Investigation of the relationship between LRRK2 and α-synuclein in Parkinson's disease

Giuseppe Madaro

A thesis submitted in partial fulfilment of the requirements for the degree of Doctor of Philosophy

The University of Sheffield

School of Medicine and Population Health

Division of Neuroscience

September 2023

Abstract

Mutations in the *LRRK2* gene which encodes Leucine-rich repeat kinase 2 (LRRK2) are the most common monogenic cause of Parkinson's disease (LRRK2-PD). Like sporadic PD, LRRK2-PD is characterised by intraneuronal inclusions, prion-like spreading of aggregated α-synuclein, and dopaminergic neuron degeneration. LRRK2 is a protein with GTPase and kinase activity which regulates several biological functions, including autophagy and subcellular trafficking.

We have previously shown that LRRK2 interacts with histone deacetylase 6 (HDAC6), a cytoplasmic deacetylase that regulates inflammation, axonal trafficking, and clearance of ubiquitinated protein aggregates via aggrephagy. Preliminary data indicate that LRRK2 may regulate HDAC6 by phosphorylation and that the kinase hyperactive LRRK2 mutant G2019S disrupts ubiquitin-dependent aggresome formation in PD. HDAC6 and LRRK2 have been independently linked to clearance and propagation of aggregated α-synuclein. However, how LRRK2 mutations cause α-synuclein pathology remains elusive. Therefore, this thesis aimed to characterise the interaction between LRRK2 and HDAC6 and establish the role of LRRK2 and HDAC6 in α-synuclein metabolism.

We observed that LRRK2 kinase activity influences its binding to HDAC6, but does not regulate ubiquitin-dependent aggresome formation, NLRP3 inflammasome activation or microtubule acetylation. We did not find evidence that PFF-induced α-synuclein aggregates are targeted to the aggresome via HDAC6. However, HDAC6 inhibition led to accumulation of both soluble and PFF-induced α-synuclein aggregates, indicating a role of HDAC6 in α-synuclein homeostasis under physiological and pathological conditions. Additionally, LRRK2 kinase inhibitors increased α-synuclein expression levels but had no impact on seeded α-synuclein aggregation. No changes were detected in basal α-synuclein secretion and subcellular localisation upon either LRRK2 or HDAC6 inhibition.

Our data indicate that both LRRK2 and HDAC6 may be involved in α-synuclein homeostasis by influencing its clearance and aggregation. Future research will elucidate how LRRK2 regulates HDAC6 functions and how these intersect with α-synuclein dyshomeostasis.

Acknowledgements

First, I would like to thank the Battelle Institute for generously funding this project through the Jeffrey Wadsworth PhD studentship.

This work wouldn't have been possible without the supervision of Prof Kurt J. De Vos, whose expertise greatly influenced the direction of my research. I am deeply grateful for his constant presence throughout all the phases of my PhD and for encouraging invaluable internal and international exchanges. I extend my sincere appreciation to my second supervisor Prof Heather Mortiboys for her availability in addressing any matters related to this research.

A substantial part of this work owes much to the collaboration with Dr. Laura Volpicelli-Daley's group at the University of Alabama at Birmingham. A special mention goes to Charlotte F. Brzozowski for her indispensable contribution to setting up the experiments involving preformed α-synuclein fibrils and mice.

I wish to thank all my fellow lab group members who have played a significant part in my academic development and who have been instrumental in supporting my lab routine during the COVID-19 pandemic, in particular Dr. Lily Koryang, Dr. Emma F. Smith, Dr. Claudia S. Bauer, and Natalie Pye. Above all, I owe the most to Dr. Valentina Basso for her genuine companionship, both within and beyond the academic sphere. In addition, I would like to thank all the members of the Grierson and Twelvetrees labs for their constructive feedback and advice.

A PhD journey would not go very far without the mentorship of a group of trusted allies. Thanks to Dr. Ilaria Giovannelli, Dr. Leonardo Contreas, Dr. Matilde Sassani, Dr. Paolo Marchi, Dr. Michela Pulix, Dr. Aina Mogas Barcons, and Kayal Vizhi Muthukrishnan for enriching my PhD experience and for significantly contributing to a healthy work-life balance.

Lastly, I am grateful to my family for expressing excitement for my research and supporting me from across the Channel. And to Ian, for being by my side in every moment of this crazy journey.

Contents

List of figures

List of tables

Abbreviations

6-OHDA	*6-hydroxydopamine*
aa	*Amino acid*
AGE	*Advanced glycation end-product*
ANK	*Ankyrin repeats*
ANOVA	*One-way analyses of variance*
APLP1	*Amyloid precursor-like protein 1*
ASO	*Antisense oligonucleotide*
ATAT1	*α-tubulin acetyltransferase 1*
ATP	*Adenosine triphosphate*
AurA	*Aurora A*
BAG3	*Bcl-2-associated athanogene 3*
BiFC	*Bimolecular fluorescence complementation*
BMDM	*Bone marrow-derived macrophages*
BSA	*Bovine serum albumin*
C-terminus	*Carboxy-terminus*
CDK5	*Cyclin dependent kinase 5*
CFTR	*Cystic fibrosis transmembrane conductance regulator*
CHIP	*Carboxyl terminal of Hsp70/Hsp90 interacting protein*
CK2	*Casein kinase 2*
CMA	*Chaperone-mediated autophagy*
COR	*C-terminal of Roc*
Cts	*Cathepsin*
Cx32	*Connexin 32*
Da	*Dalton*
DA	*Dopamine*

DAT	*Dopamine transporter*
DD	*Deacetylase domains*
DIV	*Day in vitro*
DJ-1	*Daisuke-Junko-1 protein*
DMB	*Dynein motor binding domain*
DMEM	*Dulbecco's modified Eagle's medium*
DMSO	*Dimethyl sulfoxide*
DNAJC5	*DnaJ Heat Shock Protein Family (Hsp40) Member C5*
DRP1	*Dynamin-related protein 1*
E	*Embryonic day*
EDTA	*Ethylenediaminetetraacetic acid*
EGFP	*Enhanced green fluorescent protein*
EGFR	*Epidermal growth factor receptor*
ELISA	*Enzyme-linked immunosorbent assay*
EndoA	*EndophilinA*
ER	*Endoplasmic reticulum*
ERK	*Extracellular signal-regulated kinase*
ESCRTIII	*Endosomal sorting complex required for transport III*
EV	*Empty vector*
GBA	*Glucocerebrosidase*
GFP	*Green fluorescent protein*
GRK2	*G protein-coupled receptor kinase 2*
GSK3β	*Glycogen synthase kinase 3β*
GTP	*Guanosine triphosphate*
GWAS	*Genome-wide association studies*
HBSS	*Hank's Balanced Salt Solution*
HDAC	*Histone deacetylase*

HDAC6	*Histone deacetylase 6*
HEK293	*Human embryonic kidney 293*
HSC70	*Heat shock cognate 70 kDa*
HSF1	*Heat shock factor 1*
HSP70	*Heat shock protein 70 kDa*
HSP90	*Heat shock protein 90 kDa*
IL-1β	*Interleukin 1β*
JIP4	*JNK-interacting protein 4*
KD	*Knockdown*
KO	*Knockout*
LAG3	*Lymphocyte activation gene 3*
LAMP2A	*Lysosomal-associated membrane protein 2A*
LB	*Luria-Bertani*
LBs	*Lewy Bodies*
LC3	*Microtubule-associated protein light chain 3*
LCD	*Low complexity domain*
LDH	*Lactate dehydrogenase*
LNs	*Lewy neurites*
LPS	*Lipopolysaccharide*
LRR	*Leucine-rich repeats*
LRRK2	*Leucine-rich repeat kinase 2*
LRS	*Leucyl-tRNA synthetase*
LSD	*Least Significant Difference*
LYTL	*LYsosomal Tubulation/sorting driven by LRRK2*
M	*Molar*
MAPS	*Misfolding-associated protein secretion*
MEF	*Mouse embryonic fibroblast*

Miro	*Mitochondrial Rho*
MPTP	*1-methyl-4-phenyl-1,2,3,6-tetrahydropyridine*
MT	*Microtubule*
MTOC	*Microtubule-organising centre*
mTor	*Mammalian target of rapamycin*
N-terminus	*Amino-terminus*
NAC	*Non-amyloid-β component*
NAT	*N-terminal acetyl transferase*
NEDD4	*Neuronally expressed developmentally down-regulated gene 4*
NES	*Nuclear export signal*
NeuN	*Neuronal nuclear protein*
NF	*Neurofilament*
NLRC4	*NLR Family CARD Domain Containing 4*
NLRP3	*Nucleotide-binding domain, leucine-rich repeat, and pyrin domain-containing protein 3*
NLS	*Nuclear localisation signal*
NSF	*N-ethylmaleimide sensitive fusion*
O-GlcNAc	*O-linked N-acetyl-glucosamine*
OGA	*O-GlcNAcase*
OGT	*O-GlcNAc transferase*
OMM	*Outer mitochondrial membrane*
ON	*Overnight*
OPA1	*Optic atrophy 1*
OPTN	*Optineurin*
PBS	*Phosphate-Buffered Saline*
PCC	*Pearson's correlation*
PD	*Parkinson's disease*

PFA	*Paraformaldehyde*
PFFs	*Preformed fibrils*
PIN1	*Peptidyl-prolyl cis/trans isomerase NIMA-interacting 1*
PINK1	*PTEN-induced putative kinase 1*
PKA	*cAMP-dependent protein kinase*
PKCα	*Protein kinase Cα*
PRKN	*Parkin*
PRR	*pattern recognition receptor*
PRX	*Peroxiredoxin*
pS129	*Shospho-S129*
PTM	*Post-translational modification*
RNS	*Reactive nitrogen species*
Roc	*Ras of complex protein*
ROS	*Reactive oxygen species*
rpm	*Revolutions per minute*
RRID	*Research Resource Identifier*
RT	*Room temperature*
S	*Svedberg*
SD	*Standard deviation*
SDS-PAGE	*Sodium dodecyl sulphate polyacrylamide gel electrophoresis*
SE14	*Ser-Glu tetra decapeptide repeat domain*
SEM	*Standard error of mean*
SERCA	*Sarcoendoplasmic Reticulum Calcium ATPase*
SIAH	*Seven in absentia homolog*
siRNA	*Small interfering RNA*
SIRT	*Sirtuin*

SNARE	*Soluble N-ethylmaleimide-sensitive factor attachment protein receptor*
SNCA	*Synuclein Alpha*
SNpc	*Substantia nigra pars compacta*
SNpr	*Substantia nigra pars reticulata*
SOD1	*Superoxide dismutase 1*
SUMO	*Small ubiquitin-related modifier*
TB	*Terrific broth*
TBS	*Tris-buffered saline*
TH	*Tyrosine hydroxylase*
TLR2	*Toll-like receptor 2*
tMCC	*Thresholded Mander's colocalization coefficient*
TNT	*Tunnelling nanotube*
TOM	*Translocase of the outer membrane*
TPPP1/p25	*Tubulin polymerization-promoting protein-1*
Tub A	*Tubastatin A*
TX-100	*Triton X-100*
Ub	*Ubiquitin*
UPS	*Ubiquitin-proteasome system*
USP1	*Ubiquitin Specific Protease 1*
VAMP2	*Vesicle-associated membrane protein 2*
VDAC1	*Voltage-dependent anion channel 1*
Veh	*Vehicle*
vGLUT1	*Vesicular glutamate transporter 1*
VPS35	*Vascular protein sorting 35*
Wnt	*Wingless-related integration site*
WT	*Wild type*

YFP	*Yellow fluorescent protein*
ZnF-UBP	*Zinc finger ubiquitin-binding domain*

1 Introduction

1.1 Parkinson's disease

1.1.1 Parkinson's disease: clinical and pathological features

Parkinson's disease (PD) is a complex, multi-system neurodegenerative disorder characterised by a strong motor component. The most common clinical signs include resting tremors, slowing of movements (bradykinesia), muscular rigidity and postural imbalance. As the disease progresses, symptoms become more pervasive until they compromise the ability to accomplish primary everyday tasks such as walking or eating. Though an accurate diagnosis often coincides with the onset of the first motor dysfunctions, these are usually anticipated and accompanied by a complex spectrum of non-motor symptoms. The latter are grouped into behavioural (anxiety, depression, sleep disorders, etc.), cognitive (dementia, psychosis, hallucinations, etc.) and autonomic (constipation, incontinence, orthostatic hypotension, etc.) (Reviewed by Tolosa *et al.*, 2021). PD usually emerges after the age of 50, following a prodromal phase that can last up to one decade. Yet, less frequent early-onset cases have been recorded and are often linked to hereditary or environmental factors (Kolicheski *et al.*, 2022).

The exact aetiology of PD remains elusive. The most widely accepted hypothesis proposes a crosstalk between genetic risk factors (genomic mutations and polymorphisms) and the co-occurrence of multiple environmental contributors, including exposure to pollutants or heavy metals, lifestyle, microbial infections, gut dysbiosis, inflammation and many others (Patrick *et al.*, 2019; Cabezudo *et al.*, 2020).

PD is the most common neurodegenerative disorder after Alzheimer's disease with an incidence of 1-2% and accounts for more than 6 million cases worldwide (Feigin *et al.*, 2019; Tysnes *et al.*, 2017). Since age is one of the leading risk factors of PD, this number is expected to grow in line with the increase in the world population life expectancy. The latest projections predict that PD prevalence could grow to up to 17 million cases by 2040 (Dorsey *et al.*, 2018). To date, all available treatment options

focus on mitigating PD symptoms. Although the clinical protocols currently in place significantly improve the quality of life of people with the disease, symptomatic treatments tend to fail over time, as neurodegeneration becomes more severe (Church, 2021). The research into a treatment capable of halting or slowing down the course of PD is still ongoing. Numerous strategies have been proposed and tested over decades of intense exploration but most of them have failed in clinical trials. Nonetheless, at least three drugs have recently made it into phase 3 and many more are currently undergoing earlier clinical testing, bringing new hope for a disease that still does not have a cure (McFarthing *et al.*, 2022).

1.1.1.1 Dopaminergic neurodegeneration

The core PD symptoms are directly linked to the progressive loss of dopaminergic neurons in the substantia nigra pars compacta (SNpc) and in the adjacent ventral tegmental area (VTA), both located in the midbrain (de Rijk *et al.*, 1997). These nuclei project to the striatum and modulate voluntary movement through their indirect connections with the thalamus and the motor cortex (Gerfen, 2022). Extensive neurodegeneration is also observed in autonomic, motor and neuromodulatory areas of the brainstem (Seidel *et al.*, 2015). The disruption of key neuronal circuits provokes pattern and activity changes in surviving neurons, which cause most of the non-motor symptoms (McGregor *et al.*, 2019).

The reason of the selective vulnerability of this neuronal population is one of the major unresolved questions which will help identify the causes of PD. Particular attention has been given to the unique structural and functional features of SN dopaminergic neurons, which may explain some cell-autonomous mechanisms of neurodegeneration. Neurons in the SNpc project to the striatum with a highly intricate arborisation architecture (Matsuda *et al.*, 2009). This implies the engagement in a high number of synaptic connections, which requires an intense energetic demand (Pissadaki and Bolam, 2013). Additionally, free cytoplasmic dopamine and its metabolic intermediates are susceptible to oxidation. This generates highly unstable side-products such as dopamine-o-quinone, 5,6-indolequinone and aminochrome, which may react with lipids and proteins contributing to metabolic failure and protein aggregation (Latif *et al.*, 2021). Moreover, midbrain dopaminergic neurons display autonomous pacemaker activity, which involves large cytosolic Ca^{2+} oscillations

(Grace *et al.*, 1983; Grace *et al.*, 1989). Dysregulation of Ca^{2+} signalling has been linked to bioenergetic unbalance and oxidative stress (Zampese *et al.*, 2020). Taken together these elements may represent a source of vulnerability of the dopaminergic neurons in the midbrain, which base their survival on a fragile metabolic balance.

1.1.1.2 Lewy pathology

Similar to other neurodegenerative disorders, PD progression is intertwined with a profound protein homeostasis unbalance leading to protein misfolding and aggregation. A distinctive histopathological feature of most PD cases is the deposition of intracytoplasmic inclusions known as Lewy Bodies (LBs) and Lewy Neurites (LNs), depending on their subcellular location (Henderson *et al.*, 2019). LBs and LNs mainly consist of insoluble aggregates of the presynaptic protein α-synuclein interspersed with fragmented organelles, cytoskeletal components and other aggregated proteins (Spillantini *et al.*, 1997; Lashuel, 2020). The process of α-synuclein aggregation begins when liquid condensates of natively unfolded α-synuclein monomers transition to insoluble, β-sheet-rich oligomers. These aggregates act as nucleation centre for the recruitment and pathological conversion of other natively folded monomers, which polymerise into proteolysis-resistant fibrils (Tofaris, 2022). Oligomers and fibrils can be released from diseased cells and taken up by surrounding neurons and glia (Stefanis *et al.*, 2019). This contributes to propagation of α-synuclein pathology and is linked to neurotoxicity and neuroinflammation (Mehra *et al.*, 2019). Because of its ability to spread across the brain, Lewy pathology is not only found in the substantia nigra but also in other extranigral regions of the brainstem and in the cerebral cortex (Hughes *et al.*, 1992). Deposition of α-synuclein aggregates advances following a stereotypical pattern through interconnected brain areas and partially overlaps with disease progression (Braak *et al.*, 2002; Braak *et al.*, 2003). Chapter 1.2 is dedicated to the role of α-synuclein pathology and LBs formation in PD.

1.1.2 Parkinson's disease genetics

Genetic variations are accountable for the development of PD only in a modest percentage of cases estimated around 15-25% (Day *et al.*, 2021; He *et al.*, 2020). Additionally, most monogenic factors display pleiotropy and incomplete penetrance: the same genetic mutations can give rise to a wide spectrum of severity and onset

age. In some extreme cases, carriers might not even develop any pathology during the course of their lives (Day and Mullin, 2021). This testifies the complex interaction between multiple genetic factors and environment in the aetiology of PD, many of which still await to be discovered.

Historically, the study of inheritance patterns in large families affected by PD led to the identification of the first rare but highly penetrant mendelian factors. To date, mutations in over 20 genes have been linked to familial PD, although in some cases the connection with the disease has not been fully clarified (Tab 1.1; Blauwendraat *et al.*, 2020). Recent advancements in sequencing technologies which powered the latest genome-wide association studies (GWAS) enabled the identification of 90 highly diffused genetic variants and polymorphism which moderately increase the lifetime risk to develop PD (for a more comprehensive review, see Nalls *et al.*, 2019 and Ye *et al.*, 2022). Below we report the most significant genetic loci and their relevance in PD.

1.1.2.1 SNCA

In 1996, a study conducted by Polymeropoulos and colleagues on the segregation of genetic markers with hereditary parkinsonism led to the identification of the first genetic locus directly connected to PD (Polymeropoulos *et al.*, 1996). Originally named Park1, the region mapped on chromosome 4q21-q23 contains the *SNCA* gene encoding for α-synuclein. To date, genomic multiplications and seven missense mutations in the *SNCA* gene (A30P, E46K, H50Q, G51D, A53V, A53T, and A53E) have been described as the cause of autosomal-dominant forms of PD with high penetrance (Fig. 1.1; Polymeropoulos *et al.*, 1997; Krüger *et al.*, 1998; Singleton *et al.*, 2003; Zarranz *et al.*, 2004; Appel-Cresswell *et al.*, 2013; Kiely *et al.*, 2013; Pasanen *et al.*, 2014; Yoshino *et al.*, 2017). Soon after its discovery, α-synuclein was identified as the main component of the proteinaceous lesions commonly observed in PD brains (Spillantini *et al.*, 1998). More recently, polymorphisms in the promoter and the distal enhancer region of the *SNCA* gene have been linked to increased risk of PD (Maraganore *et al.*, 2006; Soldner *et al.*, 2016). These breakthroughs have driven the scientific community's interest on clarifying the properties of α-synuclein for last 30 years. We reported the main findings in Chapter 1.2 .

1.1.2.2 LRRK2

Mutations in the *LRRK2* gene encoding leucin-rich repeat kinase 2, are the most common cause of dominantly inherited PD, accounting for approximately 5% of genetic PD worldwide and up to 40% of all PD cases in some North African and Jewish cohorts (Paisán-Ruíz *et al.*, 2004; Zimprich *et al.*, 2004; Healy *et al.*, 2008). LRRK2-PD is characterised by incomplete penetrance and slow progression. LRRK2 is a multifunctional protein involved in a large number of biological pathways, including lysosomal integrity, mitochondrial homeostasis, autophagy, vesicle trafficking and cell motility, with more being discovered every year (Taylor *et al.*, 2020). Since most of the LRRK2 mutations causing neurodegeneration result in an overall increase of LRRK2 kinase activity, the protein has originally been linked to PD through the hypothesis of a toxic gain-of-function (West *et al.*, 2007). However, recent evidence demonstrates a more intricate mechanism of action (Usmani *et al.*, 2021). We dedicated Chapter 1.3 to the functions of LRRK2 and its role in PD.

1.1.2.3 VPS35

Mutations in the *VPS35* gene are associated with PD through an autosomal dominant inheritance pattern (Vilariño-Güell *et al.*, 2011; Zimprich *et al.*, 2011). This locus encodes vascular protein sorting 35, which forms a heterotrimer with VPS29 and VPS26 at the core of the multimeric retromer complex. The retromer complex plays a cargo-binding role in recycling membrane proteins between endosomes, trans-Golgi network and plasma membrane (Cunningham *et al.*, 2020). A role of VPS35 in synaptic vesicles cycle has also been reported (Ye *et al.*, 2020). VPS35-linked PD is considered rare, affecting only 0.2% of the European population and is virtually indistinguishable from sporadic PD (Lesage *et al.*, 2020). On a cellular level, VPS35 mutations cause disruption of endosomal dynamics, autophagy impairment, mitochondrial disruption and α-synuclein accumulation leading to loss of dopaminergic neurons (Bono *et al.*, 2020; Hanss *et al.*, 2021).

1.1.2.4 GBA1

GBA1 mutations cause autosomal recessive early-onset parkinsonism which often overlaps with Gaucher's disease, a metabolic disorder caused by lysosomal storage disruption (Aharon-Peretz *et al.*, 2004; Clark *et al.*, 2005; Gan-Or *et al.*, 2008). *GBA1*-

PD risk varies depending on the specific mutation and is usually linked to more severe dementia (Lesage *et al.*, 2011). In general, all the *GBA1* mutations linked to PD cause loss-of-function of the lysosomal enzyme glucocerebrosidase (GCase), involved in the metabolism of sphingolipids and cholesterol. Inactive GCase leads to endo-lysosomal system dysfunction and lipid homeostasis unbalance (Gegg *et al.*, 2022). Poor autophagolysosomal flux and interaction with unprocessed GCase substrates has been linked to impaired α-synuclein degradation and protein aggregation (Zunke *et al.*, 2018). Interestingly, GCase expression is consistently downregulated in sporadic PD, highlighting the importance of lysosomes in initiating and propagating the disease (Murphy *et al.*, 2014).

1.1.2.5 PRKN and PINK1

Mutations of the E3 ubiquitin ligase parkin (*PRKN*) and phosphatase and tensing homolog (PTEN)-induced kinase 1 (*PINK1*) are the cause of an early-onset, autosomal recessive form of PD (Kitada *et al.*, 1998; Valente *et al.*, 2004). These two proteins cooperate in the cellular pathway involved in selective degradation of mitochondria by macroautophagy known as mitophagy (Onishi *et al.*, 2021). Under physiological conditions, PINK1 is constitutively imported into the mitochondrial intermembrane space, cleaved, and returned to the cytoplasm for proteasomal degradation. In case of mitochondrial damage, the loss in membrane potential causes PINK1 to stall on the outer mitochondrial membrane (OMM), homodimerize and auto-phosphorylate. Activated PINK1 phosphorylates PRKN as well several ubiquitinated targets on the OMM. PRKN shows high affinity for phosphorylated ubiquitin and its E3 ubiquitin ligase activity is activated by phosphorylation. This triggers a positive feedback loop of ubiquitination and phosphorylation. Phosphorylated polyubiquitin chains are sensed by adapter proteins which eventually mediate engulfment of the dysfunctional mitochondria into an autophagosome (Onishi *et al.*, 2021). Dysregulation of the PINK1/ PRKN signalling leads to accumulation of dysfunctional mitochondria, redox unbalance, ROS production, and apoptosis (Ge *et al.*, 2020).

1.1.2.6 PARK7

Loss-of-function mutations in Parkinson protein 7 (PARK7, also known as Daisuke-Junko-1 protein, DJ-1) cause autosomal recessive PD characterised by early onset.

This protein is ubiquitously expressed and its activity lays at the crossroad of a few key molecular pathways (Bonifati *et al.*, 2003). It exerts a pro-survival, antioxidant, cytoprotective function by activating ERK1/2; it activates PI3K/Akt to inhibit apoptosis and stimulate cell proliferation; it suppresses the pro-apoptotic ASK1 and p53 pathways; it activates the anti-oxidative stress Nrf2 transcription factors to prevent apoptosis and regulate mitophagy (Neves *et al.*, 2022).

Table 1.1 Genetic risk factors for PD. The column marked with an asterisk indicates an estimate which takes into account the number of independent families in which a link between gene mutations and PD was reported, evidence of disease-related functional changes, and availability of publications reporting no links between gene variants and PD (adapted from Blauwendraat *et al.*, 2020).

Gene	Mutation	Note	Year of discovery	Proposed disease mechanism	Inheritance	Frequency	Nominated by GWAS	Confidence as actual PD gene*
SNCA	Missense or multiplication	Often with dementia	1997, 2003	Gain of function or overexpression	Dominant	Very rare	Yes	Very high
PRKN	Missense or loss of function	Often early onset	1998	Loss of function	Recessive	Rare	No	Very high
UCHL1	Missense	..	1998	Loss of function?	Dominant	Unclear	No	Low
PARK7	Missense	Often early onset	2003	Loss of function	Recessive	Very rare	No	Very high
LRRK2	Missense	..	2004	Gain of function	Dominant	Common	Yes	Very high
PINK1	Missense or loss of function	Often early onset	2004	Loss of function	Recessive	Rare	No	Very high
POLG	Missense or loss of function	Atypical PD	2004	Loss of function?	Dominant	Rare	No	High
HTRA2	Missense	..	2005	Unclear	Dominant	Unclear	No	Low
ATP13A2	Missense or loss of function	Atypical PD	2006	Loss of function	Recessive	Very rare	No	Very high
FBXO7	Missense	Often early onset	2008	Loss of function	Recessive	Very rare	No	Very high
GIGYF2	Missense	..	2008	Unclear	Dominant	Unclear	No	Low
GBA	Missense or loss of function	..	2009	Likely loss of function	Dominant (incomplete penetrance)	Common	Yes	Very high
PLA2G6	Missense or loss of function	Often early onset	2009	Loss of function	Recessive	Rare	No	Very high
EIF4G1	Missense	..	2011	Unclear	Dominant	Unclear	No	Low
VPS35	Missense	..	2011	Loss of function	Dominant	Very rare	No	Very high
DNAJC6	Missense or loss of function	Often early onset	2012	Loss of function	Recessive	Very rare	No	High
SYNJ1	Missense or loss of function	Often atypical PD	2013	Loss of function	Recessive	Very rare	No	High
DNAJC13	Missense	Same family as *TMEM230*	2014	Unclear	Dominant	Unclear	No	Low
TMEM230	Missense	Same family as *DNAJC13*	2016	Loss of function?	Dominant	Unclear	No	Low
VPS13C	Missense or loss of function	..	2016	Loss of function	Recessive	Rare	Yes	High
LRP10	Missense or loss of function	..	2018	Loss of function?	Dominant	Unclear	No	Low

1.1.3 PD and environmental "modifiers"

PD is a heterogeneous disorder where genetic and environmental factors closely interact to influence risk, penetrance, and prognosis of the disease (Jacobson *et al.*, 2019; He *et al.*, 2020). Numerous environmental "modifiers" have been identified over the course of observational studies which helped contextualise the varied PD panorama.

Well-documented inverse relationships have been found between PD risk and lifestyle behaviours such as smoking (Domenighetti *et al.*, 2022) or caffeine consumption (Ren and Chen, 2020). Moderate to high levels of physical exercise not only have a protective impact but have proven to be an effective adjuvant of symptomatic treatments (Fang *et al.*, 2018; Gamborg *et al.*, 2022). Despite being a consistent risk factor for other neurodegenerative disorders, the impact of alcohol consumption in PD is ambiguous, with studies reporting positive, null and negative effects (Peng *et al.*, 2020; Mitchell *et al.*, 2022). Finally, abuse of illicit drugs such as heroin and amphetamine-like stimulants has been correlated with increased risk of PD (Ferreira *et al.*, 2020).

In addition to personal habits, specific working and living environments may enhance exposure to pesticides, heavy metals and solvents linked to increased risk of PD.
Paraquat and rotenone are two infamous examples of chemical compounds used in agriculture which cause severe dopaminergic neuronal loss. The herbicide Paraquat was widely commercialised in the early 1960s and subsequently restricted following reports of acute neurotoxicity. Exposure to Paraquat causes α-synuclein upregulation and selective nigrostriatal degeneration by interfering with mitochondrial respiration. This results in heavy ROS production, which accelerates protein oxidation and aggregation (Manning-Bog *et al.*, 2002; Sherer *et al.*, 2003). Rotenone is a broad-spectrum insecticide which interferes with the electron transport chain by inhibiting mitochondrial complex I (Fang and Casida, 1999). Chronic exposure to rotenone is associated with α-synuclein pathology, dopaminergic toxicity and increased risk of PD (Heikkila *et al.*, 1985; Ferrante *et al.*, 1997; Tanner *et al.*, 2011).
Trichloroethylene (TCE) is a versatile industrial solvent banned in EU since 2010 (Liu *et al.*, 2018). Chronic exposure to this substance can increase by five times the risk of PD (Goldman *et al.*, 2012). Today, TCE is an ubiquitous and persistent environmental

contaminant found in air, soil and groundwater which is thought to contribute to the steady increment in PD incidence (Dorsey *et al.*, 2023).

As for organic compounds, contamination by heavy metals (Hg, Pb, Cu, Mn, Al, Fe, Mg, Zn, Bi, and Tl) may result from intense industrial pollution. Over time, heavy metals can dramatically alter neuronal metabolism and mitochondrial function causing neurotoxicity. Additionally, the direct interaction between α-synuclein an bivalent cations can promote the transition from soluble multimers to pathogenic oligomers (Bjorklund *et al.*, 2018).

Several epidemiologic studies warned about the risks of exposure to environmental pollutants since young age in highly industrialised areas (Ritz *et al.*, 2015; Grova *et al.*, 2019). Children and young adults are more vulnerable to changes in the brain physiology which may trigger neurodegeneration later in life. These include accumulation of α-synuclein, alterations of the innate immune response and neuroinflammation (Calderón-Garcidueñas *et al.*, 2008).

Some interesting associations between inflammation, infectious agents and PD have also been identified (Smeyne *et al.*, 2021). These include influenza viruses such as H1N1, which caused the 1918 pandemic (Henry *et al.*, 2010), and the avian influenza virus H5N1 (Jang *et al.*, 2009). Other common infections potentially linked to PD are hepatitis C and *Helicobacter pylori* (Smeyne *et al.*, 2021). Medium and long-term effects of COVID19 on neurodegeneration have been reported (Prudencio *et al.*, 2021; Douaud *et al.*, 2022). Future longitudinal studies will help clarify possible effects of the SARS-CoV-2 pandemic on PD incidence.

1.2 α-synuclein and its role in Parkinson's disease

The strong influence that α-synuclein exerts in shaping PD pathology and progression is evidenced by at least four major observations. First, alterations of the *SNCA* gene locus, including mutations, duplications and polymorphisms, are causative or increase the risk of PD (Blauwendraat *et al.*, 2020). Second, α-synuclein monomers have the propensity to self-assemble into neurotoxic fibrils similar to those found in LBs and LNs (Alam *et al.*, 2019). Third, α-synuclein levels are consistently upregulated in sporadic PD (Jowaed *et al.*, 2010). Finally, α-synuclein overexpression causes dopaminergic neurodegeneration in several animal models (Cooper *et al.*, 2018; Gómez-Benito *et al.*, 2020). Here we summarise the physiological role of α-synuclein and the pathological changes associated to PD.

1.2.1 α-synuclein expression and functions

The human synucleins protein family encompasses three proteins encoded by distinct genes: α-, β- and γ-synuclein (Spillantini *et al.*, 1995; Lavedan *et al.*, 1998; Lavedan *et al.*, 1998). Among these, α-synuclein is the most widely studied for its involvement in PD. α-synuclein is a small protein of 140 amino acids (aa), is mainly expressed in the presynaptic compartment and is one of the most abundant proteins in the brain (Jakes *et al.*, 1994; Iwai *et al.*, 1995). Under physiological conditions, α-synuclein adopts a wide range of secondary structures, among which a random coil monomer is statistically favoured. Partial α-helix folding and formation of dynamic homotetramers has also been described (Bartels, Choi and Selkoe, 2011; Wang *et al.*, 2011). Like most intrinsically disordered proteins, the possibility for α-synuclein to form organised 3D structures depends on the surrounding environment and the presence of interacting partners (Bondos *et al.*, 2022).

α-synuclein contains three biochemically distinct domains (Fig. 1.1). The lysine-rich, positively charged, N-terminal domain spans from aa 1 to 60 and can fold into two α-helix stretches (low complexity domains, LCDs) connected by a flexible linker. This secondary structure is stabilised by the interaction with phospholipid bilayers, especially small diameter vesicles (Davidson *et al.*, 1998; Bussell and Eliezer, 2003). The central hydrophobic region (aa 61-96), known as non-amyloid-β component (NAC), harbours a stretch of 12 aa which is necessary and sufficient to form the

proteolysis resistant fibril core (Giasson *et al.*, 2001). Lastly, the C-terminus comprises aa 97-140. This highly acidic and negatively charged region is rich in proline residues and characterised by an intrinsically disordered structure. α-synuclein C-terminus is involved in high affinity interactions with bivalent cations, other proteins and membranes (Binolfi *et al.*, 2006; Bernal-Conde *et al.*, 2020; S. Zhang *et al.*, 2021).

The function of synuclein is not well understood, mostly because knockout (KO) animal models do not manifest any major phenotypical anomalies. This is probably due to a compensatory effect of the two, non-aggregation-prone α-synuclein isoforms β-and γ-synuclein (Anwar *et al.*, 2011; Senior *et al.*, 2008). Early studies on α-synuclein KO mice recorded a faster synaptic recovery rate in response to paired pulse stimulation, leading to the hypothesis of a role in presynaptic homeostasis and neurotransmitter release (Abeliovich *et al.*, 2000). α-synuclein may regulate synaptic transmission by enhancing the formation of the SNARE complex through the interaction with VAMP2 (Burré *et al.*, 2010; Hawk, Khounlo and Shin, 2019; Sun *et al.*, 2019). This chaperone function accelerates the kinetics of neurotransmitter release (Huang *et al.*, 2018; Logan *et al.*, 2017) and is linked to the formation of α-helix-rich α-synuclein tetramers (Burré, Sharma and Südhof, 2014; Nuber *et al.*, 2018). α-synuclein can also directly bind to negatively charged membranes and influence their curvature (Ferreon *et al.*, 2009; Westphal *et al.*, 2013). As a result, α-synuclein may facilitate membrane bending and promote pore dilation and neurotransmitter exocytosis (Logan *et al.*, 2017). α-synuclein may also regulate synaptic transmission by modulating Ca^{2+} influx (Danzer *et al.*, 2007), or by regulating dopamine transporter (DAT)-mediated reuptake of neurotransmitter from the synaptic cleft (Butler *et al.*, 2015).

In addition to the presynaptic terminus, α-synuclein has been found in other cellular compartments and in association with membrane-bound organelles, although its non-synaptic roles are even more enigmatic. α-synuclein can interact with mitochondria and be translocated to the intermembrane space (Li *et al.*, 2007; Nakamura *et al.*, 2008). Its function in mitochondria is probably linked to translocation of mitochondrial components, membrane remodelling and respiratory enzyme regulation (Liu *et al.*, 2009; Loeb *et al.*, 2010). Interaction of α-synuclein with organelles such as endoplasmic reticulum (ER), Golgi apparatus, and the endolysosomal system has been proposed to influence vesicle trafficking, lipid metabolism, membrane

remodelling and regulation of membrane channels (Bernal-Conde *et al.*, 2020; Vidović and Rikalovic, 2022). Finally, a small fraction of α-synuclein is located in the nucleus. Direct interaction of α-synuclein with histones suggests a role in chromatin remodelling and gene expression regulation (Goers *et al.*, 2003).

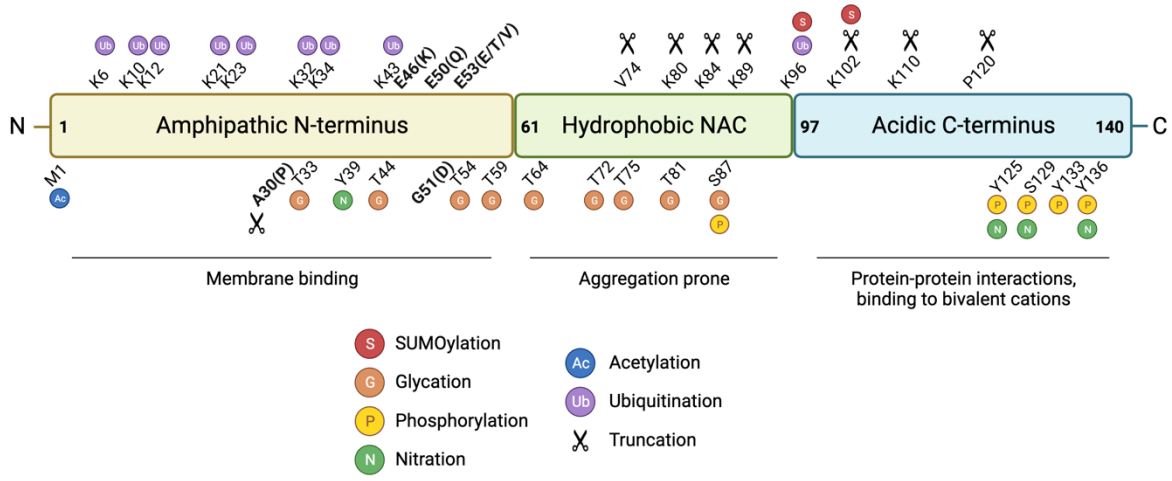

Figure 1.1 Schematic representation of α-synuclein structure and overview of the main post-translational modifications. The N-terminal domain is reported in yellow, the central non-amyloid-β component (NAC) in green and the intrinsically disorder C-terminal domain in light blue. Residues subject to post-translational modifications are labelled. α-synuclein mutations related to genetic PD are reported in bold. Created with BioRender.com.

1.2.2 Routes of α-synuclein degradation

According to the current view of PD progression, the unbalance between α-synuclein synthesis and degradation is an early event that precedes oligomer formation and neurodegeneration (Lehtonen *et al.*, 2019). Protein homeostasis relies on a network of molecular pathways that regulate protein translation, folding, trafficking, refolding, and degradation. Newly synthesised peptides are co-translationally guided into their final three-dimensional conformation by the intervention of folding factors such as molecular chaperones, co-chaperones, oxidoreductases and *cis/trans* isomerases (Balchin *et al.*, 2020). Given the high complexity of the folding process and the biophysical and biochemical stress to which mature proteins undergo, misfolding events are relatively frequent. This triggers the activation of stress pathways such as the unfolded protein response and the heat shock response which ultimately increase the expression of protein chaperones and co-chaperones (Hetz *et al.,* 2020; Gu *et al.*, 2023). Molecular chaperones perform an indispensable quality control function on the proteome by facilitating protein refolding and directing terminally misfolded substrates towards the most appropriate degradation route (Jayaraj *et al.*, 2020; Kawagoe *et al.*, 2022).

Mammalian cells mainly rely on two cellular structures to achieve protein clearance, both linked to α-synuclein degradation: the proteasome and the lysosome. The proteasome is a unique supramolecular multi-protease complex composed by a 20S barrel-like catalytic core and two 19S regulatory subunits (Martinez-Fonts *et al.*, 2020). A series of ATP-dependent conformational changes thread the misfolded protein through the catalytic core of the proteasome where it gets processed into small peptides (Sahu *et al.*, 2021). Proteins can be targeted to the proteasome through the conjugation of a polyubiquitin tail, which acts as degradation signal. This pathway is knowns as the ubiquitin-proteasome system (UPS; Tracz *et al.*, 2021; Zajicek *et al.*, 2021).

The term “autophagy” refers to the degradation of cellular components via the lysosomal pathway. Autophagy is further classified into macroautophagy, chaperone-mediated autophagy (CMA), and microautophagy depending on whether the substrate is delivered to the lysosome via autophagic vesicles, guided by chaperones or through invagination of the lysosomal membrane, respectively (Yu *et al.*, 2018; Kirkin, 2020;

Wang *et al.*, 2022). During macroautophagy, entire portions of the cytoplasm or selected substrates are engulfed by a double-membrane vesicle forming an autophagosome (Johansen *et al.*, 2020). Following tethering and fusion with a lysosome, the contents of the newly formed autophagolysosome are digested by the action of proteolytic enzymes (Kumar *et al.*, 2022). CMA is a specialised form of autophagy which mainly targets soluble proteins containing the pentapeptide motif KFERQ, recognised by heat shock cognate 70 (HSC70). This cytoplasmic chaperone transports CMA targets to the lysosome where lysosome-associated membrane protein 2A (LAMP2A) mediates protein threading and translocation to the lysosome lumen for degradation (Bourdenx *et al.*, 2021).

Numerous lines of evidence establish a connection between both the proteasomal and autophagolysosomal pathways and regulation of α-synuclein homeostasis. The role of the proteasome in the clearance of α-synuclein emerged from numerous studies, although its impact appears to be contingent upon the cellular environment and the α-synuclein species under consideration (Fig. 1.2a, b). Tests based on overexpression cellular models and purified proteasome systems suggest that α-synuclein is targeted to the proteasome via both ubiquitin-dependent and -independent mechanisms (Bennett *et al.*, 1999; Tofaris, *et al.*, 2001; Webb *et al.*, 2003; Emmanouilidou *et al.*, 2010; Shabek *et al.*, 2012). In contrast, other studies based on endogenously expressed α-synuclein in PC12 cells and cortical neurons did not evidence significant changes in α-synuclein expression and ubiquitination (Rideout *et al.*, 2001; Rideout *et al.*, 2002). The key to clarify these apparently contradictory data may lie in a work of Emmanouilidou and coworkers, who suggested that the 26S proteasome exclusively targets intermediate-size soluble α-synuclein oligomers formed as a result of α-synuclein accumulation (Emmanouilidou *et al.*, 2010). Hence, the proteasome may process a subset of α-synuclein species or mutant isoforms which may be variably enriched based on cell type and experimental conditions (Webb *et al.*, 2003).

A number of studies suggest that macroautophagy is involved in clearance of overexpressed α-synuclein and its oligomeric intermediates (Fig. 1.2c; Webb *et al.*, 2003; Lee *et al.*, 2004). α-synuclein C-terminal is robustly ubiquitinated by the E3 ubiquitin ligase neuronally expressed developmentally down-regulated gene 4 (NEDD4). The conjugation with K63-linked polyubiquitin represents a strong autophagy localisation signal (Vogiatzi *et al.*, 2008; Tofaris *et al.*, 2011). The

importance of autophagy in α-synuclein homeostasis is supported by studies in mice lacking components of the autophagy machinery showing high levels of aberrantly modified synuclein (Ahmed *et al.*, 2012; Friedman *et al.*, 2012). Interestingly, some authors observed that large fibrillar aggregates are resistant to proteolytic degradation even via macroautophagy (Lee *et al.*, 2004; Tanik *et al.*, 2013).

In addition to macroautophagy, CMA has also been linked to α-synuclein clearance (Fig. 1.2d). α-synuclein includes a CMA recognition motif and studies based on cellular models report the involvement of CMA in degradation of α-synuclein monomers and dimers (Cuervo *et al.*, 2004; Martinez-Vicente *et al.*, 2008a). Inhibition of CMA causes α-synuclein build up and aggregation in overexpression models and in primary neurons (Vogiatzi *et al.*, 2008). α-synuclein accumulation has also been reported in mice in which LAMP2A had been knocked down (Rothaug *et al.*, 2015). Nonetheless, *in vivo* data display some ambiguity. In fact, in these models α-synuclein dyshomeostasis cannot be uniquely attributed to CMA dysfunction (Rothaug *et al.*, 2015). Additionally, negative results collected *in vivo* may be affected by poor cell type specificity and lack of spatial resolution (Xilouri *et al.*, 2016). It is worth mentioning that CMA downregulation and increased α-synuclein half-life have been observed in post mortem PD brains, which corroborates the pathogenic relevance of this pathway (Alvarez-Erviti *et al.*, 2010).
Ebrahimi-Fakhari and coworkers dissected α-synuclein turnover in a transgenic mouse model using a cranial window approach combined with multiphoton microscopy. Topical pharmacological inhibition of the proteasome or of the autophagolysosomal pathway revealed a functional connection between the two degradation routes in α-synuclein homeostasis. The first prevails under normal conditions, the second intervenes upon increased α-synuclein burden (Ebrahimi-Fakhari *et al.*, 2011).

Taken together, these studies indicate that multiple degradation pathways regulate α-synuclein protein levels under physiological conditions. This synergistic effect is heightened in pathology, where the coexistence of multiple cytotoxic species requires the contemporary engagement of selective clearance routes.

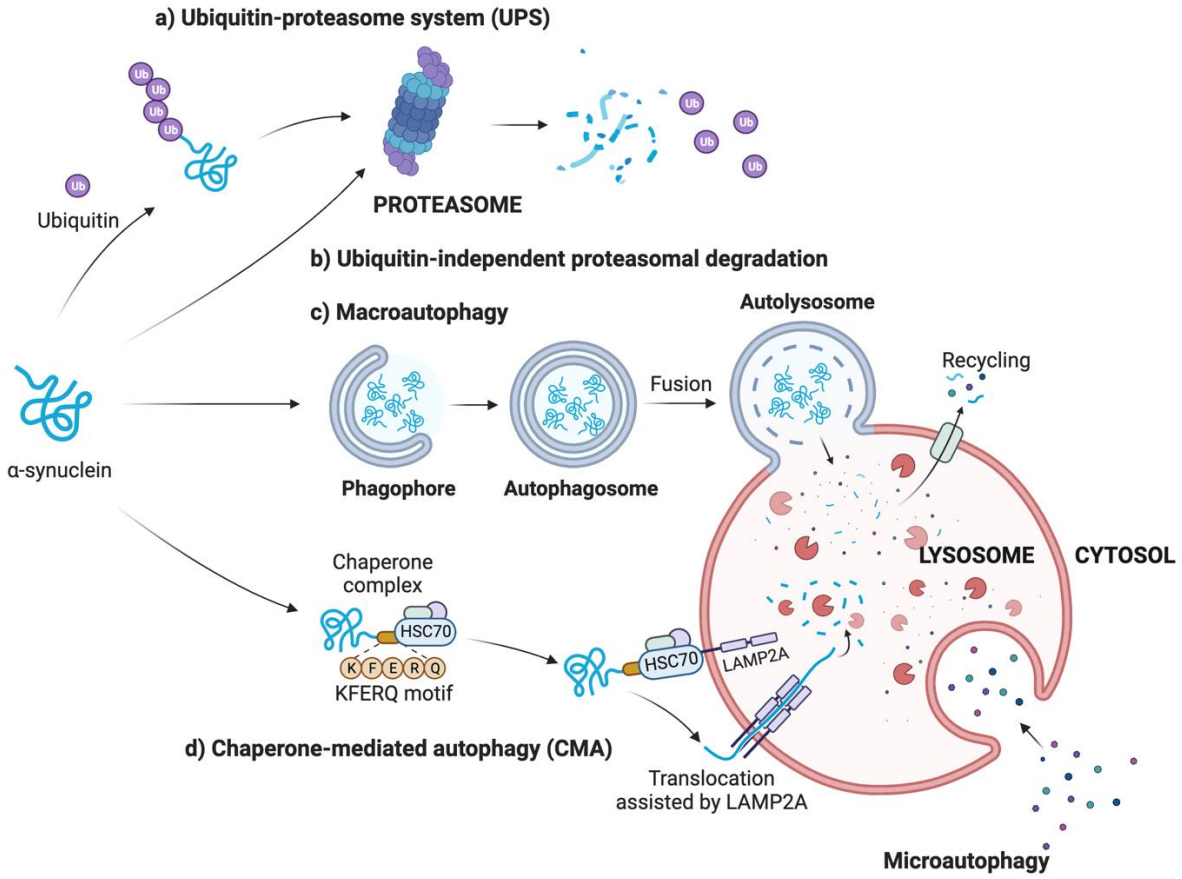

Figure 1.2 Mechanisms of α-synuclein degradation. Natively folded and soluble oligomeric α-synuclein is targeted to the proteasome via the ubiquitin-proteasome system (UPS) **a)** or via an ubiquitin-independent chaperone-mediated mechanism **b)**. Soluble, oligomeric, or aggregated α-synuclein can be targeted to the autophagolysosomal pathway **c)**. Chaperone-mediated autophagy (CMA) mostly processes monomeric α-synuclein and soluble α-synuclein oligomers **d)**. Created with BioRender.com.

1.2.3 α-synuclein aggregation and Lewy body formation

α-synuclein exists within the cells in a spectrum of interconvertible species that can influence neuronal biology in different ways (Alam *et al.*, 2019). Under physiological conditions, the two LCDs sited in the N-terminus of the protein facilitate weak intermolecular interactions and the formation of phase separation intracytoplasmic domains (Jónsson *et al.*, 2012; Guerrero-Ferreira *et al.*, 2018). In PD, these liquid condensates drive the aggregation of α-synuclein into β-sheet-rich amyloid structures which are highly cytotoxic (Fig. 1.3; Serio *et al.*, 2000; Cremades *et al.*, 2012; Narayanan *et al.*, 2019). The aggregation process starts with a rate-liming phase corresponding to the formation of a metastable fibril nucleus (Conway, Harper and Lansbury, 1998). This insoluble core templates the assembly of other native-state monomers into protofilaments and amyloid fibrils initiating an exponential polymerization phase (Fig. 1.3; Hijaz *et al.*, 2020).

α-synuclein fibrils are composed by two protofilaments intertwined into a left-handed helix. Residues 37–99 are involved in the formation of the fibril core, where they adopt a β-hairpin, serpentine Greek key shape. The N- and C- terminal regions protrude from the axis of the fibril forming a solvent-accessible mantle. Four distinct fibril architectures have been described, which reflect polymorphisms of the β-folding conformation and of the protofibrils interface, both influenced by α-synuclein mutations (Mirecka *et al.*, 2014; B. Li *et al.*, 2018; Guerrero-Ferreira *et al.*, 2018; Y. Li *et al.*, 2018).

Spontaneous nucleation of α-synuclein aggregates in physiological conditions is a statistically rare event (Cremades *et al.*, 2012). As a result, any synergistic perturbations of the cellular microenvironment which increase the kinetic stability of the system can accelerate the pathological conversion of the protein and trigger a ripple effect.

As previously mentioned, seven *SCNA* gene mutations have been linked to genetic PD (Fig.1.1). Although they don't affect the partially folded conformation of the soluble monomer, they all consistently increase α-synuclein aggregation propensity, albeit through different mechanisms (Balestrino *et al.*, 2020; Ghosh *et al.*, 2013; J. Li *et al.*, 2001). Both A53T and E46K improve the thermodynamic stability of the fibril by speeding up the elongation phase (Conway *et al.*, 2000). The A30P and G51D mutants

increase the kinetics of the nucleation core by reducing lipid binding (Choi *et al.*, 2004; Fortin *et al.*, 2004). Conversely, the E46K mutation promotes α-synuclein clustering and overcrowding on the surface of cell membranes and enhances contacts between α-synuclein N- and C-termini (Choi *et al.*, 2004).

Lipid binding has proven to have a dual role in α-synuclein aggregation. On the one hand, the interaction of α-synuclein with membranes favours α-helical conformations, which antagonise β-sheets folding and support the physiological function of the protein by multimer formation (Zhu *et al.*, 2003; Burré *et al.*, 2014). On the other hand, α-synuclein enrichment onto vesicles and organelle surfaces generates microdomains where the high local concentration increases the probability of nucleation events (Lee *et al.*, 2002; Comellas *et al.*, 2012). This equilibrium depends on phospholipid composition, vesicle size and relative α-synuclein concentrations (Burré *et al.*, 2014; Galvagnion *et al.*, 2016). The interplay between α-synuclein and lipids can also be observed in the heterogeneous ultrastructure of the LB, of which lipids are an important component. LB are usually organised around a dense core crowded with dysmorphic and fragmented organelles (mostly ER, mitochondria, autophagosomes and lysosomes) interspersed with α-synuclein fibrils. Pathologically modified α-synuclein is stratified in concentric layers around the LB together with misplaced cytoskeletal components (Fig. 1.3; Shahmoradian *et al.*, 2019; Moors *et al.*, 2021). This characteristic of the LB led to the alternative hypotheses that α-synuclein pathology may originate on the surface of dysfunctional organelles or that the latter may be trapped during the process of LB formation (Shahmoradian *et al.*, 2019).

Another factor influencing α-synuclein solubility is the presence of metallic solutes. The acidic, intrinsically disordered α-synuclein C-terminus is involved in electrostatic interactions with cations, predominantly Ca^{2+}. Ions promote aggregation by neutralising α-synuclein charge, disturbing the intramolecular interactions between N- and C- termini and exposing the NAC region to self-assemble (Stephens *et al.*, 2020). Similar to ions, low pH partially neutralises the positive charge of the C-terminal domain. This in turn reduces the electrostatic repulsion between monomers and increases the nucleation propensity of partially folded intermediates (Uversky *et al.*, 2001).

Finally, α-synuclein post-translational modifications (PTMs) can have a significant impact on nucleation e polymerisation of α-synuclein aggregates (Fig. 1.1).

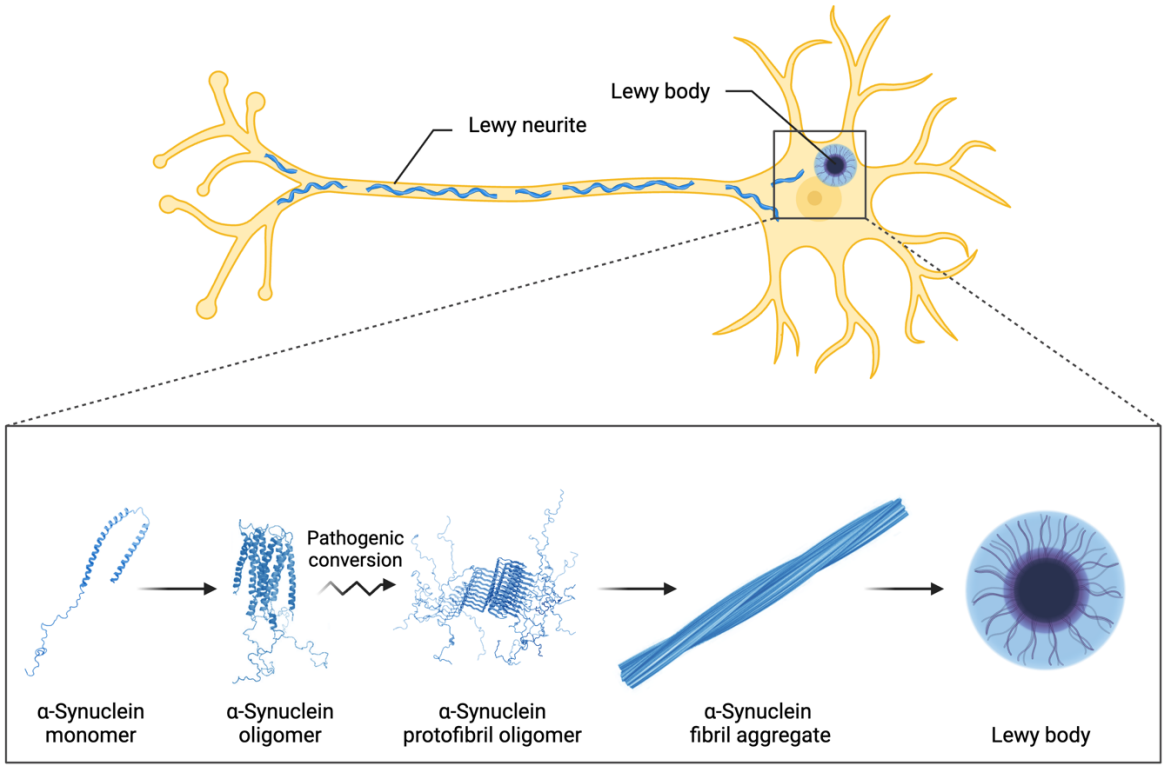

Figure 1.3 Stages of α-synuclein misfolding and aggregation. Under physiological conditions, α-synuclein monomers adopt a wide range of unfolded or partially folded conformations which include the formation of homodimers and homotetramers. Because of intrinsic or microenvironmental factors, α-synuclein soluble oligomers can convert into insoluble β-sheet-rich aggregates. These act as nucleation centres for the template conversion of native α-synuclein monomers into highly ordered amyloid fibrils. α-synuclein fibrils affecting dysmorphic neuronal projections (Lewy neurites) are retrogradely accumulated into a perinuclear inclusion (Lewy body). Created with BioRender.com.

1.2.4 α-synuclein post-translational modifications and Lewy pathology

In addition to the effects of the surrounding cellular environment, α-synuclein conformation strictly depends on changes in the biophysical properties of the protein. More than 300 different PTMs have been so far identified, some of which may either have a pathological role in PD or limit the impact of α-synuclein aggregation (Schmidt *et al.*, 2022). Among the best characterised PTMs there are phosphorylation, acetylation, O-GlcNAcylation, SUMOylation ubiquitination, and truncation (Fig.1.1; Tab 1.2). In addition to enzymatically regulated PTMs, α-synuclein can be modified by several oxidative reactions. These include oxidation and nitration of methionine residues, oxidative tyrosine dimerization, conjugation with oxidative dopamine adducts, and glycation, which promote aggregation by cross-linking and loss of electrostatic repulsion between α-synuclein monomers (Fig. 1.1, Tab 1.2; Yoo *et al.*, 2022). This section focuses on the most common α-synuclein PTMs, with a particular accent on the most relevant for the present work.

1.2.4.1 Phosphorylation

Phosphorylation is the most studied among α-synuclein PTMs and one of the first to be linked to PD pathology. α-synuclein contains two serine (S87 and S129) and 4 tyrosine residues (Y39, Y125, Y133, and Y136) which can undergo phosphorylation and modulate α-synuclein aggregation propensity and cytotoxicity (Fig. 1.1, Tab 1.2; Kawahata *et al.*, 2022). Above all, a consistent body of research aimed to disentangle the enigmatic function of S129 phosphorylation (pS129) in PD, which is still debated. While under physiological conditions only 4% of α-synuclein displays this PTM, more than 90% of α-synuclein in LBs and LNs is phosphorylated on S129, suggesting a role of pS129 in inclusion formation (Fujiwara *et al.*, 2002b; Anderson *et al.*, 2006). Notably, pS129 occurs early in PD progression compared to other PTMs (Sonustun *et al.*, 2022).

To date, the protein kinases reported to target this residue include casein kinase I and II (CKs; Okochi *et al.*, 2000), G protein-coupled receptor kinases 1, 2, 5 and 6 (GRKs; Pronin *et al.*, 2000), LRRK2 (Qing, Zhang, *et al.*, 2009a), polo-like kinase 2 (PLK2; Inglis *et al.*, 2009), protein kinase C-related kinase (PKR; Reimer *et al.*, 2018), and LK6/Mnk2a (Zhang *et al.*, 2015).

Early studies indicated that α-synuclein is hyperphosphorylated by CK2 following proteasome inhibition. This suggests that pS129 may direct α-synuclein to proteasomal degradation (Waxman and Giasson, 2008; Chau *et al.*, 2009). In agreement, the half-life of pS129-α-synuclein is lower than that of its non-phosphorylated isoform (Machiya *et al.*, 2010). Subsequently, a link between pS129 and α-synuclein clearance via the lysosomal pathway was also described (Oueslati *et al.*, 2013; Dahmene *et al.*, 2017). Along the same lines, a role of the lysosome in efficiently processing small phosphorylated aggregates but not large fibrils has been confirmed in other studies (Arawaka *et al.*, 2017; Peng *et al.*, 2018).

From a pathological perspective, pS129 has been associated with both cytotoxic and cytoprotective outcomes. A number of studies reported that α-synuclein hyperphosphorylation leads to more severe neurotoxicity (Zhang *et al.*, 2015; Karampetsou *et al.*, 2017; Reimer *et al.*, 2018). Increased aggregation propensity was described in SH-SY5Y cells (Smith *et al.*, 2005), leading to activation of the unfolded protein response and cell death (Sugeno *et al.*, 2008). Another pathological mechanism by which pS129 may induce cytotoxicity is the displacement of α-synuclein from intracellular membranes to mitochondria, causing oxidative stress (Arawaka *et al.*, 2006; Kuwahara *et al.*, 2012; Di Maio *et al.*, 2016). Moreover, pS129 increases α-synuclein affinity for membrane receptors such as LAG3 and APLP1. This enhances the internalisation rate and seeding capacity of α-synuclein oligomers and fibrils (S. Zhang *et al.*, 2021). Similar pro-aggregation and neurotoxic effects of pS129 have been confirmed *in vivo* (Karampetsou *et al.*, 2017).
In stark contrast, other studies in cellular and animal models found that pS129 is a neuroprotective PTM (Gorbatyuk *et al.*, 2008; Oueslati *et al.*, 2012; Tenreiro *et al.*, 2014; Ghanem *et al.*, 2022). Specifically, pS129 reduced seeded aggregation *in cellulo*, in hippocampal organoids and in mice and was observed to predominantly occur following α-synuclein aggregation (Sano *et al.*, 2021; Ghanem *et al.*, 2022).

1.2.4.2 Ubiquitination

Studies in post-mortem brains revealed that a consistent fraction of α-synuclein forming LBs is K63-linked polyubiquitinated (Tofaris *et al.*, 2003; Anderson *et al.*, 2006; Alexopoulou *et al.*, 2016). α-synuclein ubiquitination may act as a signal for both

proteasomal and lysosomal degradation, although a few ubiquitin-independent mechanisms also concur to α-synuclein clearance (Chapter 1.2.2).
NEDD4 has been identified as the main E3 ubiquitin ligase involved in α-synuclein ubiquitination (Tofaris *et al.*, 2011; Na *et al.*, 2012). By targeting K21 and K96, NEDD4 improves α-synuclein clearance and reduces α-synuclein-mediated toxicity in yeast, *Drosophila*, rats and patient-derived iNeurons (Chung *et al.*, 2013; Davies *et al.*, 2014). *De novo* α-synuclein ubiquitination on the lysine residues 45, 58, and 60 was recently linked to α-synuclein loading into endosomes and lysosome-dependent degradation (Zenko *et al.*, 2023).

By contrast, monoubiquitination of α-synuclein by the E3 ligases seven in absentia homolog (SIAH) 1 and 2 was shown to promote aggregation and toxicity (J. T. Lee *et al.*, 2008; Rott *et al.*, 2008).

1.2.4.3 SUMOylation

SUMOylation is the covalent conjugation of small ubiquitin-related modifier (SUMO) moieties to a target lysine residue (Mandel and Agarwal, 2022). This PTM increases in response to cell stressors and plays important roles in signalling pathways related to PD, such as regulation of DJ-1 activity, mitochondrial dynamics and expression of genes involved in mitochondrial and lysosomal maintenance (Harder *et al.*, 2004; Zhou *et al.*, 2004; Guerra De Souza *et al.*, 2016; Savyon *et al.*, 2020). Notably, SUMO is upregulated in PD models and in patient brains, and is consistently found within α-synuclein lesions (Weetman *et al.*, 2013; Rott *et al.*, 2017).
SUMOylation was reported to increase α-synuclein propensity to form aggregates (Krumova *et al.*, 2011; Abeywardana and Pratt, 2015). Although some studies proposed that SUMOylation targets α-synuclein to the proteasome (Kim *et al.*, 2011; Oh *et al.*, 2011), more recent evidence indicates that this PTM antagonises ubiquitination and redirects α-synuclein towards endosome-mediated degradation and secretory routes (Kunadt *et al.*, 2015; Rott *et al.*, 2017).

1.2.4.4 N-terminal acetylation

More than 80% of the human proteome is N-terminally acetylated either co-translationally or post-translationally by a class of enzymes named N-terminal acetyl transferases (NATs). This irreversible modification has important consequences on

protein function, folding, half-life, interactions, and localisation (Aksnes *et al.*, 2019; Deng *et al.*, 2021). Physiological α-synuclein N-terminal acetylation promotes α-helical secondary structures, which increase α-synuclein affinity to membranes, promote protein-protein interactions, and protect from aggregation (Anderson *et al.*, 2006; Öhrfelt *et al.*, 2011; Bartels *et al.*, 2014; Bell *et al.*, 2022). Based on the evidence available in literature, Iyer and colleagues proposed that N-terminal acetylation may prime α-synuclein for additional PTMs, although its role in PD is yet to be clarified (Iyer *et al.*, 2022).

1.2.4.5 O-GlcNAcylation

Conjugation of O-linked N-acetyl-glucosamine (O-GlcNAcylation) is a form of protein glycosylation involving the hydroxyl groups of threonine and serine residues. This PTM is regulated by the antagonistic action of O-GlcNAc transferase (OGT) and O-GlcNAcase (OGA) enzymes (Lee *et al.*, 2021).
O-GlcNAcylation predominately occurs in the NAC region of α-synuclein. This PTM reduces α-synuclein aggregation and prevents oligomer spreading without interfering with α-synuclein membrane binding properties (Marotta *et al.*, 2015; Lewis *et al.*, 2017). Additionally, α-synuclein O-GlcNAcylation counteracts calpain-mediated proteolytic cleavage, which produces highly amyloidogenic peptides (Levine *et al.*, 2017).

1.2.4.6 Nitration

Nitration is a non-enzymatic oxidative reaction resulting from the mismatch between production of free radicals as a side-product of mitochondrial respiration and their neutralisation by the cellular antioxidant systems (Tahavvori *et al.*, 2023). As previously mentioned, dopaminergic neurons are energetically demanding neuronal cell types which are intrinsically more susceptible to incur oxidative stress (Trist *et al.* , 2019). α-synuclein and oxidative stress display a reciprocal relationship. If on one side oxidative stressors can trigger α-synuclein aggregation (Paxinou *et al.*, 2001), accumulation of α-synuclein monomers and oligomers inhibit complex I and interfere with mitochondrial respiration (Junn *et al.*, 2002; Chinta *et al.*, 2010). Under oxidative stress and in presence of reactive nitrogen species (RNS) α-synuclein undergoes nitration on four tyrosine residues (Y39, Y125, Y133 and Y136). Nitration reduces α-

synuclein affinity for lipid bilayers and increases fibril formation (Hodara *et al.*, 2004). It has been shown that nitration leads to the formation of 3,3-dityrosine cross-links between α-synuclein monomers, which are converted into nucleation centres (Souza *et al.*, 2000; Takahashi *et al.*, 2002).
In PD, α-synuclein nitration occurs following S129 phosphorylation and has been proposed to contribute to the deposition of α-synuclein inclusions (Sonustun *et al.*, 2022).

1.2.4.7 Glycation

Glycation is a non-enzymatic reaction promoted by aging and hyperglycaemia. It occurs when a reducing sugar (such as glucose) reacts with an amino group (Maillard reaction) generating unstable carbonyl and dicarbon intermediates which, in turn, react with exposed lysine residues (Abdelkader *et al.*, 2022). This process leads to the formation of advanced glycation end-products (AGEs), which have been linked to PD and other age-related diseases (Abdelkader *et al.*, 2022). Being glycation a slow reaction, it primarily affects long-lived proteins, including α-synuclein (Konig *et al.*, 2018). α-synuclein glycation has been reported in LBs and has been shown to promote oligomerisation and α-synuclein-mediated toxicity (Vicente Miranda *et al.*, 2017). Interestingly, diabetes mellitus, a chronic disorder characterised by unbalanced glucose metabolism, is linked to increased production of AGEs and constitutes a significant risk factor for PD (Yang *et al.*, 2017; Khalid *et al.*, 2022).

Table 1.2 Most common α-synuclein post-translational modifications (PTMs) and their impact on α-synuclein aggregation propensity. (Adapted from Brembati *et al.*, 2023).

PTMs	Residue	Effect	References
Phosphorylation	S87	Limits aggregation	(Paleologou *et al.*, 2010)
	S129	Promotes aggregation	(Fujiwara *et al.*, 2002a; Smith *et al.*, 2005; Karampetsou *et al.*, 2017)
		Limits aggregation	(Gorbatyuk *et al.*, 2008; Oueslati *et al.*, 2012; Tenreiro *et al.*, 2014; Ghanem *et al.*, 2022)
	Y39	Promotes aggregation	(Mahul-Mellier *et al.*, 2014; Brahmachari *et al.*, 2016; Dikiy *et al.*, 2016)
	Y125	Limits aggregation	(Negro *et al.*, 2002; Chen *et al.*, 2009; Kosten *et al.*, 2014)
Ubiquitination	K (many identified)	Promotes degradation	(Tofaris *et al.*, 2011; Engelender *et al.*, 2022; Zenko *et al.*, 2023)
SUMOylation	K	Limits aggregation	(Krumova *et al.*, 2011)
	K	Protects from degradation	(Rott *et al.*, 2017; Rousseaux *et al.*, 2018)
N-terminal acetylation		Inhibits aggregation	(Bell *et al.*, 2023)
O-GlcNAcylation	T72	Inhibits aggregation	(Marotta *et al.*, 2015; Levine *et al.*, 2017, 2019)
	S87	Inhibits aggregation	(Lewis *et al.*, 2017)
Nitration	Y39	Promotes oligomerization	(Hodara *et al.*, 2004)
	Y125	Promotes dimerization	(Takahashi *et al.*, 2002; Hodara *et al.*, 2004)

	Y133	Promotes aggregation	(Hodara *et al.*, 2004)
	Y136	Promotes aggregation	(Hodara *et al.*, 2004)
Glycation	K	Promotes oligomerization	(Vicente Miranda *et al.*, 2017)

1.2.5 Spreading of α-synuclein pathological aggregates

A common feature to most prion-like neurogenerative pathologies is the template conversion of proteins of the same type into a pathological form that can propagate to other cells (Prusiner, 2001; Carlson *et al.*, 2021). In PD, α-synuclein acts as an infectious agent which replicates itself and spreads from diseased to healthy cells across the brain. α-synuclein pathology propagates following a stereotypical pattern first described by Braak and co-workers (Braak *et al.*, 2003a; Braak *et al.*, 2003b). According to the Braak hypothesis, α-synuclein pathology may be triggered by environmental factors such as infectious agents or toxins interacting with the enteric nervous system and the olfactory bulb. From the peripheral nervous system α-synuclein aggregation would reach the basal structures of the brain "climbing" through the vagal nerve. By comparing disease progression to the histological features of post-mortem PD brains, Braak and co-workers found that lesions initially affect the dorsal motor nucleus of the glossopharyngeal and vagal nerves and the anterior olfactory nucleus. From the brain stem, the disease ascends towards anatomically interconnected brain areas, gradually involving the anteromedial and temporal mesocortex. The staging of inclusions spreading partially correlates with autonomic, motor, and cognitive deterioration (Braak *et al.*, 2003a; Braak *et al.*, 2003b).

Several canonical and non-canonical mechanisms have been implicated in the secretion of α-synuclein, some of which are based on passive diffusion or release, while others rely on finely regulated processes. Monomeric but not aggregated α-synuclein can passively translocate across the cell membrane (Ahn *et al.*, 2006) with a modality that may depend on existing membrane pores rather than direct diffusion across the lipid bilayer (Lee *et al.*, 2005b; H. J. Lee *et al.*, 2008). Another passive form of communication between cells is represented by tunnelling nanotubes (TNTs), intercellular membranous bridges with a diameter ranging between 50 and 200 nm. TNTs contribute to spreading of α-synuclein aggregates *in vitro*, but their role *in vivo* has not been demonstrated (Abounit *et al.*, 2016; Rostami *et al.*, 2017).
Many regulated mechanisms also influence α-synuclein secretion. One of the best characterised is exosomes release, which occurs when a multivesicular body fuses with the cell membrane. Exosomes are small extracellular vesicles (100 nm in diameter) involved in long-distance paracrine signalling and inter-cell exchange

(Kalluri *et al.*, 2020). Release of α-synuclein via the exosomal pathway is calcium dependent (Emmanouilidou *et al.*, 2010) and is exacerbated by autophagy impairment, lysosomal dysfunction and oxidative stress (Alvarez-Erviti *et al.*, 2011; Fussi *et al.*, 2018; Zhang *et al.*, 2018). This secretion route might have a considerable impact on α-synuclein-related toxicity. Exosome-bound α-synuclein is more transmissible and has higher seeding propensity compered to freely diffusible oligomers (Stuendl *et al.*, 2016)

Unconventional ER/ Golgi-dependent exocytosis has also been proposed as a possible spreading mechanism, which is upregulated by proteasomal inhibition and mitochondrial damage (Lee *et al.*, 2005b). This secretion route depends on a stress-induced clearance pathway named misfolding-associated protein secretion (MAPS). When the canonical protein degradation routes are overwhelmed, the ER-associated deubiquitylase USP1, the molecular chaperone HSC70 and the co-chaperone DNAJC5 recruit misfolded cytosolic proteins onto the surface of the ER for deubiquitylation. These substrates are subsequently loaded into ER-associated late endosomes for secretion (Lee *et al.*, 2016; Xu *et al.*, 2018).

Finally, release of α-synuclein has been linked to 14-3-3 proteins. These are molecular chaperones highly expressed in the brain where they are involved in trafficking of cellular components (Giusto *et al.*, 2021). Wang and colleagues found that 14-3-3 proteins facilitate aggregates secretion from the neurons but their binding with secreted oligomers also limits their uptake, seeding properties, spreading and toxicity (Wang *et al.*, 2018).

Once dispersed in the extracellular milieu, α-synuclein can be actively internalised by other neuronal and glial cells. A few receptors have been so far identified which can accelerate this process. The gap junction protein connexin-32 (Cx32) was shown to mediate the uptake of α-synuclein oligomers by neurons and oligodendrocytes (Reyes *et al.*, 2019).α-synuclein pathogenic oligomers can also bind with high affinity to lymphocyte activation gene 3 (LAG3) expressed on immune cells and amyloid precursor-like protein 1 (APLP1) expressed in the brain (S. Zhang *et al.*, 2021).

Additionally, heparan sulphate proteoglycans (HSPGs), a family glycoproteins expressed on the cell surface, contribute to endocytosis of α-synuclein aggregates (Holmes *et al.*, 2013).

A recent study described a role for innate immunity in α-synuclein spreading. Membranes receptors such as Toll-like receptor 2 (TLR2) sense the presence of potentially cytotoxic stimuli and activate the inflammatory response. α-synuclein aggregates bind to TLR2 expressed by neurons leading to a higher internalisation rate. At the same time, astrocytes and microglia exploit TLR2-dependent endocytosis to attenuate the extracellular α-synuclein burden (Kim *et al.*, 2021). Neurons may rely on the higher clearance capacity of these support cells in early stages on the disease (Loria *et al.*, 2017). Astrocytes in particular have been observed to form a network connected via TNTs which allows them to redistribute α-synuclein burden and ease mitochondrial and ER stress (Rostami *et al.*, 2017).

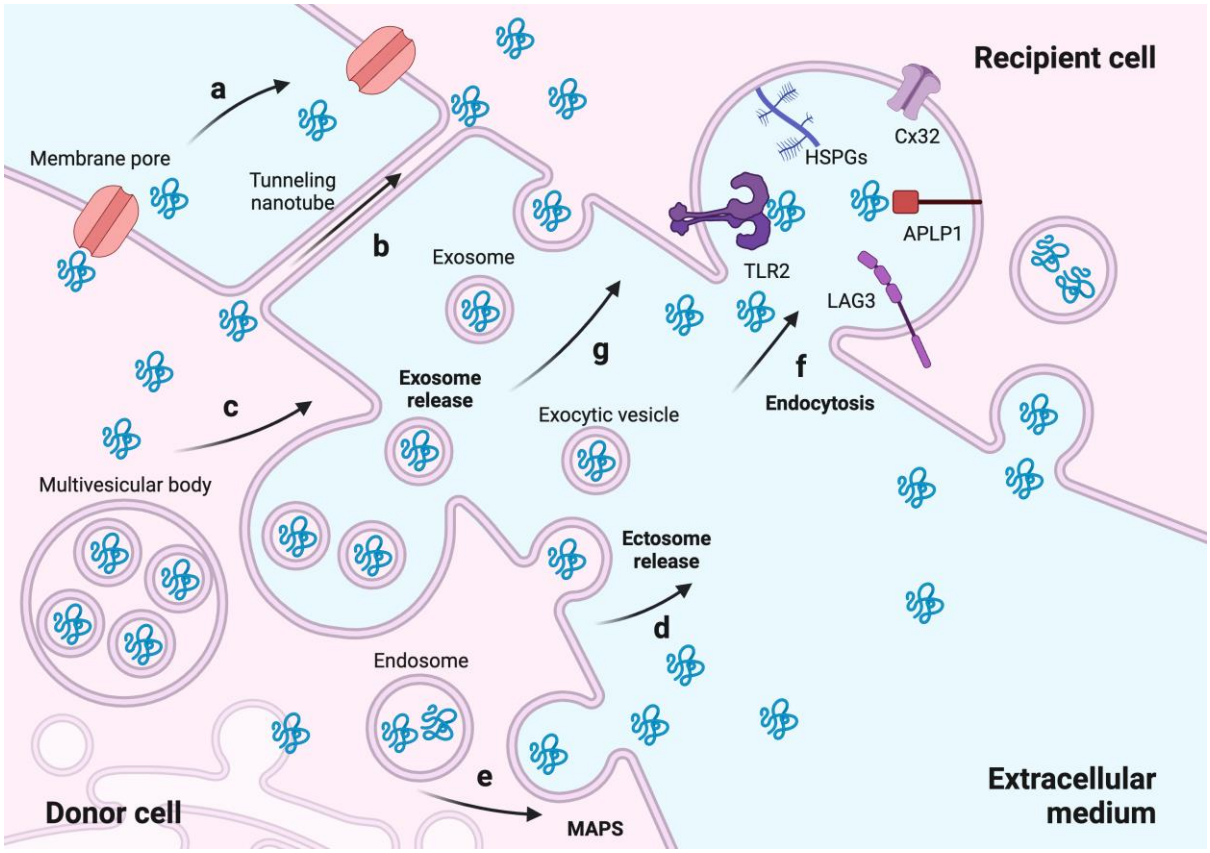

Figure 1.4 Mechanisms of propagation of a-synuclein pathology. α-synuclein can passively diffuse to the extracellular milieu and to other cells through membrane pores **a)** or via tunnelling nanotubes **b)**. It can also be actively secreted via the release of exosomes **c)**, exocytic vesicles **d)** or via a non-canonical secretory pathway named misfolding-associated protein secretion (MAPS) **e)**. Membrane-bound α-synuclein can undergo internalization through vesicular fusion with the recipient membrane **g)**. Freely diffusible α-synuclein can be internalised via endocytosis. α-synuclein uptake can be promoted by binding to cell type-specific membrane receptors such as lymphocyte activation gene 3 (LAG3), amyloid precursor-like protein 1 (APLP1), Connexin 32 (Cx32), heparan sulphate proteoglycans (HSPGs), and Toll-like receptor 2 (TLR2) **f)**. Created with BioRender.com.

1.2.6 Impact of α-synuclein pathology

Accumulation of α-synuclein soluble oligomers and proto-fibrils impinges on the delicate neuronal homeostasis provoking the impairment of several cell functions. α-synuclein mutations, overexpression and aggregation have been linked to loss of membrane integrity (Danzer *et al.*, 2007), mitochondrial dysfunction and oxidative stress (Hsu *et al.*, 2000), inhibition of the ubiquitin-proteasome system (Snyder *et al.*, 2003), synaptic dysfunction (Scott *et al.*, 2010), microtubule (MT) destabilisation (Alim *et al.*, 2004), cellular trafficking impairment, inflammation, and epigenetic changes (Bernal-Conde *et al.*, 2020; He *et al.*, 2020). Similar cytotoxic effects have been described in supporting cell types (Reyes *et al.*, 2014; Lindström *et al.*, 2017; Díaz *et al.*, 2019). Nonetheless, our understanding of the mechanisms that relate the many species of α-synuclein to neurodegeneration in PD is still fragmentary.

One of the major mechanisms through which α-synuclein aggregates induce cell toxicity is their ability to disrupt membrane integrity. α-synuclein aggregates have been observed extracting lipids from amphipathic bilayers and sequestering them into newly formed fibrils (Zhu, Li and Fink, 2003; Reynolds *et al.*, 2011). Fusco and colleagues described the presence of a highly lipophilic element and a structured region into α-synuclein oligomers which are incorporated into lipid bilayers and disrupt their integrity (Fusco *et al.*, 2017). Loss of subcellular compartmentalisation can result in the dispersion of cytotoxic metabolites or proteolytic enzymes, akin to what occurs with lysosomes. α-synuclein aggregates damage the lysosomal membrane causing the release of their contents, which elicits mitochondrial dysfunction, production of ROS and inflammation (Freeman *et al.*, 2013). Permeabilization of the plasma membrane causes the uncontrolled influx of Ca^{2+} ions. Dysregulation of Ca^{2+} signalling leads to neuronal death by free-radical stress (Angelova *et al.*, 2016; Deas *et al.*, 2016). α-synuclein can also interfere with Ca^{2+} homeostasis at the level of the ER, the main storage site of Ca^{2+} within the cell. α-synuclein aggregates bind to and upregulate the Sarcoendoplasmic Reticulum Calcium ATPase (SERCA) causing an increase in cytosolic Ca^{2+} (Betzer *et al.*, 2018).

We previously mentioned the elusive physiological interaction between α-synuclein and mitochondria (Li *et al.*, 2007; Nakamura *et al.*, 2008). Dysregulation of this partnerships has been linked to mitochondrial dysfunction, which in turn causes α-

synuclein oxidation and further aggregation. α-synuclein overexpression has been linked to mitochondria fragmentation which precedes organelle dysfunction (Kamp *et al.*, 2010; Plotegher *et al.,* 2014; Ordonez *et al.*, 2018). These changes are independent from any canonical mitochondrial fission mechanisms and seem to be related to α-synuclein's membrane-bending properties (Varkey *et al.*, 2010; Nakamura *et al.*, 2011). α-synuclein soluble oligomers, rather than larger fibrils cause influx of Ca^{2+} which results in mitochondrial swelling, depolarisation and release of cytochrome C (Luth *et al.*, 2014). These toxic species may induce mitochondrial damage by interfering with some key transmembrane channels and complexes. Pathogenic PTMs such as pS129 impair the trafficking of mitochondrial proteins by inhibiting the mitochondrial import machinery. Phosphorylated α-synuclein binds to translocase of the outer membrane 20 (TOM20) and disrupts the interaction with the co-receptor TOM22 causing loss of membrane potential and ROS production (Di Maio *et al.*, 2016). An interaction between α-synuclein and voltage-dependent anion channel 1 (VDAC1) has also been studied (Lu *et al.*, 2013). This protein is expressed on the outer mitochondrial membrane and is part of mitochondrial permeability transition pore which regulates the exchange of ions and metabolites in the mitochondria and can induce uncoupling and mitochondria-mediated apoptosis. Soluble, prefibrillar α-synuclein reversibly interacts with and inhibits VDAC1 blocking the exchange of proteins and substrates. It can also translocate through the channel in a voltage-dependent manner and reach in IMM. Here it inhibits the respiratory complexes causing the blockage of the respiratory chain an oxidative stress (Rostovtseva *et al.*, 2015).

Protein dyshomeostasis is another pathological feature that is both cause and consequence of synucleinopathy and is further exacerbated by α-synuclein misfolding. Oxidised, phosphorylated and aggregated α-synuclein escapes CMA degradation and disrupts this clearance route by binding to LAMP2A and interfering with the lysosomal membrane translocation mechanism (Martinez-Vicente *et al.*, 2008b). In addition to the lysosomal pathway, the proteasome is a parallel degradation route for α-synuclein significantly affected by α-synuclein mutants and oligomers (Emmanouilidou *et al.*, 2010a; Lindersson *et al.*, 2004). In line with this, pharmacological stimulation of the proteasome has shown a positive impact on PD models (Zhou *et al.*, 2019).

Neurodegeneration in PD is often preceded by changes in neurotransmission. It has been shown that α-synuclein pathology interferes with synaptic function and impinges on neuronal activity. α-synuclein pathology causes age-dependent redistribution of SNARE complex components and interferes with dopamine release (Garcia-Reitböck *et al.*, 2010). Large α-synuclein aggregates and oligomers bind synaptoberin-2 and hamper the interaction between vSNARE and tSNARE components (Choi *et al.*, 2013; Hawk *et al.*, 2019). α-synuclein has also been observed to disrupt dopamine reuptake by inhibiting dopamine active transporter (DAT, Lundblad *et al.*, 2012). These pathological changes lead to a reduction in nigro-striatal dopamine levels which translates into a reduction of voluntary movements in rats (Tofaris *et al.*, 2006).

α-synuclein is physiologically present in traces in the nucleus where it interacts with histones. A role in stress induced transcription regulation has been reported by Siddiqui and colleagues in neurotoxin-induced models and in PD patients (Siddiqui *et al.*, 2012). Oxidative stress enhances nuclear α-synuclein translocation which causes an architectural chromatin rearrangement and induces aberrant neurotoxic transcription of cell cycle-related genes (Ma *et al.*, 2014; Pinho *et al.*, 2019).

Finally, dispersion of amyloid aggregates can trigger non-cell autonomous pathogenic mechanisms mediated by microglia and astrocytes. Microglia can be activated by the neuronal release of α-synuclein oligomers. These particles are internalised by binding to TLR2 and are processed as an antigen triggering an adaptive autoimmune response (Kim *et al.*, 2013). Activated microglia secrete inflammatory cytokines which allow infiltration and differentiation of a cluster of CD4+ cells into pro inflammatory T helper lymphocytes (Su and Zhou, 2021). Astrocytes contribute to neuroinflammation by acting as antigen presenting cells, a role that has been confirmed in PD patients (Rostami *et al.*, 2020).

1.3 LRRK2 in physiology and pathology

Mutations in the *LRRK2* gene (originally identified as *PARK8*, mapped on chromosome 12p11.2-q13.1) are the most common cause of genetic PD (Funayama *et al.*, 2002; Paisán-Ruíz *et al.*, 2004; Zimprich *et al.*, 2004). LRRK2-linked PD (LRRK2-PD) is characterised by a dominant inheritance pattern and incomplete penetrance estimated between 24% and 100%, depending on the mutation (Paisán-Ruíz *et al.*, 2004; Zimprich *et al.*, 2004; Healy *et al.*, 2008; Marder *et al.*, 2015). In addition to missense mutations affecting the protein sequence, several polymorphisms of the *LRRK2* locus are known to modify the risk of developing PD over the lifetime (Nalls *et al.*, 2019).

As opposed to other monogenic risk factors, LRRK2-PD is usually characterised by a more benign clinical picture compared to idiopathic PD, with less severe autonomic symptoms, slower progression and milder cognitive impairment (Sosero and Gan-Or, 2023; Vollstedt *et al.*, 2023). Additionally, LRRK2 is consistently upregulated in sporadic PD (Di Maio *et al.*, 2018). These characteristics make the study of LRRK2 functions and dysregulation particularly attractive to extrapolate pathogenic mechanisms valid across multiple PD backgrounds (Saunders-Pullman *et al.*, 2019).

1.3.1 LRRK2 molecular structure

LRRK2 is a 286 kDa multi-functional protein containing a GTPase and a serine-threonine kinase domain (Berwick *et al.*, 2019; Marchand *et al.*, 2020). The presence of a tandem Ras of complex proteins (Roc)- C-terminal of Roc (COR) domain collocates LRRK2 within the ROCO protein superfamily (Marín, 2008). The N-terminus of the protein contains armadillo, ankyrin, and leucine-rich repeat (LRR) domains. A WD40 domain occupies LRRK2's C-terminus. The non-catalytic domains provide a scaffold for the catalytic core and mediate dimerization and protein-protein interactions (Fig. 1.5; Guaitoli *et al.*, 2016).

LRRK2 is ubiquitously expressed throughout the body (Biskup *et al.*, 2007). The highest expression levels are recorded in kidneys, lungs and immune cells, where the major abnormalities are observed in LRRK2 KO models (Tong *et al.*, 2010; Herzig *et al.*, 2011; Fuji *et al.*, 2015). In the brain, LRRK2 is mainly found in areas receiving dopaminergic connections, rather than dopaminergic nuclei themselves (Gaiter *et al.*,

2006; Giesert *et al.*, 2013). Within the cell, the protein is mostly cytoplasmatic but it is cyclically recruited to the surface of intracellular membranes. Here LRRK2 exerts an important part of its biochemical roles (Berger *et al.*, 2010).

LRRK2 underpins a range of key signalling pathways and organelle functions, including autophagy, cellular trafficking, endocytosis, synaptic maturation, calcium signalling, and translational control (Berwick *et al.*, 2019). Above all, LRRK2 is a multilevel regulator of the autophagolysosomal pathway which coordinates endocytic vesicles sorting and phagosome-lysosome fusion (Gómez-Suaga *et al.*, 2012; Hockey *et al.*, 2015; Eguchi *et al.*, 2018). LRRK2 also plays important roles in innate immunity- and inflammation, as attested by the link between LRRK2 genetic variants and infectious or autoimmune diseases such as leprosy, tuberculosis Crohn's disease (Härtlova *et al.*, 2018; Hui *et al.*, 2018; Fava *et al.*, 2019; Kim, Suh and Joe, 2022; Yan *et al.*, 2022; Oun *et al.*, 2023). Finally, LRRK2 is involved in ciliogenesis and centrosomal cohesion. Dysregulation of these biological functions have important implications for cell polarity and neurodevelopment (Shakya *et al.*, 2021; Usmani *et al.*,2021).

The following sections provide an overview of LRRK2 regulation and summarise some of the key pathogenic mechanisms which link LRRK2 to PD.

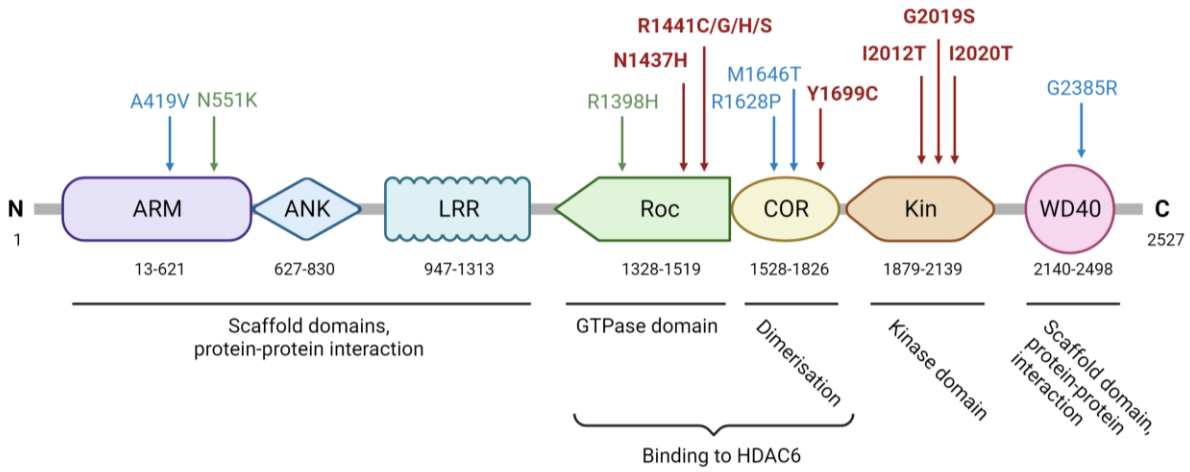

Figure 1.5 LRRK2 protein structure and PD-linked mutations. From the N-terminus to the C-terminus, LRRK2's domains are: armadillo (ARM), ankyrin (ANK), leucine-rich repeat (LRR), Ras of complex (Roc), C-terminal of Roc (COR), kinase (Kin), and WD40. LRRK2's catalytic core encompasses the Roc-COR and the kinase domain. All other domains play scaffolding roles and are involved in the binding to LRRK2's interactome. The confirmed pathogenic LRRK2 mutations linked to familial PD (in red) cluster within LRRK2's catalytic domains and impinge on its enzymatic activity. The risk variants are reported in blue and the protective variants are indicated in green. Created with BioRender.com.

1.3.2 LRRK2 enzymatic activity

1.3.2.1 LRRK2 structure-based activation mechanism

Over the last decade, the intricate network of signalling pathways in which LRRK2 is involved has been progressively uncovered, yet the mechanisms governing its regulation remain a focal point in PD studies. An essential part of LRRK2 activity depends on the binding to GTP and GDP, which occurs within the micromolar range (dissociation constants [K_d] are 4.1 ± 0.3 μM for GTP and 1.2 ± 0.1 μM for GDP) (Wu *et al.*, 2019). Mutations blocking LRRK2 interaction with GTP, such as T1348N, cause loss of kinase activity (Ito *et al.*, 2007; West *et al.*, 2007; Wu *et al.*, 2019). LRRK2 GTPase and kinase domains are involved in a structural and functional crosstalk that modulates LRRK2 activity. Several studies confirmed that LRRK2 can homodimerize in physiological solutions thanks to head-to-head or tail-to-tail interactions between WD40 or COR domains (Deng *et al.*, 2008; Gotthardt *et al.*, 2008; Daniëls *et al.*, 2011; Deniston *et al.*, 2020). The highly dynamic equilibrium between monomeric and dimeric status is regulated by GTP turnover and determines the association of LRRK2 with intracellular membranes. GDP-bound LRRK2 is recruited onto organelle surfaces and forms dimers, which represent a kinase-active molecular status (Greggio *et al.*, 2008; Berger, Smith and Lavoie, 2010; Civiero *et al.*, 2012; Deyaert *et al.*, 2017). Exchange of GDP with GTP induces dimer dissociation and return to a freely diffusible form (Deyaert *et al.*, 2017). Membrane recruitment dimerization and activation has been reported in macrophages and microglia in response to TLR4 stimulation, mTOR inhibition and lysosomal stress (Berger *et al.*, 2010; Schapansky *et al.*, 2014; Herbst *et al.*, 2020).

1.3.2.2 LRRK2 regulation

The finding that Rab29 mutations cause a PD phenotype superimposable with LRRK2 hyperactivity helped collocate these two proteins in the same pathway (MacLeod *et al.*, 2013). This small GTPase (also known as Rab7L1, located in the PARK16 locus) seems to play a structural role in LRRK2 kinase activity activation, at least in overexpression models. Rab29 facilitates the recruitment of LRRK2 to the *trans*-Golgi network, which enhances the molecular proximity between LRRK2 and its membrane-bound Rab GTPase substrates resulting in Rab hyperphosphorylation (Purlyte *et al.*,

2018; Gomez *et al.*, 2019; Kuwahara *et al.*, 2020). Notably, the hyperphosphorylation of Rab proteins recorded in LRRK2 pathogenic backgrounds seems not to uniquely depend on direct LRRK2 kinase upregulation. Mutations that interfere with LRRK2 GTPase activity yield even higher Rab protein phosphorylation compared to kinase mutants due to increased LRRK2 recruitment to endosomal membranes (Rinaldi *et al.*, 2023).

According to the latest model, LRRK2 binds to non-phosphorylated, membrane-anchored Rab29 through a binding site located in the armadillo domain (Nagai-Ito *et al.*, 2022; Vides *et al.*, 2022). This site also shows affinity for other Rab substrates, including Rab8A, Rab10, Rab32 and Rab38. The formation of LRRK2-enriched membrane microdomains facilitates phosphorylation of Rab29, which shifts to a higher affinity binding site in the LRRK2 N-terminal. This initiates a feed-forward activation loop which allows the recruitment of more LRRK2 molecules and the phosphorylation of other Rabs (Vides *et al.*, 2022).

Conflicting results published by the same research team, seem to challenge Rab29 importance as a LRRK2 regulator. Rab29 KO or overexpression in mice does not influence the phosphorylation of LRRK2 substrates. Additionally, no changes in Rab phosphorylation were recorded upon LRRK2 stimulation or mutant LRRK2 expression in a Rab29 KO background (Kalogeropulou *et al.*, 2020). This might indicate that Rab29 recruits LRRK2 to intracellular membranes only in specific cellular and molecular contexts or that another not yet identified activator may influence LRRK2 activity.

The interplay between LRRK2 and Rab29 may be downstream to VPS35, another protein related to genetic PD. VPS35 is a positive regulator of LRRK2 kinase activity, while the D620N mutation causes a toxic gain of function, resulting in the hyperphosphorylation of LRRK2's targets (Mir *et al.*, 2018). Additionally, expression of wild-type but not of the PD-causing mutant VPS35-D620N rescues the organelle sorting defect caused by LRRK2 dysregulation in KO mice and drosophila (MacLeod *et al.*, 2013).

In addition to Rab29, cAMP-dependent protein kinase (PKA) has also been proposed as a putative LRRK2 regulator. PKA phosphorylates several LRRK2 residues, some of which are mutated in PD (Muda *et al.*, 2014).

1.3.2.3 Impact of Parkinson's disease-linked mutations on LRRK2 activity

Several LRRK2 amino acid substitutions have been identified as pathogenic (N1437H, R1441C/G/H/S, Y1699C, I2012T, G2019S, I2020T) or as risk variants for PD (A419V, R1628P, M1646T, and G2385R) (Funayama *et al.*, 2005; Tomiyama *et al.*, 2006; Healy *et al.*, 2008; Aasly *et al.*, 2010; Ross *et al.*, 2011; Gopalai *et al.*, 2014; Li *et al.*, 2015; Fan *et al.*, 2016; Mata *et al.*, 2016). On the other hand, at least two variants exert a protective effect (N551K and R1398H; Fig. 1.5) (Hui *et al.*, 2018). Among the pathogenic mutations, the G2019S is by far the most common, particularly among Berber and Ashkenazi Jewish communities and in patients with European heritage (Tan *et al.*, 2005; Shu *et al.*, 2019). PD-associated mutations impact the crosstalk between Roc-COR and Kinase domain and their individual activities in different ways, although the overall effect is a pathogenic kinase upregulation. This is reflected in the consistent increase in phosphorylation levels of a subset of LRRK2 substrates and of the autophosphorylation site S1292 (Sheng *et al.*, 2012; Steger *et al.*, 2016, 2017).
The three mutations affecting the kinase activation loop, I2012T, G2019S and I2020T, directly boost LRRK2 kinase activity (Sheng *et al.*, 2012). The other pathogenic mutations affect the Roc GTPase (R1441C/G/H and N1437H) and COR domain (Y1699C). R1441C/G/H and Y1699C increase LRRK2 affinity for GTP and suppress hydrolysis to GDP. This extends the residence time of the nucleotide within the GTP binding pocket and increases LRRK2's active state lifetime (Daniëls *et al.*, 2011; Liao *et al.*, 2014). The N1437H mutation locks LRRK2 into a dimer with low binding affinity to GTP and diminished GTPase activity. This impairs LRRK2 dimerization cycle by decreasing the nucleotide exchange rate (Huang *et al.*, 2019).

1.3.2.4 LRRK2 inhibitors

As previously mentioned, LRRK2 hyperactivation is not only found in carriers of LRRK2 mutations but is also a common feature among sporadic PD cases (Di Maio *et al.*, 2018). This motivated the race towards the development of selective, brain-penetrant LRRK2 kinase inhibitors as a possible strategy to treat LRRK2-PD first, and-hopefully- other non-related PD cases in the future. Progress has been slowed down by concerns about possible side-effects following downregulation of such a ubiquitously expressed protein.

The most potent and selective LRRK2 kinase inhibitors available so far are classed as type I and lock the Asp-Phe-Gly (DFG) regulatory motif of the kinase domain into a closed conformation ("DFG-in", Gilsbach *et al.*, 2015; J. D. Scott *et al.*, 2017). Acute *in vivo* studies involving type I inhibitors evidenced similar phenotypes to LRRK2 KO models, including lysosomal abnormalities in kidney proximal tubule cells and formation of lamellar bodies in lung type II cells (Herzig *et al.*, 2011). Studies conducted on non-human primates confirmed the emergence of lung alterations following subacute administration of type I LRRK2 inhibitors. These encompass hypertrophy and hyperplasia of type 2 pneumocytes and intra-alveolar infiltration of macrophages and neutrophils (Baptista *et al.*, 2020; Miller *et al.*, 2023). These changes are mainly detected at a histological level and do not seem to compromise organ function (Fuji *et al.*, 2015; Baptista *et al.*, 2020). A major confounding effect in the assessment of type I inhibitor efficacy and safety is the interference with LRRK2 expression levels by increasing ubiquitination and proteasomal degradation (Zhao *et al.*, 2015). As a consequence, distinguishing side-effects arising solely from LRRK2 inhibition from those due to decreased protein expression presents a significant challenge.

Conversely, type II inhibitors lock the kinase domain in a "DFG-out" conformation. This type of inhibitors is less studied and has lower target specificity compared to type I. Nonetheless, by observing the opposing effects that type I and type II kinase inhibitors exert on the interaction between LRRK2 and MTs, some authors suggested that type II inhibitors might have reduced side-effects (see below, Deniston *et al.*, 2020).

1.3.3 Cellular roles of LRRK2

1.3.3.1 Subcellular trafficking

One of the best characterised LRRK2 cellular functions is the orchestration of subcellular dynamics. A phosphoproteomic screening conducted in mouse embryonic fibroblasts expressing LRRK2 gain-of-function mutants led to the identification of a subgroup of small Rab GTPases (Rab3a/b/c/d, Rab8a/b, Rab10, Rab12, Rab29, Rab35 and Rab43) as putative LRRK2 substrates (Steger *et al.*, 2016). These proteins act as molecular hubs to regulate every aspect of membrane dynamics, from biogenesis to transport, tethering, and fusion. Rab proteins can switch from a GDP-

bound inactive status to a GTP-bound, membrane-associated active status. This transition is regulated by guanine nucleotide exchange factors (GEFs), GTPase-activating proteins (GAPs) and GDP-dissociation inhibitors (GDIs) and determines the recruitment of effectors that mediate membrane cycles (Homma *et al.*,2021). Pathological phosphorylation of Rab proteins prevents the binding to GDIs and causes aberrant accumulation at the target membrane. This impacts on their ability to translocate to the compartments where their activity is required (Steger *et al.*, 2016).

Another way LRRK2 may regulate subcellular trafficking is by interacting with the MT cytoskeleton. LRRK2 directly binds to three of the eight human β-tubulin isoforms (TUBB, TUBB4, and TUBB6) and is enriched in areas of intense MT remodelling, such as the growth cone. LRRK2 may stabilise MTs, support axonal trafficking and growth cone expansion by regulating α-tubulin acetylation. In fact, LRRK2 expression is inversely correlated to this PTM (Law *et al.*, 2014).

A pathological LRRK2 gain-of-function was hypothesised based on the observation that, in overexpression models, most PD-linked mutants (N1437H, R1441C/G, Y1699C, I2020T) lead to the formation of LRRK2 filaments surrounding MTs. Interestingly, wild type, G2019S and I2012T LRRK2 can be induced to display the same phenotype under administration of type I LRRK2 kinase inhibitors (Kett *et al.*, 2012; Ramírez *et al.*, 2017; Schmidt *et al.*, 2019). LRRK2 filaments have a right-handed double helix structure with the GTPase domain facing the MT surface and the kinase domain protruding from it (Deniston *et al.*, 2020; Watanabe *et al.*, 2020). The interface between LRRK2 and MTs and the residues involved in this interaction have been recently characterised (Snead *et al.*, 2022). Aberrant LRRK2 polymerisation primarily occurs along stretches of deacetylated MTs (Godena *et al.*, 2014), is promoted by GTP binding (Ramírez *et al.*, 2017) and strictly depends on conformational changes of the kinase domain (Deniston *et al.*, 2020). A closed conformation, promoted by binding to type I kinase inhibitors, allows fibril formation. Conversely, an open kinase domain conformation, stabilised by type II inhibitors, prevents LRRK2 oligomerisation at the MT interface (Deniston *et al.*, 2020; Weng *et al.*, 2023). Strikingly, pharmacological or genetic upregulation of MT acetylation abolishes LRRK2 polymerisation (Godena *et al.*, 2014). Since deposition of LRRK2 filaments obstructs MT-based trafficking, some authors proposed that these might act

as a roadblock for the bidirectional motion of molecular motors and their associated cargoes (Godena *et al.*, 2014; Deniston *et al.*, 2020).

Although LRRK2 polymerisation might represent an overexpression artefact, impaired vesicle endocytosis and cellular trafficking are common features of LRRK2-PD also reported in more physiological models (Cho *et al.*, 2014; Pfeffer, 2018). Endogenous expression of LRRK2-G2019S or R1441H in iPSC-derived knock-in human neurons disrupts autophagosome dynamics. Mechanistically, hyperactive LRRK2 recruits the motor adaptor JNK-interacting protein 4 (JIP4) to the surface of autophagic vesicles in a kinase-dependent manner. The affected autophagosomes engage aberrant contacts with kinesin. This results in a tug-of-war between kinesin and cytoplasmic dynein forcing vesicles to stall (Boecker *et al.*, 2021; Dou *et al.*, 2023). Interestingly, Dou and colleagues did not observe defects in mitochondria and lysosomal trafficking upon LRRK2 hyperactivity, which suggests the impairment of an autophagosome-specific transport mechanism (Dou *et al.*, 2023).

1.3.3.2 Autophagolysosomal pathway

Several studies described the implications of LRRK2 dysregulation for autophagy and mitophagy, which place LRRK2 at the core of lysosomal pathway regulation. As previously mentioned, it is widely accepted that LRRK2 is selectively recruited to intracellular membranes. Here, the phosphorylation of a subgroup of Rab GTPases would sustain essential homeostatic mechanisms. Yet, most of the current knowledge in the field has been extrapolated from stress models, leaving important gaps in our understanding of the physiological role of LRRK2 in autophagy.

The first indication of a link between LRRK2 and protein turnover came from the evidence that LRRK2-KO mice display marked lysosomal dysfunction in the kidney (Tong *et al.*, 2010). Later work on immune cells revealed a deficit in autophagy initiation and accumulation of autophagic substrates in LRRK2 knockdown models (Schapansky *et al.*, 2014). Experiments performed under lysosomal stress conditions in immortalised cell lines revealed that LRRK2-dependent phosphorylation of Rab8a and Rab10 at the surface of endolysosomal membranes prevents lysosomal enlargement and promotes lysosomal secretion (Eguchi *et al.*, 2018). LRRK2 translocates to damaged endolysosomes and facilitates the recruitment of molecular

machineries which promote lysosomal repair and prevent lysophagy. These include endosomal sorting complex required for transport III (ESCRTIII) and the Rab effectors EH-domain-binding protein 1 (EHBP1) and EHBP1L1 (Eguchi *et al.*, 2018; Herbst *et al.*, 2020). In primary astrocytes, LRRK2-mediated phosphorylation of Rab10 and Rab35 recruits the motor adapter JIP4 which supports the formation of LAMP1-negative membranous tubules releasing cargoes from damaged lysosomes. This process named LYsosomal Tubulation/sorting driven by LRRK2 (LYTL) by Bonet-Ponce and colleagues, has been proposed as a non-canonical membrane sorting response to lysosomal stress (Bonet-Ponce *et al.*, 2020).
Independently form Rab signalling, LRRK2 regulates macroautophagy by phosphorylating Beclin-1 and the mammalian target of rapamycin (mTor) regulator Leucyl-tRNA synthetase (LRS, Manzoni *et al.*, 2016; Ho *et al.*, 2018).

Considering the protective LRRK2 function described in physiological contexts, it may seem counterintuitive that, in PD, LRRK2 hyperactivity leads to accumulation of early autophagosomes and partially digested autophagy substrates (Rocha *et al.*, 2020). LRRK2 inhibition showed protective effects in a rotenone based model reproducing the aberrant autophagosomes phenotype observed in PD-patients (Rocha *et al.*, 2020). Moreover, LRRK2 inhibitors have proved effective to ameliorate the lysosomal abnormalities in mouse astrocytes carrying PD-causative GBA1 mutations (Sanyal *et al.*, 2020). Similar improvements were observed in DA neurons reprogrammed from PD patients carrying either LRRK2 or GBA1 mutations. Inhibition of LRRK2 kinase activity increases GCase activity in a pathological cellular context with a mechanism mediated by Rab10 (Ysselstein *et al.*, 2019). These studies indicate that LRRK2 hyperactivity may lead to a pathogenic gain-of-function, which may override the cytoprotective LRRK2 roles. One of these pathogenic mechanisms has been characterized in the context of CMA, where LRRK2 mutants impede substrate import into the lysosome by binding to LAMP-2A (Orenstein *et al.*, 2013).

A role of LRRK2 on α-synuclein turnover and spreading has been proposed, although the mechanisms linking LRRK2 mutations to α-synuclein pathology remain elusive.
A study from Volpicelli-Daley's group reports that LRRK2 overexpression promotes α-synuclein clearance and prevents aggregation upon exposure to α-synuclein preformed fibrils (PFFs) in primary neurons and in rat brains. In contrast, the kinase hyperactive LRRK2 mutant G2019S significantly increases α-synuclein pathology.

Administration of LRRK2 inhibitors ameliorates the pathological phenotype, supporting pharmacological manipulation of the pathway as a potential therapeutic protocol (Volpicelli-Daley *et al.*, 2016). More recently, MacIsaac and colleagues confirmed the increased susceptibility of LRRK2-G2019S expressing neurons to fibril-induced α-synuclein aggregation and the beneficial outcome of LRRK2 downregulation (MacIsaac *et al.*, 2020).

1.3.3.3 Synaptic activity

Accumulating data indicate that LRRK2 influences synaptic architecture and function by regulating the transport of synaptic components as well as the molecular events leading to neurotransmitter release. A few studies correlated LRRK2 kinase activity with sorting of synaptic vesicles. Cirnaru and coworkers reported a reduction in the rate of synaptic vesicles trafficking and depression of synaptic activity following acute LRRK2 kinase inhibition (Cirnaru *et al.*, 2014). Recent evidence links LRRK2 to axonal transport of lysosome-related dense core vesicles, involved in synaptogenesis and release of neuropeptides and neurotrophic factors. Mutations in Lrrk (a LRRK2 orthologue) lead to UNC-104 (a kinesin orthologue)-dependent accumulation of dense core vesicles at the synaptic bouton of the neuromuscular junction in *Drosophila* (Inoshita *et al.*, 2022). LRRK2 may also regulate the recruitment of specific synaptic proteins, as it has been shown for α-synuclein. LRRK2 inhibition increases anterograde trafficking of α-synuclein and enrichment of the protein at the presynaptic compartment (Brzozowski *et al.*, 2021).

At the synaptic site, LRRK2 engages with an intricate network of protein-protein interactions which influence the dynamics of the recycling synaptic vesicle pool (Shin *et al.*, 2008; Piccoli *et al.*, 2011). LRRK2 phosphorylates and increases the ATPase activity of N-ethylmaleimide sensitive fusion (NSF). This protein couples ATP hydrolysis with disassembly of the SNARE complex following an exocytic event and makes it available for subsequent release cycles (Cirnaru *et al.*, 2014; Belluzzi *et al.*, 2016). LRRK2 hyperactivity not only augments neurotransmitter release but it also interferes with clathrin-mediated vesicle endocytosis by interacting with EndophilinA (EndoA) and auxilin, two components of the endocytic machinery. EndoA participates in synaptic vesicles recycling by influencing membrane curvature and promoting vesicle uncoating (Kaksonen *et al.*, 2018). Expression of LRRK2-G2019S in

Drosophila results in EndoA hyperphosphorylation and inhibits membrane tubulation and endocytosis at the neuromuscular junction (Matta *et al.*, 2012). The opposite phenotype was observed in a LRRK2-deficient background (Matta *et al.*, 2012). Under physiological conditions, auxilin cooperates with EndoA and with the chaperone HSC70 to remove the clathrin coat from the cytoplasmic surface of newly endocytosed vesicles. LRRK2-R1441C hyperphosphorylates auxilin, blocks vesicle endocytosis and causes depletion of the synaptic vesicle pool in PD patient-derived dopaminergic neurons (Nguyen *et al.*, 2018).

Taken together, these studies show that the overall effect of LRRK2 kinase activity upregulation is an increase in the probability of neurotransmitter release. This effect has been corroborated *in vivo* by recording an increase in paired pulse depression in substantia nigra pars reticulata (SNpr) neurons and glutamatergic neurons in LRRK2-G2019S mice (Sitzia *et al.*, 2022).

1.3.3.4 Mitochondria

Loss of mitochondrial integrity is a typical signature of PD that results from deregulation of quality control pathways and impaired autophagic turnover. LRRK2 hyperactivity has been associated with accumulation of faulty mitochondria in PD. In addition to regulating the flux of substrates through the lysosomal pathway, which is essential for the clearance of damaged mitochondria, LRRK2 can directly affect mitochondrial network dynamics and functionality.

LRRK2 is physiologically associated with the outer mitochondrial membrane (West *et al.*, 2005; Biskup *et al.*, 2006). Here, a group of mitochondrial Rho (Miro) GTPases operate as mitochondrial stress sensors. Miro proteins anchor the organelle to molecular motor complexes and mediate mitochondrial trafficking. In case of mitochondrial depolarisation, Miro proteins are promptly degraded via the UPS, leading to mitochondrial arrest and PINK1/PRKN mediated mitophagy (Kruppa and Buss, 2021). Work involving iPSC-derived neurons revealed that LRRK2 forms a complex with Miro which promotes degradation. PD-mutations prevent LRRK2-Miro interaction, delay mitophagy and lead to accumulation of faulty mitochondria (Hsieh *et al.*, 2016).

Mitochondrial quality control is also achieved by recruiting Rab10 to the membrane of damaged mitochondria in a PINK1/PRKN-dependent manner. Rab10 mediates the

recruitment of the autophagy receptor optineurin (OPTN) to the mitochondria surface and facilitates the engagement of the mitophagy molecular machinery. Mutant LRRK2 causes sequestration of hyperphosphorylated Rab10 onto abnormal membrane compartments, blocking an important mechanism of mitochondrial turnover (Wauters *et al.*, 2020).

Besides mitophagy, LRRK2 influences mitochondrial network dynamics by interacting with several members of the dynamin GTPase superfamily, including dynamin-related protein 1 (DRP1), OPA1 and mitofusin1 (Stafa *et al.*, 2014). In particular, DRP1-based mitochondrial fission isolates damaged portions of the mitochondrial network and precedes mitophagy (Fenton *et al.*, 2021). LRRK2 overexpression and mutations are linked to increased recruitment of DRP1 and reduced recruitment of PRKN to the mitochondrial membrane under stress conditions, leading to mitochondria fragmentation and aggregation (Wang *et al.*, 2012; Bonello *et al.*, 2019).

Altogether, impairment of mitochondrial integrity and disruption of the turnover mechanisms of cellular components result in oxidative stress, which accelerates protein misfolding and aggregation (Ryan *et al.*, 2015).

1.4 HDAC6

1.4.1 HDAC6 molecular structure and functions

Histone deacetylase 6 (HDAC6) is a ubiquitous and evolutionarily conserved member of a family of 18 enzymes (Fig. 1.6). HDAC6 is a large, 1255 amino acid protein with an apparent molecular weight of approximately 160 kDa (Fig. 1.7). The singularity of this class IIb histone deacetylase consists in the tandem duplication of the class I/II deacetylase homology domain (Grozinger, Hassig and Schreiber, 1999). The two functionally related HDAC6 deacetylase domains, termed DD1 and DD2, are separated by a flexible linker which constitutes the dynein motor binding domain (DMB, Y. Zhang *et al.*, 2006). At the C-terminal, HDAC6 has a Ser-Glu tetra decapeptide repeat domain (SE14), and a zinc finger ubiquitin-binding domain (ZnF-UBP, also known as BUZ). HDAC6 contains two nuclear export signal (NES) and one nuclear localisation signal (NLS), which together with the SE14 domain, regulate the distribution of the protein between cytoplasm and nucleus (Fig. 1.7; Han *et al.*, 2009; Y. Liu *et al.*, 2012; Seigneurin-Berny *et al.*, 2001).

HDAC6 lysine deacetylase activity targets numerous cytoplasmic substrates, which explains its multifaceted role in cellular physiology (Fig. 1.7). α-tubulin is the main HDAC6 substrate (Hubbert *et al.*, 2002), through which HDAC6 regulates cytoskeletal stability (see below). The panel of key HDAC6 targets includes cortactin (Zhang *et al.*, 2007), heat shock protein 90 (HSP90; Kovacs *et al.*, 2005; Scroggins *et al.*, 2007), β-catenin (Y. Li *et al.*, 2008), peroxiredoxins (Prx, Parmigiani *et al.*, 2008) and survivin (Riolo *et al.*, 2012), through which HDAC6 regulates strategic cellular functions such as autophagy, actin-dependent cell motility, protein turnover, Wnt signalling, mitigation of oxidative stress, cell survival and cell cycle progression. Finally, a deacetylase-independent role of HDAC6 in lymphocytes polarity, mobility and migration has also been described (Cabrero *et al.*, 2006).

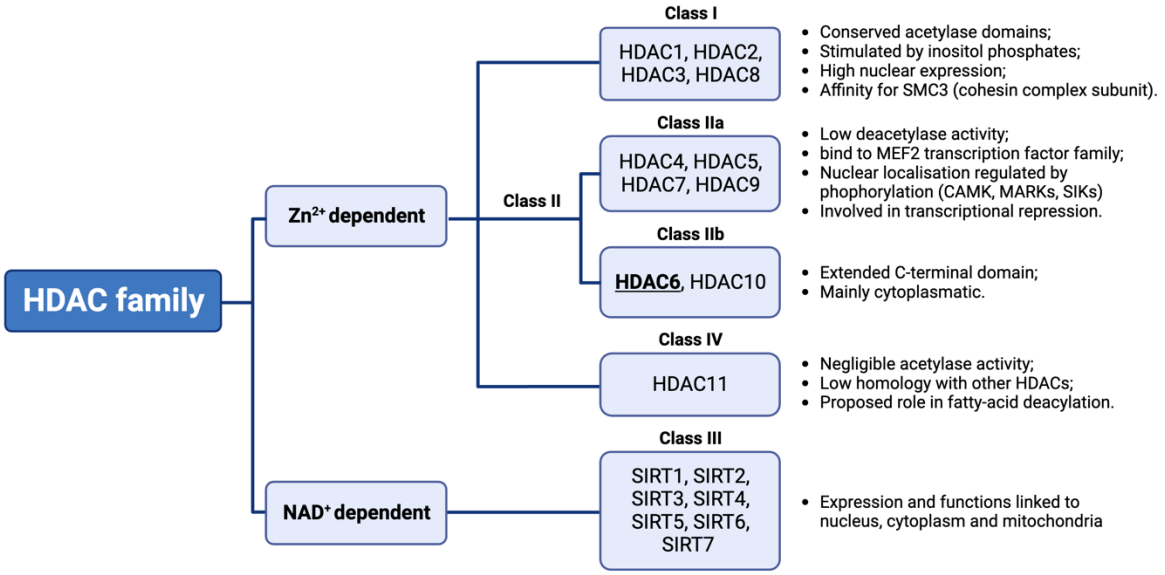

Figure 1.6 The histone deacetylase (HDAC) protein family. Human HDACs are grouped in four classes based on their homology, structure, and functions. A brief description of each class is reported (Jones *et al.*, 2008; Walkinshaw *et al.*, 2013; Hudson *et al.*, 2015; Watson *et al.*, 2016; Kutil *et al.*, 2018; Zhao and Zhou, 2019). HDAC6 is grouped with HDAC10 in Class IIb. These two HDACs differ from the others by an extended C-terminus containing cytoplasmic localisation signals and anchoring domains. Created with BioRender.com.

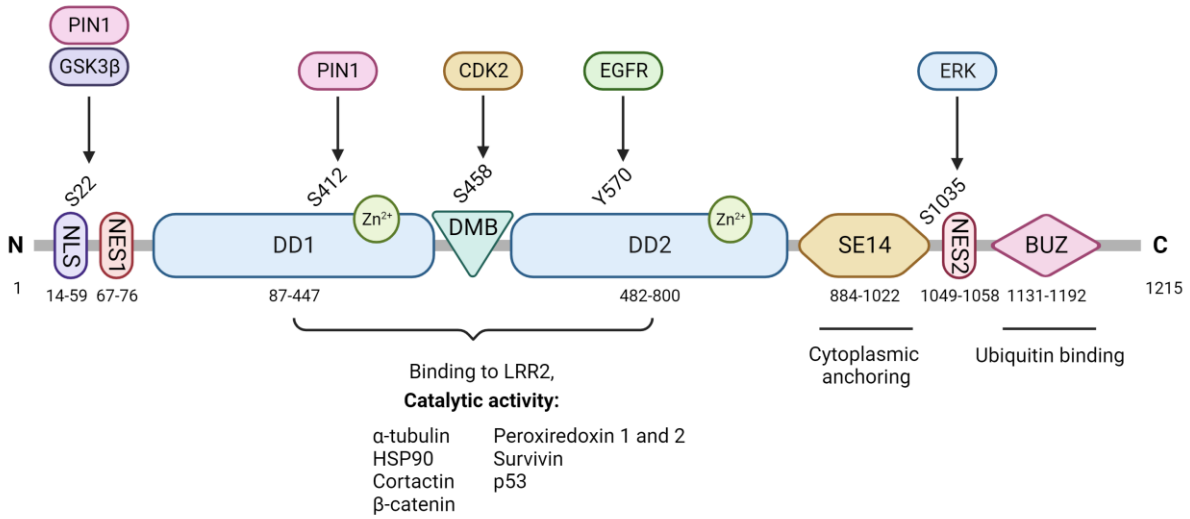

Figure 1.7 Schematic representation of the molecular structure of human HDAC6. HDAC6 is a unique class IIb histone deacetylase which contains two deacetylase domains (DD) and is mainly expressed in the cytoplasm. An ubiquitin-binding zinc-finger domain (BUZ) mediates the interaction between HDAC6 and polyubiquitinated protein aggregates. Binding to dynein occurs through the dynein motor binding domain (DMB). The main HDAC6 cytoplasmic substrates are listed. Arrows indicate the confirmed HDAC6 phosphorylation sites and the related protein kinases linked to HDAC6 phosphorylation. NLS= nuclear localization signal; NES= nuclear export signal; SE14= Ser-Glu tetra decapeptide repeat domain. Created with BioRender.com.

1.4.2 Role of HDAC6 in cellular trafficking and motility

MTs are highly dynamic hollow cytoskeletal components consisting of heterodimers of α- and β-tubulin organised into protofilaments (Rolls *et al.*, 2021). MTs undergo a wide range of post translational modifications that can influence their stability, dynamics and protein-protein interactions (Bär *et al.*, 2022; Naren *et al.*, 2023). Among these, acetylation of α-tubulin at the K40 residue stands out as particularly enigmatic. This is because, despite involving the luminal side of the microtubule, it influences the activity of molecular motors that engage with the filament's outer surface (L'Hernaul *et al.*, 1985; LeDizet *et al.*, 1987). Two studies observed that MT acetylation weakens the interaction between protofilaments (Portran *et al.*, 2017; Xu *et al.*, 2017). The authors proposed that this increases MTs elasticity and improves resilience to mechanical ageing and stress-related breakage (Portran *et al.*, 2017; Xu *et al.*, 2017).

K40 acetylation is tuned by the antagonistic action of α-tubulin acetyltransferase 1 (ATAT1) and HDAC6 (Akella *et al.*, 2010; Shida *et al.*, 2010). On the one hand, ATAT1 catalyses the conjugation of an acetyl group to this lysine residue. On the other hand HDAC6 erases this modification and reduces MT acetylation levels (Zhang *et al.*, 2003). By deacetylating tubulin, HDAC6 influences biological functions including subcellular trafficking (Dompierre *et al.*, 2007), cell adhesion and motility (Castro-Castro *et al.*, 2012; Kalebic *et al.*, 2013), autophagy (Geeraert *et al.*, 2010), and neuronal development (Ageta-Ishihara *et al.*, 2013; G. W. Kim *et al.*, 2013; Wei *et al.*, 2018).

1.4.3 Role of HDAC6 in aggrephagy

Besides its enzymatic activity, HDAC6 plays an essential role as a protein chaperone to direct the degradation of protein aggregates under proteotoxic stress conditions (Fig. 1.8). As outlined above, terminally misfolded proteins are escorted to the proteasome or to the lysosome for clearance. These physiological degradation pathways may be overwhelmed by the persistence of cellular stressors such as gene mutations, oxidative and metabolic stress, impaired protein clearance, ageing, inflammation, and toxins. This leads to accumulation of protein aggregates in the cytoplasm. One of the mechanisms of misfolded protein clearance activated in response to prolonged proteotoxic stress is known as "aggrephagy" (Johnston, Ward and Kopito, 1998; Øverbye, Fengsrud and Seglen, 2007; Zaarur *et al.*, 2008; Ben-

Gedalya *et al.*, 2011; Matsumoto *et al.*, 2018). Protein aggregates are retrogradely trafficked to the microtubule-organizing centre (MTOC) and accumulate into a membrane-free juxtanuclear inclusion named “aggresome” (Johnston, Ward and Kopito, 1998). This organelle primarily consists of misfolded or unfolded proteins which form structured or amorphous aggregates (Kopito, 2000; Øverbye *et al.*, 2007). Mature aggresomes are surrounded by a cage of intermediate filaments: keratin and vimentin in non-neuronal cells, neurofilaments in neurons (Kopito, 2000; Iwata, Christianson, *et al.*, 2005). Rearrangement of the intermediate filament cytoskeleton is a late event in aggresome formation which relies on MT-based trafficking and is essential for aggresome clearance (Biskou *et al.*, 2019; Morrow *et al.*, 2020). Vimentin facilitates the correct positioning of proteostasis-related machineries to the aggresome and its subsequent dismantling by macroautophagy and proteasomal degradation (Wigley *et al.*, 1999; Levine and Klionsky, 2004; Hao *et al.*, 2013). Notably, aggresomes exhibit several similarities with LBs, including juxtanuclear localisation, disruption of the intermediate filament network, and presence of ubiquitinated protein aggregates, along with numerous components of the aggrephagy pathway, such as protein chaperones, proteasomes, dynein and HDAC6 (Miki *et al.*, 2011; Shen *et al.*, 2018).

Trafficking of misfolded proteins into aggresomes relies on two complementary transport mechanisms: one ubiquitin-dependent, the other ubiquitin-independent.

While K48/K11-linked polyubiquitin chains encode proteasomal targeting signals, misfolded proteins tagged with K63-linked ubiquitin are steered towards autophagic clearance routes (Tan *et al.*, 2008). p62’s ubiquitin binding domain displays high affinity for the more extended conformation of K63-linked ubiquitin chains attached to protein aggregates. Aggregate-bound p62 homopolymerizes and mediates the sequestration of misfolded proteins into a p62 body (Fig. 1.8; Long *et al.*, 2008; Wooten *et al.*, 2008). p62 bodies are liquid-liquid phase separation domains normally cleared by LC3-mediated selective autophagy (Zaffagnini *et al.*, 2018). Under intense proteotoxic stress, p62 bodies progressively accumulate, which triggers the recruitment of HDAC6. HDAC6 binds to the c-terminal ends of unanchored K63-linked ubiquitin chains embedded within the protein aggregates and acts as a cargo adaptor for the molecular motor cytoplasmic dynein (Kawaguchi *et al.*, 2003; Ouyang *et al.*, 2012). This allows the retrograde trafficking of aggresome precursors into an aggresome (Hook *et al.*, 2002; Kawaguchi *et al.*, 2003; Bjørkøy *et al.*, 2005). Both p62 and HDAC6 are necessary in ubiquitin-dependent aggrephagy. It has been shown that

depletion of either proteins results in disruption of this transport mechanism (Calderilla-Barbosa *et al.*, 2014).

For completeness, we mention that ubiquitin-independent aggresome formation does not require HDAC6 and relies on a different set of molecular chaperones. These include as HSP70, the HSP70-interacting ubiquitin ligase carboxyl terminal of Hsp70/Hsp90 interacting protein (CHIP), the HSP70 co-chaperone Bcl-2-associated athanogene 3 (BAG3) and molecular adaptors such as the 14-3-3 protein family (García-Mata *et al.*, 1999; Wigley *et al.*, 1999; Gamerdinger *et al.*, 2011; Zhang and Qian, 2011).

Several mechanisms contribute to the regulation of ubiquitin-dependent aggrephagy. Although HDAC6 mainly plays a structural role in this pathway, its deacetylase activity is also required for aggresome formation (Kawaguchi *et al.*, 2003; Yan *et al.*, 2013). The function of HDAC6 enzymatic activity in aggrephagy has not yet been clarified. Other studies explored the impact of HDAC6 phosphorylation on aggresome formation. CK2 phosphorylates HDAC6 on S458 increasing its deacetylase activity and promotes aggresome formation and clearance (Watabe *et al.*, 2011). Another putative HDAC6 phosphorylation site is S22, which may be targeted by glycogen synthase kinase 3β (GSK3β). GSK3β-mediated S22 phosphorylation has been correlated with an increase in HDAC6 deacetylase activity. Accordingly, inhibition of the Akt/GSK3β pathway has been shown to reduce S22 phosphorylation resulting in increased tubulin acetylation and mitochondrial trafficking (Fig. 1.8; Chen *et al.*, 2010).

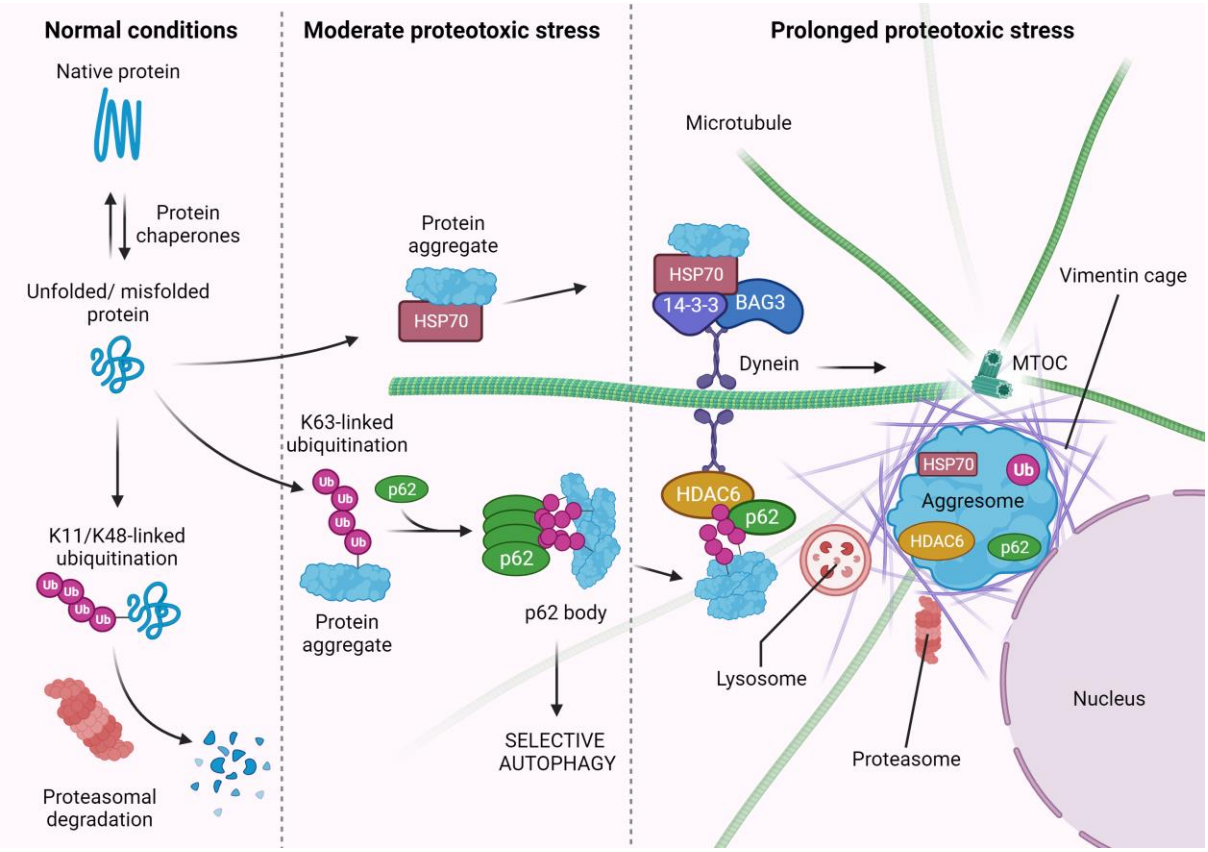

Figure 1.8 Ubiquitin-dependent and ubiquitin-independent mechanisms of sequestration of protein aggregates into aggresomes. Under physiological conditions, misfolded proteins are either refolded or tagged with K11/K48-linked polyubiquitin and degraded via the ubiquitin-proteasome system. If the chaperone and the protein degradation systems fail or are overwhelmed, misfolded proteins form oligomers and aggregates. K63-linked polyubiquitinated aggregates are sequestered by p62 into a p62 body and are degraded by selective autophagy. If the proteotoxic stress persists, HDAC6 binds to the polyubiquitin chains embedded within the protein aggregate and acts as a cargo adaptor for the dynein motor complex. Protein aggregates that are not subject to polyubiquitination are intercepted and recruited to dynein by a complex of molecular chaperones including heat shock protein 70 (HSP70), Bcl-2-associated athanogene 3 (BAG3) and members of the 14-3-3 protein family. Protein aggregates are trafficked to the microtubule organizing centre (MTOC) and accumulate into an aggresome. The reorganization of the intermediate filament cytoskeleton promotes the recruitment of lysosomes and proteasomes, leading to gradual degradation of the organelle. Created with BioRender.com.

1.4.4 HDAC6 and neurodegeneration

In the previous section we summarised the important role played by HDAC6 in the clearance of protein aggregates under prolonged protein stress conditions. Protein dyshomeostasis is a recurrent trait of PD which often culminates in accumulation of α-synuclein aggregates. An increasing body of research indicates that many molecular pathways regulated by HDAC6 may carry significant consequences for PD pathogenesis. However, the literature presents contrasting perspectives, with studies emphasizing the positive, null, or negative effects of HDAC6 activity on the molecular and cellular phenotypes of PD.

Studies reporting a neuroprotective effect of HDAC6 in PD models often focus on the ability of HDAC6 to preserve protein homeostasis either by preventing protein misfolding or by sequestering cytotoxic α-synuclein oligomers into larger, more stable inclusions. HDAC6 has been proposed to prevent α-synuclein aggregation in mice by activating the heat shock response (Du *et al.*, 2014). Under physiological conditions, HDAC6 forms a complex with heat-shock transcription factor 1 (HSF1) and HSP90. Ubiquitin-bound HDAC6 is released from the complex, which derepresses HSF1. Active HSF1 induces the expression of several heat-shock protein-encoding genes which mitigate misfolded protein stress (Boyault *et al.*, 2007; Pernet *et al.*, 2014).
Other studies indicate that α-synuclein clearance relies on dynein retrograde transport and HDAC6 activity (Cai *et al.*, 2009; Su *et al.*, 2011). It has been reported that HDAC6 recruits α-synuclein into perinuclear aggresome-like bodies in SH-SY5Y and PC12 cells expressing A53T α-synuclein treated with MPP^+. HDAC6 KO interferes with the condensation of α-synuclein into inclusions, causing relocation of the protein to the nuclear compartment and apoptosis (Su *et al.*, 2011). A similar HDAC6-dependent cytoprotective mechanism has been documented in a transgenic *Drosophila* model expressing human α-synuclein. HDAC6 promotes the formation of large α-synuclein inclusions to counter the accumulation of cytotoxic oligomers. Animals lacking HDAC6 display more severe DA neuron loss, retinal degeneration, and locomotor dysfunction (Du *et al.*, 2010).

Notably, studies dissecting different aspects of the complex PD phenotype, such as loss of lysosomal integrity, inflammation, oxidative stress, and axonal trafficking impairment, reported significant improvements upon HDAC6 depletion or inhibition.

With respect to α-synuclein turnover, HDAC6 inhibitors reduced α-synuclein levels, prevented dopaminergic neuronal loss and reduced astrocyte reactivity in rats expressing human α-synuclein in the SN. Mechanistically, HDAC6 inhibition promoted CMA upregulation, which also resulted in lower pS129 levels (Francelle *et al.*, 2020). HDAC6 inhibition was also found to protect from dopaminergic neuronal loss and promote a partial motor rescue in a *Danio rerio* MPP^+-induced model of PD (Pinho *et al.*, 2016). Similarly, administration of HDAC6 inhibitors ameliorated dopaminergic degeneration in mice treated with the neurotoxin 6-hydroxydopamine (6-OHDA). 6-OHDA causes HDAC6 overexpression, leading to deacetylation and inactivation of Prx1 and Prx2, two components of the antioxidant system. The resulting oxidative stress has been shown to ameliorate upon HDAC6 inhibition (Jian *et al.*, 2017). We previously showed that expression of PD-related LRRK2 mutants R1441C or Y1699C causes formation of LRRK2 filaments along deacetylated MT stretches and impairs mitochondrial trafficking. This correlates with locomotor deficit in the corresponding transgenic *Drosophila* model. Either genetic or pharmacological HDAC6 manipulation prevents association of mutant LRRK2 with MTs and rescues the pathological phenotypes both *in vitro* and *in vivo* (Godena *et al.*, 2014). Interestingly, administration of HDAC6 inhibitors was linked to amelioration of cognitive and motor phenotypes and reduced misfolded protein deposition in other models of neurodegenerative disorders. These include Alzheimer's disease (Kim *et al.*, 2012; Selenica *et al.*, 2014; Zhang *et al.*, 2014; Sreenivasmurthy *et al.*, 2022), Charcot-Marie-Tooth disease (D'Ydewalle *et al.*, 2011; Benoy *et al.*, 2018; Mo *et al.*, 2018), amyotrophic lateral sclerosis (Taes *et al.*, 2013; Guo *et al.*, 2017; Rossaert *et al.*, 2019), Rett syndrome (Xu *et al.*, 2014; Gold *et al.*, 2015), Huntington disease (Dompierre *et al.*, 2007; Bobrowska *et al.*, 2011; Guedes-Dias *et al.*, 2015), and fragile X syndrome (Kozikowski *et al.*, 2019). In most cases, these improvements were sustained by the augmentation of tubulin acetylation levels, which rescues MT-dependent trafficking of organelles and proteins. Collectively, these reports substantiate the adverse impact of HDAC6 in neurodegeneration, particularly in the context of Parkinson's disease.

In contrast with what was said above, a recent study based on a MPTP-induced mouse model reported that HDAC6 has neither positive nor negative effects on acute neurotoxicity. Wilde-type (WT) and HDAC6 KO mice did not display any significant

differences in dopaminergic degeneration, microglia activation, α-synuclein levels and apoptotic markers (Zhao *et al.*, 2023).

Given the multifaceted role of HDAC6 in regulating cellular homeostasis, it is possible that the contradictory outcomes of HDAC6 manipulation recorded in PD may depend on the limited range of pathogenic mechanisms recapitulated by each model. From a wider perspective, HDAC6 deacetylase activity might perform both positive and negative roles within this pathological context.

1.5 Hypothesis and aims

Preliminary data from our research group suggest that LRRK2 regulates the recruitment of misfolded proteins into aggresomes and that ubiquitin-dependent aggresome formation is compromised in LRRK2-PD (Lucas *et al.*, 2019). LRRK2 establishes a direct binding with HDAC6 via its Roc domain and may catalyse the phosphorylation of HDAC6 at S22 (pS22). pS22 was found to be necessary and sufficient to support trafficking of ubiquitinated protein aggregates into aggresomes (Lucas *et al.*, 2019). The gain of function LRRK2 mutation G2019S may affect the binding between LRRK2 and HDAC6 and disrupt ubiquitin-dependent aggresome formation in HEK293 cells and iAstrocytes derived from PD patients (Lucas *et al.*, 2019). Multiple reports indicate that LBs and aggresomes share striking similarities and may originate from partially overlapping mechanisms. HDAC6 may mitigate α-synuclein toxicity by sequestering pathogenic α-synuclein oligomers into inclusions, subsequently cleared via aggrephagy.

LRRK2 is involved in sorting of organelles and membranes. Evidence suggests that LRRK2 influences α-tubulin K40 acetylation, despite lacking direct deacetylase activity. HDAC6 serves as the main α-tubulin deacetylase and its enzymatic activity is regulated by phosphorylation. In addition to its role in aggrephagy, the interaction with LRRK2 may impact HDAC6 functions related to MT acetylation and subcellular trafficking. Subcellular localization, clearance, aggregation, and propagation of α-synuclein depend on MT-based transport, a process modulated by tubulin acetylation.

We hypothesize that HDAC6 may directly link LRRK2 activity to α-synuclein clearance. In this scenario, LRRK2 may regulate the recruitment of α-synuclein aggregates into aggresomes through a kinase dependent mechanism. Dysregulation of the LRRK2-HDAC6 interplay would contribute to α-synuclein toxicity and pathology in PD.
Moreover, we hypothesise that the interaction between LRRK2 and HDAC6 could be involved in α-synuclein subcellular localisation and secretion by regulating MT acetylation.

Therefore, the aims of this project were as follows:

- to investigate the mechanism by which LRRK2 regulates HDAC6;

- to establish the impact of ubiquitin-dependent aggrephagy on clearance of α-synuclein aggregates;
- to elucidate the role of LRRK2 and HDAC6 in α-synuclein metabolism and trafficking.

2 Materials and methods

2.1 Materials and reagents

2.1.1 Buffers and media

Table 2.1 Composition of buffers, solutions, and culture media. All chemicals were purchased from Sigma-Aldrich, unless stated otherwise. Buffers were made up to volume with ultrapure H_2O, unless otherwise specified.

Name	Composition
Cell culture	
Phosphate-Buffered Saline (PBS)	137 mM NaCl, 2.7 mM KCl, 10 mM Na_2HPO_4, 1.8 mM K_2HPO_4; pH adjusted to 7.4 with HCl.
Trypsin Solution	0.25% trypsin, no phenol red (Gibco) in PBS.
Complete DMEM	Dulbecco's Modified Eagle Medium with 4.5 g/l glucose (DMEM; Thermo Scientific), 10% foetal bovine serum (FBS; Sigma-Aldrich) and 1 mM Na pyruvate (Sigma-Aldrich).
HBSS	485 ml of HBSS (Invitrogen) were supplemented with 6 ml of 1 M HEPES pH 7.4 (Invitrogen), 3 mL of 50 U ml^{-1} penicillin and 50 µg ml^{-1} streptomycin (Gibco), 6 ml of 100 mM Pyruvic Acid (Invitrogen) and 100 ml of ultra-pure H_2O. Final volume= 600 ml.
Digestion Buffer	20 U/ml papain (Worthington Biochemical Corporation), 0.2 µg/ µl L-cysteine, 1.1 µM EDTA in HBSS. The solution was gently rotated at RT for 30 min and filter-sterilised immediately before use.
DNase Solution	50 µU/mL DNase (Sigma-Aldrich) in ice-cold plating media.

Plating Medium	Neurobasal medium (Invitrogen), 5% FBS, 1% Glutamax (Invitrogen), 2% B27 supplement (Invitrogen), 50 U ml^{-1} penicillin (Gibco) and 50 µg ml^{-1} streptomycin (Gibco).
Neuronal Medium (mouse neurons)	Neurobasal medium (Invitrogen), 1% Glutamax (Invitrogen), 2% B27 supplement (Invitrogen).
Neuronal Medium (rat neurons)	Neurobasal medium (Gibco, Life Technologies), 2 mM L-glutamine (Lonza), 1% B27 supplement (Invitrogen), 100 IU/ml penicillin (Lonza), 100 mg/ml streptomycin (Lonza).
Coating Buffer	0.1 mg/ml poly-D-lysine hydrobromide (Sigma-Aldrich), 50 mM boric acid (Sigma-Aldrich); pH 8.5.
Flush Medium	DMEM, 10% FBS, 100 IU/ml penicillin (Lonza), 100 mg/ml streptomycin (Lonza).
L929 Conditioned Medium	L929 cells were cultured for 10 days in DMEM (Thermo Scientific) supplemented with 10% FCS (Gibco). Conditioned medium was filtered through a 0.2 µm filter and stored at -20 ºC.
BMDM Growth Medium	DMEM, 15% L929 Conditioned Medium,10% FBS, 100 IU/ml penicillin (Lonza), 100 mg/ml streptomycin (Lonza).
Cell lysis and immunoblot	
BRB80	80 mM K-PIPES (pH 6.8), 1 mM EDTA, 1 mM $MgCl_2$, 1% NP40 (IGEPAL CA-630), 150 mM NaCl, 10 mM NaF, 1 mM Na_2VO_4, 10 mM β-glycerophosphate, 5 mM $Na_4P_2O_7$; for cell lysis, BRB80 was complemented with 1x Protease Inhibitor Cocktail (Thermo Scientific).
20x Tris-buffered Saline (TBS)	400 mM Tris, 3 M NaCl; pH adjusted to 7.4 with HCl.

Triton X-100 Extraction Buffer	1% v/v Triton X-100, 1x Protease Inhibitor Cocktail, 1x PhosSTOP Phosphatase inhibitor Cocktail (Roche) in 1x TBS.
SDS Extraction Buffer	2% sodium dodecyl sulphate (SDS), 1x Protease Inhibitor Cocktail, 1x PhosSTOP Phosphatase inhibitor Cocktail in 1x TBS.
5x Laemmli buffer	300 mM Tris HCl (pH 6.8), 25% glycerol (Fisher Scientific), 25% β -mercaptoethanol,10% SDS, 0.01% bromophenol blue.
Resolving Gel (7.5%)	375 mM Tris-HCl (pH 8.8), 7.5% acrylamide-bis-acrylamide (National Diagnostics), 0.1% SDS, 0.1% ammonium persulfate (APS), 0.1% TEMED. Used to separate proteins of molecular weight >100 kDa.
Resolving Gel (10%)	375 mM Tris-HCl (pH 8.8), 10% acrylamide-bis-acrylamide, 0.1% SDS, 0.1% APS, 0.1% TEMED. Used to separate proteins of molecular weight between 40 and 100 kDa.
Resolving Gel (15%)	375 mM Tris-HCl (pH 8.8), 15% acrylamide-bis-acrylamide, 0.1% SDS, 0.1% APS, 0.1% TEMED. Used to separate proteins of molecular weight <40 kDa.
Stacking Gel (6%)	125 mM Tris HCl (pH 6.8), 6% acrylamide-bis-acrylamide, 0.1% SDS, 0.06% APS, 0.3% TEMED.
10x Tris-Glycine Buffer	250 mM Tris base, 1.92 M glycine; pH 8.3.
Running Buffer	1x Tris-Glycine Buffer, 0.1% SDS.
Transfer Buffer	1x Tris-Glycine Buffer, 20% methanol (Fisher Scientific).
Ponceau Stain	0.1% Ponceau S, 5% acetic acid.
TBS-Tween-20 (TBS-T)	1x TBS, 0.1% Tween-20

Immunofluorescence	
Antigen Retrieval Solution	10 mM sodium citrate, 0.05% Tween-20; pH 6.0.

2.1.2 Plasmids

Table 2.2 Plasmid DNA used for transfection of immortalised cell lines. Kan= kanamycin; Amp= ampicillin.

Name	Protein	Backbone	Antibiotic resistance	Source
2xMyc-LRRK2	Human LRRK2 WT	pCMV-Tag 3B	Kan	Mark Cookson (NIH) (Addgene #25361)
2xMyc-LRRK2-D1994A	Human LRRK2 (D1994A)	pCMV-Tag 3B	Kan	In house mutagenesis of Addgene #25361 (Lucas *et al.*, 2019)
2xMyc-LRRK2-R1441C	Human LRRK2 (R1441C)	pCMV-Tag 3B	Kan	Mark Cookson (NIH, Addgene #25363)
2xMyc-LRRK2-Y1699C	Human LRRK2 (Y1699C)	pCMV-Tag 3B	Kan	Mark Cookson (NIH, Addgene #25364)
2xMyc-LRRK2-G2019S	Human LRRK2 (G2019S)	pCMV-Tag 3B	Kan	Mark Cookson (NIH, Addgene #25362)
FLAG-HDAC6	Human HDAC6	pCI-neo-FLAG	Amp	In house cloning (Lucas *et al.*, 2019)
FLAG-HDAC6-S22A	Human HDAC6-S22A	pCI-neo-FLAG	Amp	In house mutagenesis (Lucas *et al.*, 2019)

GFP-250	Human p115 (aa 1- 252)	pEGFP-C2	Kan	Elizabeth Sztul (University of Alabama at Birmingham)
GFP-CFTRΔF508	Human CFTR CFTRΔF508	pEGFP-C1	Kan	Ron Kopito (Stanford)
GFP-Rab8a	Human Rab8a	pEGFP-C1	Kan	Gift from Andrew Peden (University of Sheffield)
pCI-neo empty vector	- -	pCI-neo	Amp	Promega
α-synuclein-A53T	Human α-synuclein-A53T	pCI-neo	Amp	In house cloning
α-synuclein-WT	Human α-synuclein-WT	pCI-neo	Amp	In house cloning
α-synuclein-YFP	Human α-synuclein-WT	pcDNA4	Amp	Gift from Ulf Dettmer (Harvard Medical School)

2.1.3 Drugs

Table 2.3 List of drugs for treatments. Information about Suppliers and preparation of the stock solutions are reported. DMSO was purchased from Sigma-Aldrich. All stock solutions were stored at -20 °C.

Name	Supplier	Stock concentration	Solvent
Ampicillin	Sigma-Aldrich	100 mg/ml	H_2O
ATP	Sigma-Aldrich	100 mM	H_2O
GSK2578215A	Tocris	5 mM	DMSO
HG-10-102-01	Calbiochem	5 mM	DMSO
Kanamycin	Sigma-Aldrich	50 mg/ml	H_2O
LPS	Sigma-Aldrich	2 mg/ ml	H_2O
MG132	Sigma-Aldrich	10 mM	DMSO
MLi-2	Tocris	200 µM	DMSO
Tubastatin A	Sigma-Aldrich	20 mM	DMSO

2.1.4 Antibodies

Table 2.4 List of primary and secondary antibodies used for western blot (WB), immunofluorescence (IF) and immunoprecipitation (IP). RRID= Research Resource Identifier, available at https://www.rrids.org/; Gg= *Gallus gallus domesticus* (chicken); Ea= *Equus africanus asinus* (donkey); Cp= *Cavia porcellus* (guinea pig); Ch= *Capra hircus* (goat); Mm= *Mus musculus* (mouse); Oc= *Oryctolagus cuniculus* (rabbit); Rn= *Rattus norvegicus domestica* (rat).

Antibody	Host	Supplier	RRID	Application
Primary antibodies				
Anti-acetyl-α-tubulin (6-11B-1)	Mm	Sigma-Aldrich	AB_2819178	WB 1:5,000
Anti-F4/80	Rn	Abcam	AB_1140040	IF 1:1,000
Anti-FLAG (M2)	Mm	Sigma-Aldrich	AB_259529	WB 1:2,000
Anti-FLAG M2 Magnetic Beads	Mm	Sigma-Aldrich	AB_2637089	IP: 10 µl
Anti-GAPDH (14C10)	Oc	Cell Signaling Technology	AB_561053	WB 1:2,000
Anti-GFP (JL-8)	Mm	TaKaRa Biology	AB_10013427	WB 1:5,000
Anti-HDAC6 (D2E5)	Oc	Cell Signaling Technology	AB_10891804	IF 1:200
Anti-IL-1β	Oc	Abcam	AB_308765	WB 1:1,000
Anti-myc (9B11)	Mm	Cell Signaling Technology	AB_331783	WB 1:2,000 IF 1:2,000 IP: 1:250
Anti-NeuN	Gg	Millipore	AB_11205760	IF 1:500
Anti-neurofilament	Gg	Abcam	AB_2149618	IF 1:5,000

Anti-P62/ SQSTM1 antibody	Oc	Proteintech	AB_10694431	IF 1:500
Anti-Phopsho HDAC6-S22	Oc	Abcam	AB_942257	WB 1:500
Anti-phospho-Rab10-T73 (MJF-R21)	Oc	Abcam	AB_2811274	WB 1:1,000
Anti-phospho-Rab8a-T72 (MJF-R20)	Oc	Abcam	AB_2814988	WB 1:1,000
Anti-phospho-α-synuclein-S129	Oc	Abcam	AB_869973	WB 1:500 IF 1:1,000
Anti-Rab10 (D36C4)	Oc	Cell Signaling Technology	AB_10828219	WB 1:1,000
Anti-tyrosine hydroxilase	Gg	Abcam	AB_1524535	IF 1:1,000
Anti-ubiquitin	Mm	Cytoskeleton	AB_2884970	WB 1:1,000 IF 1:250
Anti-vGLUT1	Cp	Synaptic Systems	AB_887878	IF 1:1,000
Anti-vimentin	Gg	Millipore	AB_11212377	IF 1:4,000
Anti-α-synuclein	Mm	Synaptic Systems	AB_2619811	WB 1:1,000 IF 1:500
Anti-α-tubulin	Oc	Abcam	AB_2288001	WB 1:10,000
Anti-α+β-synuclein	Oc	Abcam	AB_869971	WB 1:1,000 IF 1:200
Secondary antibodies				

Alexa 488 anti-rabbit IgG	Ch	Thermo Fisher Scientific		AB_2576217	IF 1:500
Alexa 568 anti-rabbit IgG	Ea	Thermo Fisher Scientific		AB_2534017	IF 1:500
Alexa Fluor 488 anti-mouse IgG	Ch	Thermo Fisher Scientific		AB_2556548	IF 1:500
Alexa Fluor 555 anti-guinea pig IgG	Ch	Thermo Fisher Scientific		AB_2535856	IF 1:500
Alexa Fluor 568 anti-mouse IgG	Ch	Thermo Fisher Scientific		AB_144696	IF 1:500
Alexa Fluor 680 anti-rabbit IgG	Ea	Stratech		AB_2340627	WB 1:25,000
Alexa Fluor 790 anti-mouse IgG	Ea	Stratech		AB_2340870	WB 1:25,000
Anti-mouse immunoglobulins/HRP	Ch	Agilent		AB_2617137	WB 1:5,000
Anti-rabbit immunoglobulins/HRP	Ch	Agilent		AB_2617138	WB 1:5,000
Cy5 anti-chicken IgY	Ea	Jackson ImmunoResearch Labs		AB_2340365	IF 1:500

2.2 Methods

2.2.1 Plasmid DNA purification

Ultracompetent XL10-Gold *E. coli* strains (Agilent Technologies) transformed with the plasmids listed in Tab 2.2 were suspended in 25% glycerol and indefinitely stored at -80 °C. For small-scale plasmid expansion and purification, a stab of bacterial cells was streaked onto a Luria-Bertani (LB) Agar (Sigma-Aldrich) plate containing either 100 ug/ ml ampicillin or 50 ug/ ml kanamycin according to corresponding plasmid-mediated resistance and incubated overnight (ON) at 37 °C. Single bacterial colonies were picked and inoculated in 5 ml of LB Broth (Sigma-Aldrich) supplemented with 100 ug/ ml ampicillin or 50 ug/ ml kanamycin and incubated ON at 37 °C with shaking at 220 rpm. To encourage growth and increase culture yield, Terrific Broth (TB; Sigma-Aldrich) was used instead of LB Broth to grow bacterial strains containing LRRK2 constructs. Bacteria were pelleted by centrifugation at 4,000 rcf for 5 min and plasmid DNA was extracted and purified using a NucleoSpin Plasmid Miniprep kit (Macherey-Nagel) according to manufacturer's instructions. Plasmids encoding LRRK2 constructs were purified using a ZymoPURE Plasmid Miniprep Kit (Zymo Research) according to manufacturer's instructions for higher DNA yield. For large-scale expansion of plasmid DNA, a starter culture was made by picking single bacterial colonies and inoculating them into 5 ml of the appropriate growth medium at 37 °C for 8 h with shaking at 220 rpm. The starter culture was then used to inoculate 500 ml of the same growth medium type. The bacterial culture was incubated in a 2 l flask at 37 °C ON with shaking at 220 rpm. Plasmid DNA was purified using a QIAGEN Plasmid Maxi Kit (Qiagen) following manufacturer's instructions and reconstituted in nuclease-free water (Qiagen).

DNA concentration was determined using a NanoDrop 1000 Spectrophotometer (Thermo Scientific). Either Elution Buffer AE (Macherey-Nagel), ZymoPURE Elution Buffer (Zymo Research) or nuclease-free water (Qiagen) were used as blank, depending on the kit used for DNA purification. All three DNA extraction protocols utilised in this work consistently yielded pure DNA with a ratio of absorbance at 260 nm and 280 nm above the 1.8 theoretical threshold.

2.2.2 Cell culture

2.2.2.1 Immortalised cell lines and plasmid transfection

HeLa, HEK293, COS7, SHSY-5Y were cultured in Complete DMEM at 37°C in a CO_2 incubator and regularly tested for mycoplasma contamination. Cells were passaged twice a week after reaching 90% confluency. Cells were rinsed with PBS and incubated in prewarmed Trypsin Solution for 4 min at 37°C. Trypsin was quenched by adding two volumes of Complete DMEM, then cells were gently detached by pipetting and diluted into an appropriated volume of Complete DMEM for passaging or plating.

Cells were transiently transfected at ~80% confluency the day after plating. Plasmid DNA was purified as described in chapter 2.2.1. pCI-neo empty vector (EV) was used as negative control in all experiments. Plasmid DNA was diluted in OptiMEM (Gibco, Life Technologies) and mixed by vortexing (Tab. 2.5). For co-transfection experiments, half the amount of DNA reported in Tab. 2.5 was used for each plasmid and mixed in a 1:1 ratio. 3 µl of TurboFect Transfection Reagent (Thermo Scientific) were added per each µg of plasmid DNA (Tab. 2.5) and immediately vortexed for 10 s. The transfection mix was incubated at room temperature (RT) for 20 min, dispensed to the cells and immediately mixed by gently rocking the plate side to side. Cells were returned to the CO_2 incubator for 6 h, then the media was replaced with fresh Complete DMEM. Drug treatments were administered 24 h post transfection.

Table 2.5 Plasmid DNA transfection with TurboFect

Plate	DNA (µg/ well)	TurboFect (µl/ well)	Final OptiMEM vol (µl/ well)
10 cm	10	30	1000
6-well	2	6	200
12-well	1	3	100
24-well	0.5	1.5	50

2.2.2.2 Isolation of bone marrow-derived macrophages from mice

Young adult mice were culled by cervical dislocation. Femurs and tibias were dissected, cleared of any visible traces of muscle and connective tissues, briefly sterilised in 70% ethanol, and rinsed in sterile PBS. The epiphyses were removed and the bone marrow was flushed with Flush Medium into a sterile tube using a 1 ml syringe with a 25G needle. The cell suspension was homogenised by pipetting up and down with a micropipette. $5 \cdot 10^5$ cells were plated in 10 ml of BMDM Growth Medium into sterile 10 cm bacterial dishes and incubated at 37 °C in a CO_2 incubator. At day *in vitro* (DIV) 1, 10 ml of fresh BMDM Growth Medium were added to each dish. At DIV 5, 7 and 9 cells were fed with a 1:1 mix of fresh and conditioned BMDM Growth Medium centrifuged for 5 min at 500 rcf to remove non-adherent cells. At DIV11 cells were detached with ice-cold PBS on ice for 10 min, precipitated by centrifugation for 4 min at 400 rcf and resuspended in BMDM Growth Medium. BMDMs were seeded into 12-well plates at a density of $2 \cdot 10^5$ cells/ well or on glass coverslip into 24-well plates at a density of $1 \cdot 10^5$ cells/ well. Experiments or immunostaining were performed at DIV14.

2.2.2.3 Isolation of primary neurons from mice

Pregnant CD1 mice were purchased from Charles River (Wilmington, MA). P0 mice pups were cryoanesthetised on ice. Brains were extracted in ice-cold HBSS and dissected in Hibernate E (Brainbits) on ice using sterile surgical instruments. Hippocampal and cortical sections were collected into separate 15 ml conical tubes and stored in Hibernate E on ice for the entire duration of the procedure. Tissue samples were rinsed twice with HBSS and incubated with Digestion Buffer for 45 min at 37 °C. Samples were resuspended in ice-cold DNase solution and inverted three times, then immediately rinsed once with ice-cold plating media and twice with ice-cold HBSS. Brain tissue was homogenised by pipetting, diluted in ice-cold Plating Medium and filtered through a 40 mm nylon mesh cell strainer (Fisher Scientific). Cells were counted and plated on glass coverslips at a density of 100,000 cells per well in a 24-well plate or 500,000 cells per well in a 6-well plate. Both plates and coverslips were previously coated with PDL Coating Buffer for 1.5 h at 37 °C and rinsed twice with sterile ultrapure water. Neurons were allowed to settle ON at 37 °C in a CO_2

incubator, then Plating Medium was replaced with Neuronal Medium. At DIV7 neurons were fed with a 1:1 mix of fresh and conditioned Neuronal Medium.

2.2.2.4 Isolation of cortical neurons form rats

Primary cortical neurons were kindly provided by Dr Claudia S. Bauer. Neurons were isolated from embryonic day 18 (E18) Sprague Dawley rat embryos (Charles River) as previously described (Seibenhener and Wooten, 2012) and seeded in 24-well plates at a density of 100,000 cells per well. Neurons were maintained in Neuronal Medium and incubated at 37°C in a CO_2 incubator. At DIV5, 8 and 12, neuronal cultures were fed with a 1:1 mix of fresh and conditioned Neuronal Medium.

2.2.2.5 Drug treatments

Proteasome inhibition was obtained by administering 5 µM MG132, unless otherwise specified. HDAC6 deacetylase activity was inhibited with 10 µM tubastatin A. LRRK2 kinase activity was inhibited with either 100 nM MLi-2, 3 µM GSK2578215A, or 3 µM HG-10-102-01. A corresponding volume of sterile DMSO was used as control in all experiments. Incubation times varied based on the experiment and the cell line used and are reported individually in the Results sections of this work.

2.2.3 Inflammasome activation assay

DIV14 BMDMs were treated with 1 ng/ ml Lipopolysaccharide (LPS) and either DMSO, tubastatin A or MLi-2 in 400 µl of fresh BMDM Growth Medium per well. Exactly 3.5 h post LPS administration, 20 µl of a 100 mM ATP stock solution were added to each well to a final concentration of 5 mM. 20 µl of sterile ultrapure H_2O were used as control. Exactly 4 h post LPS administration, conditioned media samples were collected and centrifuged for 5 min at 1500 rcf to remove cell debris and the supernatant was transferred into clean tubes on ice. BMDMs were washed twice in PBS, scraped in 120 µl of 2x Laemmli Buffer, needle-sheared, and either stored at -20 °C or processed by SDS-PAGE/ immunoblot.

The concentration of secreted IL-1β in the conditioned media was measured using a Mouse IL-1β beta Uncoated ELISA (Invitrogen) according to manufacturer's instructions. Samples were loaded onto a transparent 96-well plate (Corning Costar 9018 ELISA) both undiluted and serially diluted 1:2 and 1:4 in fresh BMDM Growth

Medium. Each sample dilution was run in duplicate and fresh BMDM Growth Medium was used for blank subtraction. Absorbance was read at 450 nm on a PheraSTAR FS plate reader (BMG Labtech). Only values falling within the dynamic range of the method were used for data analysis.

2.2.4 α-synuclein preformed fibrils

2.2.4.1 Synthesis

Recombinant mouse full-length α-synuclein was purified as previously described (Volpicelli-Daley *et al.*, 2014) and stored at -80 °C.

Monomeric α-synuclein aliquots were thawed on ice and centrifuged at 100,000 rcf for 60 minutes at 4° C to remove any aggregated material. The supernatant was collected and protein concentration was calculated by measuring absorbance at 280 nm on a NanoDrop 1000 (Thermo Scientific) spectrophotometer using the mouse α-synuclein molar extinction coefficient ε= 7450 $M^{-1}cm^{-1}$. A solution of 50 mM NaCl and 10 mM Tris pH 7.5 was used as blank. To synthesise preformed fibrils (PFFs), monomeric α-synuclein was diluted to 5 mg/ ml in 500 µl of PBS, placed into a sealed Protein LoBind 1.5 ml Tube (Eppendrof) and incubated for 7 days at 37 °C under shaking at 1,000 rpm. PFFs were separated from the non-polymerised monomer solution by centrifugation at 17,000 rcf for 10 minutes at RT, then the pellet was resuspended in 250 µl of PBS. To measure the concentration of the PFF suspension, 5 µl of PFFs were mixed with 5 µl of 8 M of guanidinium chloride and incubated for 1 h at RT. Absorbance at 280 nm was read on a NanoDrop 1000 spectrophotometer and α-synuclein concentration was calculated as above. A 1:1 mix of PBS and 8 M of guanidinium chloride was used as blank. The PFFs suspension was diluted to 5 mg/ ml in PBS, split into 22 µl aliquots and stored at -80 °C.

2.2.4.2 Administration

On the day of the experiment, PFFs were thawed at RT and transferred into a 1.5 ml polystyrene sonication tube (Acive Motif), sealed, and sonicated on a Q800R3 Qsonica Sonicator in pulsating mode with an amplitude of 30%, process time of 15 min, pulse-on time of 3 s, pulse-off time of 2 s and temperature of 15 °C. To assess PFFs' size, freshly sonicated PFFs were diluted 1:500 in PBS and loaded onto a DynaPro NanoStar Dynamic Light Scattering Detector (Wyatt Technology) run by

Dynamics software (Waters Corporation; version 8.1.1.89). 5 measurements of 10 acquisitions each were made per each sonication cycle. Sonication was considered successful if PFFs showed a unimodal size distribution with an average main radius ranging between 10 and 100 nm.

For experiments performed in COS7 cells, freshly sonicated PFFs were diluted to 1 µg/ ml in Complete DMEM and incubated for 24 h. Sterile PBS was used as negative control. Any additional drug treatments were also incubated at this stage. For experiments performed in primary mouse cortical neurons, PFFs were diluted to 2 µg/ ml in fresh Neuronal Medium, added to an equal volume of conditioned neuronal media (final concentration= 1 µg/ ml) and incubated for 7 d.

2.2.5 α-synuclein secretion assay

Cells were plated in a 24-well plate. SH-SY5Y cells expressing wild type α-synuclein were incubated with either DMSO, tubastatin A, GSK2578215A or HG-10-102-01 for 16 h. DIV13 rat cortical neurons or were incubated with the same inhibitors for 24 h. Drug treatments were administered in 250 ul of media per well in duplicate. Post incubation, cells were washed in PBS and lysed in 50 ul of 2.5x Laemmli Buffer per well, needle-sheared, and either stored at -20 °C or processed by SDS-PAGE/ immunoblot. Conditioned media samples were centrifuged for 5 min at 1,000 rcf to remove cell debris. 200 ul of supernatant were mixed with 50 ul of 5x Laemmli Buffer and either stored at -20 °C or processed by dot blot. To assess treatment toxicity, the release of lactate dehydrogenase (LDH) was quantified on conditioned media samples in duplicate by using a colorimetric Non-Radioactive Cytotoxicity Assay (Cyto Tox 96, Promega) following manufacturer's instructions. Fresh culture medium was used as blank. Absorbance at 490 nm was read on a PheraSTAR FS plate reader. Relative cell survival was calculated by dividing the average absorbance of each treatment by the average absorbance of the DMSO-treated control per each biological replicate.

2.2.6 Immunoblotting

2.2.6.1 Cell lysis and immunoprecipitation

Cells were rinsed with PBS and scraped on ice in 750 µl (10 cm dish) or 100 µl (6-well plate) of BRB80 Buffer. Crude lysates were incubated at 4° C under gentle mixing for

30 minutes and then cleared by centrifugation at 17,000 rcf at 4° C for 20 minutes. Protein concentration was measured by colorimetry using a Bradford Bio-Rad Protein Assay (Bio-Rad) according to manufacturer's instructions. Absorbance was read at 595 nm on a S1200 Diode Array Spectrophotometer (WPA) and protein concentration was calculated using a bovine serum albumin (BSA) standard (Thermo Scientific). Samples were diluted to 1 µg/ µl in 1x Laemmli Buffer and either stored at -20 °C or processed by SDS-PAGE/ immunoblot.

For Co-immunoprecipitation assays, total cell lysates were diluted to 2 µg/ µl in 1 ml of BRB80. Myc-tagged proteins were immunoprecipitated by incubating protein lysates with an anti-myc antibody for 16 h at 4°C under gentle mixing and then with 10 µl of Protein G Mag Sepharose Xtra (Cytiva) bead slurry for 2 h at 4°C under gentle mixing. Protein G beads were previously blocked with 2% BSA (Fisher Scientific) in BRB80 ON at 4°C to prevent aspecific protein binding. FLAG-tagged proteins were immunoprecipitated by using 10 µl of anti-FLAG M2 Magnetic Beads slurry incubated for 16 h at 4°C under shaking. Immunocomplexes were separated from the flow through using a magnetic stand (Ambion) and washed 5 times with 500 µl of ice-cold BRB80. Buffer residues were carefully aspirated with a micropipette and the immunoprecipitates were resuspended in 50 µl of 2.5x Laemmli Buffer and immediately processed by SDS-PAGE/ immunoblot.

2.2.6.2 Sequential protein extraction

Experiments were performed in 6-well plates. Cells were moved onto ice, rinsed with PBS and scraped in 300 µl of ice-cold Triton X-100 Extraction Buffer per well. Crude cell lysates were transferred to a benchtop centrifuge tube and sonicated on ice with a probe Vibra Cell sonicator (Sonics) for 10 s in pulsating mode (1 s on, 1 s off) with 30% amplitude. Lysates were incubated on ice for 30 min and then centrifuged at 17,000 rcf for 15 min at 4 °C. The supernatant, named triton X-100-soluble protein (TX-100), was collected. The pellet was resuspended in 300 µl of ice-cold Triton X-100 Extraction Buffer, centrifuged at 17,000 rcf for 15 min at 4 °C and the supernatant was discarded. This step was repeated twice, then the pellet was resuspended in 150 µl of RT SDS Extraction Buffer and sonicated for 15 s in pulsating mode (1 s on, 1 s off) with 30% amplitude. Protein concentration of the TX-100 fraction was measured by colorimetry using a Pierce BCA Protein Assay Kit (Thermo Scientific) according to

manufacturer's instructions. Samples were run in triplicate and absorbance was read at 562 nm on a PheraSTAR FS plate reader. TX-100 fractions were diluted to 1 µg/µl in 1x Laemmli Buffer and SDS fractions were diluted in 1x Laemmli Buffer using the same dilution factor calculated for the corresponding TX-100 fraction. Protein samples were either stored at -20 °C or processed by SDS-PAGE/ immunoblot.

2.2.6.3 SDS-PAGE and immunoblot

Protein samples diluted in Laemmli Buffers were denatured at 95 °C for 5 min, except those intended for detection of LRRK2. From 15 to 60 µg of protein or up to 45 µl of sample were loaded per lane onto an SDS-polyacrylamide gel and separated in Running Buffer applying a constant voltage of 120 V using a Mini-PROTEAN Tetra Cell gel electrophoresis system (Bio-Rad). A Precision Plus All Blue Prestained Protein Standard (Bio-Rad) was run in parallel with all samples as a molecular weight marker. After separation, samples were transferred onto 0.2 µm nitrocellulose (GE Healthcare, for detection of α-synuclein) or 0.45 µm PVDF-FL (Merck) blotting membrane in Transfer Buffer using a Criterion Blotter (Bio-Rad) by applying a constant voltage of 100 V for 30 min (for detection of proteins smaller than 75 kDa) or 30 V for 16 h (for detection of proteins above 75 kDa).

Samples obtained from sequential protein extraction were stained using a Total protein staining Li-COR Revert™ 700 kit, acquired on a Li-COR Odyssey Fc Imaging System and de-stained according to manufacturer's instructions. In all other cases, protein transfer was confirmed by incubating membranes with Ponceau Solution for 1 minute followed by washes with ultrapure H_2O.

Membranes intended for α-synuclein detection were fixed wiht 2% formaldehyde (Sigma-Aldrich) in PBS for 30 minutes followed by two washes with PBS for 5 minutes. Membranes were blocked with 5% BSA (detection of phosphorylated epitopes) or 5% non-fat dry milk (Bio-Rad, any other epitopes) in TBS-T for 1 h at RT under shaking. Membranes intended for Rab10 and phopsho-Rab10-T73 were blocked with EveryBlot Blocking Buffer (Bio-Rad) for 5 min at RT under shaking.

Primary antibodies were diluted in 5% BSA (detection of phosphorylated epitopes) or 5% non-fat dry milk (any other epitopes) in TBS-T according to Tab. 2.4 and incubated either for 1 h at RT or ON at 4°C. Antibodies anti-Rab10 and phopsho-Rab10-T73 were diluted in SignalBoost Immunoreaction Enhancer Solution A (Millipore) according to Tab. 2.4 and incubated ON at 4°C. Membranes were washed 3 times with TBS-T

for 10 min and incubated with secondary antibodies diluted in TBS-T for 1 h at RT (Tab. 2.4). Membranes intended for detection of Rab10 and phopsho-Rab10-T73 were incubated with HRP-conjugated secondary antibodies diluted in SignalBoost Immunoreaction Enhancer Solution B (Millipore) for 1 h at RT. Membranes incubated with fluorescent secondary antibodies were washed 3 times with TBS-T for 10 min and imaged on a Li-COR Odyssey Fc Imaging System. Membranes incubated with HRP-conjugated antibodies were incubated with SuperSignal West Pico Chemiluminescent Substrate (Thermo Scientific) for 5 min prior to acquisition.

2.2.6.4 Dot blot immunodetection of secreted α-synuclein

Conditioned media samples mixed with Laemmli Buffer were incubated at 95 °C for 5 min. 200 ul of sample per well were applied onto a Bio-Dot Microfiltration Apparatus (Bio-Rad) mounting a 0.2 µm nitrocellulose blotting membrane (GE Healthcare) equilibrated with PBS. An equal volume of fresh culture media mixed 4:1 with 5x Laemmli Buffer and treated in parallel with conditioned media samples was used as blank. 20 µl of total cell lysate were loaded as positive control. Protein samples were dot-blotted by applying vacuum, rinsed once with PBS, and fixed with 2% formaldehyde in PBS for 30 min. Fixing solution was removed by applying vacuum and rinsed with PBS. Membranes were removed from the Microfiltration Apparatus, washed with TBS-T, and blocked with 5% non-fat dry milk in TBS-T for 1 h at RT. Antibodies incubation and signal detection was performed as described above.

2.2.6.5 Densitometry analysis

Chemiluminescent or fluorescent signal from immunoblots detected on a Li-COR Odyssey Fc Imaging System was quantified using Image Studio Software (LI-COR Biosciences UK Ltd, Cambridge, UK; version 5.5.4). Protein bands were manually selected using the “Draw Rectangle” tool. Median background was measured at the top and bottom border of each box and automatically subtracted. Signal intensity was normalised to a loading control and expressed as fold change to control treatment. Dot blot experiments were quantified in grid mode selecting the blank sample well for automatic subtraction of User-Defined median background. Signal intensity was normalised to control.

2.2.7 Immunofluorescence and microscopy

2.2.7.1 Immunofluorescence staining of HeLa, HEK293, SHSY-5Y, and BMDMs

Cells were washed with PBS and fixed with 4% formaldehyde in PBS for 30 min. The fixing solution was washed with PBS and quenched with 50 mM NH_4Cl (Sigma-Aldrich) in PBS for 10 min. Cells were permeabilised with 0.2% triton X-100 in PBS for 3 min and then blocked with 0.2% cold water fish gelatine (Sigma-Aldrich) in PBS (blocking solution) for 30 min to reduce aspecific antibody binding. Primary antibodies were diluted in blocking solution as per Tab. 2.4 and incubated for either 3 h (antibodies anti- HDAC6, p62, ubiquitin and vimentin) or 1 h (all other antibodies) at RT in a sealed humidified container. Samples were washed and incubated with blocking solution for 10 min at RT. Secondary antibodies were diluted in blocking solution and incubated for 1 h at RT (Tab. 2.4). Samples were washed three times with blocking solution and counterstained with 1 ng/ µl Hoechst 33342 (Thermo Scientific) in PBS for 10 min. Samples were rinsed with PBS and mounted onto microscopy glass slides (Fisherbrand) with fluorescence mounting medium (Dako).

2.2.7.2 Immunofluorescence staining of COS7 and primary neurons

Cells were washed with PBS and fixed in 4% paraformaldehyde (PFA, ProSciTech), 4% sucrose (Sigma-Aldrich) in PBS for 30 min at RT. Samples obtained from experiments involving PFFs administration were fixed with 4% PFA, 4% sucrose, 1% triton X-100 in PBS for 30 min at RT. Samples were washed 4 times with 0.05% saponin (Sigma-Aldrich) in PBS and blocked with 3% BSA, 0.05% saponin in PBS (blocking solution) for 30 min at RT. Primary antibodies were diluted in blocking solution as per Tab. 2.4 and incubated in a sealed container either for 3 h at RT (experiments on COS7 cells) or ON at 4 °C (experiments on primary neurons). Samples were washed 4 times with 0.05% saponin in PBS and incubated for 1 h at RT with secondary antibody and 1 ng/ µl Hoechst 33342 (Thermo Scientific) diluted in blocking solution (Tab. 2.4). Finally, samples were rinsed with PBS and mounted onto glass microscope slides (Fisherbrand) using ProLong Gold Antifade Mountant (Invitrogen).

2.2.7.3 Immunofluorescence staining of brain sections

Fixed mouse brain sections were kindly provided by Charlotte F. Brzozowski from the University of Alabama at Birmingham (USA). Mice were treated as previously described (Luk *et al.*, 2012). In brief, 4.5-month-old C57BL/6 mice were bilaterally injected into the striatum with either freshly sonicated PFFs or monomeric α-synuclein (injection coordinates: AP from bregma: +1.0; ML from bregma: +/-2.0; DV from dura: -3.2; injection speed: 500 nl/ min; injection volume: 2 uL per site; protein concentration: 5 mg/ ml). Mice were culled 6 weeks post-injection and perfused with 20 ml of saline solution prior to brain extraction. Brains were harvested and dissected on ice. Samples were fixed with 4% PFA for 2 days, incubated in 30% sucrose-PBS for 2 days and snap frozen at -45°C in 2-methylbutane. 40 µm thick coronal sections obtained with a freezing microtome.

Brain sections were washed three times with PBS and incubated in Antigen Retrieval Solution for 1 h at 37 °C. Samples were washed with PBS and incubated in 5% goat serum (Gibco), 0.1% Triton X-100 in PBS for 1 h at RT under shaking. Primary antibodies were diluted in 5% goat serum in PBS and incubated for 24 h at 4 °C under gentle shaking (Tab. 2.4). After rinsing with PBS, brain sections were incubated in secondary antibody and 1 ng/ µl Hoechst 33342 (Thermo Scientific) in 5% goat serum in PBS for 2 h at RT under shaking (Tab. 2.4). Tissues were washed with PBS and mounted onto SuperFrost Plus microscope slides (Fisherbrand) using ProLong Gold Antifade Mountant (Invitrogen).

2.2.7.4 Confocal microscopy and image analysis

Images of immunostained cells were acquired using a 63x HCX PL APO 1.4 NA oil objective on a Leica SP5 confocal microscope (Leica Microsystems Ltd., Milton Keynes, UK) using LAS AF software (Leica Microsystems). Laser intensities, pinhole aperture, detector gains, and acquisition settings were kept constant during experiments to ensure comparability.

Endogenous aggresomes were counted in Fiji software (Schindelin *et al.*, 2012; version 2.9.0/1.53t) using the Cell Counter plugin by quantifying the number of cells containing a single, round, perinuclear, ubiquitin/ p62/ HDAC6- positive inclusion surrounded by a circular basket of vimentin filaments. α-synuclein-positive aggresomes were quantified by counting the number of α-synuclein-YFP expressing

cells containing a single, round, perinuclear, YFP-positive inclusion surrounded by a circular basket of vimentin filaments. Data were expressed as percentage of the total. Synaptic terminal imaging was performed with a scan format of 2048x2048. Images were analysed in Fiji and the JACoP plugin was used to calculate the thresholded Mander's colocalization coefficient (MCC) and the Pearson's correlation coefficient (PCC).

PFFs-treated primary neurons and mouse brain sections were imaged as z-stacks (step size 0.2 µm); maximal projection images were generated using Fiji.

2.2.8 Data analysis

Data calculations were performed using Microsoft Excel (Microsoft Corporation, Redmond, WA, USA; version 16.74) and statistical analysis was performed in Prism 9 (GraphPad Software, LLC; version 9.5.1). Statistical significance between experimental groups was determined by one-way analyses of variance (ANOVA) or unpaired two-tailed t-test as indicated. Multiple comparisons following ANOVA were performed using uncorrected Fisher's Least Significant Difference (LSD) test. Sample sizes, number of independent replicates and other details are reported in the figure legends.

3 Investigation of the interaction between LRRK2 and HDAC6

3.1 Introduction

Prolonged downregulation of the ubiquitin-proteasome system (UPS) leads to misfolded protein stress and stimulates aggrephagy as a supplementary route of protein clearance. In this context, HDAC6 sequesters protein aggregates into an aggresome by binding K63-linked polyubiquitin chains and acting as a cargo adapter for cytoplasmic dynein. The formation of a complex between HDAC6 and dynein is a crucial step in trafficking ubiquitinated protein aggregates into an aggresome (Kawaguchi *et al.*, 2003). In fact, the interaction between HDAC6 and the molecular motor complex increases upon proteasomal inhibition (Kawaguchi *et al.*, 2003; Lucas *et al.*, 2019).

Previous work form the De Vos lab identified a novel role of LRRK2 in regulating HDAC6-dependent recruitment of ubiquitinated protein aggregates into aggresomes (Lucas *et al.*, 2019). Mechanistically, LRRK2 was found to interact with HDAC6 and phosphorylate HDAC6 on serine 22 (HDAC6-S22). This correlates with enhanced interaction of HDAC6 with cytoplasmic dynein and effective recruitment of the ubiquitinated cargo into aggresomes. It was also observed that the phosphodeficient HDAC6 mutant S22A is insensitive to aggrephagy activation, suggesting a role of S22 phosphorylation in aggresome formation. Additional indication of a regulatory function of LRRK2 kinase activity comes from the evidence the kinase-dead mutant LRRK2-D1994A does not support ubiquitin-dependent aggresome formation. Finally, it was found that upregulation of the interaction between HDAC6 and cytoplasmic dynein induced by proteasome inhibition is similarly disrupted upon LRRK2 knock-down. This further confirms LRRK2 as an upstream regulator of the pathway.

Counterintuitively, LRRK2-G2019S, which has enhanced kinase activity, was also found to impair aggresome formation. This observation possibly indicates a more complex interplay between LRRK2 and HDAC6 that the phosphorylation model cannot entirely explain.

In the same study, the binding between LRRK2 and HDAC6 was dissected leading to the observation that both HDAC6 deacetylase domains independently interact with LRRK2 Roc-COR domain. This interaction is affected by either functional or

pathogenic mutations that modify LRRK2 kinase activity. In particular, the kinase hyperactive LRRK2 mutant G2019S showed reduced binding to HDAC6. Conversely, more HDAC6 co-immunoprecipitated with the kinase dead mutant D1994A, indicating a stronger interaction. The opposing effect of these two mutations on the binding with HDAC6 suggests that the interaction is regulated by LRRK2 kinase activity. Moreover, LRRK2 hyperactivity may impair the binding between these molecular partners. If we hypothesize that the binding between LRRK2 and HDAC6 contributes to aggrephagy induction- rather than the sole LRRK2 enzymatic activity-, we might explain why LRRK2-G2019S is equally disruptive to aggresome formation as it is LRRK2 deficiency.

Similarly to aggresome formation, HDAC6 was recently found to regulate an aggresome-like mechanism that mediates innate immunity through inflammasome activation (Magupalli *et al.*, 2020). The inflammasome is a multicomponent protein complex assembled in response to infections, inflammation and many other potentially cytotoxic stimuli. One of the most extensively studied inflammasome activation mechanisms involves nucleotide-binding domain, leucine-rich repeat, and pyrin domain-containing protein 3 (NLRP3) and causes the release of pro-inflammatory cytokines such as interleukin 1β (IL-1β, Martinon *et al.*, 2002). Canonical NLRP3 inflammasome activation requires two steps. Inflammasome priming occurs when an extracellular ligand (such as bacterial toxins or pro-inflammatory cytokines) engages with a pattern recognition receptor (PRR, such as Toll-like receptors, NOD-like receptors or cytokine receptors). This results in activation of the transcription factor NF-κB and expression of inflammasome components, including NLRP3 and the IL-1β precursor pro-IL-1β (Bauernfeind *et al.*, 2009). The co-occurrence of a second danger signal (external ATP, ion imbalance, mitochondrial impairment, lysosomal damage, trans-Golgi disassembly, etc.) translates into the assembly of the NLRP3 inflammasome, an event known as inflammasome activation. This triggers the cleavage of pro-caspase-1 into the two subunits composing active caspase-1. Caspase-1, in turn, cleaves pro-IL-1β, which maturates into IL-1β, and activates the pore-forming protein gasdermin D leading to cytokine release and pyroptosis (Dong *et al.*, 2022; He *et al.*, 2015; Lei *et al.*, 2018).

Magupalli and colleagues reported that NLRP3 inflammasome assembly relates on ubiquitin/HDAC6-mediated retrograde transport of the inflammasome components to the MTOC. They observed that HDAC6 inhibition impairs inflammasome activation

and IL-1β secretion. It was proposed that the enrichment of the inflammasome molecular actors at the MTOC not only promotes a more efficient response to stressors, but it would also facilitate autophagic degradation of the inflammasome to resolve inflammation (Magupalli *et al.*, 2020).

LRRK2 is emerging as a key regulator of innate immunity. LRRK2 is highly expressed in peripheral immune cells and was found to promote NLR family CARD domain-containing protein 4 (NLRC4) inflammasome activation (Liu *et al.*, 2017; Gan *et al.*, 2021). LRRK2 alterations predispose to diseases characterised by a strong inflammatory component, including PD (Ahmadi Rastegar *et al.*, 2020). LRRK2-G2019S is known to cause more pronounced microgliosis and astrogliosis in rodent models of PD, which correlates with increased neuroinflammation and a more severe neurodegenerative phenotype (Lin *et al.*, 2009; Daher *et al.*, 2015; Bieri *et al.*, 2019). On the contrary, LRRK2 KO is linked to anti-inflammatory effects not just in the context of α -synuclein pathology but also in response to other neuroinflammatory agents, both biological and inorganic (Daher *et al.*, 2014; Puccini *et al.*, 2015; Chen *et al.*, 2018).

If LRRK2 regulates HDAC6 role on inflammasome activation in a similar way as we previously found about aggresome formation, we predict that LRRK2 kinase inhibition should reduce inflammasome activation.

3.2 Results

3.2.1 LRRK2 kinase activity is not required for HDAC6-linked aggresome formation

Our previous data indicate that LRRK2 kinase activity may regulate aggresome formation via HDAC6 phosphorylation. Here, we tested if LRRK2 kinase activity is required for aggresome formation in two commonly used cell lines: Hela and COS7. In these *in vitro* systems, aggresome formation can be induced by prolonged proteasome inhibition. HeLa or COS7 cells were treated with MG132 for 16 h to inhibit the proteasome and induce accumulation of protein aggregates into aggresomes. LRRK2 was inhibited with MLi-2, a potent and highly selective LRRK2 kinase inhibitor (Fell *et al.*, 2015). Since HDAC6 deacetylase activity is required for aggresome formation (Kawaguchi *et al.*, 2003), the HDAC6 inhibitor tubastatin A was used as control of aggresome formation dysregulation. Cells were fixed and immunostained using antibodies anti ubiquitin, HDAC6, p62 and vimentin. Samples were imaged on a confocal microscope and the percentage of cells containing a mature aggresome was quantified in blind. We defined an aggresome as a single, round, perinuclear inclusion, which is positive to ubiquitin, HDAC6 and p62 and is enclosed within a nest-like cage of vimentin filaments (Fig. 3.1a, d). At the time when the aggresome formation assays were performed in HeLa, we could not rely on a robust protocol to assess endogenous LRRK2 kinase activity. Hence, MLi-2 target engagement was confirmed by immunoblot by quantifying the phosphorylation level of the LRRK2 substrate Rab8a-T72 in HeLa co-expressing EGFP-Rab8a and myc-LRRK2-G2019S and exposed to the same inhibitors mix incubated in the main experiment (Fig. 3.1b). To test LRRK2 inhibition in COS7, part of the cell samples was lysed, separated by SDS-PAGE and immunoblotted using antibodies anti phospho-Rab10-T73 (Fig. 3.1e). HDAC6 inhibition was confirmed by immunoblot by quantifying tubulin acetylation levels (Fig. 3.1c, f).

Approximately 35% of HeLa cells and 60% of COS7 cells treated with MG132 showed condensation of p62, ubiquitin (HeLa) and HDAC6 (COS7) into a perinuclear inclusion. Concomitantly, the vimentin cytoskeleton underwent marked architectural reorganisation and formed a cage surrounding the aggresome. As expected, HDAC6 inhibition significantly impaired the cells' ability to recruit protein aggregates into aggresomes. In fact, the percentage of cells containing a mature aggresome was

reduced by about 1/3 compared to control in both HeLa and COS7 (~20% and ~40% respectively). Administration of tubastatin A was associated with the presence of ubiquitin-, HDAC6- and p62- positive puncta scattered across the cytoplasm. However, the formation of vimentin nest-like structures seemed overall unperturbed, which suggests the formation of ubiquitin/HDAC6-independent aggresomes. Quantification of the phosphorylation status of Rab8a or Rab10 by immunoblot confirmed that MLi-2 effectively inhibited LRRK2 under these experimental conditions (Fig. 1.1b, e). Nonetheless, samples treated with MLi-2 were morphologically indistinguishable from cells treated with MG132-only. In fact, the percentage of HeLa and COS7 cells incubated with MLi-2 harbouring an aggresome was comparable to the respective controls (Fig. 1.1a, d). Taken together, these data indicate that LRRK2 kinase activity is not required for ubiquitin/HDAC6-dependent aggresome formation in a physiological background. Hence, it is likely that LRRK2 role in aggrephagy is not mediated by its kinase activity, as previously hypothesised.

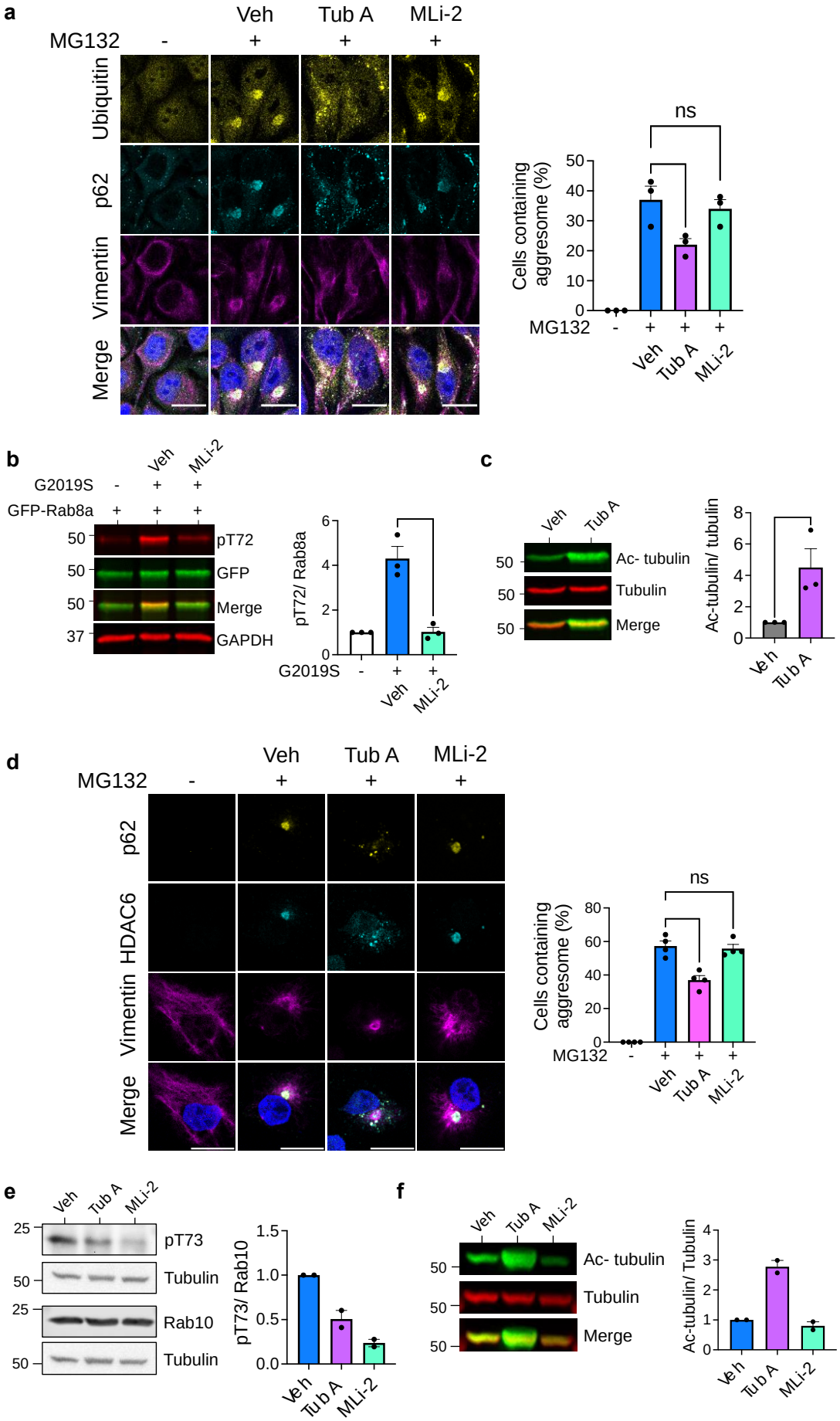
a
Veh
Tub A
MLi-2
MG132
Ubiquitin
p62
Vimentin
Merge
ns
Cells containing aggresome (%)
b
G2019S
GFP-Rab8a
pT72
GFP
Merge
GAPDH
pT72/ Rab8a
c
Ac- tubulin
Tubulin
Ac-tubulin/ tubulin
d
HDAC6
e
pT73
Rab10
pT73/ Rab10
f

Figure 3.1 LRRK2 kinase inhibition does not affect aggresome formation. a) HeLa treated with MG132 and either DMSO (Veh), MLi-2 or tubastatin A for 16 h. Samples were fixed and immunostained with antibodies anti- ubiquitin (yellow), p62 (cyan) and vimentin (magenta). Nuclei were counterstained with Hoechst (blue). The percentage of cell containing an aggresome was quantified. One-way ANOVA with Fisher's LSD test; N= 3, ~200 cells analysed per condition per experiment. **b)** HeLa transfected with GFP-Rab8a and either empty vector or myc-LRRK2-G2019S. 24 h post-transfection, samples were incubated with the same inhibitor mix used in a). Protein lysates were processed by SDS-PAGE and immunoblotted using antibodies anti- GFP, phospho-Rab8a-T72 and GAPDH. Unpaired t-test. N= 3. **c)** HeLa treated as in a) were lysed and processed by SDS-PAGE and immunoblotted using antibodies anti total and acetylated-tubulin. Unpaired t-test. N= 3. **d)** COS7 treated as in a) fixed and immunostained using antibodies anti- p62 (yellow), HDAC6 (cyan) and vimentin (magenta). Nuclei were counterstained with Hoechst (blue). The percentage of cell containing an aggresome was quantified. One-way ANOVA with Fisher's LSD test; N= 4, ~150 cells analysed per condition per experiment. **e)** COS7 treated as in a) were lysed, processed by SDS-PAGE and immunoblotted using antibodies anti- phospho-Rab10-T73, Rab10 and tubulin. N= 2. **f)** COS7 treated as in a) were lysed, processed by SDS-PAGE and immunoblotted using antibodies anti total and acetylated-tubulin. N= 2.
All data are shown as mean± SEM. ns= non-significant; *= p≤ 0.05; **= p≤ 0.01; ***= p≤ 0.001. Scale bar= 20 µm.

3.2.2 LRRK2 kinase activity does not regulate NLRP3 inflammasome activation

We previously mentioned the similarities between the molecular dynamics leading to aggresome formation and inflammasome activation. Both processes involve retrograde trafficking of ubiquitinated protein cargoes mediated by HDAC6. Based on the indication that LRRK2 may regulate HDAC6 by phosphorylation, we investigated if LRRK2 kinase activity modulates the inflammasome activation response in DIV14 murine bone marrow- derived macrophages (BMDMs). In brief, bone marrow was harvested from young adult male mice and differentiated for 14 days into BMDMs in BMDMs growth medium. At day DIV14, cell samples were fixed and immunostained using an antibody anti F4/80 to assess the complete differentiation of the myeloid precursors into mature macrophages (Fig. 3.2a). DIV14 BMDMs were incubated with LPS for 4 h to induce inflammasome priming. Either tubastatin A or MLi-2 were added to the culture media at this step. 30 minutes before samples collection, primed macrophages were exposed to ATP to induce inflammasome activation and IL-1β secretion. Cells were lysed in 2.5x Laemmli buffer, processed by SDS-PAGE and immunoblotted for pro-IL-1β and tubulin (Fig. 3.2b). Conditioned media samples were collected and analysed with a commercial enzyme-linked immunosorbent assay (ELISA) for quantitative detection of mouse IL-1β (Fig. 1.2 c). HDAC6 inhibition was confirmed by immunoblot on total cell lysates using an anti- acetylated tubulin antibody (Fig. 3.2d).

LPS administration effectively induced inflammasome priming, detected as a surge in pro-IL-1β expression. Additional exposure to extracellular ATP caused NLRP3 inflammasome activation. This resulted in the maturation of pro-IL-1β into IL-1β and its subsequent secretion, which correlated with a decrease in the level of pro-IL-1β detected by immunoblot. In agreement with Magupalli and colleagues, HDAC6 inhibition with tubastatin A significantly mitigated the overexpression of pro-IL-1β in response to LPS (Fig. 1.2 b). Concomitantly, tubastatin A also reduced IL-1β secretion upon ATP administration (Fig. 1.2 c). This confirms that HDAC6 is required for both NLRP3 inflammasome priming and activation. As opposed to HDAC6 inhibition, MLi-2 administration did not produce any detectable effect on pro-IL-1β expression and IL-1β secretion in response to pro-inflammatory stimuli (Fig. 3.2b, c). Thus, similarly to what we observed on aggresome formation, LRRK2 kinase activity does not regulate NLRP3 inflammasome priming and activation.

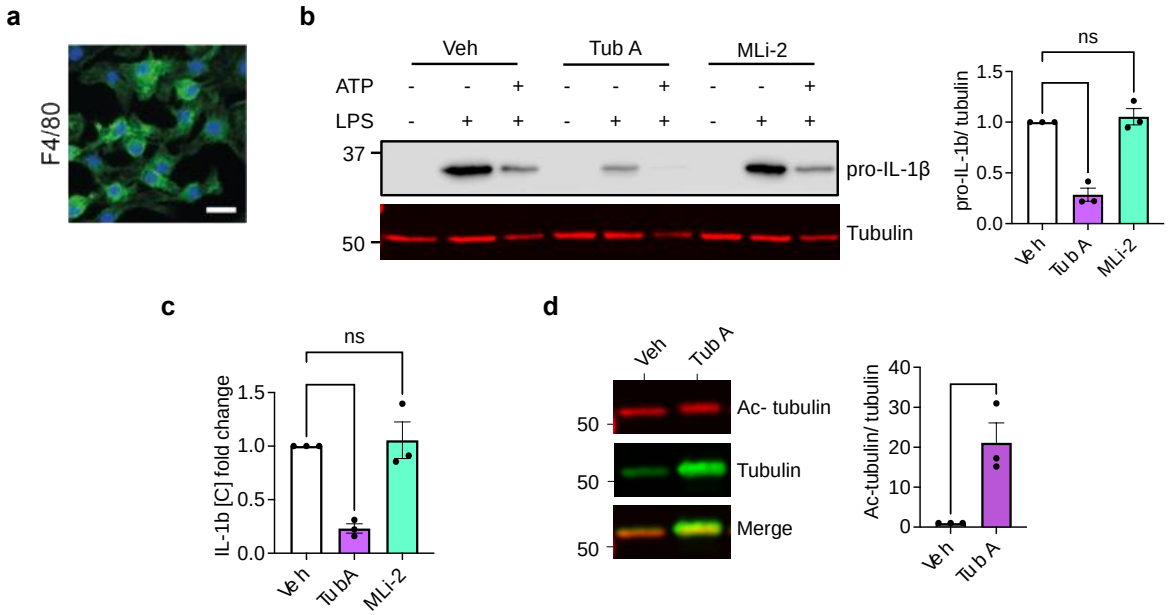

Figure 3.2 LRRK2 kinase inhibition does not affect inflammasome activation. a) DIV14 BMDMs fixed and immunostained with an antibody anti- F4/80 (green). Nuclei were counterstained with Hoechst (blue). Scale bar= 20 µm. **b)** DIV14 BMDMs were exposed to lipopolysaccharide (LPS) and either DMSO (Veh), tubastatin A (tub A) or MLi-2 for 4 h. ATP was added 30 min before samples collection. Protein lysates were processed by SDS-PAGE and immunoblotted using antibodies anti- pro-IL-1β and tubulin. The graph shows the quantification of pro-IL-1β expression level upon inflammasome priming by LPS administration. One-way ANOVA with Fisher's LSD test; N= 3. **c)** ELISA quantification of the concentration IL-1β secreted in the conditioned media of BMDMs treated with LPS+ ATP as described in b). One-way ANOVA with Fisher's LSD test; N= 3. **d)** Protein lysates of BMDMs treated with either DMSO (Veh) or tubastatin A for 4 h were separated by SDS-PAGE and immunoblotted using antibodies anti- total and acetylated tubulin. Unpaired t-test. N= 3.
All data are shown as mean± SEM; ns= non-significant; **= p≤ 0.01; ***= p≤ 0.001.

3.2.3 LRRK2 does not regulate HDAC6-S22 phosphorylation

In a previous study conducted in the De Vos lab, a siRNA knockdown (KD) approach was used to conclude that LRRK2 promotes ubiquitin-dependent targeting of protein aggregates to the aggresome by phosphorylating HDAC6-S22. It was observed that MG132 administration increases the interaction between HDAC6 and dynein. This change is prevented by LRRK2 KD or expression of the phospho-deficient mutant HDAC6-S22A (Lucas *et al.*, 2019). Nevertheless, our latest data collected by utilising targeted inhibitors suggest that LRRK2 kinase activity is not required in aggresome formation. To clarify this contradicting evidence, we investigated the effect of LRRK2 inhibition on HDAC6-S22 phosphorylation upon induction of proteotoxic stress.

First, we confirmed the specificity of the antibody anti- phosphorylated HDAC6-S22 used by Lucas and colleagues (Abcam, RRID: AB_942257). FLAG-tagged HDAC6 either WT or the phospho-deficient mutant S22A was transfected into HEK293 cells. 24 h post-transfection, samples were lysed, processed by SDS-PAGE, and immunoblotted using antibodies anti- FLAG and phosphorylated HDAC6. Next, we used LRRK2 kinase inhibitors to test whether LRRK2 modifies HDAC6-S22 phosphorylation status. FLAG-HDAC6 was transiently expressed in HEK293 cells. 24 h post-transfection samples were treated with MG132 to stimulate aggrephagy activation and promote HDAC6 phosphorylation. LRRK2 was inhibited by treating samples with MLi-2. After 2 h of incubation, cells were lysed, processed by SDS-PAGE, and immunoblotted using antibodies anti- FLAG and phopsho-HDAC6-S22. LRRK2 inhibition was confirmed by assessing Rab10-T73 phosphorylation levels.

The antibody anti-phosphorylated HDAC6 herein tested showed high specificity for the S22 phospho-site. In fact, no signal was detected when the HDAC6 phospho-deficient mutant S22A was expressed (Fig. 1.3a). No changes in HDAC6 phosphorylation were observed upon 2 h of proteasome inhibition (Fig. 3.3b). This suggests that HDAC6-S22 phosphorylation does not increase upon proteotoxic stress or that a longer incubation might be required to observe any changes. MLi-2 administration reduced Rab10-T73 phosphorylation by more than 75% (Fig. 1.3c). However, LRRK2 inhibition had no effect on the basal phosphorylation level of HDAC6-S22 (Fig. 3.3b). This indicates that LRRK2 might not be the main kinase targeting HDAC6 on this residue.

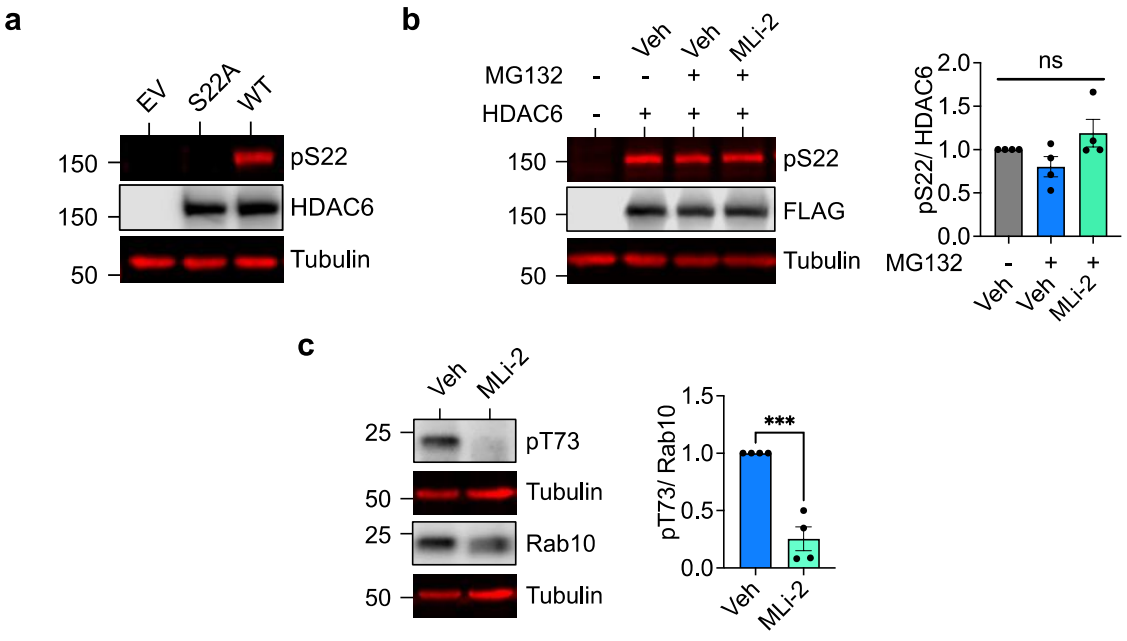

Figure 3.3 LRRK2 does not phosphorylate HDAC6-S22. a) HEK293 expressing either an empty vector (EV) or FLAG-HDAC6 WT or phospho-deficient (S22A) were lysed and processed by SDS-PAGE. Samples were immunoblotted using antibodies anti- phospho-HDAC6-S22, FLAG and tubulin. N=2 **b)** HEK293 expressing FLAG-HDAC6 were treated with MG132 and MLi-2 for 2 h. Protein lysates were processed by SDS-PAGE and immunoblotted using antibodies anti- phospho-HDAC6-S22 (Abcam, RRID: AB_942257), FLAG and tubulin. One-way ANOVA; N= 4. **c)** Protein samples from b) were immunoblotted using antibodies anti- phospho-Rab10-T73, Rab10 and tubulin. Unpaired t-test; N= 4.

All data are shown as mean± SEM; ns= non-significant; ***= p≤ 0.001.

3.2.4 The binding between LRRK2 and HDAC6 is affected by LRRK2 kinase activity

Our previous data indicate an inverse correlation between LRRK2 kinase activity and its interaction with HDAC6. The gain-of-function LRRK2 mutation G2019S impairs the binding between LRRK2 and HDAC6, which may translate into an aggresome formation deficit (Lucas *et al.*, 2019). Here we aimed to confirm if LRRK2 activation status influences this interaction by using LRRK2 kinase inhibitors.

HEK293 were transfected with either WT or G2019S myc-LRRK2 and FLAG-HDAC6. The day after transfection samples were treated with MLi-2 for 4 h. Total protein lysates were incubated with an anti-myc antibody to precipitate LRRK2. The resulting immune pellets were separated by SDS-PAGE and both myc-LRRK2 and FLAG-HDAC6 were detected by immunoblot (Fig. 3.4a). LRRK2 inhibition was confirmed by immunoblot by assessing Rab8a-T72 phosphorylation on HEK293 expressing myc-LRRK2-G2019S and EGFP-Rab8a incubated with the same media used for the main experiment (Fig. 3.4 b).

In line with previous findings, the G2019S mutation significantly reduced the amount of HDAC6 that co-immunoprecipitated with LRRK2. This confirms that the kinase hyperactive G2019S mutant displays a pathological molecular phenotype characterised by weaker binding to HDAC6. Inhibition of LRRK2 kinase activity by MLi-2 administration restored the interaction between the two proteins to the same levels as WT LRRK2. However, due to the high variability of the experimental output, no significant effect was detected on the amount of HDAC6 interacting with WT LRRK2 upon LRRK2 kinase inhibition (Fig. 3.4a, second bar of the histogram).

These data point out that the binding between LRRK2 and HDAC6 is affected by pathological upregulation of LRRK2 kinase activity. Such effect can be rescued by pharmacological LRRK2 inhibition. We did not find evidence that downregulation of WT LRRK2 promotes the interaction with HDAC6.

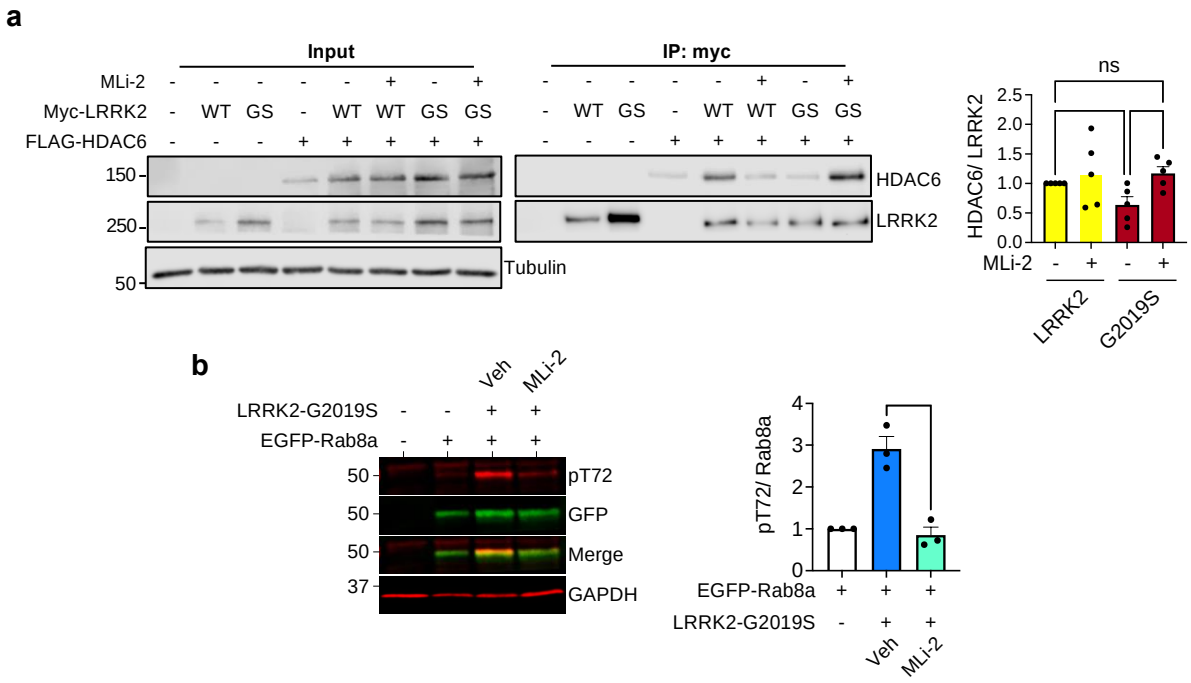

Figure 3.4 Kinase inhibition rescues the interaction between LRRK2-G2019S and HDAC6. a) HEK293 expressing either WT or G2019S myc-LRRK2 and FLAG-HDAC6 were treated with MLi-2 for 4 h. Cells were lysed and LRRK2 was immunoprecipitated using an anti-myc antibody. Both the total cell lysates (Input) and the immune pellets (IP) were processed by SDS-PAGE and immunoblotted using antibodies anti- FLAG, myc, and tubulin. One-way ANOVA with Fisher's LSD test; N= 5. **b)** HEK293 transfected with GFP-Rab8a and either empty vector or myc-LRRK2-G2019S. 24 h post-transfection, samples were incubated with the same inhibitor mix used in a). Protein lysates were processed by SDS-PAGE and immunoblotted using antibodies anti- GFP, phospho-Rab8a-T72 and GAPDH. Unpaired t-test. N= 3.

All data are shown as mean± SEM; ns= non-significant; *= p≤ 0.05; **= p≤ 0.01.

3.3 Discussion

Previous data from our group indicate that both LRRK2 KO and expression of the kinase dead LRRK2 mutant D1994A have a similar negative impact on ubiquitin-dependent targeting of protein aggregates to the aggresome. This suggests that LRRK2 kinase activity is required to sustain aggresome formation. To test this hypothesis, we used the potent and highly selective kinase inhibitor MLi-2 and measured the effect of LRRK2 inhibition on aggresome formation induced by proteasome inhibition. Under these conditions, ubiquitinated protein aggregates accumulated into an aggresome surrounded by displaced vimentin filaments. Here, they colocalized with p62 and HDAC6. Administration of the HDAC6 inhibitor tubastatin A partially disrupted the targeting of ubiquitinated aggregates to the aggresome, which confirmed the engagement of a HDAC6-dependent transport mechanism. In contrast to our prediction, LRRK2 inhibition- confirmed by assessing the phosphorylation levels of established LRRK2 substrates- did not affect the percentage of cells forming ubiquitin-dependent aggresomes. Our findings were corroborated in two unrelated fibroblast-like cell lines.

Following the hypothesis of a kinase-dependent regulation of HDAC6 by LRRK2, we explored other cytoplasmic functions of this histone deacetylase. Recent reports indicate that HDAC6 mediates assembly and activation of the NLRP3 inflammasome through a trafficking mechanism similar to aggresome formation (Magupalli *et al.*, 2020). In line with the work of Magupalli and colleagues, HDAC6 inhibition in BMDMs reduced the expression of pre-IL-1β upon NLRP3 inflammasome priming. We also recorded a significantly lower secretion of mature IL-1β in response to inflammasome NLRP3 activation. However, similar to what we found for aggresome formation, LRRK2 inhibition had no effect on NLRP3 inflammasome priming and activation.

Our data align with the work of Liu and co-workers, who found that neither LRRK2 KO nor LRRK2 kinase inhibition influence NLRP3 inflammasome activation. In fact, they observed that LRRK2 is an upstream activator of the NLRC4 inflammasome signalling (Liu *et al.*, 2017). In contrast, Pajarillo and colleagues reported that LRRK2 mediates the neuroinflammatory response caused by exposure to manganese via kinase-dependent activation of the NLRP3 inflammasome (Pajarillo *et al.*, 2023). It has been proposed that Rab10 overactivation dysregulates the autophagolysosomal pathway, resulting in leakage of lysosomal enzymes that sustain the proteolytic activity of the

inflammasome (Bruchard *et al.*, 2013; dos Santos *et al.*, 2018; Pajarillo *et al.*, 2023). However, the effect of LRRK2 expression on trafficking and clearance of inflammasome components has not been assessed. Hence, the occurrence of HDAC6-dependent effects is unknown in this context. It should be noted that the work by Pajarillo and colleagues was conducted on LRRK2 overexpression models rather than in a physiological LRRK2 background (Liu *et al.*, 2017; Pajarillo *et al.*, 2023). This suggests that the studies mentioned above focus on two different aspects of LRRK2 regulation. One examines the physiological role of the kinase (Liu *et al.*, 2017), whereas the other describes a pathogenic gain-of-function caused by LRRK2 upregulation, which can be mitigated by the administration of LRRK2 inhibitors (Pajarillo *et al.*, 2023).

In general, LRRK2 inhibition or KD are linked to anti-inflammatory and neuroprotective effects in acute α-synuclein overexpression rat models (Daher *et al.*, 2014, 2015). Intriguingly, inhibition of NLRP3 inflammasome has been consistently shown to protect against PD phenotypes, as opposed to the NLRC4 inflammasome (Gordon *et al.*, 2018; Haque *et al.*, 2020). Thus, further work is needed to fully resolve the mechanisms by which LRRK2 supports natural immunity and contributes to inflammation.

Altogether, our results contradict our original hypothesis and suggest that HDAC6's role as a cargo adaptor in aggrephagy and NLRP3 inflammasome activation does not require LRRK2 kinase activity. Combined with the indication that LRRK2 KO impairs the trafficking of ubiquitinated protein aggregates into aggresomes, these data indicate that LRRK2 regulates HDAC6 via a kinase-independent mechanism.

In the work leading up to this project, HDAC6 was proposed as a LRRK2 substrate based on *in vitro* phosphorylation assays followed by mass spectrometry analyses. These experiments led to the identification of HDAC6-S22 as the main putative HDAC6 phosphorylation site targeted by LRRK2. This was corroborated by the indication that LRRK2 overexpression increases HDAC6-S22 phosphorylation (Lucas *et al.*, 2019). It was also indirectly suggested that LRRK2-dependent phosphorylation of HDAC6-S22 increases the interaction between HDAC6 and dynein following accumulation of aggrephagy substrates (Lucas *et al.*, 2019). These data are in contrast with the evidence presented here that shows that LRRK2 kinase activity is not required to induce HDAC6-dependent aggresome formation. Hence, to clarify this

apparent contradiction we investigated the effective impact of LRRK2 kinase activity on HDAC6-S22 phosphorylation utilising a pharmacological approach. Firstly, we did not find confirmation that the disruption to protein clearance caused by proteasome inhibition leads to HDAC6-S22 hyperphosphorylation. Nevertheless, this should be further investigated in an extensive time-course experiment. Additionally, LRRK2 kinase inhibition did not change HDAC6-S22 phosphorylation. For comparison, we recorded a ~75% decrease in Rab10 phosphorylation levels, a well-defined LRRK2 substrate.

HDAC6 is targeted by a heterogeneous group of kinases, including Aurora A (AurA; Pugacheva *et al.*, 2007), epidermal growth factor receptor (EGFR; Deribe *et al.*, 2009), glycogen synthase kinase 3β (GSK3β; Chen *et al.*, 2010), casein kinase 2 (CK2; Watabe *et al.*, 2011), protein kinase Cα (PKCα; Zhu *et al.*, 2011), G protein-coupled receptor kinase 2 (GRK2; Lafarga *et al.*, 2012), extracellular signal-regulated kinase (ERK; Williams *et al.*, 2013), and peptidyl-prolyl cis/trans isomerase NIMA-interacting 1 (PIN1; Chuang *et al.*, 2018). With the exception of EGFR, which inhibits HDAC6 activity, all the other aforementioned kinases enhance HDAC6 downstream effects, including aggrephagy, tubulin deacetylation, depression of subcellular trafficking and increase of cell motility. To date, the confirmed HDAC6 phosphorylation sites encompass 4 serine (S22, S412, S458 and S1035) and one tyrosine residue (Y570; Fig. 1.7). In the specific case of S22 phosphorylation, at least two kinases were found to modulate this PTM. By targeting S22, GSK3β increases HDAC6 deacetylase activity and reduces axonal trafficking of mitochondria in hippocampal neurons (Chen *et al.*, 2010). Concomitantly, PIN1-dependent S22 phosphorylation promotes cell migration and invasion in lung cancer cells (Chuang *et al.*, 2018). None of these studies explored the impact of S22 phosphorylation on aggrephagy. On the other hand, CK2 has been specifically found to increase aggresome formation and clearance by phosphorylating S458 (Watabe *et al.*, 2011). Given the convergence of multiple pathways on the same serine residue, it is possible that the contribution of LRRK2 to S22 phosphorylation may be masked by other kinases. Thus, LRRK2 inhibition does not result in any detectable changes, as opposed to LRRK2 overexpression (Lucas *et al.*, 2019). Additionally, although LRRK2 might physiologically target S22, this PTM may regulate biological processes other than aggresome formation. Finally, it is worth mentioning that a recent study did not detect any changes in HDAC6-S22 phosphorylation in SH-SY5Y cells stably expressing either WT or G2019S LRRK2 (Lin *et al.*, 2020). This

opens to the possibility that the LRRK-dependent phosphorylation of HDAC6-S22 originally detected by Lucas and colleagues may be an experimental artefact.

Once we excluded direct HDAC6 phosphorylation as a putative mechanism by which LRRK2 supports aggresome formation, we researched evidence of alternative models by focussing on the binding between LRRK2 and HDAC6. It was previously found that loss and gain of function mutations have opposing effects on the interaction between LRRK2 and HDAC6 (Lucas *et al.*, 2019). The kinase dead LRRK2 mutant D1994A binds more strongly to HDAC6 compared to WT LRRK2. Conversely, the kinase hyperactive G2019S mutant shows reduced binding (Lucas *et al.*, 2019). This suggests that LRRK2 kinase activity influences its binding to HDAC6 and that the hyperactivity of the G2019S mutant may lead to abnormal binding affinity. We confirmed this hypothesis by inhibiting LRRK2, which rescued the binding between LRRK2-G2019S and HDAC6.

LRRK2 harbours numerous heterologous and auto-phosphorylation sites, some of which are located in the binding site for HDAC6, namely the Roc-COR domain (Lucas *et al.*, 2019; Marchand *et al.*, 2020). Among these, a cluster of at least 10 independently confirmed autophosphorylation sites (S1292, S1343, T1348, T1368, S1403, T1404, T1410, T1444, T1491, and T1503) is consistently hyperphosphorylated in G2019S-LRRK2 (Marchand *et al.*, 2020). It is possible that the aberrant autophosphorylation of the Roc-COR domain caused by kinase upregulation may interfere with the recruitment of HDAC6 and impinge upon aggrephagy. Future work will confirm if rescuing the interaction between LRRK2-G2019S and HDAC6 is sufficient to restore HDAC6-dependent aggresome formation in a G2019S background.

Our data support a model were aggresomal targeting of ubiquitinated aggregates relies on the binding between LRRK2 and HDAC6 rather than LRRK2 kinase activity. As our understanding of the processes regulated by LRRK2 becomes more detailed, the mechanisms by which this protein operates acquire new levels of complexity. LRRK2 is emerging as an important signalling scaffold which enhances protein-protein contacts. This scaffolding function has been described for Wnt signalling and for the ASK1-MKK3/6-p38 MAPK pathway, where LRRK2 scaffolding properties facilitate the interaction between pathway components and increase their activation efficiency (Berwick and Harvey, 2012; Yoon *et al.*, 2017). Notably, this function is altered by PD-

causative LRRK2 mutations (Berwick and Harvey, 2012). The literature also offers examples of LRRK2 operating independently from its basal kinase activity. LRRK2 interacts with high affinity with the MT associated protein tau and with cyclin dependent kinase 5 (CDK5). The formation of a ternary complex increases CDK5-mediated tau phosphorylation (Shanley *et al.*, 2015). Another work found that the PD-linked variant E193K does not influence LRRK2 kinase activity but prevents mitochondrial fission by interfering with the recruitment of DRP1 (Perez Carrion *et al.*, 2018).

We can speculate that LRRK2 may play a similar role in aggrephagy by bringing together HDAC6 and its activator(s) to promote aggresome formation. This would explain why aggresome formation is not affected by LRRK2 kinase inhibitors under physiological conditions. To the best of our knowledge, the only HDAC6 kinase so far identified as a LRRK2 interactor is GSK3β (Lin *et al.*, 2010), which regulates HDAC6 deacetylase activity by phosphorylation (Chen *et al.*, 2010; Manca *et al.*, 2019; Singh *et al.*, 2019). Although modulation of HDAC6 enzymatic activity can impact ubiquitin-dependent aggresome formation (Kawaguchi *et al.*, 2003), a direct connection between GSK3β and aggrephagy has never been explored.

We acknowledge that a model where LRRK2 provides a scaffold for HDAC6 and a not yet identified activator cannot explain why the kinase-inactivating mutation D1994A- which strengthens the binding to HDAC6- does not promote aggresome formation (Lucas *et al.*, 2019). It is possible that this mutation interferes with the recruitment of the hypothetical HDAC6 activator. This should be verified by testing other kinase inactive mutants already described in literature, such as K1906A, K1906M, D1994N, D2017A, S2032A, and T2035A (Smith *et al.*, 2006; Haebig *et al.*, 2010). It would also be interesting to explore the impact of other PD-linked LRRK2 mutants on HDAC6-dependent aggresome formation. This may provide important insights on the interplay between these key regulators of protein metabolism.

4 Role of HDAC6 in the formation of Lewy body-like α-synuclein inclusions

4.1 Introduction

Progressive accumulation of ubiquitinated α-synuclein inclusions affecting the soma (Lewy bodies) and the neuronal projections (Lewy neurites) is a hallmark of both familial and sporadic PD (Spillantini *et al.*, 1997, 1998; Iwatsubo, 2003). The prion-like mechanism of α-synuclein aggregation has been extensively characterised *in vitro* and follows a sigmoidal curve (Paciotti *et al.*, 2018). During this process, soluble α-synuclein monomers coalesce to form transient oligomeric structures. These act as nucleation centres for the polymerisation of natively unfolded α-synuclein monomers into highly ordered β-sheet-rich fibrillary aggregates (Celej *et al.*, 2012; Chen *et al.*, 2018). Several factors contribute to α-synuclein nucleation and polymerisation including missense mutations, post-translational modifications, cellular microenvironment abnormalities, molecular crowding and presence of other ligands and aggregation partners (Vidović *et al.*, 2022).

The accumulation of α-synuclein oligomers and aggregates in neurons, glial cells and in the extracellular milieu eventually results in neuronal loss. Even if the multifaceted mechanisms linking α-synuclein burden to PD aetiology are not fully uncovered, there is evidence of numerous cellular physiology alterations. These encompass mitochondrial damage, oxidative stress, subcellular trafficking disruption, synaptic dysfunction, loss of membrane integrity, protein dyshomeostasis, gene expression dysregulation, DNA damage and inflammation (Ma *et al.*, 2014; Bernal-Conde *et al.*, 2020; He *et al.*, 2020; Brás and Outeiro, 2021).

Both the proteasome and autophagy (mainly CMA and macroautophagy) are involved in targeted clearance of α-synuclein monomers and aggregates. Moreover, both proteasomal and lysosomal degradation routes are affected by α-synuclein accumulation and display abnormalities in PD (Stefanis *et al.*, 2019). Particular attention has been drawn by the role played by lysosomes in PD aetiology and progression, given their central role in degradation of α-synuclein oligomers and fibrils. As such, restoration of the autophagic flux is being explored as a potential therapeutic strategy (Erekat, 2022).

Compelling evidence underly the contribution of LRRK2 in causing protein dyshomeostasis not just in hereditary PD but also in sporadic forms of the disease (Pérez-Carrión *et al.*, 2022). Additionally, it is now clear that LRRK2 alterations exacerbate most of the pathological phenotypes associated with α-synuclein aggregation (Dues *et al.*, 2020; Jeong *et al.*, 2020; O'Hara *et al.*, 2020). As already mentioned, LRRK2 was recently found to regulate aggrephagy via HDAC6. It was also observed that aggresome formation is disrupted in patient-derived iAstrocytes carrying the G2019S mutation (Lucas *et al.*, 2019). This might have important implications for the clearance of potentially cytotoxic protein aggregates, such as α-synuclein oligomers and fibrils. Even if a communal origin for aggresomes and Lewy bodies has been hypothesised (Olanow *et al.*, 2004; Tanaka *et al.*, 2004), the relevance of HDAC6-mediated aggrephagy in degradation of α-synuclein aggregates has never been fully explored. Most importantly, the majority of the studies aiming to dissect aggrephagy was carried out in non-neuronal cell lines. To the best of our knowledge, the literature lacks neuronal models of aggresome formation. In fact, little is known about how and if aggrephagy operates in the cell type most affected by α-synuclein aggregation. Therefore, we implemented an *in vitro* model to clarify whether α-synuclein aggregates are recruited into aggresomes and investigate if LRRK2/ HDAC6-linked aggrephagy contributes to α-synuclein clearance.

4.2 Results

4.2.1 Establishing a neuronal-like in vitro model of aggresome formation

The neuroblastoma cell line SH-SY5Y is an inexpensive *in vitro* model commonly used to recapitulate a few cellular and molecular aspects of PD. One of the advantages of this tool is the possibility to differentiate SH-SY5Y cells into monocultures of mature dopaminergic neurons within 6-10 days (Ioghen *et al.*, 2023).

Aggresome formation upon proteasome inhibition has been reported in SH-SY5Y in a few studies (Muqit *et al.*, 2004; Bang *et al.*, 2016; Kwon *et al.*, 2020). Hence, we tested 4 different MG132 administration protocols described in other works to establish and characterise a neuronal-like model of aggresome formation.

WT, undifferentiated SH-SY5Y were plated on glass coverslips. The following day, samples were treated with MG132 according to one of the following protocols. Protocol 1 consists of a 16 h pre-treatment step with 0.1 µM MG132, followed by an 8 h recovery step in fresh media and a 16 h treatment with 1 µM MG132 (Kwon *et al.*, 2020). Protocol 2 consists of a 16 h pre-treatment step with 0.25 µM MG132, followed by an 8 h recovery step in fresh media and a 16 h treatment with 2.5 µM MG132 (Bang *et al.*, 2016). Protocol 3 consists of an 18 h incubation with 1 µM MG132 (Iqbal *et al.*, 2020). Protocol 4 (which mimics the conditions previously tested on HeLa and COS7) consists of an 18 h incubation with 5 µM MG132. Post incubation, cells were fixed and immunostained using antibodies anti- ubiquitin, p62 and vimentin and imaged on a confocal microscope.

As opposed to what we observed in HeLa and COS7 cell lines (Fig. 1.1 a, d), only a few SH-SY5Y cells (less than 10 per coverslip) were found to harbour a perinuclear ubiquitin- and p62- positive inclusion (consistent with ubiquitin/HDAC6-dependent aggresome formation). By visual examination, Protocol 3 was the most effective at inducing ubiquitin-dependent aggresome formation in SH-SY5Y. However, the high cell toxicity caused by prolonged proteasome inhibition and the unexpectedly low number of cells forming detectable ubiquitin-positive aggresomes prevented any accurate quantification. Across all the conditions, most of the cells presented a vimentin nest-like structure that did not enwrap any ubiquitin or p62 speckles (Fig. 4.1a).

Since reorganisation of the vimentin cytoskeleton is often linked to misfolded protein stress and aggresome formation, we investigated if the appearance of a vimentin cage

in SH-SY5Y is an HDAC6-dependent phenomenon. SH-SY5Y were plated on glass coverslips and treated with 1 µM MG132. 10 µM tubastatin A was used to inhibit HDAC6. Samples were incubated for 18 h, then fixed and immunostained using antibodies anti- ubiquitin and vimentin. Images were acquired on a confocal microscope. To confirm the intracellular accumulation of ubiquitinated protein aggregates upon proteasome inhibition, part of the cell samples was processed by sequential protein extraction. In brief, cells were lysed in TBS+ 1% triton X-100 and centrifuged. The supernatant, named triton-soluble protein fraction, was collected and the insoluble pellet was resuspended in TBS+ 2% SDS to obtain the SDS-soluble protein fraction. The triton-soluble fraction virtually contains all the soluble, non-aggregated protein pool. On the contrary, the SDS-soluble fraction mostly contains protein oligomers, polymers and aggregates. Protein samples were separated by SDS-PAGE and immunoblotted using an anti-ubiquitin antibody.

Proteasome inhibition caused rearrangement of the vimentin cytoskeleton into a perinuclear nest-like structure in about 55% of the cells. However, no ubiquitin-positive inclusions were found. HDAC6 inhibition had no detectable effect on this phenotype. In fact, the percentage of cells treated with tubastatin A containing a vimentin cage was comparable to control (Fig. 4.1b). This indicates that the formation a vimentin cage in these experimental conditions does not relate on an HDAC6-dependent mechanism. Hence, in this model, the presence of a vimentin nest-like structure does not represent a marker of ubiquitin-dependent aggresome formation. Immunoblot analysis of the soluble/ insoluble protein fractions revealed an enrichment of ubiquitinated proteins in the SDS-soluble pool upon MG132 administration, in line with accumulation of ubiquitinated, triton-insoluble protein aggregates (Fig. 4.1c). Altogether, this suggests that ubiquitin-dependent aggrephagy might not be the prevalent degradation route of protein aggregates in SH-SY5Y.

In the literature, aggresomes are classified into ubiquitin-dependent and ubiquitin-independent, based on the molecular mechanisms leading to their formation (Johnston, Ward and Kopito, 1998; García-Mata *et al.*, 1999). Since we rarely detected any ubiquitin signal colocalising with vimentin, we hypothesised that most of the vimentin cages observed in SH-SY5Y may enclose a ubiquitin-independent aggresome.

Fluorescently labelled proteins have been previously used as a tool to study aggrephagy. GFP-CFTRΔF508 is a GFP-tagged mutant of the ion channel cystic

fibrosis transmembrane conductance regulator (CFTR). The ΔF508 deletion interferes with the correct folding and subcellular localisation of the protein, which undergoes polyubiquitination and proteasomal degradation (Jensen *et al.*, 1995; Ward & Kopito, 1994). Upon proteasome inhibition, GFP-CFTRΔF508 is recruited into aggresomes through a ubiquitin- and HDAC6- dependent mechanism (Johnston *et al.*, 1998; Kawaguchi *et al.*, 2003). EGFP-250 is another chimeric protein which forms aggregates. It consists of the first 250 amino acids of the Golgi-associated protein p115. Contrary to GFP-CFTRΔF508, EGFP-250 recruitment into aggresomes is ubiquitin independent (García-Mata *et al.*, 1999).

Therefore, we exploited the biological properties of GFP-CFTRΔF508 and EGFP-250 as a more sensitive method of aggresome detection. By using these fluorescent biosensors, we also aimed to elucidate the nature of the aggresomes that SH-SY5Y may form.

Either GFP-250 or GFP-CFTRΔF508 were expressed in SH-SY5Y. The day after transfection, samples were treated with 1 μM MG132 at regularly interspaced time points for up to 16 h. Cells were fixed, immunostained with an anti-vimentin antibody and imaged by confocal microscopy.

Untreated samples contained speckles of GFP-250 and GFP-CFTRΔF508 spread throughout the cytosol. Following proteasome inhibition, both constructs were progressively recruited into aggresomes. Condensation of fluorescently labelled protein aggregates around the nucleus occurred after 8 h of MG132 treatment. Recruitment of the fluorescent probes into a mature aggresome was observed after 12 h of incubation. The formation of the organelle was accompanied by rearrangement of the vimentin cytoskeleton around the perinuclear protein aggregate inclusion (Fig. 4.1d). Also in this case, exposure to MG132 resulted in partial sample loss, which was exacerbated by high expression of the fluorescent constructs. Again, only a few cells per coverslip expressing either GFP-250 or GFP-CFTRΔF508 were found to contain a fluorescently labelled aggresome, which limited the possibility to conduct accurate quantification. Nonetheless, these experiments prove that both ubiquitin-dependent and independent aggresome formation is possible in SH-SY5Y, even if at different rate to other cell lines tested. We can speculate that SH-SY5Y may activate different pathways to support misfolded protein clearance, which might also include secretion. The reduced aggrephagy rate might as well explain the increased susceptibility of these cells to prolonged proteasome inhibition. Although this neuronal-like model may

have limited exploitability for quantitative studies, expression of GFP-250 or GFP-CFTRΔF508 in SH-SY5Y offers a simple tool to visualise the relative subcellular distribution of putative aggrephagy substrates.

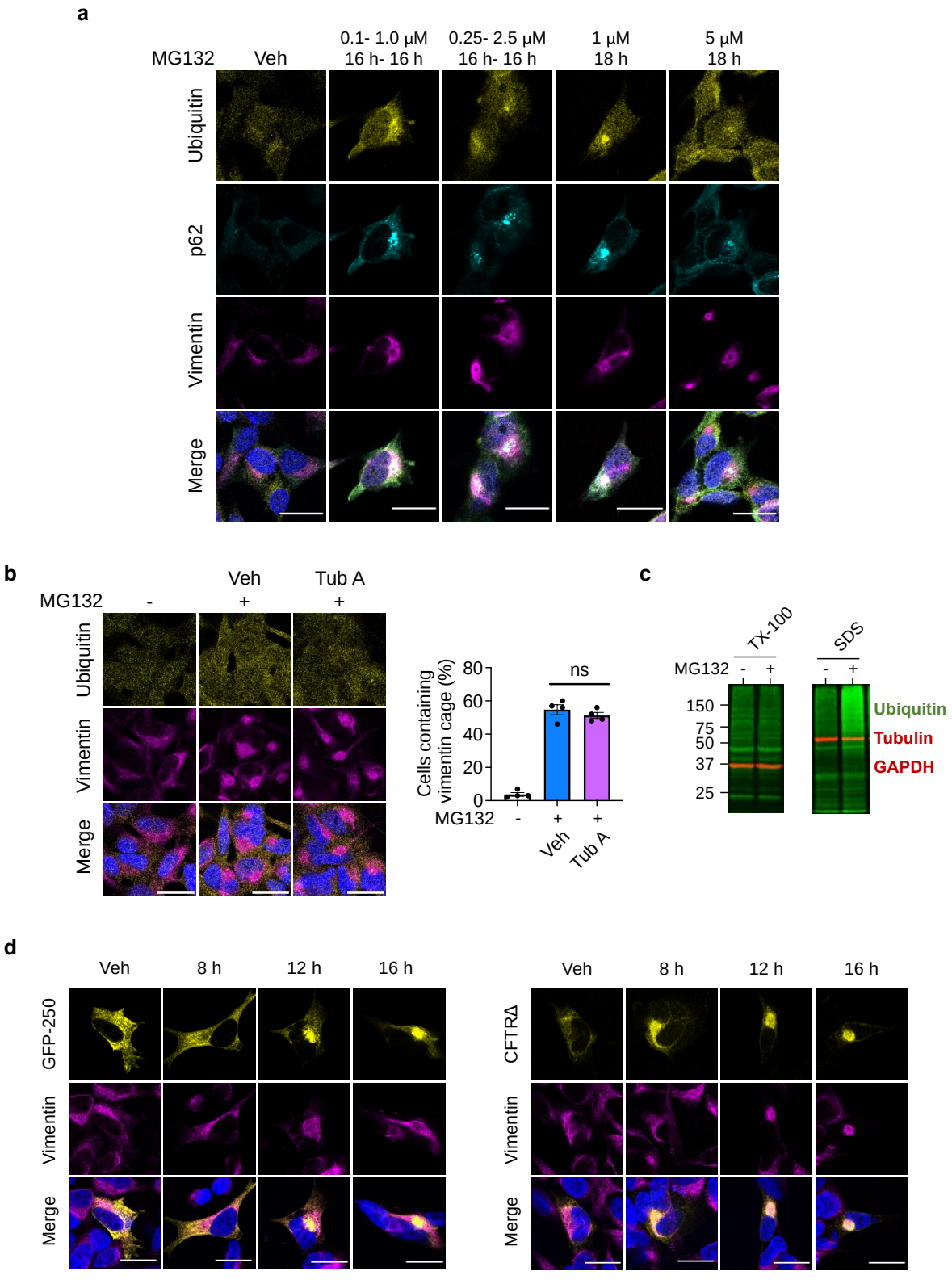

Figure 4.1 SH-SY5Y cells form both ubiquitin-dependent and ubiquitin-independent aggresomes. a) SH-SY5Y exposed to either DMSO (Veh) or MG132 following 4 different administration patterns were fixed and immunostained using antibodies anti- ubiquitin (yellow), p62 (cyan) and vimentin (magenta). Nuclei were counterstained with Hoechst (blue). 0.1- 1.0 µM, 16 h- 16 h= 16 h incubation with 0.1 µM MG132 followed by an 8 h recovery in fresh

media and a 16 h incubation with 1.0 µM MG132; 0.25- 2.5 µM, 16 h- 16 h= 16 h incubation with 0.25 µM MG132 followed by an 8 h recovery in fresh media and a 16 h incubation with 2.5 µM MG132; 1 µM, 18 h = 18 h incubation with 1 µM MG132; 5 µM, 18 h = 18 h incubation with 5 µM MG132. Scale bar= 20 µm. N= 2. **b)** SH-SY5Y treated with 1 µM MG132 and tubastatin A for 18 h were fixed and immunostained using antibodies anti- ubiquitin (yellow) and vimentin (magenta). Nuclei were counterstained with Hoechst (blue). The percentage of cells containing a vimentin cage was quantified. Data are shown as mean± SEM; unpaired t-test. ns= non-significant. Scale bar= 20 µm. N= 4, ~150 cells analysed per condition per experiment. **c)** SH-SY5Y treated as in b) were processed by sequential protein extraction. Protein samples were separated by SDS-PAGE and immunoblotted using antibodies anti-ubiquitin, GAPDH (triton X-100-soluble fraction, TX-100) or tubulin (SDS- soluble fraction, SDS). N= 2. **d)** SH-SY5Y were transfected with either GFP-250 or GFP-CFTRΔF508 (CFTRΔ), in yellow. The day after transfection, samples were treated with either DMSO (Veh) or 1 µM MG132 at increasing time points. Cells were fixed and immunostained using an antibody anti-vimentin (magenta). Nuclei were counterstained with Hoechst (blue). Scale bar= 20 µm. N= 2.

4.2.2 Overexpressed α-synuclein is not recruited into aggresomes

Phosphorylation of α-synuclein on S129 is a signature of α-synuclein intraneuronal inclusions enriched in Lewy bodies (Kawahata *et al.*, 2022). Antibodies recognising phosphorylated α-synuclein-S129 (pS129) are routinely used to detect α-synuclein aggregated species through several molecular biology techniques. Here, we used the model described in the previous section combined with antibodies raised against total and phosphorylated α-synuclein to investigate if α-synuclein aggregates are recruited into aggresomes. α-synuclein aggregation has been previously achieved in both differentiated and undifferentiated SH-SY5Y treated with MG132 (Iqbal *et al.*, 2020). To mimic α-synuclein dyshomeostasis and promote aggregation, we inhibited the proteasome in SH-SY5Y expressing either WT or A53T α-synuclein. The A53T mutation increases α-synuclein aggregation propensity and causes autosomal dominant PD (Polymeropoulos *et al.*, 1997; Conway *et al.*, 2000).

Undifferentiated SH-SY5Y were transfected with either WT or A53T untagged human α-synuclein and either GFP-250 or GFP-CFTRΔF508. The day after transfection, cells were treated with 1 μM MG132 for 12 h. Samples were fixed, immunostained using antibodies anti-α-synuclein, pS129 and vimentin and imaged by confocal microscopy. To test the occurrence of insoluble α-synuclein aggregates, part of the samples was processed by sequential protein extraction in TBS+ 1% triton X-100 and then TBS+ 2% SDS. Protein samples were separated by SDS-PAGE and immunoblotted using antibodies anti- α-synuclein, pS129 and ubiquitin.

In all the conditions tested, both total and pS129 α-synuclein staining appeared homogeneously distributed across the cytoplasm, with no detectable signs of protein aggregation. MG132 administration promoted both ubiquitin-independent and ubiquitin-dependent aggresome formation, confirmed by the presence of GFP-250 or GFP-CFTRΔF508 inclusions and by the formation of a vimentin cage. However, α-synuclein did not colocalise with these structures (Fig. 2.2a). Immunoblot analysis of the protein fractions revealed that most of the α-synuclein pool was extracted by the TBS+ 1% triton X-100 buffer while no signal was detected in the SDS-soluble fraction. An increase in pS129 was observed in the triton X-100-soluble fraction upon proteasome inhibition. However, this did not correspond to the formation of any phosphorylated α-synuclein aggregates detectable in the SDS-soluble fraction. Analysis of the distribution of the ubiquitinated protein pool confirmed an increase in

the ubiquitin signal upon MG132 administration both in the triton X-100- and the SDS-soluble fraction (Fig. 4.2b). This is compatible with accumulation of triton X-100-insoluble protein oligomers and aggregates.
Taken together, these data point out that α-synuclein overexpression combined with pathogenic mutations and protein turnover stress by proteasome inhibition are insufficient conditions to induce α-synuclein aggregation in this cellular model.

LRRK2 mutations which enhance LRRK2 kinase activity are associated to increased α-synuclein pathology in several *in vitro* and *in vivo* models (Volpicelli-Daley *et al.*, 2016; Longo *et al.*, 2017; Bieri *et al.*, 2019). Additionally, α-synuclein aggregation has been reported in SH-SY5Y expressing either WT or G2019S LRRK2 72 h post-transfection (Kondo *et al.*, 2011). Hence, we tested if expression of PD-linked LRRK2 mutants would induce recruitment of α-synuclein into aggresomes in SH-SY5Y cells.
WT or A53T α-synuclein and myc-tagged LRRK2 were expressed in SH-SY5Y. WT LRRK2 was compared to three PD-linked LRRK2 mutants (R1441C, Y1699C and G2019S); the kinase dead LRRK2 mutant D1994A was used as negative control. Cells were fixed 72 h post-transfection, immunostained using antibodies anti- α-synuclein, myc and vimentin and imaged by confocal microscopy.
Even under these experimental conditions, α-synuclein staining was uniformly distributed across the cytoplasm with no detectable signs of relocation or aggregation. The vimentin cytoskeleton was not affected by any major changes, further indicating the absence of aggresomes (Fig. 2.2c).

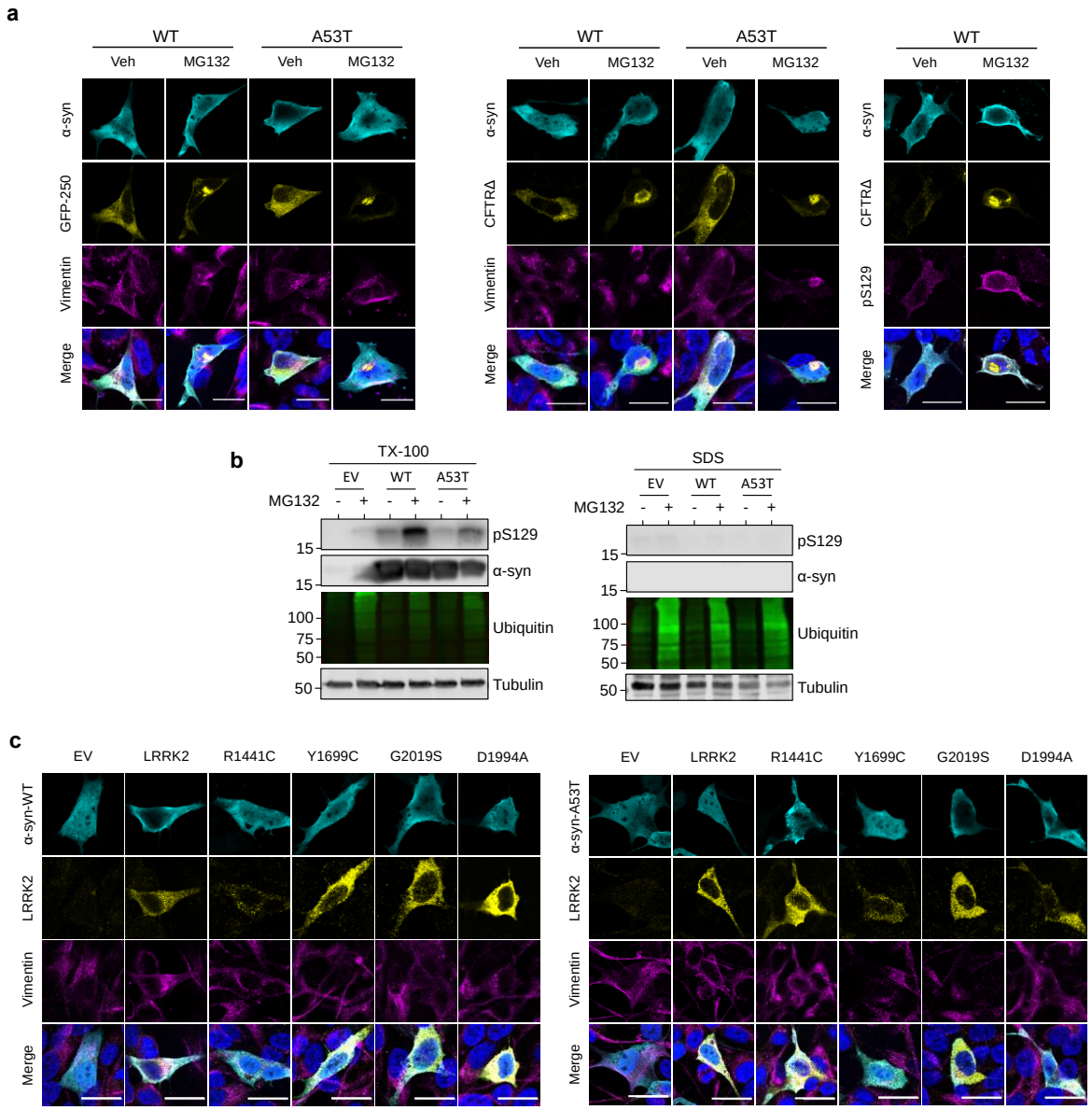

Figure 4.2 Overexpressed α-synuclein does not accumulate into aggresomes. a) SH-SY5Y were transfected with either WT or A53T α-synuclein and either GFP-250 or GFP-CFTRΔF508 (CFTRΔ). The day after transfection samples were treated with either DMSO (Veh) or 1 μM MG132 for 12 h. Cells were fixed and immunostained using antibodies anti- α-synuclein (cyan), vimentin and pS129 (both in magenta). GFP is shown in yellow. Nuclei were counterstained with Hoechst (blue). Scale bar= 20 μm. N= 4. **b)** SH-SY5Y transfected with either an empty vector (EV) or α-synuclein (either WT or A53T) were incubated with 1 μM MG132 for 12 h and processed by sequential protein extraction. Protein samples were separated by SDS-PAGE and immunoblotted using antibodies anti- pS129, α-synuclein, ubiquitin and tubulin. TX-100= triton X-100-soluble protein fraction; SDS= SDS-soluble protein fraction. N= 2. **c)** SH-SY5Y transfected with either WT (left panel) or (right panel) α-synuclein and either an empty vector (EV) or myc-LRRK2 (WT, R1441C, Y1699C, G2019S or D1994A). Cells were fixed 72 h post-transfection and immunostained using antibodies anti α-synuclein (cyan), myc (yellow) and vimentin (magenta). Nuclei were counterstained with Hoechst (blue). Scale bar= 20 μm. N= 2.

4.2.3 The impact of HDAC6 on α-synuclein aggregation is aggrephagy independent

α-synuclein aggregation is a fundamental requirement to address the hypothesis of aggregated α-synuclein being cleared via HDAC6-dependent aggrephagy. The experiments conducted in SH-SY5Y clearly indicate that proteasome inhibition causes accumulation of protein aggregates which are eventually recruited into aggresomes. However, such stress conditions seem not to induce α-synuclein aggregation in our model.

In PD, misfolded α-synuclein acts as a template for the conversion of soluble monomers into pathogenic β-sheet-rich aggregates (Tofaris, 2022). The seeding properties of α-synuclein aggregates have been exploited for years to study PD pathophysiology in several *in vitro* and *in vivo* models. α-synuclein preformed fibrils (PFFs) can be synthetised from recombinant α-synuclein monomers under appropriate environmental conditions. After sonication, PFFs fragments ranging between 10 and 100 nm can be taken up by neurons or other cell types and trigger further α-synuclein aggregation (Volpicelli-Daley *et al.*, 2014). To investigate the role of ubiquitin/HDAC6-mediated aggrephagy on clearance of α-synuclein aggregates we adopted an *in vitro* model under development in Dr Volpicelli-Daley's lab at the University of Alabama at Birmingham. This is based on the administration of sonicated PFFs in COS7 cells expressing fluorescently labelled α-synuclein. We also exploited this cellular model to investigate if LRRK2 kinase activity modulates the formation α-synuclein inclusions. It has been previously shown that the presence of YFP fused to α-synuclein C-terminus does not interfere with the template conversion of natively folded α-synuclein to insoluble fibrils (Luk *et al.*, 2009; Tanik *et al.*, 2013). Additionally, the presence of a fluorescent tag allows to focus our observations on *de novo* α-synuclein aggregation and to distinguish from mere internalisation of untagged PFF fragments.

COS7 cells were transfected with human WT α-synuclein C-terminally tagged with YFP (α-syn-YFP). 24 h post-transfection cells were exposed to 1 μg/ ml of freshly sonicated mouse α-synuclein PFFs. Sterile PBS was used as control. Either tubastatin A or MLi-2 were administered at this stage. 8 h after PFFs administration, MG132 was added to the media and incubated for 16 h. Cells were fixed 24 h post PFFs administration in 4% PFA, 4% sucrose,1% triton X-100 in PBS. The presence of triton

X-100 in the fixation buffer allows most of the soluble proteins to be leached from the sample. In this way, insoluble protein aggregates are preserved while the freely diffusible protein background is washed off. Samples were immunostained with antibodies anti- HDAC6 and vimentin and imaged on a confocal microscope. The percentage of cells transfected with α-syn-YFP containing a perinuclear inclusion surrounded by a vimentin cage was quantified in blind. The percentage of cells transfected with α-syn-YFP containing aggresomes that were positive for both α-synuclein and HDAC6 was also assessed.

To study the impact of HDAC6 and LRRK2 inhibition on α-synuclein aggregation at a molecular level, part of the cell samples was processed by sequential protein extraction in TBS+ 1% triton X-100 and TBS+ 2% SDS. Protein fractions were separated by SDS-PAGE and immunoblotted using antibodies anti- YFP and pS129. A commercial fluorescent protein stain (Li-COR Revert^{TM} 700) was used as loading control to normalise α-synuclein signal in the triton X-100- and in the SDS-soluble protein fractions. LRRK2 inhibition was confirmed by immunoblot on total cell lysates by assessing Rab10-T73 phosphorylation (Fig. 4.3d). HDAC6 inhibition was confirmed on total cell lysates by quantifying tubulin acetylation levels (Fig. 4.3c).

Cells incubated with PBS displayed diffuse residual α-synuclein fluorescence in the nucleus, but not in the cytoplasm. PFFs administration induced aggregation of α-syn-YFP, which formed intracytoplasmic fibrillary structures. Approximately 20% of the cells expressing α-syn-YFP recruited α-synuclein into an aggresome-like perinuclear inclusion surrounded by a vimentin basket. α-synuclein colocalised with HDAC6 into an aggresome in less than 1% of the cells, suggesting that HDAC6 is not involved in trafficking α-synuclein aggregates to the organelle. HDAC6 inhibition had no effect on the formation of α-synuclein-positive inclusions, which further confirms that α-synuclein aggregates are recruited into aggresomes via a ubiquitin/HDAC6-independent mechanism. LRRK2 inhibition did not cause any significant changes in the aggregation phenotype. Finally, proteasome inhibition induced the formation of HDAC6-positive aggresomes, as previously observed, but had no effect on the percentage of α-synuclein-positive aggresomes. This indicates that the UPS has limited impact on the degradation α-synuclein under these conditions. Upon proteasome inhibition, the percentage of aggresomes which were positive for both α-synuclein and HDAC6 significantly increased to ~5% (Fig. 4.3a). It is likely that, under

additional misfolded protein stress, multiple trafficking mechanisms converge into the genesis of an aggresome, where ubiquitinated and non-ubiquitinated proteins coexist. Immunoblot analysis of the sequentially extracted protein fractions showed a clear enrichment of α-synuclein in the SDS-soluble pool upon PFFs administration, consistent with α-synuclein aggregation (Fig. 4.3b, bottom panel). On the contrary, α-synuclein was only detectable in traces in the SDS-soluble protein fraction of samples treated with the PBS control. This reflects what we observed by immunofluorescence. Administration of HDAC6 inhibitors caused a significant increase in α-synuclein aggregates detected in the SDS-soluble fraction. This, combined with our data on aggresome formation, suggests that HDAC6 is involved at some level in the turnover of α-synuclein, but not through aggrephagy. Given the increase in α-synuclein aggregation detected by immunoblot, a parallel increase in the percentage of cells harbouring an α-synuclein-positive aggresome would be expected. However, this was not the case. In line with the results collected by immunofluorescence analysis, neither LRRK2 nor proteasome inhibitors altered the distribution of α-synuclein between triton X-100- and SDS-soluble protein pools. However, MG132 administration increased the total amount of protein extracted by the SDS buffer. This confirms that LRRK2 kinase activity does not play a significant role in α-synuclein aggregation under these experimental conditions. Likewise, the UPS is not involved in the degradation of the α-synuclein species present in this cellular model (Fig. 4.3b, bottom panel).

In line with previous reports, α-synuclein-S129 phosphorylation consistently increased upon proteasome inhibition both in the soluble and aggregated protein pools (Fig. 4.3 b, right panel). A smaller but significant increase in pS129 was also detected in the triton X-100-soluble fraction upon HDAC6 inhibition. This post-translational modification increases in response to proteasome and lysosome inhibition (Machiya *et al.*, 2010; Waxman *et al.*, 2008). One of the functions of HDAC6 is to promote autophagy by deacetylating cortactin, a component of the molecular machinery implicated in the autophagosome-lysosome fusion (Lee *et al.*, 2010). Thus, HDAC6 inhibition may disrupt protein homeostasis to a different extent to UPS by disturbing the autophagic flux. In turn, this might trigger α-synuclein hyperphosphorylation.

Taken together, these results suggest that α-synuclein aggregates are recruited into aggresomes via a mechanism that does not rely on HDAC6 and is not influenced by LRRK2 kinase activity.

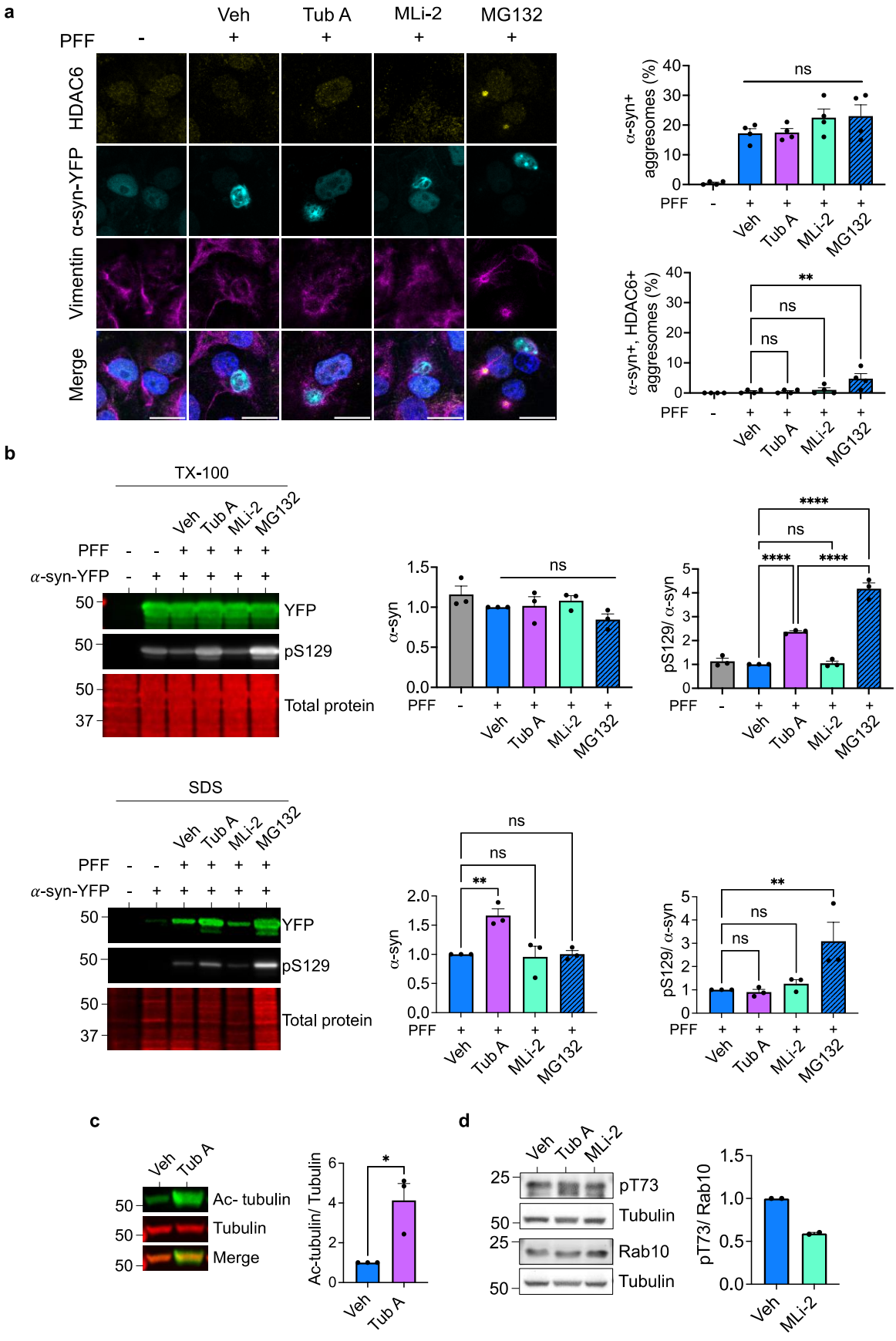
a
Veh
Tub A
MLi-2
MG132
PFF
HDAC6
α-syn-YFP
Vimentin
Merge
α-syn+ aggresomes (%)
α-syn+, HDAC6+ aggresomes (%)
ns
**
b
TX-100
SDS
α-syn-YFP
YFP
pS129
Total protein
α-syn
pS129/ α-syn
****
c
Ac- tubulin
Tubulin
Merge
Ac-tubulin/ Tubulin
*
d
pT73
Rab10
pT73/ Rab10

Figure 4.3 HDAC6 does not regulate the accumulation of α-synuclein aggregates into aggresomes. a) COS7 were transfected with human α-synuclein-YFP (cyan). 24 h post-transfection cells were treated with either PBS or mouse PFFs and either DMSO (Veh), tubastatin A or MLi-2. 8 h after PFFs administration, MG132 was added to the media. Cells were fixed 24 h post PFFs administration and immunostained with antibodies anti- HDAC6 (yellow) and vimentin (magenta). Nuclei were counterstained with Hoechst (blue). Graphs show the percentage of transfected cells containing an α-synuclein-positive aggresome (upper graph) and the percentage of transfected cells containing an α-synuclein- and HDAC6-positive aggresome (lower graph). One-way ANOVA with Fisher's LSD test; N= 4, ~150 cells analysed per condition per experiment. Scale bar= 20 µm. **b)** COS7 cells treated as in a) were processed by sequential protein extraction. The triton X-100 soluble protein fraction (TX-100) and the SDS-soluble protein fraction (SDS) were separated by SDS-PAGE and immunoblotted using antibodies anti- YFP and pS129. A commercial total protein stain was used as loading control for normalisation. One-way ANOVA with Fisher's LSD test; N= 3. **c)** Total cell lysates of COS7 cells treated as in a) were processed by SDS-PAGE and immunoblotted using antibodies anti total and acetylated-tubulin. Unpaired t-test. N= 3. **d)** Total cell lysates of COS7 cells treated as in a) were processed by SDS-PAGE and immunoblotted using antibodies anti- phospho-Rab10-T73, Rab10 and tubulin. N= 2.
All data are shown as mean± SEM. ns= non-significant; *= p≤ 0.05; **= p≤ 0.01; ****= p≤ 0.0001.

4.2.4 Colocalization between α-synuclein inclusions and aggrephagy markers in neurons

In vitro systems such as COS7 cells represent a simple tool to dissect conserved molecular pathways and obtain quick biological readouts. However, observations collected in fibroblast-like cell lines lacking the subcellular specialisation of the neuron might not reflect the high spatial complexity found in the brain. Another possible limitation of this model is the exogenous expression of α-synuclein, which might lead to changes in cell physiology. For these reasons, we researched additional evidence of aggrephagy being activated in neurons upon α-synuclein aggregation. To corroborate the formation of intraneuronal α-synuclein inclusions from an aggresomal perspective, we inoculated α-synuclein PFFs in primary mouse cortical neurons and in mouse brains in collaboration with Dr Volpicelli-Daley's team. Neurofilaments (NF) were used along with ubiquitin and p62 as putative markers of aggresome formation in neurons. These intermediate filaments are displaced from the axonal compartment and surround inclusion bodies in PD and other neurodegenerative disorders (Mayer *et al.*, 1989). NF relocation has been confirmed in primary hippocampal neurons incubated with PFFs and in PD patients' inclusions and seem to be functional to the maturation of the LB (Mahul-Mellier *et al.*, 2020; Moors *et al.*, 2021).

Primary mouse cortical neurons were extracted at P0 and cultured in Neuronal Media for 7 days (see Methods). At DIV7, neurons were incubated with 1 µg/ ml of freshly sonicated mouse α-synuclein PFFs. PBS was used as negative control. 5 µM MG132 was added to the culture media 16 h prior fixation. Samples were fixed at DIV14 in 4% PFA, 4% sucrose, 1% triton X-100 in PBS, immunostained with antibodies anti- pS129, ubiquitin, p62 and NF and imaged on a confocal microscope. The antibodies anti-HDAC6 and Hsc70 available in our lab were also validated on mouse cortical neurons, but no cross-reactivity was observed in this species (image not shown).

PFFs administration induced misfolding and aggregation of endogenous α-synuclein in mouse cortical neurons after 7 days of incubation. α-synuclein pathology mainly affected neuronal projections in form of non-ubiquitinated pS129-positive filaments and puncta. Scattered α-synuclein aggregates were also found in the soma, but no aggresome-like inclusions were observed. p62 did not colocalise with phosphorylated α-synuclein. NF were mainly detected in neuronal projections and were not perturbed

by α-synuclein aggregation. Ultimately, MG132 administration did not cause any visible changes in the subcellular distribution of the markers examined (Fig. 4.4a).

The structure and subcellular localisation of α-synuclein aggregates found in cultured neurons after 7 days suggest that this model is likely to represent an earlier stage of α-synuclein pathology than what described in COS7. In fact, a previous study based on PFFs administration in primary hippocampal neurons described the formation of ubiquitin-, p62- and NF- positive LB-like inclusions after 21 days of incubation (Mahul-Mellier *et al.*, 2020). Additional work is required to optimise this *in vitro* model and clarify the role of HDAC6 in the formation of LB in neurons.

Finally, colocalization of α-synuclein lesions with aggresomal markers was also researched *in vivo* in mice. Two 4.5-month-old C57BL/6 mice were bilaterally injected into the striatum with either PFFs or monomeric α-synuclein (protein concentration: 5 mg/ ml, injection volume: 2 uL per site) and culled 6 weeks post-injection. Brains were dissected and fixed. Sections of the striatum and of the substantia nigra pars compacta (SNpc) were immunostained using the following antibodies: pS129, p62, ubiquitin, NF, neuronal nuclear protein (NeuN, a pan-neuronal marker), and tyrosine hydroxylase (TH, a dopaminergic neuronal marker). Images were acquired on a confocal microscope in z-stack mode.

Lewy neurites and larger perinuclear yarn-like aggregates were observed in the cortex (Fig. 4.4b) and in TH+ neurons in the SNpc (Fig. 4.4c) of mice injected with PFFs but not monomeric α-synuclein. Most pS129-positive inclusions colocalised with ubiquitin and p62. Interestingly, NF were displaced from the axonal compartment and recruited to the α-synuclein inclusions in the cortex. Likewise, TH aggregation and colocalization with LB-like inclusions was observed in the SNpc as previously reported in PD patients (Kawahata *et al.*, 2009; Moors *et al.*, 2021).

Overall, the perinuclear α-synuclein inclusions found in the brain of mice injected with PFFs resembled the aggresome-like structures described in COS7 cells expressing α-syn-YFP (Fig. 4.4b, Fig. 4.3a). Nevertheless, in contrast with the dense, onion skin-type LB ultrastructure emphasized by Moors and colleagues (Moors *et al.*, 2021), the inclusions detected in our models appeared thread-like and less compacted around a dense core (Fig. 4.4b).

The models so far investigated might represent an intermediate stage in α-synuclein pathology which lies between the emergence of α-synuclein fibrils and the formation of a mature inclusion body. Further experiments will clarify if the α-synuclein inclusions

observed in mouse brains have an aggresomal origin and if HDAC6 plays a role in their formation.

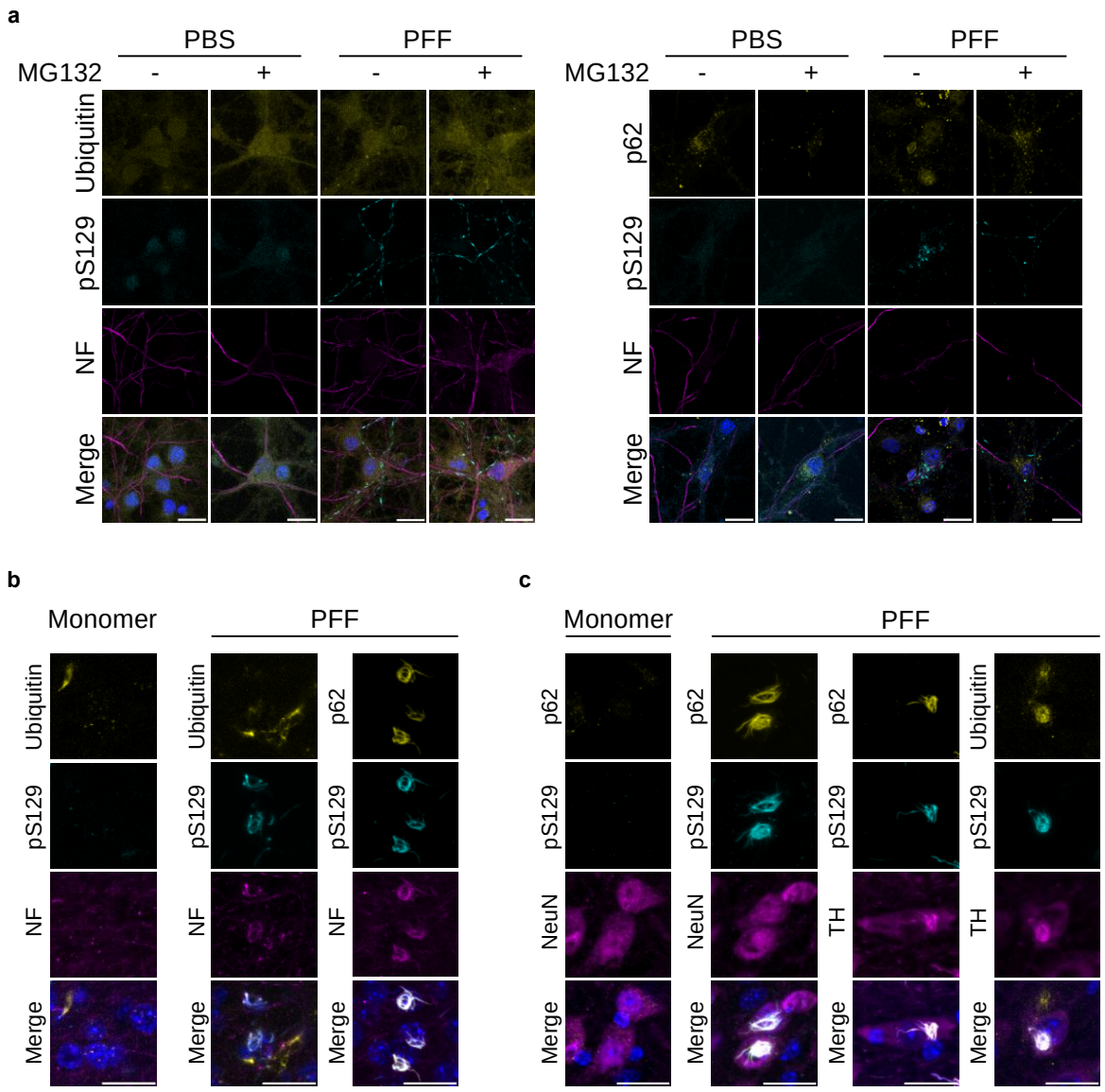

Figure 4.4 Colocalization of α-synuclein inclusions with aggresome markers in primary neurons and *in vivo*. a) DIV7 mouse cortical neurons were exposed to either PBS or mouse PFFs and incubated for 7 days. Either DMSO or MG132 were added 16 h before fixation. Neurons were fixed at DIV14 and immunostained with antibodies anti- ubiquitin or p62 (both in yellow), pS129 (cyan) and neurofilaments (NF, magenta). Nuclei were counterstained with DAPI (blue). N= 1. Scale bar= 20 µm. **b)** 4.5-month-old mice underwent bilateral striatal injection of either monomeric α-synuclein or PFFs by stereotaxic surgery. 6 months post-injection, brains were dissected and fixed. Cortical brain sections were immunostained using antibodies anti- ubiquitin or p62 (both in yellow), pS129 (cyan) and NF (magenta). Nuclei were counterstained with DAPI (blue). N= 1. Scale bar= 20 µm. **c)** Sections of the substantia nigra par compacta of the same mice described in b) were immunostained using antibodies anti-ubiquitin or p62 (both in yellow), pS129 (cyan) and NF or tyrosine hydroxylase (TH, both in magenta). Nuclei were counterstained with DAPI (blue). N= 1. Scale bar= 20 µm.

4.3 Discussion

α-synuclein aggregation is one of the most prominent features linking sporadic and genetic PD which is exacerbated by LRRK2 mutations (Dues and Moore, 2020). The causality of LRRK2 dysregulation in PD aetiology has been confirmed across an extensive range of models, where LRRK2 mutations recapitulate most of the pathological changes observed in sporadic PD (Seegobin *et al.*, 2020). The recent evidence that the PD-causative G2019S LRRK2 mutation disrupts HDAC6-dependent aggrephagy (Lucas *et al.*, 2019) motivated our interest in establishing the impact of this key cellular response to proteotoxic stress on α-synuclein homeostasis in neurons.

Previous studies reported aggresome formation in both naïve and differentiated SH-SY5Y cells in response to proteasome inhibition. Here, we combined four treatment patterns described by other authors and immunofluorescence protocols successfully applied in other sections of this work to establish a neuronal-like model of ubiquitin-dependent aggresome formation. The treatment protocols compared differed in MG132 concentration, incubation times and number of incubation cycles.

Unlike other human and simian cell lines used in this work, naïve SH-SY5Y cells did not tolerate exposure to MG132 for more than 12 h, even at low doses. In fact, all four treatment schemes assessed in this study caused marked sample loss. The susceptibility of SH-SY5Y to proteasome inhibition may indicate that the proteasome is the main route of protein quality control in this cell line, as well as the potential deficiency of other mechanisms of misfolded protein clearance. Most of the surviving cells displayed rearrangement of the vimentin cytoskeleton compatible with aggresome formation. However, no ubiquitin, p62 or HDAC6 (data not shown) colocalised with these structures, suggesting the preferential activation of a ubiquitin-independent aggresome formation mechanism. In fact, assembly of ubiquitin-dependent aggresomes was rarely observed in this cell line, despite the accumulation of ubiquitinated TX-100-insoluble protein aggregates. The additional observation that tubastatin A did not perturb the formation of vimentin cages further suggests that these originate from an HDAC6-independent process.

To confirm the engagement of either one or the other transport mechanism of misfolded protein aggregates into aggresomes and clarify the nature of the vimentin basket formed upon proteasomal inhibition, we utilised the molecular probes GFP-

CFTRΔF508 and GFP-250. These two constructs have been originally used to characterise aggresome formation and are recruited into the organelle with ubiquitin-dependent and -independent mechanisms, respectively (Johnston *et al.*, 1998; García-Mata *et al.*, 1999). Since both fluorescent probes were accumulated into a vimentin-bound juxtanuclear inclusion upon proteasome inhibition, we concluded that both ubiquitin-dependent and -independent aggresome formation mechanisms are supported in SH-SY5Y cells. It is possible that HDAC6-dependent trafficking of misfolded substrates into aggresomes is stimulated by the overload of misfolded proteins obtained by expressing GFP-CFTRΔF508. Hence, the two fluorescent probes were used as a molecular tool to efficiently visualise aggresomes in SH-SY5Y and verify the targeting of α-synuclein aggregates. These constructs offer the additional advantage of discriminating between alternative recruitment mechanisms.

Many factors contribute to the formation of metastable α-synuclein oligomers which act as nucleation cores for the assembly of insoluble aggregates. These encompass mutations and high local α-synuclein concentrations (Vidović and Rikalovic, 2022). The latter can either result from abnormal expression or inefficient clearance mechanisms (Tofaris, 2022). Besides other degradation routes, the proteasome provides a significant contribution to α-synuclein metabolism, at least in overexpression PD models (Bi *et al.*, 2021). Following previous reports (Zhou and Freed, 2004; Opazo *et al.*, 2008; Iqbal *et al.*, 2020), we combined overexpression of α-synuclein mutants and proteasome inhibition to trigger α-synuclein aggregation.
In our hands, the neuroblastoma cell line SH-SY5Y clearly reacted to MG132 administration by accumulating TX-100-insoluble protein aggregates and recruiting both misfolded protein reporters into aggresomes. Additionally, we detected an increase in pS129, in line with previous observations (Chau *et al.*, 2009). However, the combination of PD-mimicking conditions tested in this model did not lead to any detectable α-synuclein aggregation. Moreover, the increase in α-synuclein phosphorylation recorded in this experimental context supports the hypothesis of a stress-induced, protective PTM (Paleologou *et al.*, 2008; Weston *et al.*, 2021; Ghanem *et al.*, 2022), rather than a pro-aggregation, cytotoxic factor (Fujiwara *et al.*, 2002a; Chen and Feany, 2005; Arawaka *et al.*, 2006; Gorbatyuk *et al.*, 2008). As a result, we could not confirm if part of the α-synuclein pool is targeted to the aggresome under proteotoxic stress conditions in this neuronal-like model. We could also not replicate

α-synuclein aggregation induced by expression of LRRK2 mutants reported by other authors in patient-derived neurons (Zhao *et al.*, 2020) and SH-SY5Y, specifically (Kondo *et al.*, 2011).

Our results differ from the reports we based our *in vitro* model on. Iqbal and co-workers described α-synuclein aggregation and accumulation into aggresomes upon proteasome inhibition in both HeLa and non-differentiated SH-SY5Y expressing either wildtype or mutant α-synuclein. However, the enrichment of the protein within the vimentin cage was not clearly evidenced and the presence of insoluble α-synuclein aggregates was not further corroborated. Additionally, the percentage of cells showing aggresomes was not indicated (Iqbal *et al.*, 2020). Previous studies reported spontaneous aggregation of overexpressed wildtype or mutant α-synuclein and formation of aggresomes in HEK293 and N27 cells 24 h post-transfection (Zhou and Freed, 2004; Opazo *et al.*, 2008). Opazo and colleagues also observed an increase in the percentage of cells containing aggregates upon proteasome inhibition (Opazo *et al.*, 2008).
Cancer-derived cell lines tend to evolve under the selective pressure of specific culture conditions. This generates high genetic heterogeneity of the same lines cultured by different groups, which affect morphology, growth rate, gene expression patterns and even responsiveness to drug treatments (Ben-David *et al.*, 2018). In a cellular context where multiple pathways participate to α-synuclein homeostasis (Stefanis *et al.*, 2019), it is plausible that small metabolic changes can have a significant impact on the cell response to proteotoxic stress. Hence, it is unfortunate but not completely unexpected that the SH-SY5Y strain available in our lab may behave differently to what observed by other groups.

With the more general aim to investigate whether α-synuclein aggregates are substrate of aggrephagy and clarify the role of HDAC6 in α-synuclein pathology, we administered α-synuclein PFFs in COS7 cells expressing human α-synuclein-YFP. This simian fibroblastoid cell line offers the advantage of a flat morphology, well suited for live recording of subcellular dynamics that may be required in possible follow up experiments. Additionally, we consistently yielded high numbers of HDAC6-positive aggresomes in COS7 following proteasome inhibition (Fig. 3.1d). This indicates effective engagement of the aggresome formation molecular apparatus. LB-like

inclusions have been thoroughly characterised in QBI-HEK293 and HEK293 cells expressing α-synuclein seeded with PFFs (Luk *et al.*, 2009; Tanik *et al.*, 2013). These aggregates show strong immunoreactivity for phosphorylated α-synuclein, HSP70, HSP90, ubiquitin, proteasome components and for the autophagosome markers p62 and LC3. Additionally, they are stained by the amyloid-specific dye thioflavin S, engulf membrane-bound organelles, and display a similar ultrastructure to LB (Luk *et al.*, 2009; Tanik *et al.*, 2013).

In line with previous studies, internalised PFFs acted as nucleation sites for aggregation of α-synuclein monomers. Seeded aggregates displayed a spectrum of morphologies including puncta, fibrils, and aggresome-like inclusions surrounded by vimentin. *De novo* α-synuclein aggregation rather than sole PFFs phagocytosis was confirmed by the sequestration of YFP within the protein inclusions, which were resistant to fixation in presence of 1% triton X-100. Moreover, α-synuclein-YFP was extracted with TBS/SDS only upon exposure to PFFs and was detected by immunoblot as a band of approximately 40 kDa (wildtype α-synuclein has an apparent molecular weight of 17 kDa). About 20% of cells expressing α-synuclein-YFP exposed to PFFs recruited the fluorescent construct into a canonically defined aggresome (Johnston *et al.*, 1998). Nonetheless, we could exclude a ubiquitin/HDAC6-dependent transport mechanism based on three observations: i) HDAC6 did not colocalise with α-synuclein inclusions and was rarely associated with α-synuclein-positive aggresomes; ii) HDAC6 inhibition did not affect the percentage of cells containing an α-synuclein-positive aggresome; iii) proteasome inhibition did not increase the percentage of cells containing α-synuclein-positive inclusion bodies.

Besides the mechanism involving K63-linked polyubiquitination, p62 and HDAC6, other molecular chaperons act as cargo adaptors for cytoplasmic dynein and are involved in recruiting protein aggregates into aggresomes for degradation (García-Mata *et al.*, 1999). Gamerdinger and colleagues observed that aggregates of the amyotrophic lateral sclerosis-linked superoxide dismustase 1 (SOD1) mutant G85R are intercepted by the molecular chaperone HSP70. These partially oligoubiquitinated complexes are loaded on to dynein by the stress-induced co-chaperone Bcl-2-associated athanogene 3 (BAG3) and directed to the aggresome (Basso *et al.*, 2006; Gamerdinger *et al.*, 2011). The interaction between HSP70 and the co-chaperone ubiquitin ligase carboxyl terminal of HSP70/HSP90 interacting protein (CHIP) is an essential event in this ubiquitin-independent recruitment process (Zhang *et al.*, 2011).

Hence, it is possible that under the experimental conditions tested in the present work, α-synuclein aggregates are transported to the aggresome via a HSP70/BAG3-dependent mechanism.

Notably, we found that HDAC6 inhibition increased the amount of TX-100-insoluble α-synuclein-YFP. If such aggregates are recruited into aggresomes, we would expect that their accumulation should correspond to an increase in the percentage of cells forming an aggresome. However, this parameter was unchanged. A possible explanation of this apparent contradiction is that HDAC6 inhibition may impact other features of the aggresome that were not investigated, such as total volume or protein density. Alternatively, HDAC6 may be involved in the degradation of α-synuclein oligomeric species that elude aggresomal sequestration and are preferentially cleared by selective autophagy (Du *et al.*, 2014; H. J. Lee *et al.*, 2004; Webb *et al.*, 2003). HDAC6 plays an important role in autophagy by orchestrating the fusion between lysosomes and autophagosomes (Lee *et al.*, 2010; Wang *et al.*, 2019). Thus, HDAC6 inhibition may inhibit a parallel clearance route, resulting in the accumulation of insoluble α-synuclein oligomers. A third possibility is that HDAC6 may act upstream to α-synuclein aggregation by influencing protein folding. HDAC6 increases the expression of key protein chaperones such as HSP70 and HSP25 by derepressing the transcription factor heat shock factor 1 (HSF1) and promoting its translocation to the nucleus (Pernet *et al.*, 2014). On the contrary, HDAC6 inhibition attenuates the expression of heat-shock proteins (HSPs) and reduces ER stress tolerance (Li *et al.*, 2017). Most HSPs not only contribute to α-synuclein clearance, but also exert an important anti-aggregation function (Guo *et al.*, 2023).

Our findings are in apparent contradiction with previous publications indicating the involvement of HDAC6 in the formation of aggresome-like α-synuclein inclusions. Aggresomes formed by co-expressing α-synuclein and synphilin 1 in SH-SY5Y cells colocalise with HDAC6, p62, γ-tubulin and vimentin and are effectively removed by autophagy (Chung *et al.*, 2001; Wong *et al.*, 2008). However, neither the nature of such inclusions nor the direct role of HDAC6 in their formation have been investigated. It is possible that co-expression of α-synuclein and synphilin 1 leads to the occurrence of aggregated species that differ from those obtained by PFF induction (e.g., oligomers rather than fibrils). Su and co-workers claimed that HDAC6 directs aggresomal degradation of α-synuclein aggregates formed in response to the mitochondrial toxin MPP^+ in naïve PC12 and SH-SY5Y (Su *et al.*, 2011). However, the data shown do not

evidence any condensation of α-synuclein into aggresome-like structures. Additionally, the presence of aggresomes was not confirmed by any other markers. Hence, it is likely that the effect of HDAC6 on α-synuclein expression levels and cell survival in this experimental context is mostly due to other HDAC6 functions, such as redox stress buffering (Parmigiani *et al.*, 2008), heat-shock response activation (Boyault *et al.*, 2007; Pernet *et al.*, 2014), or autophagic flux regulation (Lee *et al.*, 2010). Du and colleagues observed that HDAC6 mitigates the neurodegenerative phenotype of a *Drosophila* PD model by promoting the sequestration of toxic α-synuclein oligomers into LB-like inclusions (Du *et al.*, 2010). However, based on their results, the authors could not distinguish between anti-oligomerisation and pro-aggregation effects. Additionally, the link between LB-like inclusions obtained in Drosophila and aggresomes has not been researched. Du and colleagues also indicated that the total α-synuclein levels are unaffected by HDAC6 KO or overexpression. This points towards a terminal aggregation process which eludes any clearance attempts that usually follow aggresome formation. In fact, if on one hand internalised PFFs seeds can be efficiently degraded via p62-dependent autophagy in naïve HEK293 cells (Watanabe *et al.*, 2012), LB-like inclusions are resistant to proteolysis and disrupt autophagosome clearance (Tanik *et al.*, 2013). Interestingly, a study reporting clearance of wildtype α-synuclein aggresomes also highlights the non-amyloidogenic nature of the inclusion bodies obtained by overexpressing the protein in HEK293 (Opazo *et al.*, 2008). Altogether these studies and our data support the existence of different α-synuclein strains which are directed to alternative clearance processes. Some of these lead to terminal sequestration of protein aggregates into a proteolysis-resistant inclusion.

As we mentioned above, proteasome inhibition caused the emergence of HDAC6-positive aggresomes in COS7 cells expressing α-synuclein-YFP. However, the percentage of cells containing α-synuclein aggresomes did not increase, as opposed to what would be expected for ubiquitin-dependent aggrephagy substrates (Johnston *et al.*, 1998; Ravikumar *et al.*, 2002; Wong *et al.*, 2008). MG132 administration increased the absolute amount of α-synuclein-YFP extracted by the SDS buffer. However, proteasome inhibition also causes a general increase in protein aggregation, here detected as an enrichment of the TX-100-insoluble protein pool. We chose to normalise α-synuclein-YFP by the total amount of protein loaded per lane to increase

our precision when comparing the effects of tubastatin A and MLi-2 to control. Nonetheless, this method of analysis has some limitations when the total SDS protein fraction changes in response to the treatment.

Altogether, our data indicate that the proteasome does not participate in the degradation of α-synuclein aggregates directed to the aggresome or of their precursors. We also observed that even under metabolic stress, HDAC6-positive inclusions colocalised with α-synuclein only in a small percentage of cells. This might indicate that formation of α-synuclein aggresomes and ubiquitin-dependent aggresomes are two mutually exclusive mechanisms and that the first might disrupt the other. Additional evidence should be collected to confirm this hypothesis. Another possibility is that α-synuclein inclusions seeded by PFFs may elude any regulated protein degradation mechanisms and that the accumulation into a LB-like inclusion mostly depends on the biophysical properties of the fibril. This possibility is supported by the observation that aggresome-like inclusions of a fluorescent aggrephagy substrate (a YFP-tagged huntingtin exon 1 fragment containing 72 glutamine repeats) and LB-like inclusion can coexist in the same cells without overlapping. While aggresomes resolve, LB-like inclusions persist indefinitely (Tanik *et al.*, 2013).

Similar to what we noted for HDAC6 inhibition, the increase in TX-100-insoluble α-synuclein aggregates which follows proteasome inhibition seems to conflict with the immunofluorescence data. This can be due to selectivity of the proteasome for species that are not recruited into aggresomes, such as soluble α-synuclein oligomers (Bennett *et al.*, 1999; Emmanouilidou *et al.*, 2010; Shabek *et al.*, 2012; Tofaris *et al.*, 2001; Webb *et al.*, 2003). The latter would accumulate under proteasome inhibition but may not necessarily result in higher aggresome formation rates. It is also possible that MG132 administration induced undetected changes of the aggresome architecture.

LRRK2 inhibition did not affect the accumulation of TX-100-insoluble α-synuclein aggregates or the formation of aggresome-like inclusions. Studies on rodents exposed to PFFs found that LRRK2 inhibitors are only effective in mitigating α-synuclein aggregation in G2019S and R1441G knock-in animals but not in a WT LRRK2 genetic background (Volpicelli-Daley *et al.*, 2016; Ho *et al.*, 2022). On the other hand, LRRK2 KD obtained by injection of antisense oligonucleotides effectively reduces PFF-seeded α-synuclein aggregation and improves dopaminergic neurons survival (Zhao

et al., 2017). These data are compatible with a toxic gain of function of LRRK2 kinase hyperactive mutants which can be mitigated by targeted inhibitors. In normal conditions, LRRK2 intervenes in α-synuclein aggregation with a different mechanism which does not involve its basal kinase activity. This is in analogy to what we described for the role of LRRK2 in the recruitment of protein aggregates into aggresomes. It would be interesting to explore how the COS7-based aggregation model would react to expression of LRRK2 mutants or LRRK2 KD.

Finally, we attempted to research signs of colocalization between α-synuclein aggregates and aggresomal markers in cultured neurons and in mouse brains, which more closely recapitulate the cellular and physiological context most affected by PD-changes.

PFFs are effectively endocytosed by DIV7 primary neurons and induce the conversion of endogenous α-synuclein into insoluble inclusions that recapitulate the main features of both LBs and LNs (Volpicelli-Daley *et al.*, 2011; Mahul-Mellier *et al.*, 2020). At this neuronal maturation stage, α-synuclein expression reaches its peak, which enhances the aggregation phenotype (Murphy *et al.*, 2000; Volpicelli-Daley *et al.*, 2011). α-synuclein pathology first affects the neural projections and travels retrogradely to the soma over the course of 14 d. 21 d after PFF inoculation, approximately 22% of neurons form a dense perinuclear inclusion which shares similar immunohistochemical and ultrastructural features with LB found in PD patients (Mahul-Mellier *et al.*, 2020). Due to time constrains, we limited the exploration of this model at the 7 d post PFFs inoculation benchmark. At this stage, α-synuclein aggregation mostly affected neural projections and appeared in form of scattered puncta and filaments which did not colocalise with neither ubiquitin nor p62. Additionally, proteasome inhibition for 16 h before harvesting had no visible impact on the subcellular distribution of α-synuclein pathology and of the aggresomal markers tested. Given the higher amount of time required by neurons to form perinuclear inclusions compared to COS7 cells, it is possible that they may respond to proteasome inhibition more slowly than fibroblast-like cell lines. The highly ramified neuronal morphology translates into longer distances to cover during transport of molecules and organelles. Alternatively, neurons might rely on secretion and on the scavenging role of glial cells for clearing terminally misfolded proteins rather than forming aggresomes.

Since the antibodies available in our lab did not consistently detect murine HDAC6, we decided to halt the testing on this model. Future work should aim to characterise the cooccurrence of α-synuclein inclusions and additional aggresomal markers (including HDAC6) at 14 and 21 d post PFFs inoculation and test the role of HDAC6 in the formation of LB-like inclusions in primary neurons by pharmacological and genetic manipulation.

The murine PD-model explored in this work has been extensively characterised by Luk's group and is based on the stereotaxic injection of PFF into the striatum of non-transgenic mice (Luk *et al.*, 2012; Zhang *et al.*, 2019). This is sufficient to seed the aggregation of endogenous α-synuclein in several brain areas relevant for human PD which are interconnected with the striatum. These include layers IV and V of the neocortex, olfactory bulb and SNpc (Luk *et al.*, 2012). Aggregates obtained by PFFs injection are ubiquitinated, phosphorylated, colocalise with HSP90 and p62 and are positive to thioflavin S staining (Luk *et al.*, 2012; Rey *et al.*, 2016).
Here we confirmed the immunoreactivity of seeded aggregates for pS129 and ubiquitin, as well as the colocalization with p62. We could not determine the presence of HDAC6 due to the lack of cross reactivity of the antibodies available at the time of the experiment. We observed the overlap of α-synuclein filaments with TH in the SNpc and cytoskeletal components in the cortex. Sequestration of TH and neurofilaments within LBs are commonly reported in PD patients (Kawahata *et al.*, 2009; Moors *et al.*, 2021). In this mouse model, intermediate filaments seemed engulfed within the structure of the aggregate rather than being recruited around the inclusion, as it normally occurs during aggresome and LB maturation (Morrow *et al.*, 2020; Moors *et al.*, 2021). Additionally, the loose yarn-like appearance of the α-synuclein aggregates affecting the perikaryon 6 weeks post-injection hardly compare with the multilayer structure of the LB (Shahmoradian *et al.*, 2019; Moors *et al.*, 2021) or the crowded environment of the aggresome (Dul *et al.*, 2001; Saliba *et al.*, 2002; Cohen and Taraboulos, 2003; Lehotzky *et al.*, 2004). The work by Luk and colleagues describes a stereotypical expansion of the brain regions affected by Lewy pathology at 30, 90 and 180 days post-inoculation but does not provide information about the ultrastructure of the inclusions, their maturation process and the grade of similarity to LB (Luk *et al.*, 2012). A later study shows the progressive consolidation of these aggregates, which still retain the same "spider-like" appearance after 4 months post

injection (Osterberg *et al.*, 2015). In general, this mouse model recapitulates an intermediate phase of the process leading to LB maturation and closely mimics a prodromal/early PD stage (Rey *et al.*, 2016). We propose that similarities between induced aggregates, aggresomes and LBs should be researched in older mice.

Studies attempting to pinpoint the impact of HDAC6 in rodent models of PD used approaches that complicate the discrimination between concomitant effects of the induction treatments on multiple cellular systems. Francelle and colleagues reported the amelioration of the neurodegenerative phenotype in rats transduced with α-synuclein and treated with HDAC6 inhibitors (Francelle *et al.*, 2020). The positive role of HDAC6 inhibition in this context is liked to activation of CMA and mitigation of neuroinflammation; α-synuclein aggregation has not been investigated (Francelle *et al.*, 2020). Zhao and colleagues used a MPTP-induced mouse model and observed that HDAC6 KO has no significant impact on neurodegeneration. However, the authors did not explore changes in α-synuclein homeostasis (Zhao *et al.*, 2023).

As opposed to overexpression and MPTP-induced models, PFF inoculation offers the advantage of specifically focussing on a disease-causing mechanism naturally occurring in PD in a more physiological context. Combined with HDAC6 inhibitors or with a HDAC6 deficient genetic background (Zhang *et al.*, 2008b; J. Zhao *et al.*, 2023), it could represent a valuable tool to corroborate *in vitro* findings on the mechanisms converging in LB formation.

5 Role of LRRK2 and HDAC6 signalling in α-synuclein trafficking and secretion

5.1 Introduction

α-synuclein is a critical element of the synaptic vesicle cycle and is actively transported to the pre-synaptic terminal (Anderson *et al.*, 2020). It has been proposed that, in PD, the elevated α-synuclein concentration in this compartment promotes spontaneous nucleation events leading to aggregation (Tofaris *et al.*, 2006; Lundblad *et al.*, 2012). A peculiarity of α-synuclein aggregates is their ability to spread from diseased to healthy neurons, where they act as template for the pathological conversion of soluble α-synuclein monomers (J. Y. Li *et al.*, 2008; Kordower *et al.*, 2008). The process of α-synuclein spreading follows a stereotypical pattern, mostly influenced by the relative connectivity of the brain areas involved (Braak *et al.*, 2003). Even if direct membrane damage partially contributes to the diffusion of aggregates from affected neurons to the extracellular milieu, α-synuclein secretion mostly occurs at the axonal terminal and is regulated by activity-dependent exocytosis (Fontaine *et al.*, 2016; Lee *et al.*, 2005; Yamada *et al.*, 2018). In addition, other non-canonical secretory mechanisms mediate α-synuclein spreading, including exosome release (Emmanouilidou *et al.*, 2010; Alvarez-Erviti *et al.*, 2011) and interneuronal transmission via tunnelling nanotubes (Dieriks *et al.*, 2017).

Both preservation of functional synaptic architecture and the secretory and uptake events occurring at the presynaptic terminal rely on the subcellular trafficking of molecules and organelles (Kapitein *et al.*, 2015; Xie *et al.*, 2017). In this context, LRRK2 and HDAC6 play a crucial role through complementary mechanisms. LRRK2 phosphorylates several members of the Rab GTPases protein family, which operate as molecular switches for the fine regulation of vesicular trafficking (Steger *et al.*, 2016). On the other hand, HDAC6 removes α-tubulin acetylation, a marker of stable MTs which promotes intracellular transport (Hubbert *et al.*, 2002; Dompierre *et al.*, 2007; Reed *et al.*, 2006).

Our data on the interaction between LRRK2 and HDAC6 suggest that LRRK2 signalling may intersect HDAC6 functions at some level. Notably, LRRK2 interacts with MTs and its expression inversely correlates with MTs acetylation (Caesar *et al.*,

2013; Deniston *et al.*, 2020; Gandhi *et al.*, 2008; Law *et al.*, 2014). Recent evidence indicates that LRRK2 kinase inhibition increases the axonal trafficking of α-synuclein towards the pre-synaptic compartment (Brzozowski *et al.*, 2021). Pathogenic LRRK2 mutants form filaments along deacetylated MTs stretches which interfere with axonal transport. Both aberrant LRRK2 filamentation and impaired subcellular trafficking can be rescued upon pharmacological and genetic manipulation of MTs acetylation status (Godena *et al.*, 2014). Since HDAC6 is the main tubulin deacetylase (Hubbert *et al.*, 2002; Zhang, Sohee Kwon, *et al.*, 2008), we hypothesised that LRRK2 may regulate MTs acetylation via HDAC6. This, in turn, might influence the way α-synuclein is transported to the presynaptic terminal and have important implications on the nucleation, accretion and secretion of α-synuclein aggregates in PD.

5.2 Results

5.2.1 LRRK2 kinase activity does not regulate HDAC6 deacetylase activity

The binding between LRRK2 and HDAC6 and the role played by LRRK2 in sustaining HDAC6-dependendent aggresome formation suggest a functional interplay between these two proteins. So far, we showed that LRRK2 kinase activity does not regulate HDAC6 chaperone function in the context of aggresome formation and NLRP3 inflammasome activation. Nonetheless, HDAC6 is a phospho-protein whose deacetylase activity is tuned by phosphorylation (reviewed by Losson *et al.*, 2020). Although we could not confirm S22 as a phosphorylation site targeted by LRRK2, we cannot exclude the possibility that LRRK2 might modify other HDAC6 residues and regulate its enzymatic activity. Therefore, we tested if LRRK2 regulates HDAC6 by phosphorylation in HEK293 and COS7 cells. If this hypothesis is verified, inhibition of LRRK2 kinase activity should result in a change in the acetylation levels of HDAC6 substrates. Because MT deacetylation is one of the main HDAC6 functions which also influences cellular transport, we assessed α-tubulin acetylation level as readout of HDAC6 enzymatic activity.

HEK293 were treated with either tubastatin A or MLi-2 for 12 h. Total cell lysates were separated by SDS-PAGE and immunoblotted using antibodies anti- total and acetylated tubulin. LRRK2 kinase inhibition was confirmed by immunoblot by quantifying Rab8a-T72 phosphorylation on HEK293 transfected with myc-LRRK2-G2019S and EGFP-Rab8a and incubated with the same media used for the main experiment (Fig. 5.1b).

Baseline tubulin acetylation was readily detected in control samples and underwent a threefold increase upon HDAC6 inhibition. In contrast, LRRK2 inhibition did not perturb tubulin acetylation (Fig. 5.1a).

To confirm this result, we repeated a similar experiment in COS7 cells. Samples were treated with either tubastatin A or MLi-2 for 16 h. Total protein lysates were separated by SDS-PAGE and immunoblotted using antibodies anti- total and acetylated tubulin. LRRK2 kinase inhibition was confirmed by immunoblot by quantifying Rab10-T73 phosphorylation (Fig. 5.1d).

Data collected in COS7 recapitulated what we reported in HEK293. Tubastatin A administration consistently increased tubulin acetylation by about 4 times compared to baseline, but no effect resulted from LRRK2 inhibition (Fig. 3.1c).

Since LRRK2 kinase inhibition did not cause any detectable changes in tubulin acetylation in any of the cell systems tested, we can conclude that LRRK2 kinase does not regulate HDAC6 deacetylase activity by phosphorylation *in cellulo*.

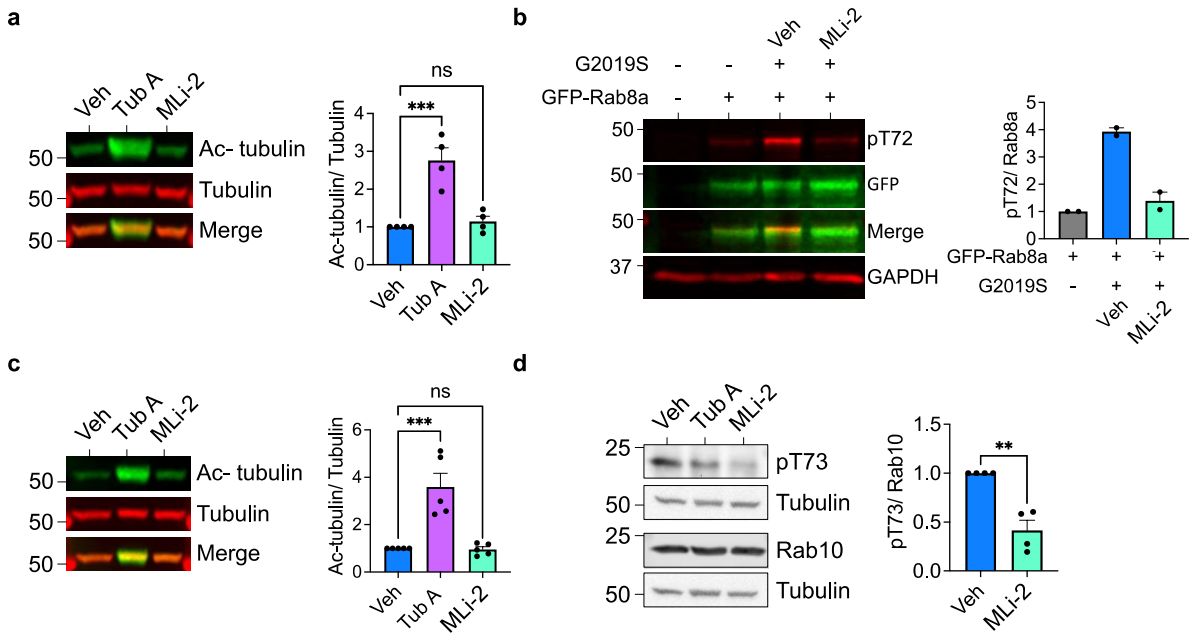

Figure 5.1 HDAC6 deacetylase activity is not regulated by LRRK2 kinase activity. a) HEK293 incubated with either DMSO (veh), tubastatin A (Tub A) or MLi-2 for 12 h. Total cell lysates were processed by SDS-PAGE and immunoblotted using antibodies anti- acetylated and total tubulin. One-way ANOVA with Fisher's LSD test; N= 4. **b)** HEK293 transfected with GFP-Rab8a and either an empty vector or myc-LRRK2-G2019S. 24 h post-transfection, samples were incubated with the same inhibitor mix used in a). Protein lysates were processed by SDS-PAGE and immunoblotted using antibodies anti- GFP, phospho-Rab8a-T72 and GAPDH. N= 2. **c)** COS7 incubated with either DMSO (veh), tubastatin A (Tub A) or MLi-2 for 16 h. Total cell lysates were processed as in a). One-way ANOVA with Fisher's LSD test; N= 5. **d)** Protein samples from c) separated by SDS-PAGE and immunoblotted using antibodies anti phospho-Rab10-T73, total Rab10 and tubulin. Unpaired t-test. N= 4.
All data are shown as mean± SEM; ns= non-significant; **= p≤ 0.01; ***= p≤ 0.001.

5.2.2 Role of LRRK2 and HDAC6 on α-synuclein subcellular localisation

According to Brzozowski and colleagues, LRRK2 kinase inhibition increases the anterograde axonal transport of α-synuclein and results in the accumulation of the protein at the pre-synaptic terminal (Brzozowski *et al.*, 2021). This effect can be detected as a positive change in colocalization between α-synuclein and other proteins normally expressed in this subcellular compartment, such as vesicular glutamate transporter 1 (vGLUT1).

Based on our hypothesis of an interplay between LRRK2 and HDAC6 and given the importance of HDAC6 in subcellular trafficking, we investigated if LRRK2 interacts with HDAC6 to regulate targeting of α-synuclein to the synapse. To compare the effect of LRRK2 and HDAC6 inhibition on α-synuclein subcellular localization, we tested the colocalization of α-synuclein and the pre-synaptic marker vGLUT1 in hippocampal and cortical mouse neurons treated with either MLi-2 or tubastatin A. Two different treatment administration patterns were compared to distinguish between long-term and short-term effects of LRRK2 and HDAC6 inhibition.

The 1-week treatment is based on the protocol described by Brzozowski and colleagues (Brzozowski *et al.*, 2021). Samples were treated as follows: neurons were fed with a 1:1 mix of fresh and conditioned neural media at DIV7; either 100 nM MLi-2 or 10 μM tubastatin A were added at this step and incubated for 7 days. To explore possible short-term effects of LRRK2 and HDAC6 inhibition, a 24 h treatment incubation protocol was tested in parallel. Thus, samples were treated as follows: neurons were fed with a 1:1 mix of fresh and conditioned neural media at DIV7 and 13; at DIV13 either 100 nM MLi-2 or 10 μM tubastatin A were added and incubated for 24 h.

All the samples were fixed at DIV14, immunostained using anti- α-synuclein and vGLUT1 antibodies and imaged on a confocal microscope. Colocalization between α-synuclein and vGLUT1 was calculated by applying two different mathematical approaches. The thresholded Mander's colocalization coefficients for α-synuclein (tMCC1) represents the ratio of positive pixels in the α-synuclein channel overlapping with positive pixels in the vGLUT1 channel. tMCC ranges from 0 to 1, where 0 indicates no overlap and 1 complete overlap. We did not show the reverse coefficient (tMCC2), assuming that vGLUT1 subcellular distribution is not affected by the treatments. Despite tMCC being an intuitive measure of "how well" pixels in channel A colocalize

with pixels in channel B, this coefficient is influenced by the intensity of the two signals. The Pearson's correlation coefficient (PCC) ranges between -1 and +1 and indicates how much the pixel intensities in two channels are related by a linear equation. PCC= -1 indicates that signal in channel A is excluded from the areas where signal in channel B is present and vice versa; PCC= 0 means that the two signals are randomly distributed; PCC= 1 indicates perfect linear relation between the two signals. This method is unaffected by signal intensity and background (Dunn *et al.*, 2011).
Part of the samples was lysed in TBS+ 2% SDS, separated by SDS-PAGE and immunoblotted to detect phospho-Rab10-T73, acetylated tubulin, α-synuclein and vGLUT1.

Effective LRRK2 inhibition was marked by a decrease in Rab10-T73 phosphorylation after 7 days and 24 h of MLi-2 incubation (Fig. 3.2b, d, g, i). Interestingly, HDAC6 inhibition resulted in Rab10-T73 dephosphorylation similarly to MLi-2 administration.
Quantification of tubulin acetylation levels did not unequivocally confirm HDAC6 inhibition. Nonetheless, a proportional increase in total and acetylated α-tubulin was detected in all biological replicates, suggesting an effect of tubastatin A administration (Fig 3.2e, j). In contrast with Brzozowski and colleagues' work, we did not observe any significant differences in the subcellular distribution of α-synuclein in hippocampal neurons after 7 days of LRRK2 kinase inhibition (Fig. 3.2a). Unexpectedly, exposure to 10 μM tubastatin A for 1 week caused severe neuronal death. For this reason, no data could be collected on the long-term effect of HDAC6 inhibition on α-synuclein trafficking.
No differences in α-synuclein subcellular localisation were detected upon either LRRK2 or HDAC6 inhibition for 24 h (Fig. 3.2c). One possible explanation may be ascribed to the timescale of the phenomena being observed. Brzozowski and colleagues reported an increase in anterograde axonal trafficking of α-synuclein as soon as 30 minutes post MLi-2 administration. Yet, detectable changes in the overall neuronal architecture might occur in more than 24 h. Additionally, neurons treated for 24 h showed a different morphology compared to those incubated for 7 days (Fig. 3.2a, c). Neuronal projections appeared irregular and more disorganised, with most α-synuclein and vGLUT1 accumulating into swollen synaptic terminals similar to apoptotic vesicles. The main difference between the 24 h and the 1-week treatment protocols is the supplementary feeding step at the time of drugs administration, 24 h

prior to harvesting. It is likely that the addition of fresh media or DMSO represents a stressor from which neurons recover after a few days. This might influence the experimental readout. Cortical and hippocampal neurons showed the same overall behaviour (Fig. 3.2f, h).

Our data indicate that LRRK2 inhibition does not affect α-synuclein targeting to synapse neither in hippocampal nor in cortical neurons. This was tested after 24 h and 7 days of incubation with the LRRK2 kinase inhibitor MLi-2. Inhibition of HDAC6 for 24 h did not influence the colocalization between α-synuclein and vGLUT1, which indicates that HDAC6 has no short-term effects on α-synuclein subcellular localization.

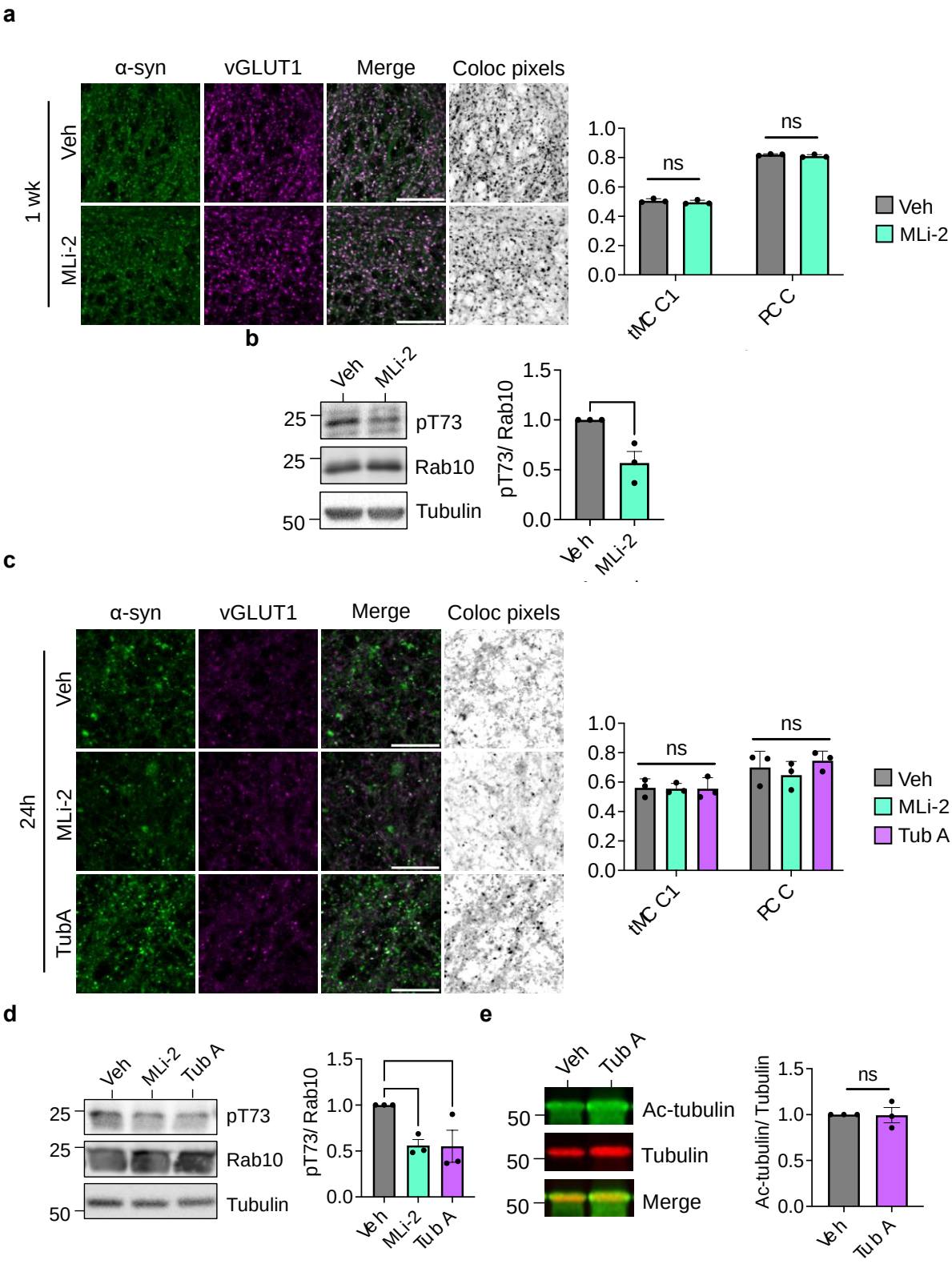
a
α-syn
vGLUT1
Merge
Coloc pixels
1 wk
Veh
MLi-2
ns
ns
tMC C1
PC C
Veh
MLi-2
b
Veh
MLi-2
25
pT73
25
Rab10
50
Tubulin
pT73/ Rab10
c
α-syn
vGLUT1
Merge
Coloc pixels
24h
Veh
MLi-2
TubA
ns
ns
tMC C1
PC C
Veh
MLi-2
Tub A
d
Veh
MLi-2
Tub A
25
pT73
25
Rab10
50
Tubulin
pT73/ Rab10
e
Veh
Tub A
50
Ac-tubulin
50
Tubulin
50
Merge
Ac-tubulin/ Tubulin
ns

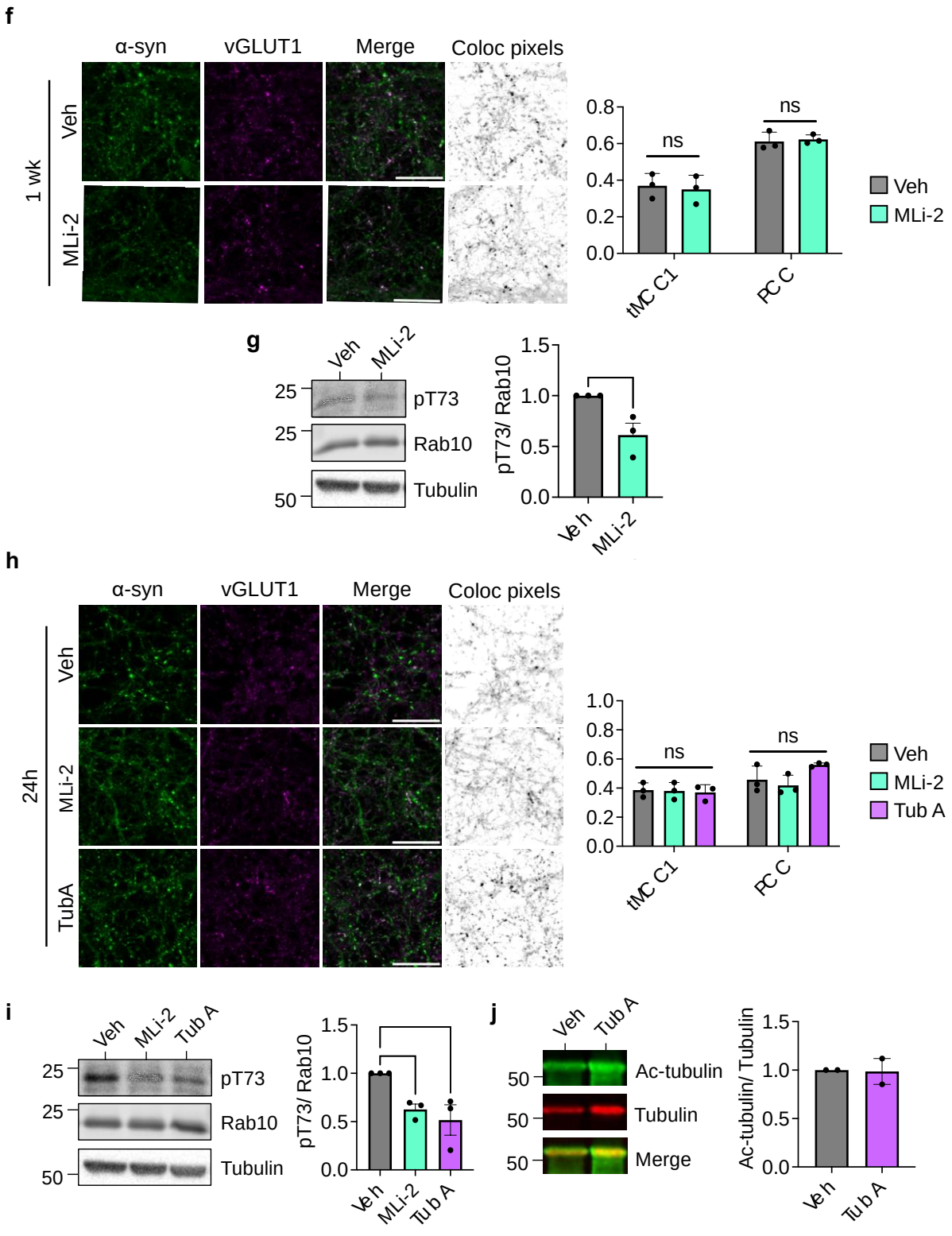

Figure 5.2 Inhibition of LRRK2 kinase activity does not influence presynaptic targeting of α-synuclein. a) DIV7 mouse hippocampal neurons were incubated with either DMSO (Veh) or MLi-2 for 7 days. At DIV14, cells were fixed and immunostained using antibodies anti α-synuclein (green) and vGLUT1 (magenta). The black and white colocalization map shows the areas where α-synuclein signal overlaps with vGLUT1. Graphs report the thresholded Menders' colocalization coefficient for α-synuclein over vGLUT1 (tMCC1) and the Pearson's

correlation coefficient (PCC) of the two signals. One-way ANOVA. Scale bar= 20 μm. N=3 **b)** Total protein extracts of hippocampal neurons treated as in a) were processed by SDS-PAGE and immunoblotted using antibodies anti- phospho-Rab10-T73, total Rab10 and tubulin. Unpaired t-test. N= 3. **c)** DIV13 mouse hippocampal neurons were incubated with either DMSO (Veh), MLi-2 or tubastatin A for 24 h. At DIV14, cells were fixed and immunostained using antibodies anti α-synuclein (green) and vGLUT1 (magenta). Colocalised pixels are shown in grey. Graphs report the tMCC1 and PCC of the two signals. One-way ANOVA. Scale bar= 20 μm. N=3 **d)** Total protein extracts of hippocampal neurons treated as in c) were processed by SDS-PAGE and immunoblotted using antibodies anti- phospho-Rab10-T73, total Rab10 and tubulin. One-way ANOVA with Fisher's LSD test; N= 3. **e)** Total protein extracts of hippocampal neurons treated as in c) were processed by SDS-PAGE and immunoblotted using antibodies anti- total and acetylated and tubulin. Unpaired t-test. N= 3. **f)** DIV7 mouse cortical neurons were incubated with either DMSO (Veh) or MLi-2 for 7 days. At DIV14, cells were fixed and immunostained using antibodies anti α-synuclein (green) and vGLUT1 (magenta). Colocalised pixels are shown in grey. Graphs report the tMCC1 and PCC of the two signals. One-way ANOVA. Scale bar= 20 μm. N=3 **g)** Total protein extracts of hippocampal neurons treated as in f) were processed by SDS-PAGE and immunoblotted using antibodies anti- phospho-Rab10-T73, total Rab10 and tubulin. Unpaired t-test. N= 3. **h)** DIV13 mouse cortical neurons were incubated with either DMSO (Veh), MLi-2 or tubastatin A for 24 h. At DIV14, cells were fixed and immunostained using antibodies anti α-synuclein (green) and vGLUT1 (magenta). Colocalised pixels are shown in grey. Graphs report the tMCC1 and PCC of the two signals. One-way ANOVA. Scale bar= 20 μm. N=3 **i)** Total protein extracts of cortical neurons treated as in h) were processed by SDS-PAGE and immunoblotted using antibodies anti- phospho-Rab10-T73, total Rab10 and tubulin. One-way ANOVA with Fisher's LSD test; N= 3. **j)** Total protein extracts of cortical neurons treated as in h) were processed by SDS-PAGE and immunoblotted using antibodies anti- total and acetylated and tubulin. N= 2. All data are shown as mean± SEM; ns= non-significant; *= p≤ 0.05.

5.2.3 LRRK2 and HDAC6 regulate physiological α-synuclein turnover

The ability of LRRK2 and HDAC6 to modulate α-synuclein pathology underlines the involvement both proteins in α-synuclein homeostasis. In Chapter 4.2.3 we showed that HDAC6 inhibition promotes the accumulation of aggregates stimulated by inoculation of α-synuclein PFFs (Fig. 4.3). However, neither LRRK2 nor HDAC6 seemed to contribute to clearance of α-synuclein aggregates via aggrephagy. In addition to degradation, secretion of misfolded proteins represents a mechanism by which neurons dispose of damaged cellular components. Neurons often rely on glial cells for the clearance of metabolic side-products secreted in the interstitial fluid (Yankova *et al.*, 2021). Additionally, the glial contribution to clearance of α-synuclein pathogenic species is well documented (Yi *et al.*, 2022). In this section we investigated the role played by LRRK2 and HDAC6 on physiological α-synuclein homeostasis. We focussed on the effect of HDAC6 and LRRK2 inhibition on α-synuclein secretion in undifferentiated SH-SY5Y expressing h-WT-α-synuclein and DIV14 rat cortical neurons. WT primary neurons were used to corroborate the observations extrapolated from the SH-SY5Y model and exclude possible artefacts due to transient α-synuclein expression.

Cells were treated with either tubastatin A or three structurally distinct LRRK2 kinase inhibitors: MLi-2, GSK2578215A (GSK25, Reith *et al.*, 2012) and HG-10-102-01 (HG-10, Choi *et al.*, 2012) 24 h post-transfection (SH-SY5Y cells) or at DIV13 (cortical neurons). 24 h post inhibitor administration, conditioned media samples were collected. Part of the samples was mixed with 5x Laemmli buffer and processed by dot-blot. The amount of α-synuclein secreted in the culture media was quantified by using an anti-α-synuclein antibody. This detection method was chosen over SDS-PAGE followed by immunoblotting due to its capacity to handle larger volumes of conditioned media, leading to a more robust detection of α-synuclein. Preliminary analysis of the conditioned media samples through immunoblotting did not yield bands suitable for quantification (data not shown). We reasoned that treatment incubation may influence cell survival and that apoptotic or damaged cells may as well disperse α-synuclein in the media. To exclude confounding effects leading to α-synuclein leakage, treatment-induced cell toxicity was assessed with a commercial LDH release assay and used to normalise the dot-blot readout. To test α-synuclein expression level, cell samples were lysed in 2.5x Laemmli buffer, processed by SDS-PAGE and

immunoblotted using anti- α-synuclein and pS129 antibodies. HDAC6 inhibition was confirmed on total cell lysates using anti- tubulin and acetylated tubulin antibodies.

α-synuclein was detected in conditioned media of SH-SH5Y and cortical neurons treated with DMSO, consistent with basal physiological secretion (Fig. 5.3b, f; Fontaine *et al.*, 2016). Treatment administration did not cause detectable cell toxicity in SH-SH5Y (Fig. 3.3c) but increased LDH release in neurons, indicating a mild neurotoxic effect (Fig. 5.3g). HDAC6 inhibition was confirmed in SH-SH5Y as a significant increase in tubulin acetylation (Fig. 5.3d). In rat cortical neurons the increase in tubulin acetylation correlated with an increase in tubulin expression, resulting in no significant changes of the ratio between acetylated and total tubulin. However, it is clear from the analysis of the immunoblot images that tubastatin A administration caused some changes at a protein level (Fig. 5.3h). Tubastatin A administration had no effect on the amount of α-synuclein detected in the conditioned media (normalised by cell toxicity) in both SH-SH5Y and cortical neurons (Fig. 5.3b, f). This indicates that HDAC6 does not regulate α-synuclein secretion. The effect of LRRK2 inhibition on α-synuclein secretion varied depending on the inhibitor used. MLi-2 administration had no overall effect on α-synuclein secretion. GSK25 administration slightly reduced α-synuclein secretion in SH-SH5Y but not in neurons. HG-10 reduced secretion in both SH-SH5Y and neurons by about 20-40% (Fig. 5.3b, f). Since MLi-2 is the most potent and specific LRRK2 inhibitor among those tested, we can conclude that LRRK2 kinase activity does not influence basal α-synuclein secretion. The mild, model-specific effect of GSK25 and HG-10 inhibitors may be caused by off-target inhibitory activity.

Both HDAC6 and LRRK2 inhibition caused a consistent increase in the amount of α-synuclein detected in the total cell lysates (Fig. 5.3a, e), indicating a role of both proteins in α-synuclein metabolism. Immunoblot analysis of SH-SH5Y and cortical neurons protein extracts also revealed that inhibition of HDAC6 and LRRK2 caused a significant reduction of α-synuclein-S129 phosphorylation (Fig. 5.3b, f). α-synuclein is a substrate of a panel of protein kinases including LRRK2, but the role of the latter on α-synuclein-S129 phosphorylation is controversial (Kawahata, Finkelstein and Fukunaga, 2022). Our data support LRRK2 as a kinase targeting α-synuclein-S129. In chapter 3.3, we observed that tubastatin A administration consistently inhibited Rab10-T73 phosphorylation, a well-known LRRK2 effector. This indicates that HDAC6 might regulate LRRK2 kinase activity. This would explain why HDAC6 inhibition also

results in α-synuclein-S129 dephosphorylation. Further work will confirm these hypotheses.

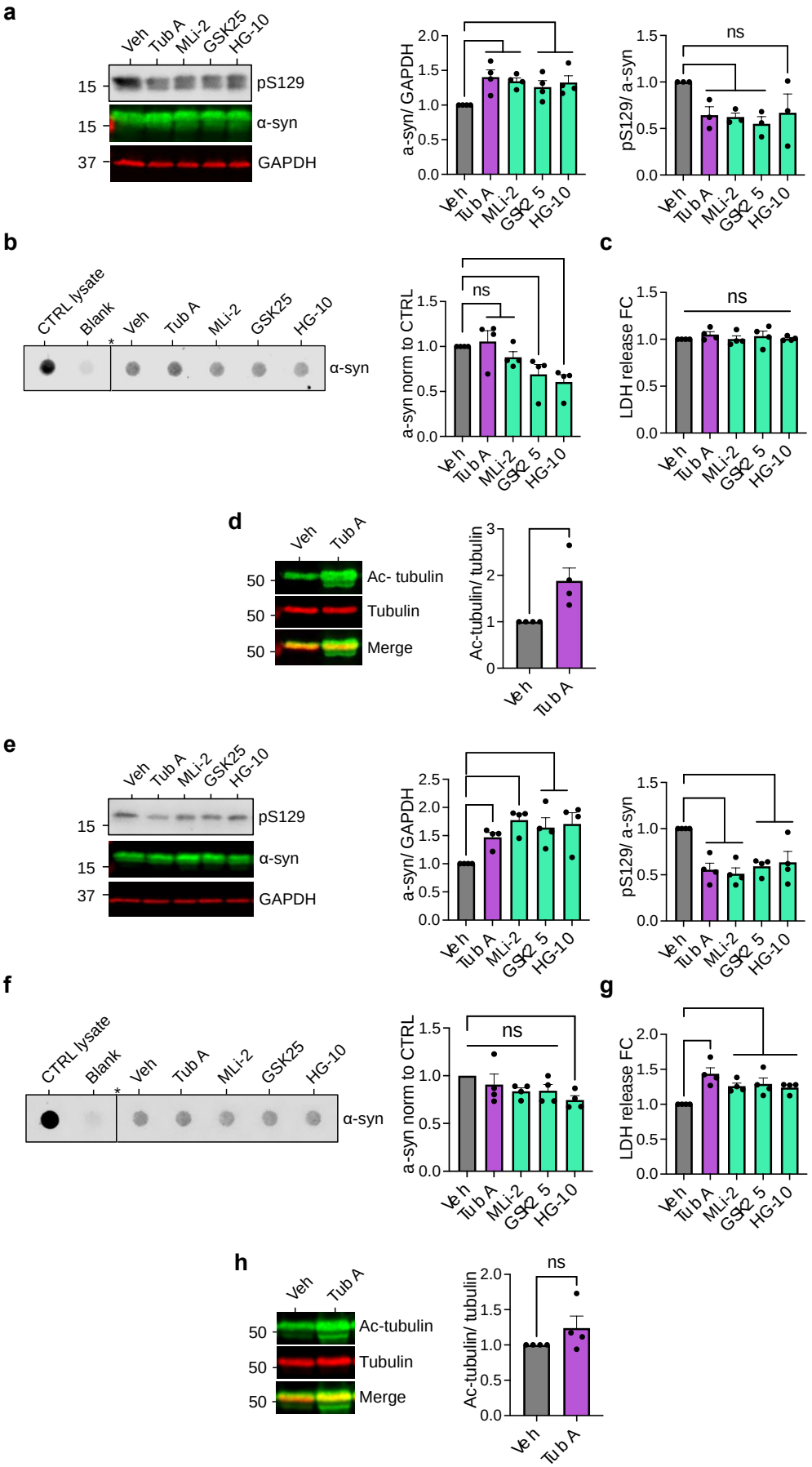
a
Veh
Tub A
MLi-2
GSK25
HG-10
15
pS129
15
α-syn
37
GAPDH
a-syn/ GAPDH
pS129/ a-syn
ns
b
CTRL lysate
Blank
α-syn
a-syn norm to CTRL
c
LDH release FC
d
Ac- tubulin
Tubulin
Merge
50
Ac-tubulin/ tubulin
e
f
g
h
Ac-tubulin

Figure 5.3 LRRK2 and HDAC6 regulate α-synuclein turnover but have no impact on α-synuclein secretion. a) SH-SY5Y were transfected with WT α-synuclein. 24 h post-transfection samples were treated with either DMSO (Veh), tubastatin A (Tub A), MLi-2, GSK2578215A (GSK25) or HG-10-102-01 (HG-10) for 24 h. Samples were lysed, processed by SDS-PAGE and immunoblotted using antibodies anti- pS129, α-synuclein and GAPDH. One-way ANOVA with Fisher's LSD test; N= 3/4. **b)** Conditioned media obtained from the samples described in a) were mixed with Laemmli buffer and processed by dot-blot using an α-synuclein antibody. The graph reports data normalised by LDH release measured in c) and expressed as ratio to vehicle-treated control. One-way ANOVA with Fisher's LSD test; N= 4. **c)** Fresh conditioned media from a) assessed with a commercial LDH release enzymatic assay. One-way ANOVA with Fisher's LSD test; N= 4. **d)** Total cell lysates obtained as in a) separated by SDS-PAGE and probed with anti- total and acetylated-tubulin antibodies. Unpaired t-test. N=4. **e)** DIV13 rat cortical neurons were treated with either Veh, Tub A, MLi-2, GSK25 or HG-10 for 24 h. Samples were lysed, processed by SDS-PAGE and immunoblotted using antibodies anti- pS129, α-synuclein and GAPDH. One-way ANOVA with Fisher's LSD test; N= 4. **f)** Conditioned media from e) processed by dot-blot and probed using an antibody anti- α-synuclein. Data are normalised based on the LDH release test reported in g) and expressed as a ratio to control. One-way ANOVA with Fisher's LSD test; N= 4. **g)** Conditioned media from e) tested with a LDH release enzymatic assay. One-way ANOVA with Fisher's LSD test; N= 4. **h)** Protein samples from e) were separated by SDS-PAGE and analysed by immunoblot using antibodies total and acetylated-tubulin. Unpaired t-test. N=4.
All data are shown as mean± SEM; ns= non-significant; *= p≤ 0.05; **= p≤ 0.01; ***= p≤ 0.001.

5.3 Discussion

In this chapter we investigated a possible mechanism by which LRRK2 may direct cellular dynamics by regulating MT acetylation via HDAC6. Although the direct role of HDAC6 as an effector of LRRK2's impact on MTs acetylation has not been directly confirmed, a few pieces of evidence support this model. First, LRRK2 does not possess any deacetylase activity. Second, LRRK2 binds to and phosphorylates HDAC6 *in vitro*. Third, both LRRK2 and HDAC6 expression levels inversely correlate with α-tubulin-K40 acetylation levels. Finally, HDAC6 inhibition rescues the tubulin acetylation loss caused by LRRK2 overexpression.

In Chapter 4.2.3 we showed that basal LRRK2 kinase activity is not required to promote HDAC6-dependent aggresome formation. However, we could not exclude if the kinase-substrate interaction observed *in vitro* between LRRK2 and HDAC6 can regulate other HDAC6 functions by modifying its deacetylase activity. Here, we further validated the biochemical significance of LRRK2-mediated HDAC6 phosphorylation by testing the effect of LRRK2 inhibition on tubulin acetylation, one of the main HDAC6 substrates (Zhang *et al.*, 2003).

LRRK2 inhibition did not affect α-tubulin acetylation in both HEK293 and COS7 cells, strongly suggesting that HDAC6 deacetylase activity is insensitive to loss of LRRK2 kinase activity. Given the positive correlation between HDAC6 deacetylase activity and the rate of HDAC6-dependent aggresome formation confirmed both elsewhere (Kawaguchi *et al.*, 2003; Watabe *et al.*, 2011) and previously in this work (Chapter 3.2.1), this result aligns with our findings on aggrephagy. This points towards the more general conclusion that HDAC6 is not physiologically regulated by LRRK2 kinase activity.

As mentioned in chapter 3.3, in specific contexts LRRK2 can operate as a signalling platform (Berwick and Harvey, 2012; Shanley *et al.*, 2015; Yoon *et al.*, 2017; Perez Carrion *et al.*, 2018). The LRRK2 Roc domain directly binds to a region of the β-tubulin monomer facing the intraluminal side of the MT in close proximity to α-tubulin-K40 (Law *et al.*, 2014). Although HDAC6 can directly bind to and deacetylates tubulin in vitro (Zhang *et al.*, 2003), it is possible that LRRK2 may facilitate the recruitment of HDAC6 to the MT and enhance the kinetics of the deacetylation reaction. Alternatively, it is possible that LRRK2 acts as a positive allosteric modulator of HDAC6 deacetylase

activity. A similar role has been proposed for tubulin polymerization-promoting protein-1 (TPPP1/p25), which regulates MTs acetylation by binding to HDAC6 and inhibiting its enzymatic activity (Schofield *et al.*, 2013). A third possibility we did not explore in this work is that the impact of LRRK2 on MTs depends on the inhibition of α-tubulin acetylation rather than the increase of the opposing enzymatic reaction. α-tubulin-K40 acetylation is predominately mediated by α-tubulin acetyltransferase 1 (ATAT1; Akella *et al.*, 2010; Siegel *et al.*, 2021). To the best of our knowledge, there are no reports of LRRK2 interacting with ATAT1. Nonetheless, LRRK2 may compete with ATAT1 for its binding to MTs keeping α-tubulin in its non-acetylated state.

α-synuclein is enriched at the pre-synaptic compartment of mature neurons. We investigated if inhibiting HDAC6 recapitulates the reported effects of LRRK2 inhibition on α-synuclein trafficking (Brzozowski *et al.*, 2021). Either hippocampal or cortical neurons were incubated with LRRK2 kinase inhibitors for either 7 d or 24 h and the colocalization between α-synuclein and the presynaptic marker vGLUT1 was assessed by confocal microscopy. Despite applying the same methods detailed by Brzozowski and colleagues (Brzozowski *et al.*, 2021), we did not observe any changes in colocalization between α-synuclein and vGLUT1 in any of the conditions and neuronal populations tested. Additionally, we could not collect information on the long-term effect of HDAC6 inhibition on presynaptic targeting of α-synuclein due to the elevated *in vitro* neurotoxicity of the dosage of tubastatin A used in this study. Moving forward, a dose-response curve could help identify a better tolerated but still effective tubastatin A concentration range. In line with LRRK2 inhibition, the 24 h tubastatin A treatment did not affect the colocalization coefficients related to α-synuclein and vGLUT1. In our experimental setup, MLi-2 was used as positive control to enhance anterograde α-synuclein trafficking, following the reports by Brzozowski and colleagues (Brzozowski *et al.*, 2021). Since their findings were not replicated, we cannot exclude the possibility of experimental artifacts masking the effect of HDAC6 on α-synuclein subcellular localisation. Interestingly, we did observe that tubastatin A consistently reduced Rab10-T73 phosphorylation, similarly to LRRK2 kinase inhibition. To our knowledge, the regulation of LRRK2 via HDAC6 has not been previously reported, neither is there evidence in literature that LRRK2 kinase activity can be regulated by acetylation. Yet, LRRK2 stability relies on the formation of a complex with the molecular chaperone heat shock protein 90 (HSP90). Inhibition of

HSP90 causes the detachment of LRRK2 from the complex and its subsequent proteasomal degradation (Wang *et al.*, 2008). HSP90 chaperone function is reversibly regulated by acetylation and depends on HDAC6 activity (Kovacs *et al.*, 2005). Thus, it is possible that HDAC6 inhibition increases HSP90 acetylation and promotes LRRK2 degradation.
Even if we could not replicate their results, the interdependence between LRRK2 kinase activity and α-synuclein subcellular distribution proposed by Brzozowski and colleagues may have crucial implications for the secretion of α-synuclein monomers and aggregates from the axon terminal (Fontaine *et al.*, 2016; Lee *et al.*, 2005; Yamada *et al.*, 2018).

Despite the body of literature describing the impact of LRRK2 dysregulation on phenotypes linked to PD encompassing α-synuclein aggregation and spreading (Ito *et al.*, 2023; Sosero *et al.*, 2023), LRRK2's role on physiological α-synuclein metabolism is still poorly investigated. Yet, alterations to basal α-synuclein clearance routes, including constitutive secretion, may drive both onset and prodromal stages of PD pathology. Here, we addressed this knowledge gap through the lens of a LRRK2/HDAC6 interaction. To investigate the role of LRRK2 kinase activity and tubulin acetylation levels on constitutive α-synuclein secretion we pharmacologically manipulated LRRK2 and HDAC6 enzymatic activities in SH-SY5Y cells expressing α-synuclein and in primary cortical neurons.
HDAC6 inhibition resulted in the accumulation of intracellular α-synuclein both under overexpression and endogenous conditions. These observations complete the data collected in PFF-induced COS7 (Chapter 4.2.3) and further emphasise the importance of HDAC6 in α-synuclein turnover. In contrast with previous reports (Guerreiro *et al.*, 2013; Brzozowski *et al.*, 2021; P. W. L. Ho *et al.*, 2022), LRRK2 inhibition also increased α-synuclein expression level in both SH-SY5Y and neurons. We also consistently observed a reduction in basal α-synuclein phosphorylation upon either LRRK2 or HDAC6 inhibition. LRRK2 has been previously proposed as a putative α-synuclein kinase which may target S129. LRRK2 binds to α-synuclein in mouse and PD patient brains and phosphorylates S129 *in vitro* (Guerreiro *et al.*, 2013; Qing *et al.*, 2009a; Qing *et al.*, 2009b). Apart from one contradictory study (Guerreiro *et al.*, 2013), several authors reported that both LRRK2 KO or inhibition reduce S129 phosphorylation in SH-SY5Y cells, mouse primary neurons, and human iNeurons

(Bieri *et al.*, 2019; Ho *et al.*, 2022). On the contrary, LRRK2 overexpression increases S129 phosphorylation (Kondo, Obitsu and Teshima, 2011; Guerreiro *et al.*, 2013). Reduced pS129 has also been observed in rats acutely expressing α-synuclein and treated with tubastatin A (Francelle *et al.*, 2020). Our data once again seem to suggest that HDAC6 may regulate LRRK2 kinase activity. As we mentioned above, the link could lie within HSP90 chaperone function (Wang *et al.*, 2008).

Since both LRRK2 and HDAC6 play a role in subcellular dynamics, we tested if the increase in α-synuclein expression caused by LRRK2 and HDAC6 inhibitors results from changes in basal α-synuclein secretion. The detection method adopted in the present work virtually allows the quantification of both membrane-bound and freely diffusible α-synuclein and is robust against cytosol leakage caused by pharmacotoxicity. We observed that neither LRRK2 kinase activity nor HDAC6 deacetylase activity are involved in basal secretion of α-synuclein both in SH-SY5Y cells and cortical neurons. This seems to align with our observation that neither HDAC6 nor LRRK2 inhibition affected α-synuclein subcellular localisation. If α-synuclein accumulated at the presynaptic compartment after 24 h of treatment, we would possibly expect a change in secretion rate. Nonetheless, given the limitations of the dot blot technique, particularly its inability to discern and exclude non-specific antibody binding, the findings on α-synuclein secretion warrant additional validation through more specific methods, such as SDS-PAGE/immunoblotting or ELISA.

The first work exploring the role of LRRK2 on α-synuclein intercellular propagation was based on SH-SY5Y and PC12 cells co-expressing either WT or G2019S LRRK2 and α-synuclein (Kondo *et al.*, 2011). Using this model, Kondo and colleagues observed that LRRK2 overexpression causes α-synuclein hyperphosphorylation and release of membrane-bound α-synuclein that can transmit to naïve cells. The authors pointed out that α-synuclein propagation is higher in cells expressing mutant LRRK2 than those transfected with the WT isoform. However, since LRRK2 overexpression was also linked to enhanced cytotoxicity, the work by Kondo and colleagues does not clarify if the release of α-synuclein in this experimental background is due to a regulated secretion mechanism or to the dispersion of apoptotic vesicles (Kondo *et al.*, 2011). A similar limitation applies to a later work utilising a bimolecular fluorescence complementation (BiFC) approach in SHSY-SY (Bae *et al.*, 2018). In this study Bae

and co-workers confirmed that LRRK2 regulates α-synuclein propagation through a kinase-dependent mechanism involving Rab35.

Our data combined with the observations of other groups seem to point towards a pathogenic gain-of-function of LRRK2 upregulation, which is exacerbated by the G2019S mutation. The hypothesis that this effect could be predominantly mediated by Rab35 is corroborated by the evidence that Rab35 hyperphosphorylation exerts the more severe impact on neurodegeneration compared to any other Rab GTPases targeted by LRRK2 (Jeong *et al.*, 2018). LRRK2 hyperactivity would hijack endosomal recycling and deviate pathogenic α-synuclein from the endolysosomal degradation pathway to a secretory route (Jeong and Lee, 2020b; Zenko *et al.*, 2023). On the other hand, LRRK2 basal activity has minimal to no effect on the constitutive release of α-synuclein from the cell, which probably relies on LRRK2- and HDAC6-independent mechanisms.

Since the administration of HDAC6 and LRRK2 inhibitors led to an increase in α-synuclein expression level with no changes in secretion, this suggests that both enzymes regulate metabolic processes occurring within the cell. Several degradation routes contribute to maintain α-synuclein homeostasis, including chaperone-mediated autophagy and selective autophagy (Cuervo *et al.*, 2004; Bandyopadhyay *et al.*, 2007). Both LRRK2 and HDAC6 have been implicated in autophagy regulation and lysosomal integrity at multiple levels (Chang *et al.*, 2021; Pang *et al.*, 2022). Thus, it is likely that the accumulation of α-synuclein observed upon HDAC6 and LRRK2 inhibition is due to a perturbance in the autophagic flux. Alternatively, HDAC6 might influence α-synuclein gene expression regulation, as it has been shown for many other genetic loci (Jo *et al.*, 2022). Either of these possibilities await further corroboration.

6 Discussion

6.1 Re-evaluation of the interaction between LRRK2 and HDAC6

LRRK2 mutations and genetic polymorphisms are the most frequent cause of inherited PD (Cherian *et al.*, 2023). LRRK2-PD closely- but not entirely- recapitulates most of the clinical and pathological features of sporadic PD, including changes in α-synuclein metabolism and accumulation of intraneuronal protein inclusions (Taymans *et al.*, 2023; Trinh *et al.*, 2023). All the ascertained pathogenic LRRK2 mutations cluster within LRRK2's catalytic domains and impinge on the enzymatic activity of the protein resulting in gain- and loss-of-function pathogenic mechanisms (Ito *et al.*, 2023). LRRK2 is often upregulated in sporadic PD (Di Maio *et al.*, 2018), which further remarks the mutual connection between changes in LRRK2 activity and loss of dopaminergic neurons. Thus, uncovering how LRRK2 operates in physiology and pathology will help gain valuable insights to address neurodegeneration (Hu *et al.*, 2023).

Our team recently found that a key stress-induced protein quality control mechanism mediated by HDAC6 depends on LRRK2 and is impaired by the gain-of-function mutation G2019S (Lucas *et al.*, 2019). HDAC6 plays a major role in targeting polyubiquitinated aggregates to the aggresome, an important cellular response to a sudden surge in misfolded proteins (Kawaguchi *et al.*, 2003). Intriguingly, HDAC6 was found in LB from PD patients, together with LRRK2 and other elements of the aggresome molecular apparatus (Alegre-Abarrategui *et al.*, 2008; Lee *et al.*, 2002; Mazzetti *et al.*, 2020; McNaught *et al.*, 2002; Miki *et al.*, 2011; Perry *et al.*, 2008). Taken together, these observations support the hypothesis of a connection between aggresome formation and the mechanisms leading to deposition of insoluble α-synuclein inclusions in PD (Olanow *et al.*, 2004; Tanaka *et al.*, 2004). HDAC6 is emerging as a promising disease modifying molecular target across several neurodegenerative disorders for its importance in autophagolysosomal pathways, axonal trafficking and mitochondrial dynamics (Lopresti, 2020). Although increasing evidence documents the neuroprotective effect of HDAC6 modulation in PD, the role attributed to this histone deacetylase in several protein quality control mechanisms and in the accumulation of α-synuclein aggregates complicates the interpretation of the experimental readouts. As we summarised in Chapter 1.4.4, HDAC6

pharmacological or genetic downregulation shifts the equilibrium of α-synuclein pathogenic species from large, relatively stable inclusions towards smaller cytotoxic oligomers. Because of its role in aggrephagy and MT-based transport, HDAC6 may represent a critical link between LRRK2 dysregulation and α-synuclein pathology initiation and spreading.

In the present thesis we aimed to address the unresolved questions invited by the work of Lucas and colleagues by further characterising the relationship between LRRK2 and HDAC6 and investigating the relevance of this interplay for α-synuclein homeostasis in PD. The results of Chapters 3 and 5 taken together contradict the hypothesis that LRRK2 regulates HDAC6 by phosphorylation. In fact, we showed that LRRK2 inhibition had no impact on HDAC6 chaperone function in the context of ubiquitin-dependent aggresome formation (Fig. 3.1) and NLRP3 inflammasome activation (Fig. 3.2). Notably, both processes depend on HDAC6 deacetylase activity (Kawaguchi *et al.*, 2003; Magupalli *et al.*, 2020). Accordingly, we found that LRRK2 kinase inhibition did not perturb tubulin acetylation levels (Fig. 5.1), indicating that HDAC6 enzymatic activity is not regulated by LRRK2-dependent phosphorylation. In line with this, we did not find evidence that LRRK2 is the main kinase targeting HDAC6-S22, a residue previously described to regulate HDAC6 deacetylase activity (Chen *et al.*, 2010) and to be phosphorylated by LRRK2 *in vitro* (Lucas *et al.*, 2019). On the other hand, we showed that LRRK2 kinase hyperactivity disrupted the binding between LRRK2 and HDAC6, which was rescued upon LRRK2 inhibition (Fig. 3.4). This provides further insights on the loss-of-function mechanism by which LRRK2-G2019S affects the recruitment of ubiquitinated aggregates into aggresomes and opens the possibility of pharmacological intervention to restore this cellular function.

HDAC6-mediated aggresome formation has been implicated in the sequestration of several aggregated proteins known for their centrality in other proteinopathies, including CFTR (Kawaguchi *et al.*, 2003), huntingtin (Iwata *et al.*, 2005), DJ-1 (Olzmann *et al.*, 2007), tau (Ding *et al.*, 2008) and SOD1 (Xia *et al.*, 2015). Similarly, HDAC6 has been linked to α-synuclein homeostasis (Du *et al.*, 2010; Du *et al.*, 2014; Su *et al.*, 2011), even though its contribution to the clearance of α-synuclein aggregates via aggrephagy is unclear (Francelle *et al.*, 2020). Therefore, in Chapter 4 we established an *in vitro* model to characterise the recruitment of aggregated α-

synuclein into aggresomes and investigate the role of HDAC6 and LRRK2 in this process. We found that PFF-induced α-synuclein inclusions were targeted to the aggresome independently from HDAC6 deacetylase activity and LRRK2 kinase activity (Fig. 4.3). On the other hand, HDAC6 inhibition led to consistent accumulation of α-synuclein insoluble species that were not targeted to the aggresomes (Fig. 4.3). These data exclude HDAC6-dependent aggrephagy as a plausible mechanism of clearance of α-synuclein aggregates and suggest that a different set of molecular chaperones and cargo adaptors may transport α-synuclein to the organelle (Basso *et al.*, 2006; Gamerdinger *et al.*, 2011). Meanwhile, our results indicate that HDAC6 regulates the accumulation of aggregated α-synuclein via alternative pathways, possibly by promoting its lysosomal degradation (Lee *et al.*, 2010; Wang *et al.*, 2019) or by preventing further aggregation (Du *et al.*, 2014; Pernet *et al.*, 2014; Li *et al.*, 2017). The involvement of LRRK2 in this function remains to be clarified. In Chapter 4 we also explored possible overlaps between the mechanisms leading to the formation of aggresomes and LB-like α-synuclein inclusions in neurons (Fig. 4.4a) and mouse brains (Fig. 4.4b). However, the neuronal and *in vivo* models presented in this section require further optimisation.

In addition to its function as a cargo adaptor, HDAC6 is an important cytoplasmic deacetylase which targets α-tubulin (Hubbert *et al.*, 2002). Likewise, LRRK2 expression levels inversely correlate with tubulin acetylation, although the mechanism ruling these changes has not been characterised (Law *et al.*, 2014). Since tubulin acetylation impacts on MT stability and molecular motor function, in Chapter 5 we investigated if LRRK2 and HDAC6 regulate α-synuclein subcellular localisation and constitutive secretion. We did not find evidence that α-synuclein targeting to the synaptic terminal depends on LRRK2 kinase activity or HDAC6 deacetylase activity (Fig. 5.1). In accordance, no changes in basal α-synuclein secretion were observed upon either LRRK2 or HDAC6 inhibition (Fig. 5.3b, f). Notably, we found that both proteins influence α-synuclein expression level and phosphorylation on S129 (Fig. 5.3a, e). This indicates that both LRRK2 and HDAC6 are involved in α-synuclein homeostasis.

Our results point towards a model where LRRK2 regulates HDAC6 via a mechanism that requires interaction between the two proteins and is regulated by LRRK2 kinase activity but is independent of direct phosphorylation of HDAC6 by LRRK2. Based on

the currently available data, we can only speculate that LRRK2 may either facilitate the contacts between HDAC6 and its activators and substrates or that the binding to LRRK2 may induce a conformational change in HDAC6 which enhances its deacetylase activity. According to this model, the kinase hyperactive mutation G2019S would impair HDAC6-dependent aggresome formation by disrupting the interaction between LRRK2 and HDAC6. Since this molecular phenotype can be restored by inhibiting LRRK2, we propose that such pathological loss-of-function may be caused by an increase in LRRK2 autophosphorylation of the docking site for HDAC6.

6.2 Impact of HDAC6 and LRRK2 on α-synuclein homeostasis

This work highlights the importance of HDAC6 in regulating soluble and aggregated α-synuclein levels. Nonetheless, we did not find evidence that HDAC6 regulates basal α-synuclein secretion or mediates the recruitment of α-synuclein aggregates into aggresomes.

Besides its role in aggresome formation, HDAC6 regulates other pathways that converge on protein homeostasis. By deacetylating cortactin, HDAC6 promotes the assembly of the F-actin network leading to fusion of autophagosomes to lysosomes (Lee *et al.*, 2010; Zhang *et al.*, 2007). In this way, it may act on the pool of α-synuclein species cleared via the autophagolysosomal pathway (Lee *et al.*, 2004; Petroi *et al.*, 2012; Webb *et al.*, 2003). HDAC6-mediated deacetylation of HSP90 promotes the interaction between the latter and its co-chaperone p23 and enhances HSP90 chaperone activity (Kovacs *et al.*, 2005). HSP90 is known for guiding protein folding and promoting stability of its targets, including LRRK2 (Chiosis *et al.*, 2023; Wang *et al.*, 2008). Interestingly, HSP90 plays a pro-aggregation role in PD by stabilising α-synuclein monomers, preventing α-synuclein ubiquitination and promoting the assembly of oligomers and fibrils (Falsone *et al.*, 2009). Conversely, HSP90 inhibition reduces α-synuclein oligomerisation and alleviates α-synuclein-induced dopamine deficiency in PD (Putcha *et al.*, 2010; McFarland *et al.*, 2014; Xiong *et al.*, 2015). By forming a complex with HSP90 and the transcription factor HSF1, HDAC6 acts as a repressor of the heat shock response. Binding of HDAC6 to ubiquitinated cellular aggregates destabilises the complex and activates HSF1-dependent expression of heat-shock genes, such as HSP70 and HSP25 (Boyault *et al.*, 2007). HSP70 has been found within α-synuclein inclusions in PD brains, suggesting a role in their formation

(Auluck *et al.*, 2002). *In vitro* studies revealed that HSP70 cooperates with its co-chaperones HSP40 and HSP110 to dismantle both intracellular and extracellular α-synuclein fibrils and release non-toxic monomers (Danzer *et al.*, 2011; Wentink *et al.*, 2020). This translates into a protective effect on dopaminergic neurons in PD (Auluck *et al.*, 2002; Klucken *et al.*, 2004). Moreover, a role of HSP70 in LRRK2 stability and subcellular localisation has been reported, which may have important implications for LRRK2-dependent neurotoxicity (Lichtenberg *et al.*, 2011; Fukuzono *et al.*, 2016). Thus, HDAC6 may influence α-synuclein metabolism via mechanisms that do not necessarily involve aggrephagy or secretion. Additionally, LRRK2-dependent activation of HDAC6 may represent the initial step of a regulatory loop which terminates with LRRK2 destabilisation and inactivation.

Our results obtained using LRRK2 inhibition introduce an additional layer of complexity. On the one hand, LRRK2 kinase inhibitors had no effect on the accumulation of α-synuclein aggregates into aggresomes or on the formation of triton-X100-insoluble α-synuclein species in COS7 cells induced with PFFs (Fig. 4.3). On the other hand, they increased α-synuclein levels in SH-SY5Y and cortical neurons (Fig. 5.3). This indicates that basal LRRK2 kinase activity may support the turnover of soluble but not aggregated α-synuclein. LRRK2 mutations have a well-documented negative impact on LAMP2A activity and on CMA (Orenstein *et al.*, 2013). This suggests that LRRK2 may stabilise a fundamental route of degradation of α-synuclein monomers and oligomers (di Domenico *et al.*, 2019; Ho *et al.*, 2020). Therefore, LRRK2 inhibition might impact CMA in a WT background. LRRK2 has also been implicated in the regulation of every stage of the autophagolysosomal pathway, from phagophore formation to autophagosome maturation, fusion of the autophagosome to the lysosome, regulation of the autophagolysosomal pH and degradation of the autophagy targets. However, the exact role of LRRK2 in this context is still elusive, since most available data tend to be model-specific (Madureira *et al.*, 2020). α-synuclein was found to be constitutively targeted to the lysosome through a non-canonical endosome recycling mechanism which depends on *de novo* α-synuclein ubiquitination (Zenko *et al.*, 2023). Given the importance of LRRK2 in sorting cellular vesicles and membranes and supporting lysosomal degradation, it is possible that downregulation of its activity may contribute to a partial blockage of α-synuclein clearance (Boecker, 2023).

6.3 The biological meaning of the Lewy body

The data in this work indicate that HDAC6 operates independently from aggrephagy to prevent accumulation of triton-X100-insoluble α-synuclein aggregates. On the other hand, the formation of LB-like α-synuclein inclusions was unaffected by HDAC6 and LRRK2 inhibition. Although we did not assess the impact of HDAC6 inhibition on cell survival, multiple lines of evidence support the hypothesis that insoluble α-synuclein prefibrillar species have a higher impact on cell physiology than larger aggregates (Grassi *et al.*, 2018). The cellular functions affected by the accumulation of α-synuclein oligomers span from protein degradation to mitochondrial function, ER homeostasis, synaptic activity, membrane integrity and inflammation (Lashuel *et al.*, 2002; Sharon *et al.*, 2003; Ingelsson, 2016). When compared to soluble multimers and fibrils, insoluble, proteinase-K-resistant oligomers cause the most severe impact on mitochondrial respiration and neuronal survival (Cremades *et al.*, 2012). Similar conclusions were also extrapolated from *in vivo* studies, where the elevated inter-neuronal transmissibility of oligomeric aggregates was associated to more severe neurodegenerative phenotypes (Winner *et al.*, 2011; Helwig *et al.*, 2016).

From this perspective, sequestration of cytotoxic α-synuclein oligomers into fibrils and LBs may represent a cytoprotective mechanism in response to α-synuclein misfolding, rather than being the cause of neuronal loss (Chartier *et al.*, 2018; Graves *et al.*, 2023). This is supported by the fact that elderly people can develop Lewy pathology without any overt clinical manifestations (Parkkinen *et al.*, 2007; Jellinger, 2009; Buchman *et al.*, 2012). Conversely, severity of PD symptoms does not correlate with the presence of LBs. In fact, not all sporadic PD patients develop Lewy pathology and *PRKN* gene mutations are not linked to the formation of LBs (Gaig *et al.*, 2009; Milber *et al.*, 2012; Johansen *et al.*, 2018; Chittoor-Vinod *et al.*, 2021). In LRRK2-PD, LBs are reported in approximately 40% of cases. Among these, the G2019S mutation is associated with the highest frequency compared to all the other LRRK2 variants (Gaig *et al.*, 2009; Kalia *et al.*, 2015; Takanashi *et al.*, 2018; Agin-Liebes *et al.*, 2020; Chittoor-Vinod, Jeremy Nichols and Schüle, 2021). This suggests that Lewy pathology is not the main pathogenic mechanism even in this genetic background. An interesting discrepancy between the distribution of α-synuclein oligomers and Lewy pathology emerged from a recent work conducted in post-mortem PD brains. Sekiya and collaborators

observed that PD clinical features better correlate with the brain areas affected by α-synuclein oligomerisation than with those displaying Lewy pathology (Sekiya *et al.*, 2022). By observing the stereotypical pattern by which LBs follow the emergence of α-synuclein oligomers, it was proposed that the latter appear at early stages of PD progression and subsequently condensate into larger inclusions (Sekiya *et al.*, 2022). The literature also encompasses reports that do not align with this model and suggest that Lewy pathology equally contributes to neurodegeneration. A striking example is a work published by Lashuel's lab, which evidences that LB-like inclusions and not α-synuclein oligomers cause cell dyshomeostasis and neurotoxicity (Mahul-Mellier *et al.*, 2020). The authors characterised the evolution of PFFs-induced α-synuclein inclusions in primary neurons using a multiomic approach to assess pathway abnormalities. As α-synuclein fibrils condensate from the neuronal projections into the soma, several cellular functions are progressively altered. These include cytoskeleton dynamics, axonal trafficking, mitochondrial function, autophagy upregulation, neuroinflammation, induction of ER stress and activation of apoptosis signalling (Mahul-Mellier *et al.*, 2020). It is possible that the PFFs-induced model does not recapitulate all the events leading to α-synuclein aggregation. Because of how PFFs are synthesised, the smallest aggregates present in the cell at the time of induction are fragmentated fibrils and not oligomers (Volpicelli-Daley, Luk and Lee, 2014). Likewise, it is incorrect to assume that oligomeric species are not released at later stages from the fragmentation or partial digestion of larger aggregates (Sahoo *et al.*, 2022).

In general, assessing specific effects resulting from α-synuclein aggregation still poses a challenge in the field of synucleinopathies. A major source of ambiguity derives from the use of the umbrella term "oligomers" to describe a heterogenous group of intrinsically dynamic species which rapidly convert into fibrils (Chen *et al.*, 2015; Cremades *et al.*, 2012).

In conclusion, LBs may represent the failed attempt of the diseased cell to sequester and recycle cytotoxic aggregates and faulty organelles (Moors *et al.*, 2021). The process of LB formation might depend in whole or in part on the same molecular apparatuses that generate aggresomes. However, due to the impairment of degradation pathways in PD (Behl *et al.*, 2022; Themistokleous *et al.*, 2023) and the intrinsic resilience to proteolysis of α-synuclein amyloid inclusions (Tanik *et al.*, 2013), the contents of LBs may be indefinitely trapped into this structure. Although we found

no evidence that HDAC6 deacetylase activity and LRRK2 kinase activity are involved in the formation of LB-like inclusions, they may still be determinant in earlier stages of α-synuclein aggregation cascade. Understanding the biological meaning of the LB, the mechanisms leading to its formation and possible overlaps with aggrephagy will help design more targeted therapeutic approaches for PD.

6.4 Implications for the treatment of Parkinson's disease

In contrast with the model previously formulated (Lucas *et al.*, 2019), in this thesis we showed that LRRK2 kinase activity does not regulate HDAC6-dependent aggresome formation (Fig. 3.1). We also showed that LRRK2 kinase inhibition has no detectable effects on the formation of α-synuclein inclusions in a PFF-induced cellular model (Fig. 4.3). We found that the abnormal binding of LRRK2-G2019S with HDAC6 can be rescued by inhibiting LRRK2 kinase hyperactivity (Fig. 3.4). A set of experiments is currently ongoing to assess if the effect of LRRK2 inhibitors translates into rescue of ubiquitin-dependent aggresome formation in LRRK2-G2019S-PD. Since we observed that α-synuclein aggregates are not targeted to the aggresome in a ubiquitin/HDAC6-dependent manner (Fig. 4.3), how dysregulation of this pathway relates to PD onset and progression remains to be clarified.

LRRK2 hyperactivation and upregulation have been proposed as the direct cause of cell dyshomeostasis ultimately leading to PD (summarised in Chapter 1.3). On the other hand, LRRK2 inhibition or ablation have been shown to ameliorate most cellular and physiological phenotypes which converge in the pathology. The positive effects of LRRK2 manipulation in PD include enhancement of the autophagolysosomal pathway (Ysselstein *et al.*, 2019; Obergasteiger *et al.*, 2020; Rocha *et al.*, 2020; Singh *et al.*, 2021), improved mitophagy (Singh *et al.*, 2021), increased synaptic vesicle trafficking (Pan *et al.*, 2017), reduced neuroinflammation (Daher *et al.*, 2014; D. H. Ho *et al.*, 2022), prevention of neurodegeneration (Yao *et al.*, 2013; Daher *et al.*, 2015) and improvement of motor deficit (Cording *et al.*, 2017). With respect to α-synuclein aggregation, the impact of either LRRK2 inhibition or deficiency is controversial, with some studies supporting a beneficial effect (Zhao *et al.*, 2017; Macisaac *et al.*, 2020; Obergasteiger *et al.*, 2020; P. W. L. Ho *et al.*, 2022) and others warning of the lack of inhibitor efficacy in non-mutant genetic backgrounds (Henderson *et al.*, 2018, 2019).

This suggests that LRRK2 inhibition might have variable effects of α-synuclein pathology depending on incidental genetic or environmental factors. However, administration of LRRK2 inhibitors may still be a valid strategy to curb dopaminergic neuronal loss, especially in mutant LRRK2 backgrounds. Given the overall beneficial effect ascribed to LRRK2 manipulation in preclinical studies, the exploitability of LRRK2 as a therapeutic target in PD is under careful evaluation. Increasingly potent and specific small-molecule LRRK2 inhibitors and antisense oligonucleotides (ASOs) have been developed over the last decade in a race to develop an effective disease-modifying therapy. To date, four type I kinase inhibitors (DNL201, WXWH0226, NEU-723, and BIIB122) and one ASO (BIIB-094) are undergoing phase III clinical testing (Hu *et al.*, 2023) with no severe adverse effects being reported.

Accumulating evidence remark the pivotal role of HDAC6 in neurodegeneration (Lopresti, 2020). In PD, HDAC6 inhibitors are being studied in cellular and animal models for their overall neuroprotective effect and their ability to reduce neuroinflammation (Yan *et al.*, 2020), mitigate oxidative stress (Parmigiani *et al.*, 2008; Jian *et al.*, 2017), restore mitochondrial trafficking (Godena *et al.*, 2014) and rescue cellular metabolism (Pinho *et al.*, 2016; Francelle *et al.*, 2020). With respect to α-synuclein pathology and α-synuclein-mediated neurotoxicity, HDAC6 has been shown to have both protective, null, and deleterious effects depending on the model used and the specific pathway under investigation (discussed in Section 1.4.4 and by Mazzocchi *et al.*, 2020). Our data suggest that HDAC6 inhibition has a negative impact on α-synuclein metabolism, since administration of tubastatin A increased both soluble and aggregated α-synuclein levels (Figs. 4.3 and 5.3). This context-specificity may be the consequence of how the multifaced role of HDAC6 in cell physiology intersects differences in expression of HDAC6's interaction partners and variability in active pathways. A possible source of uncertainty in the field is the general practice of addressing research questions using simplified models that extrapolate a limited set of features from the complex pathological phenotype in which PD develops. The implementation of more comprehensive experimental approaches will help clarify which HDAC6 role prevails in PD and if it should be targeted in a positive or negative way. Additionally, the use of selective inhibitors operating on either HDAC6 binding or deacetylase properties will allow to specifically address HDAC6 pathogenic impact without compromising its neuroprotective functions (Zhang *et al.*, 2021).

Ultimately, defining the potential of HDAC6 as a therapeutic target may not only benefit LRRK2-PD but could potentially improve other PD backgrounds.

6.5 Future perspectives

The results presented in this thesis about the interplay between LRRK2 and HDAC6 and its impact on aggresome formation and α-synuclein metabolism left space to some questions that should be addressed in follow up studies.

All the data reported in this work align with a model where HDAC6 is not regulated by LRRK2-dependent phosphorylation. This stimulates alternative hypotheses on how LRRK2 may influence pathways downstream to HDAC6. One possibility that should be explored is that LRRK2 may act as a signalling scaffold for HDAC6 and its activators and substrates. Once established which residues influence the binding between LRRK2 and HDAC6 (see below), this hypothesis could be tested by using binding-defective LRRK2 mutants that retain their enzymatic activity and kinase- and GTPase-dead mutants that preserve WT LRRK2 interactome. An alternative hypothesis is that LRRK2 may promote a conformational change that increases HDAC6 deacetylase activity. This could be addressed by combining *in vitro* deacetylase assays with LRRK2 pharmacological and functional manipulation. Clarifying the interplay between LRRK2 and HDAC6 will provide new tools for the targeted regulation of cellular mechanisms that may mitigate neuronal loss in PD, such as MTs acetylation, autophagy, inflammation, and activation of the heat shock response (Mazzocchi *et al.*, 2020).

In Chapter 3.4 we showed that pathological changes in LRRK2 kinase activity influence its binding to HDAC6, however the mechanism that regulates this interaction requires further investigation. The observation that this pathological phenotype can be rescued by using LRRK2 inhibitors led us to hypothesise that abnormal autophosphorylation of LRRK2's Roc-COR domain may disrupt a binding site for HDAC6. This is currently being tested by co-immunoprecipitation assays between HDAC6 and a series of phospho-deficient LRRK2-G2019S mutants. Further corroboration could be obtained *in silico* and by crosslinking mass spectrometry. The type I LRRK2 inhibitor used in this work has a similar effect on the protein spatial arrangement as the G2019S mutation, which locks the kinase domain into a compact, "closed" conformation (Agrahari *et al.*, 2019; Schmidt *et al.*, 2021). This means that

MLi-2 should inhibit the enzymatic activity of the G2019S mutant without disturbing its conformation. To completely exclude that the effect of MLi-2 on LRRK2 binding properties depends on the stabilisation of a “binding-prone” molecular conformer, rescue of the pathological molecular phenotype should be confirmed by using type II LRRK2 inhibitors. Further to this, it should be verified if improving the LRRK2-HDAC6 interaction also translates into an improvement in aggresome formation in a G2019S-LRRK2 background.
Previous work from our lab only focussed on the effect of the G2019S mutation on the recruitment of ubiquitinated aggregates into aggresomes, but no data are currently available about other PD-causative mutants. Investigating if other LRRK2 gain-of-function mutations equally impair aggrephagy will help establish if this is a relevant pathogenic mechanism across all LRRK2-PD backgrounds.

In Chapters 4 and 5 we observed that HDAC6 inhibition increased both soluble and aggregated α-synuclein levels. Future work should investigate at which level HDAC6 influences α-synuclein metabolism. Plausibly, HDAC6 may regulate α-synuclein expression, play an anti-aggregation function, promote the degradation of monomers and aggregates via the autophagolysosomal pathway or influence the secretion of α-synuclein pathogenic species. In Chapter 4, we ruled out the hypothesis that HDAC6 is involved in directing α-synuclein aggregates to the aggresome. More refined analysis should confirm if HDAC6 inhibition influences other parameters linked to the organelle architecture, such as total volume or aggregated α-synuclein density. Another question left unanswered is how α-synuclein LB-like inclusions originate. A possibility is that α-synuclein aggregates are retrogradely trafficked with a ubiquitin-independent mechanism. Colocalization analysis and pharmacological and genetic manipulation of alternative aggresome formation mechanisms will help elucidate this. Additionally, to better understand if the process leading to α-synuclein sequestration has a cytoprotective or cytotoxic effect, future experiments should be coupled with cell viability assays. Moreover, it should be investigated if LB-like inclusions are cleared from the cell or if the formation of a LB-like inclusion is a dead-end road. To address all these questions the PFF-induced neuronal model introduced in this thesis may represent a terrific tool for translatability purposes.

Finally, in this work we observed for the first time that HDAC6 inhibition reduced Rab10 phosphorylation, a *bona fide* LRRK2 kinase substrate (Steger *et al.*, 2016). This suggests that HDAC6 may either contribute to LRRK2 stability, possibly via HSP90 (Wang *et al.*, 2008), or that it may directly regulate LRRK2 kinase activity. To date, no studies have explored if LRRK2 kinase activity or stability are regulated by acetylation. Mass spectrometry analysis could reveal any possible acetylated lysine residues of LRRK2 that are modified by HDAC6.

References

Aasly, J.O. *et al.* (2010) ‘Novel pathogenic LRRK2 p.Asn1437His substitution in familial Parkinson’s disease’, *Movement disorders : official journal of the Movement Disorder Society*, 25(13), pp. 2156–2163. Available at: https://doi.org/10.1002/MDS.23265.

Abdelkader, H. *et al.* (2022) ‘Glycation-induced age-related illnesses, antiglycation and drug delivery strategies’, *The Journal of pharmacy and pharmacology*, 74(11), pp. 1546–1567. Available at: https://doi.org/10.1093/JPP/RGAC051.

Abeliovich, A. *et al.* (2000) ‘Mice lacking α-synuclein display functional deficits in the nigrostriatal dopamine system’, *Neuron*, 25(1), pp. 239–252. Available at: https://doi.org/10.1016/S0896-6273(00)80886-7.

Abeywardana, T. and Pratt, M.R. (2015) ‘Extent of inhibition of α-synuclein aggregation in vitro by SUMOylation is conjugation site- and SUMO isoform-selective’, *Biochemistry*, 54(4), pp. 959–961. Available at: https://doi.org/10.1021/BI501512M.

Abounit, S. *et al.* (2016) ‘Tunneling nanotubes spread fibrillar α-synuclein by intercellular trafficking of lysosomes’, *The EMBO Journal*, 35(19), pp. 2120–2138. Available at: https://doi.org/10.15252/embj.201593411.

Ageta-Ishihara, N. *et al.* (2013) ‘Septins promote dendrite and axon development by negatively regulating microtubule stability via HDAC6-mediated deacetylation’, *Nature communications*, 4. Available at: https://doi.org/10.1038/NCOMMS3532.

Agin-Liebes, J. *et al.* (2020) ‘Movement disorders rounds: A case of missing pathology in a patient with LRRK2 Parkinson’s disease’, *Parkinsonism & related disorders*, 74, pp. 76–77. Available at: https://doi.org/10.1016/J.PARKRELDIS.2019.11.006.

Agrahari, A.K. *et al.* (2019) ‘Molecular insights of the G2019S substitution in LRRK2 kinase domain associated with Parkinson’s disease: A molecular dynamics simulation approach’, *Journal of Theoretical Biology*, 469, pp. 163–171. Available at:

https://doi.org/10.1016/J.JTBI.2019.03.003.

Aharon-Peretz, J., Rosenbaum, H. and Gershoni-Baruch, R. (2004) ‘Mutations in the glucocerebrosidase gene and Parkinson’s disease in Ashkenazi Jews’, *The New England journal of medicine*, 351(19), pp. 1972–1977. Available at: https://doi.org/10.1056/NEJMOA033277.

Ahmadi Rastegar, D. and Dzamko, N. (2020) ‘Leucine Rich Repeat Kinase 2 and Innate Immunity’, *Frontiers in Neuroscience*, 14, p. 193. Available at: https://doi.org/10.3389/FNINS.2020.00193/BIBTEX.

Ahmed, I. *et al.* (2012) ‘Development and characterization of a new Parkinson’s disease model resulting from impaired autophagy’, *The Journal of neuroscience : the official journal of the Society for Neuroscience*, 32(46), pp. 16503–16509. Available at: https://doi.org/10.1523/JNEUROSCI.0209-12.2012.

Ahn, K.J. *et al.* (2006) ‘Amino acid sequence motifs and mechanistic features of the membrane translocation of α-synuclein’, *Journal of Neurochemistry*, 97(1), pp. 265–279. Available at: https://doi.org/10.1111/J.1471-4159.2006.03731.X.

Akella, J.S. *et al.* (2010) ‘MEC-17 is an alpha-tubulin acetyltransferase’, *Nature*, 467(7312), pp. 218–222. Available at: https://doi.org/10.1038/NATURE09324.

Aksnes, H., Ree, R. and Arnesen, T. (2019) ‘Co-translational, Post-translational, and Non-catalytic Roles of N-Terminal Acetyltransferases’, *Molecular cell*, 73(6), pp. 1097–1114. Available at: https://doi.org/10.1016/J.MOLCEL.2019.02.007.

Alam, P. *et al.* (2019) ‘α-synuclein oligomers and fibrils: a spectrum of species, a spectrum of toxicities’, *Journal of Neurochemistry*, 150(5), pp. 522–534. Available at: https://doi.org/10.1111/JNC.14808.

Alegre-Abarrategui, J. *et al.* (2008) ‘LRRK2 is a component of granular alpha-synuclein pathology in the brainstem of Parkinson’s disease’, *Neuropathology and applied neurobiology*, 34(3), pp. 272–283. Available at: https://doi.org/10.1111/J.1365-2990.2007.00888.X.

Alexopoulou, Z. *et al.* (2016) ‘Deubiquitinase Usp8 regulates α-synuclein clearance

and modifies its toxicity in Lewy body disease', *Proceedings of the National Academy of Sciences of the United States of America*, 113(32), pp. E4688–E4697. Available at: https://doi.org/10.1073/PNAS.1523597113.

Alim, M.A. *et al.* (2004) 'Demonstration of a role for α-synuclein as a functional microtubule-associated protein', *Journal of Alzheimer's Disease*, 6(4), pp. 435–442. Available at: https://doi.org/10.3233/JAD-2004-6412.

Alvarez-Erviti, L. *et al.* (2010) 'Chaperone-mediated autophagy markers in Parkinson disease brains', *Archives of neurology*, 67(12), pp. 1464–1472. Available at: https://doi.org/10.1001/ARCHNEUROL.2010.198.

Alvarez-Erviti, L. *et al.* (2011) 'Lysosomal dysfunction increases exosome-mediated alpha-synuclein release and transmission', *Neurobiology of disease*, 42(3), pp. 360–367. Available at: https://doi.org/10.1016/J.NBD.2011.01.029.

Anderson, E.N. *et al.* (2020) 'The Non-amyloidal Component Region of α-Synuclein Is Important for α-Synuclein Transport Within Axons', *Frontiers in Cellular Neuroscience*, 13. Available at: https://doi.org/10.3389/fncel.2019.00540.

Anderson, J.P. *et al.* (2006) 'Phosphorylation of Ser-129 is the dominant pathological modification of alpha-synuclein in familial and sporadic Lewy body disease', *The Journal of biological chemistry*, 281(40), pp. 29739–29752. Available at: https://doi.org/10.1074/JBC.M600933200.

Angelova, P.R. *et al.* (2016) 'Ca2+ is a key factor in α-synuclein-induced neurotoxicity', *Journal of Cell Science*, 129(9), pp. 1792–1801. Available at: https://doi.org/10.1242/JCS.180737/260219/AM/CALCIUM-IS-A-KEY-FACTOR-IN-SYNUCLEIN-INDUCED.

Anwar, S. *et al.* (2011) 'Functional alterations to the nigrostriatal system in mice lacking all three members of the synuclein family', *The Journal of neuroscience : the official journal of the Society for Neuroscience*, 31(20), pp. 7264–7274. Available at: https://doi.org/10.1523/JNEUROSCI.6194-10.2011.

Appel-Cresswell, S. *et al.* (2013) 'Alpha-synuclein p.H50Q, a novel pathogenic mutation for Parkinson's disease', *Movement Disorders*, 28(6), pp. 811–813.

Available at: https://doi.org/10.1002/mds.25421.

Arawaka, S. *et al.* (2006) 'The role of G-protein-coupled receptor kinase 5 in pathogenesis of sporadic Parkinson's disease', *The Journal of neuroscience : the official journal of the Society for Neuroscience*, 26(36), pp. 9227–9238. Available at: https://doi.org/10.1523/JNEUROSCI.0341-06.2006.

Arawaka, S. *et al.* (2017) 'Mechanisms underlying extensive Ser129-phosphorylation in α-synuclein aggregates', *Acta neuropathologica communications*, 5(1), p. 48. Available at: https://doi.org/10.1186/S40478-017-0452-6.

Auluck, P.K. *et al.* (2002) 'Chaperone suppression of alpha-synuclein toxicity in a Drosophila model for Parkinson's disease', *Science (New York, N.Y.)*, 295(5556), pp. 865–868. Available at: https://doi.org/10.1126/SCIENCE.1067389.

Auluck, P.K. and Bonini, N.M. (2002) 'Pharmacological prevention of Parkinson disease in Drosophila', *Nature Medicine 2002 8:11*, 8(11), pp. 1185–1186. Available at: https://doi.org/10.1038/nm1102-1185.

Bae, E.J. *et al.* (2018) 'LRRK2 kinase regulates α-synuclein propagation via RAB35 phosphorylation', *Nature Communications*, 9(1). Available at: https://doi.org/10.1038/s41467-018-05958-z.

Balchin, D., Hayer-Hartl, M. and Hartl, F.U. (2020) 'Recent advances in understanding catalysis of protein folding by molecular chaperones', *FEBS letters*, 594(17), pp. 2770–2781. Available at: https://doi.org/10.1002/1873-3468.13844.

Balestrino, R. and Schapira, A.H. V (2020) 'Parkinson disease', *European Journal of Neurology*, 27(1), pp. 27–42. Available at: https://doi.org/10.1111/ene.14108.

Bandyopadhyay, B. *et al.* (2007) 'Tau aggregation and toxicity in a cell culture model of tauopathy.', *The Journal of biological chemistry*, 282(22), pp. 16454–16464. Available at: https://doi.org/10.1074/jbc.M700192200.

Bang, Y. *et al.* (2016) 'LRRK2 interferes with aggresome formation for autophagic clearance', *Molecular and cellular neurosciences*, 75, pp. 71–80. Available at: https://doi.org/10.1016/J.MCN.2016.06.007.

Baptista, M.A.S. *et al.* (2020) ‘LRRK2 inhibitors induce reversible changes in nonhuman primate lungs without measurable pulmonary deficits’, *Science translational medicine*, 12(540). Available at: https://doi.org/10.1126/SCITRANSLMED.AAV0820.

Bär, J. *et al.* (2022) ‘Direct and indirect effects of tubulin post-translational modifications on microtubule stability: Insights and regulations’, *Biochimica et biophysica acta. Molecular cell research*, 1869(6). Available at: https://doi.org/10.1016/J.BBAMCR.2022.119241.

Bartels, T. *et al.* (2014) ‘N-alpha-acetylation of α-synuclein increases its helical folding propensity, GM1 binding specificity and resistance to aggregation’, *PloS one*, 9(7). Available at: https://doi.org/10.1371/JOURNAL.PONE.0103727.

Bartels, T., Choi, J.G. and Selkoe, D.J. (2011) ‘α-Synuclein occurs physiologically as a helically folded tetramer that resists aggregation’, *Nature 2011 477:7362*, 477(7362), pp. 107–110. Available at: https://doi.org/10.1038/nature10324.

Basso, M. *et al.* (2006) ‘Insoluble mutant SOD1 is partly oligoubiquitinated in amyotrophic lateral sclerosis mice’, *The Journal of biological chemistry*, 281(44), pp. 33325–33335. Available at: https://doi.org/10.1074/JBC.M603489200.

Bauernfeind, F.G. *et al.* (2009) ‘Cutting edge: NF-kappaB activating pattern recognition and cytokine receptors license NLRP3 inflammasome activation by regulating NLRP3 expression’, *Journal of immunology (Baltimore, Md. : 1950)*, 183(2), pp. 787–791. Available at: https://doi.org/10.4049/JIMMUNOL.0901363.

Behl, T. *et al.* (2022) ‘Exploring the Role of Ubiquitin-Proteasome System in Parkinson’s Disease’, *Molecular neurobiology*, 59(7), pp. 4257–4273. Available at: https://doi.org/10.1007/S12035-022-02851-1.

Bell, R. *et al.* (2022) ‘N-Terminal Acetylation of α-Synuclein Slows down Its Aggregation Process and Alters the Morphology of the Resulting Aggregates’, *Biochemistry*, 61(17), pp. 1743–1756. Available at: https://doi.org/10.1021/ACS.BIOCHEM.2C00104.

Bell, R. *et al.* (2023) ‘Effects of N-terminal Acetylation on the Aggregation of

Disease-related α-synuclein Variants', *Journal of molecular biology*, 435(1). Available at: https://doi.org/10.1016/J.JMB.2022.167825.

Belluzzi, E. *et al.* (2016) 'LRRK2 phosphorylates pre-synaptic N-ethylmaleimide sensitive fusion (NSF) protein enhancing its ATPase activity and SNARE complex disassembling rate', *Molecular neurodegeneration*, 11(1). Available at: https://doi.org/10.1186/S13024-015-0066-Z.

Ben-David, U. *et al.* (2018) 'Genetic and transcriptional evolution alters cancer cell line drug response', *Nature 2018 560:7718*, 560(7718), pp. 325–330. Available at: https://doi.org/10.1038/s41586-018-0409-3.

Ben-Gedalya, T. *et al.* (2011) 'Cyclosporin-A-induced prion protein aggresomes are dynamic quality-control cellular compartments', *Journal of cell science*, 124(Pt 11), pp. 1891–1902. Available at: https://doi.org/10.1242/JCS.077693.

Bennett, M.C. *et al.* (1999) 'Degradation of alpha-synuclein by proteasome', *The Journal of biological chemistry*, 274(48), pp. 33855–33858. Available at: https://doi.org/10.1074/JBC.274.48.33855.

Benoy, V. *et al.* (2018) 'HDAC6 is a therapeutic target in mutant GARS-induced Charcot-Marie-Tooth disease', *Brain : a journal of neurology*, 141(3), pp. 673–687. Available at: https://doi.org/10.1093/BRAIN/AWX375.

Berger, Z., Smith, K.A. and Lavoie, M.J. (2010) 'Membrane localization of LRRK2 is associated with increased formation of the highly active LRRK2 dimer and changes in its phosphorylation', *Biochemistry*, 49(26), pp. 5511–5523. Available at: https://doi.org/10.1021/BI100157U.

Bernal-Conde, L.D. *et al.* (2020) 'Alpha-Synuclein Physiology and Pathology: A Perspective on Cellular Structures and Organelles', 13, p. 1399.

Berwick, D.C. *et al.* (2019) 'LRRK2 Biology from structure to dysfunction: research progresses, but the themes remain the same', *Molecular neurodegeneration*. NLM (Medline), p. 49. Available at: https://doi.org/10.1186/s13024-019-0344-2.

Berwick, D.C. and Harvey, K. (2012) 'LRRK2 functions as a Wnt signaling scaffold,

bridging cytosolic proteins and membrane-localized LRP6', *Human Molecular Genetics*, 21(22), p. 4966. Available at: https://doi.org/10.1093/HMG/DDS342.

Betzer, C. *et al.* (2018) 'Alpha-synuclein aggregates activate calcium pump SERCA leading to calcium dysregulation', *EMBO Reports*, 19(5). Available at: https://doi.org/10.15252/EMBR.201744617.

Bi, M. *et al.* (2021) 'Expanding the role of proteasome homeostasis in Parkinson's disease: beyond protein breakdown', *Cell death & disease*, 12(2). Available at: https://doi.org/10.1038/S41419-021-03441-0.

Bieri, G. *et al.* (2019) 'LRRK2 modifies α-syn pathology and spread in mouse models and human neurons', *Acta Neuropathologica*, 137(6), p. 961. Available at: https://doi.org/10.1007/S00401-019-01995-0.

Binolfi, A.S. *et al.* (2006) 'Interaction of r-Synuclein with Divalent Metal Ions Reveals Key Differences: A Link between Structure, Binding Specificity and Fibrillation Enhancement'. Available at: https://doi.org/10.1021/ja0618649.

Biskou, O. *et al.* (2019) 'The type III intermediate filament vimentin regulates organelle distribution and modulates autophagy', *PLoS ONE*, 14(1). Available at: https://doi.org/10.1371/JOURNAL.PONE.0209665.

Biskup, S. *et al.* (2006) 'Localization of LRRK2 to membranous and vesicular structures in mammalian brain', *Annals of neurology*, 60(5), pp. 557–569. Available at: https://doi.org/10.1002/ANA.21019.

Biskup, S. *et al.* (2007) 'Dynamic and redundant regulation of LRRK2 and LRRK1 expression', *BMC Neuroscience*, 8, p. 102. Available at: https://doi.org/10.1186/1471-2202-8-102.

Bjorklund, G. *et al.* (2018) 'Metals and Parkinson's Disease: Mechanisms and Biochemical Processes', *Current Medicinal Chemistry*, 25(19), pp. 2198–2214. Available at: https://doi.org/10.2174/0929867325666171129124616.

Bjørkøy, G. *et al.* (2005) 'p62/SQSTM1 forms protein aggregates degraded by autophagy and has a protective effect on huntingtin-induced cell death', *The Journal*

of cell biology, 171(4), pp. 603–614. Available at: https://doi.org/10.1083/JCB.200507002.

Blauwendraat, C., Nalls, M.A. and Singleton, A.B. (2020) 'The genetic architecture of Parkinson's disease', *The Lancet. Neurology*, 19(2), pp. 170–178. Available at: https://doi.org/10.1016/S1474-4422(19)30287-X.

Bobrowska, A. *et al.* (2011) 'Hdac6 knock-out increases tubulin acetylation but does not modify disease progression in the R6/2 mouse model of Huntington's disease', *PloS one*, 6(6). Available at: https://doi.org/10.1371/JOURNAL.PONE.0020696.

Boecker, C.A. *et al.* (2021) 'Increased LRRK2 kinase activity alters neuronal autophagy by disrupting the axonal transport of autophagosomes', *Current Biology*, 31(10), pp. 2140-2154.e6. Available at: https://doi.org/10.1016/J.CUB.2021.02.061.

Boecker, C.A. (2023) 'The Role of LRRK2 in Intracellular Organelle Dynamics', *Journal of molecular biology*, 435(12). Available at: https://doi.org/10.1016/J.JMB.2023.167998.

Bondos, S.E., Dunker, A.K. and Uversky, V.N. (2022) 'Intrinsically disordered proteins play diverse roles in cell signaling', *Cell Communication and Signaling*, 20(1), pp. 1–26. Available at: https://doi.org/10.1186/S12964-022-00821-7/TABLES/1.

Bonello, F. *et al.* (2019) 'LRRK2 impairs PINK1/Parkin-dependent mitophagy via its kinase activity: pathologic insights into Parkinson's disease', *Human Molecular Genetics*, 28(10), pp. 1645–1660. Available at: https://doi.org/10.1093/HMG/DDZ004.

Bonet-Ponce, L. *et al.* (2020) 'LRRK2 mediates tubulation and vesicle sorting from lysosomes', *Science advances*, 6(46). Available at: https://doi.org/10.1126/SCIADV.ABB2454.

Bonifati, V. *et al.* (2003) 'Mutations in the DJ-1 gene associated with autosomal recessive early-onset parkinsonism', *Science (New York, N.Y.)*, 299(5604), pp. 256–259. Available at: https://doi.org/10.1126/SCIENCE.1077209.

Bono, K. *et al.* (2020) ‘Endosomal dysfunction in iPSC-derived neural cells from Parkinson’s disease patients with VPS35 D620N’, *Molecular Brain*, 13(1), pp. 1–15. Available at: https://doi.org/10.1186/S13041-020-00675-5/FIGURES/6.

Bourdenx, M., Gavathiotis, E. and Cuervo, A.M. (2021) ‘Chaperone-mediated autophagy: a gatekeeper of neuronal proteostasis’, *Autophagy*, 17(8), pp. 2040–2042. Available at: https://doi.org/10.1080/15548627.2021.1935007.

Boyault, C. *et al.* (2007) ‘HDAC6 controls major cell response pathways to cytotoxic accumulation of protein aggregates’, *Genes & Development*, 21(17), p. 2172. Available at: https://doi.org/10.1101/GAD.436407.

Braak, H. *et al.* (2002) ‘Staging of the intracerebral inclusion body pathology associated with idiopathic Parkinson’s disease (preclinical and clinical stages)’, *Journal of neurology*, 249 Suppl 3(3). Available at: https://doi.org/10.1007/S00415-002-1301-4.

Braak, H. *et al.* (2003) ‘Idiopathic Parkinson’s disease: Possible routes by which vulnerable neuronal types may be subject to neuroinvasion by an unknown pathogen’, *Journal of Neural Transmission*, 110(5), pp. 517–536. Available at: https://doi.org/10.1007/S00702-002-0808-2/METRICS.

Braak, Heiko *et al.* (2003) ‘Staging of brain pathology related to sporadic Parkinson’s disease’, *Neurobiology of Aging*, 24(2), pp. 197–211. Available at: https://doi.org/10.1016/S0197-4580(02)00065-9.

Brahmachari, S. *et al.* (2016) ‘Activation of tyrosine kinase c-Abl contributes to α-synuclein-induced neurodegeneration’, *The Journal of clinical investigation*, 126(8), pp. 2970–2988. Available at: https://doi.org/10.1172/JCI85456.

Brás, I.C. and Outeiro, T.F. (2021) ‘Alpha-Synuclein: Mechanisms of Release and Pathology Progression in Synucleinopathies’, *Cells*, 10(2), pp. 1–19. Available at: https://doi.org/10.3390/CELLS10020375.

Brembati, V. *et al.* (2023) ‘Alpha synuclein post translational modifications: potential targets for Parkinson’s disease therapy?’, *Frontiers in Molecular Neuroscience*, 16. Available at: https://doi.org/10.3389/FNMOL.2023.1197853.

Bruchard, M. *et al.* (2013) ‘Chemotherapy-triggered cathepsin B release in myeloid-derived suppressor cells activates the Nlrp3 inflammasome and promotes tumor growth’, *Nature medicine*, 19(1), pp. 57–64. Available at: https://doi.org/10.1038/NM.2999.

Brzozowski, C.F. *et al.* (2021) ‘Inhibition of LRRK2 kinase activity promotes anterograde axonal transport and presynaptic targeting of α-synuclein’, *Acta Neuropathologica Communications*, 9(1). Available at: https://doi.org/10.1186/S40478-021-01283-7.

Buchman, A.S. *et al.* (2012) ‘Nigral pathology and parkinsonian signs in elders without Parkinson disease’, *Annals of neurology*, 71(2), pp. 258–266. Available at: https://doi.org/10.1002/ANA.22588.

Burré, J. *et al.* (2010) ‘Alpha-synuclein promotes SNARE-complex assembly in vivo and in vitro’, *Science (New York, N.Y.)*, 329(5999), pp. 1663–1667. Available at: https://doi.org/10.1126/SCIENCE.1195227.

Burré, J., Sharma, M. and Südhof, T.C. (2014) ‘α-Synuclein assembles into higher-order multimers upon membrane binding to promote SNARE complex formation’, *Proceedings of the National Academy of Sciences of the United States of America*, 111(40), pp. E4274–E4283. Available at: https://doi.org/10.1073/PNAS.1416598111/-/DCSUPPLEMENTAL.

Bussell, R. and Eliezer, D. (2003) ‘A Structural and Functional Role for 11-mer Repeats in α-Synuclein and Other Exchangeable Lipid Binding Proteins’, *Journal of Molecular Biology*, 329(4), pp. 763–778. Available at: https://doi.org/10.1016/S0022-2836(03)00520-5.

Butler, B. *et al.* (2015) ‘Dopamine transporter activity is modulated by α-synuclein’, *Journal of Biological Chemistry*, 290(49), pp. 29542–29554. Available at: https://doi.org/10.1074/jbc.M115.691592.

Cabezudo, D., Baekelandt, V. and Lobbestael, E. (2020) ‘Multiple-Hit Hypothesis in Parkinson’s Disease: LRRK2 and Inflammation’, *Frontiers in Neuroscience*, 14. Available at: https://doi.org/10.3389/FNINS.2020.00376.

Cabrero, J.R. *et al.* (2006) ‘Lymphocyte chemotaxis is regulated by histone deacetylase 6, independently of its deacetylase activity’, *Molecular biology of the cell*, 17(8), pp. 3435–3445. Available at: https://doi.org/10.1091/MBC.E06-01-0008.

Caesar, M. *et al.* (2013) ‘Leucine-rich repeat kinase 2 functionally interacts with microtubules and kinase-dependently modulates cell migration’, *Neurobiology of disease*, 54, pp. 280–288. Available at: https://doi.org/10.1016/J.NBD.2012.12.019.

Cai, Z.L. *et al.* (2009) ‘MPP + impairs autophagic clearance of alpha-synuclein by impairing the activity of dynein’, *NeuroReport*, 20(6), pp. 569–573. Available at: https://doi.org/10.1097/WNR.0b013e32832986c4.

Calderilla-Barbosa, L. *et al.* (2014) ‘Interaction of SQSTM1 with the motor protein dynein – SQSTM1 is required for normal dynein function and trafficking’, *Journal of Cell Science*, 127(18), p. 4052. Available at: https://doi.org/10.1242/JCS.152363.

Calderón-Garcidueñas, L. *et al.* (2008) ‘Long-term Air Pollution Exposure Is Associated with Neuroinflammation, an Altered Innate Immune Response, Disruption of the Blood-Brain Barrier, Ultrafine Particulate Deposition, and Accumulation of Amyloid β-42 and α-Synuclein in Children and Young Adults’, *http://dx.doi.org/10.1177/0192623307313011*, 36(2), pp. 289–310. Available at: https://doi.org/10.1177/0192623307313011.

Carlson, G.A. and Prusiner, S.B. (2021) ‘How an Infection of Sheep Revealed Prion Mechanisms in Alzheimer’s Disease and Other Neurodegenerative Disorders’, *International journal of molecular sciences*, 22(9). Available at: https://doi.org/10.3390/IJMS22094861.

Castro-Castro, A. *et al.* (2012) ‘ATAT1/MEC-17 acetyltransferase and HDAC6 deacetylase control a balance of acetylation of alpha-tubulin and cortactin and regulate MT1-MMP trafficking and breast tumor cell invasion’, *European journal of cell biology*, 91(11–12), pp. 950–960. Available at: https://doi.org/10.1016/J.EJCB.2012.07.001.

Celej, M.S. *et al.* (2012) ‘Toxic prefibrillar α-synuclein amyloid oligomers adopt a distinctive antiparallel β-sheet structure’, *The Biochemical journal*, 443(3), pp. 719–

726. Available at: https://doi.org/10.1042/BJ20111924.

Chang, P. *et al.* (2021) 'The Role of HDAC6 in Autophagy and NLRP3 Inflammasome', *Frontiers in immunology*, 12. Available at: https://doi.org/10.3389/FIMMU.2021.763831.

Chartier, S. and Duyckaerts, C. (2018) 'Is Lewy pathology in the human nervous system chiefly an indicator of neuronal protection or of toxicity?', *Cell and tissue research*, 373(1), pp. 149–160. Available at: https://doi.org/10.1007/S00441-018-2854-6.

Chau, K.Y. *et al.* (2009) 'Relationship between alpha synuclein phosphorylation, proteasomal inhibition and cell death: relevance to Parkinson's disease pathogenesis', *Journal of neurochemistry*, 110(3), pp. 1005–1013. Available at: https://doi.org/10.1111/J.1471-4159.2009.06191.X.

Chen, Jiayan *et al.* (2018) 'Role of LRRK2 in manganese-induced neuroinflammation and microglial autophagy', *Biochemical and biophysical research communications*, 498(1), pp. 171–177. Available at: https://doi.org/10.1016/J.BBRC.2018.02.007.

Chen, L. *et al.* (2009) 'Tyrosine and serine phosphorylation of alpha-synuclein have opposing effects on neurotoxicity and soluble oligomer formation', *The Journal of clinical investigation*, 119(11), pp. 3257–3265. Available at: https://doi.org/10.1172/JCI39088.

Chen, L. and Feany, M.B. (2005) 'Alpha-synuclein phosphorylation controls neurotoxicity and inclusion formation in a Drosophila model of Parkinson disease', *Nature neuroscience*, 8(5), pp. 657–663. Available at: https://doi.org/10.1038/NN1443.

Chen, S. *et al.* (2010) 'HDAC6 Regulates mitochondrial transport in hippocampal neurons', *PLoS ONE*, 5(5). Available at: https://doi.org/10.1371/journal.pone.0010848.

Chen, S.W. *et al.* (2015) 'Structural characterization of toxic oligomers that are kinetically trapped during α-synuclein fibril formation', *Proceedings of the National Academy of Sciences of the United States of America*, 112(16), pp. E1994–E2003.

Available at: https://doi.org/10.1073/PNAS.1421204112/SUPPL_FILE/PNAS.1421204112.SAPP.PDF.

Cherian, A., K.P, D. and Vijayaraghavan, A. (2023) 'Parkinson's disease - genetic cause', *Current opinion in neurology*, 36(4). Available at: https://doi.org/10.1097/WCO.0000000000001167.

Chinta, S.J. *et al.* (2010) 'Mitochondrial alpha-synuclein accumulation impairs complex I function in dopaminergic neurons and results in increased mitophagy in vivo', *Neuroscience Letters*, 486(3), pp. 235–239. Available at: https://doi.org/10.1016/j.neulet.2010.09.061.

Chiosis, G. *et al.* (2023) 'Structural and functional complexity of HSP90 in cellular homeostasis and disease', *Nature reviews. Molecular cell biology* [Preprint]. Available at: https://doi.org/10.1038/S41580-023-00640-9.

Chittoor-Vinod, V.G., Jeremy Nichols, R. and Schüle, B. (2021) 'Genetic and Environmental Factors Influence the Pleomorphy of LRRK2 Parkinsonism', *International journal of molecular sciences*, 22(3), pp. 1–25. Available at: https://doi.org/10.3390/IJMS22031045.

Choi, B.K. *et al.* (2013) 'Large α-synuclein oligomers inhibit neuronal SNARE-mediated vesicle docking', *Proceedings of the National Academy of Sciences of the United States of America*, 110(10), pp. 4087–4092. Available at: https://doi.org/10.1073/PNAS.1218424110/-/DCSUPPLEMENTAL.

Choi, H.G. *et al.* (2012) 'Brain Penetrant LRRK2Inhibitor', *ACS Medicinal Chemistry Letters*, 3(8), p. 658. Available at: https://doi.org/10.1021/ML300123A.

Choi, W. *et al.* (2004) 'Mutation E46K increases phospholipid binding and assembly into filaments of human α-synuclein', *FEBS Letters*, 576(3), pp. 363–368. Available at: https://doi.org/10.1016/J.FEBSLET.2004.09.038.

Chuang, H.H. *et al.* (2018) 'Pin1 Is Involved in HDAC6-mediated Cancer Cell Motility', *International Journal of Medical Sciences*, 15(13), p. 1573. Available at: https://doi.org/10.7150/IJMS.27426.

Chung, C.Y. *et al.* (2013) ‘Identification and rescue of α-synuclein toxicity in Parkinson patient-derived neurons’, *Science (New York, N.Y.)*, 342(6161), pp. 983–987. Available at: https://doi.org/10.1126/SCIENCE.1245296.

Chung, K.K.K. *et al.* (2001) ‘Parkin ubiquitinates the alpha-synuclein-interacting protein, synphilin-1: implications for Lewy-body formation in Parkinson disease’, *Nature medicine*, 7(10), pp. 1144–1150. Available at: https://doi.org/10.1038/NM1001-1144.

Church, F.C. (2021) ‘Treatment Options for Motor and Non-Motor Symptoms of Parkinson’s Disease’, *Biomolecules*, 11(4), p. 612. Available at: https://doi.org/10.3390/BIOM11040612.

Cirnaru, M.D. *et al.* (2014) ‘LRRK2 kinase activity regulates synaptic vesicle trafficking and neurotransmitter release through modulation of LRRK2 macro-molecular complex’, *Frontiers in Molecular Neuroscience*, 7(MAY), p. 89503. Available at: https://doi.org/10.3389/FNMOL.2014.00049/BIBTEX.

Civiero, L. *et al.* (2012) ‘Biochemical characterization of highly purified leucine-rich repeat kinases 1 and 2 demonstrates formation of homodimers’, *PloS one*, 7(8). Available at: https://doi.org/10.1371/JOURNAL.PONE.0043472.

Clark, L.N. *et al.* (2005) ‘Pilot association study of the beta-glucocerebrosidase N370S allele and Parkinson’s disease in subjects of Jewish ethnicity’, *Movement disorders : official journal of the Movement Disorder Society*, 20(1), pp. 100–103. Available at: https://doi.org/10.1002/MDS.20320.

Cohen, E. and Taraboulos, A. (2003) ‘Scrapie-like prion protein accumulates in aggresomes of cyclosporin A-treated cells’, *The EMBO journal*, 22(3), pp. 404–417. Available at: https://doi.org/10.1093/EMBOJ/CDG045.

Comellas, G. *et al.* (2012) ‘Structural intermediates during α-synuclein fibrillogenesis on phospholipid vesicles’, *Journal of the American Chemical Society*, 134(11), p. 5090. Available at: https://doi.org/10.1021/JA209019S.

Conway, K.A. *et al.* (2000) ‘Acceleration of oligomerization, not fibrillization, is a shared property of both alpha-synuclein mutations linked to early-onset Parkinson’s

disease: implications for pathogenesis and therapy', *Proceedings of the National Academy of Sciences of the United States of America*, 97(2), pp. 571–576. Available at: https://doi.org/10.1073/PNAS.97.2.571.

Conway, K.A., Harper, J.D. and Lansbury, P.T. (1998) 'Accelerated in vitro fibril formation by a mutant α-synuclein linked to early-onset Parkinson disease', *Nature Medicine 1998 4:11*, 4(11), pp. 1318–1320. Available at: https://doi.org/10.1038/3311.

Cooper, J.F. and Van Raamsdonk, J.M. (2018) 'Modeling Parkinson's Disease in C. elegans', *Journal of Parkinson's disease*, 8(1), pp. 17–32. Available at: https://doi.org/10.3233/JPD-171258.

Cording, A.C. *et al.* (2017) 'Targeted kinase inhibition relieves slowness and tremor in a Drosophila model of LRRK2 Parkinson's disease', *NPJ Parkinson's disease*, 3(1). Available at: https://doi.org/10.1038/S41531-017-0036-Y.

Cremades, N. *et al.* (2012) 'Direct Observation of the Interconversion of Normal and Toxic Forms of α-Synuclein', *Cell*, 149(5), pp. 1048–1059. Available at: https://doi.org/10.1016/J.CELL.2012.03.037.

Cuervo, A.M. *et al.* (2004) 'Impaired degradation of mutant alpha-synuclein by chaperone-mediated autophagy', *Science (New York, N.Y.)*, 305(5688), pp. 1292–1295. Available at: https://doi.org/10.1126/SCIENCE.1101738.

Cunningham, L.A. and Moore, D.J. (2020) 'Endosomal sorting pathways in the pathogenesis of Parkinson's disease', *Progress in brain research*, 252, pp. 271–306. Available at: https://doi.org/10.1016/BS.PBR.2020.02.001.

D'Ydewalle, C. *et al.* (2011) 'HDAC6 inhibitors reverse axonal loss in a mouse model of mutant HSPB1-induced Charcot-Marie-Tooth disease', *Nature medicine*, 17(8), pp. 968–974. Available at: https://doi.org/10.1038/NM.2396.

Daher, J.P.L. *et al.* (2014) 'Abrogation of α-synuclein -mediated dopaminergic neurodegeneration in LRRK2-deficient rats', *Proceedings of the National Academy of Sciences of the United States of America*, 111(25), pp. 9289–9294. Available at: https://doi.org/10.1073/PNAS.1403215111/-

/DCSUPPLEMENTAL/PNAS.201403215SI.PDF.

Daher, J.P.L. *et al.* (2015) 'Leucine-rich Repeat Kinase 2 (LRRK2) Pharmacological Inhibition Abates α-Synuclein Gene-induced Neurodegeneration', *The Journal of biological chemistry*, 290(32), pp. 19433–19444. Available at: https://doi.org/10.1074/JBC.M115.660001.

Dahmene, M., Berard, M. and Oueslati, A. (2017) 'Dissecting the Molecular Pathway Involved in PLK2 Kinase-mediated α-Synuclein-selective Autophagic Degradation', *The Journal of biological chemistry*, 292(9), pp. 3919–3928. Available at: https://doi.org/10.1074/JBC.M116.759373.

Daniëls, V. *et al.* (2011) 'Insight into the mode of action of the LRRK2 Y1699C pathogenic mutant', *Journal of neurochemistry*, 116(2), pp. 304–315. Available at: https://doi.org/10.1111/J.1471-4159.2010.07105.X.

Danzer, K.M. *et al.* (2007) 'Different species of α-synuclein oligomers induce calcium influx and seeding', *Journal of Neuroscience*, 27(34), pp. 9220–9232. Available at: https://doi.org/10.1523/JNEUROSCI.2617-07.2007.

Danzer, K.M. *et al.* (2011) 'Heat-shock protein 70 modulates toxic extracellular α-synuclein oligomers and rescues trans-synaptic toxicity', *The FASEB Journal*, 25(1), pp. 326–336. Available at: https://doi.org/10.1096/fj.10-164624.

Davidson, W.S. *et al.* (1998) 'Stabilization of α-Synuclein Secondary Structure upon Binding to Synthetic Membranes', *Journal of Biological Chemistry*, 273(16), pp. 9443–9449. Available at: https://doi.org/10.1074/JBC.273.16.9443.

Davies, S.E. *et al.* (2014) 'Enhanced ubiquitin-dependent degradation by Nedd4 protects against α-synuclein accumulation and toxicity in animal models of Parkinson's disease', *Neurobiology of disease*, 64(100), pp. 79–87. Available at: https://doi.org/10.1016/J.NBD.2013.12.011.

Day, J.O. and Mullin, S. (2021) 'The Genetics of Parkinson's Disease and Implications for Clinical Practice', *Genes*, 12(7). Available at: https://doi.org/10.3390/GENES12071006.

Deas, E. *et al.* (2016) ‘Alpha-synuclein oligomers interact with metal ions to induce oxidative stress and neuronal death in Parkinson’s disease’, *Antioxidants and Redox Signaling*, 24(7), pp. 376–391. Available at: https://doi.org/10.1089/ARS.2015.6343/ASSET/IMAGES/LARGE/FIGURE6.JPEG.

Deng, J. *et al.* (2008) ‘Structure of the ROC domain from the Parkinson’s disease-associated leucine-rich repeat kinase 2 reveals a dimeric GTPase’, *Proceedings of the National Academy of Sciences of the United States of America*, 105(5), pp. 1499–1504. Available at: https://doi.org/10.1073/PNAS.0709098105.

Deng, S. and Marmorstein, R. (2021) ‘Protein N-Terminal Acetylation: Structural Basis, Mechanism, Versatility, and Regulation’, *Trends in biochemical sciences*, 46(1), pp. 15–27. Available at: https://doi.org/10.1016/J.TIBS.2020.08.005.

Deniston, C.K. *et al.* (2020) ‘Structure of LRRK2 in Parkinson’s disease and model for microtubule interaction.’, *Nature* [Preprint]. Available at: https://doi.org/10.1038/s41586-020-2673-2.

Deribe, Y.L. *et al.* (2009) ‘Regulation of epidermal growth factor receptor trafficking by lysine deacetylase HDAC6’, *Science signaling*, 2(102). Available at: https://doi.org/10.1126/SCISIGNAL.2000576.

Deyaert, E. *et al.* (2017) ‘A homologue of the Parkinson’s disease-associated protein LRRK2 undergoes a monomer-dimer transition during GTP turnover’, *Nature Communications*, 8(1). Available at: https://doi.org/10.1038/s41467-017-01103-4.

Díaz, E.F. *et al.* (2019) ‘Connexin 43 hemichannels and pannexin-1 channels contribute to the α-synuclein-induced dysfunction and death of astrocytes’, *Glia*, 67(8), pp. 1598–1619. Available at: https://doi.org/10.1002/GLIA.23631.

Dieriks, B.V. *et al.* (2017) ‘α-synuclein transfer through tunneling nanotubes occurs in SH-SY5Y cells and primary brain pericytes from Parkinson’s disease patients’, *Scientific reports*, 7. Available at: https://doi.org/10.1038/SREP42984.

Dikiy, I. *et al.* (2016) ‘Semisynthetic and in Vitro Phosphorylation of Alpha-Synuclein at Y39 Promotes Functional Partly Helical Membrane-Bound States Resembling Those Induced by PD Mutations’, *ACS chemical biology*, 11(9), pp. 2428–2437.

Available at: https://doi.org/10.1021/ACSCHEMBIO.6B00539.

Ding, H., Dolan, P.J. and Johnson, G.V.W. (2008) 'Histone deacetylase 6 interacts with the microtubule-associated protein tau', *Journal of neurochemistry*, 106(5), pp. 2119–2130. Available at: https://doi.org/10.1111/J.1471-4159.2008.05564.X.

di Domenico, A. *et al.* (2019) 'Patient-Specific iPSC-Derived Astrocytes Contribute to Non-Cell-Autonomous Neurodegeneration in Parkinson's Disease', *Stem cell reports*, 12(2), pp. 213–229. Available at: https://doi.org/10.1016/J.STEMCR.2018.12.011.

Domenighetti, C. *et al.* (2022) 'Mendelian Randomisation Study of Smoking, Alcohol, and Coffee Drinking in Relation to Parkinson's Disease', *Journal of Parkinson's disease*, 12(1), pp. 267–282. Available at: https://doi.org/10.3233/JPD-212851.

Dompierre, J.P. *et al.* (2007) 'Histone deacetylase 6 inhibition compensates for the transport deficit in Huntington's disease by increasing tubulin acetylation', *The Journal of neuroscience : the official journal of the Society for Neuroscience*, 27(13), pp. 3571–3583. Available at: https://doi.org/10.1523/JNEUROSCI.0037-07.2007.

Dong, S. *et al.* (2022) 'Gasdermin E is required for induction of pyroptosis and severe disease during enterovirus 71 infection', *The Journal of biological chemistry*, 298(5). Available at: https://doi.org/10.1016/J.JBC.2022.101850.

Dorsey, E.R. *et al.* (2018) 'The Emerging Evidence of the Parkinson Pandemic', *Journal of Parkinson's disease*, 8(s1), pp. S3–S8. Available at: https://doi.org/10.3233/JPD-181474.

Dorsey, E.R. *et al.* (2023) 'Trichloroethylene: An Invisible Cause of Parkinson's Disease?', *Journal of Parkinson's Disease*, 13(2), p. 203. Available at: https://doi.org/10.3233/JPD-225047.

Dou, D. *et al.* (2023) 'Regulatory imbalance between LRRK2 kinase, PPM1H phosphatase, and ARF6 GTPase disrupts the axonal transport of autophagosomes', *Cell reports*, 42(5), p. 112448. Available at: https://doi.org/10.1016/J.CELREP.2023.112448.

Douaud, G. *et al.* (2022) ‘SARS-CoV-2 is associated with changes in brain structure in UK Biobank’, *Nature*, 604(7907), pp. 697–707. Available at: https://doi.org/10.1038/S41586-022-04569-5.

Du, G. *et al.* (2010) ‘Drosophila histone deacetylase 6 protects dopaminergic neurons against α-synuclein toxicity by promoting inclusion formation’, *Molecular Biology of the Cell*, 21(13), pp. 2128–2137. Available at: https://doi.org/10.1091/MBC.E10-03-0200/ASSET/IMAGES/LARGE/ZMK0131094910008.JPEG.

Du, Y. *et al.* (2014) ‘Histone deacetylase 6 regulates cytotoxic α-synuclein accumulation through induction of the heat shock response’, *Neurobiology of Aging*, 35(10), pp. 2316–2328.

Dues, D.J. and Moore, D.J. (2020) ‘LRRK2 and Protein Aggregation in Parkinson’s Disease: Insights From Animal Models’, *Frontiers in Neuroscience*, 14, p. 719. Available at: https://doi.org/10.3389/FNINS.2020.00719/BIBTEX.

Dul, J.L. *et al.* (2001) ‘Hsp70 and antifibrillogenic peptides promote degradation and inhibit intracellular aggregation of amyloidogenic light chains’, *The Journal of cell biology*, 152(4), pp. 705–715. Available at: https://doi.org/10.1083/JCB.152.4.705.

Dunn, K.W., Kamocka, M.M. and Mcdonald, J.H. (2011) ‘A practical guide to evaluating colocalization in biological microscopy’, *Am J Physiol Cell Physiol*, 300, pp. 723–742. Available at: https://doi.org/10.1152/ajpcell.00462.2010.

Ebrahimi-Fakhari, D. *et al.* (2011) ‘Distinct roles in vivo for the ubiquitin-proteasome system and the autophagy-lysosomal pathway in the degradation of α-synuclein’, *The Journal of neuroscience : the official journal of the Society for Neuroscience*, 31(41), pp. 14508–14520. Available at: https://doi.org/10.1523/JNEUROSCI.1560-11.2011.

Eguchi, T. *et al.* (2018) ‘LRRK2 and its substrate Rab GTPases are sequentially targeted onto stressed lysosomes and maintain their homeostasis’, *Proceedings of the National Academy of Sciences of the United States of America*, 115(39), pp. E9115–E9124. Available at: https://doi.org/10.1073/PNAS.1812196115.

Emmanouilidou, E. *et al.* (2010) ‘Cell-Produced α-Synuclein Is Secreted in a Calcium-Dependent Manner by Exosomes and Impacts Neuronal Survival’, *Journal of Neuroscience*, 30(20), pp. 6838–6851. Available at: https://doi.org/10.1523/JNEUROSCI.5699-09.2010.

Emmanouilidou, E., Stefanis, L. and Vekrellis, K. (2010) ‘Cell-produced alpha-synuclein oligomers are targeted to, and impair, the 26S proteasome’, *Neurobiology of aging*, 31(6), pp. 953–968. Available at: https://doi.org/10.1016/J.NEUROBIOLAGING.2008.07.008.

Engelender, S. *et al.* (2022) ‘Can We Treat Neurodegenerative Proteinopathies by Enhancing Protein Degradation?’, *Movement disorders : official journal of the Movement Disorder Society*, 37(7), pp. 1346–1359. Available at: https://doi.org/10.1002/MDS.29058.

Erekat, N.S. (2022) ‘Autophagy and Its Association with Genetic Mutations in Parkinson Disease’, *Medical Science Monitor : International Medical Journal of Experimental and Clinical Research*, 28, pp. e938519-1. Available at: https://doi.org/10.12659/MSM.938519.

Falsone, S.F. *et al.* (2009) ‘The molecular chaperone Hsp90 modulates intermediate steps of amyloid assembly of the Parkinson-related protein alpha-synuclein’, *The Journal of biological chemistry*, 284(45), pp. 31190–31199. Available at: https://doi.org/10.1074/JBC.M109.057240.

Fan, T.S. *et al.* (2016) ‘Clinical heterogeneity of LRRK2 p.I2012T mutation’, *Parkinsonism & related disorders*, 33, pp. 36–43. Available at: https://doi.org/10.1016/J.PARKRELDIS.2016.09.008.

Fang, N. and Casida, J.E. (1999) ‘Cubé resin insecticide: identification and biological activity of 29 rotenoid constituents’, *Journal of agricultural and food chemistry*, 47(5), pp. 2130–2136. Available at: https://doi.org/10.1021/JF981188X.

Fang, X. *et al.* (2018) ‘Association of Levels of Physical Activity With Risk of Parkinson Disease: A Systematic Review and Meta-analysis’, *JAMA network open*, 1(5), p. e182421. Available at:

https://doi.org/10.1001/JAMANETWORKOPEN.2018.2421.

Fava, V.M. *et al.* (2019) ‘Pleiotropic effects for Parkin and LRRK2 in leprosy type-1 reactions and Parkinson’s disease’, *Proceedings of the National Academy of Sciences of the United States of America*, 116(31), pp. 15616–15624. Available at: https://doi.org/10.1073/PNAS.1901805116.

Feigin, V.L. *et al.* (2019) ‘Global, regional, and national burden of neurological disorders, 1990–2016: a systematic analysis for the Global Burden of Disease Study 2016’, *The Lancet Neurology*, 18(5), pp. 459–480. Available at: https://doi.org/10.1016/S1474-4422(18)30499-X.

Fell, M.J. *et al.* (2015) ‘MLi-2, a Potent, Selective, and Centrally Active Compound for Exploring the Therapeutic Potential and Safety of LRRK2 Kinase Inhibition’, *The Journal of pharmacology and experimental therapeutics*, 355(3), pp. 397–409. Available at: https://doi.org/10.1124/JPET.115.227587.

Fenton, A.R., Jongens, T.A. and Holzbaur, E.L.F. (2021) ‘Mitochondrial dynamics: Shaping and remodeling an organelle network’, *Current opinion in cell biology*, 68, pp. 28–36. Available at: https://doi.org/10.1016/J.CEB.2020.08.014.

Ferrante, R.J. *et al.* (1997) ‘Systemic administration of rotenone produces selective damage in the striatum and globus pallidus, but not in the substantia nigra’, *Brain research*, 753(1), pp. 157–162. Available at: https://doi.org/10.1016/S0006-8993(97)00008-5.

Ferreira, C. *et al.* (2020) ‘Neuroprotection or Neurotoxicity of Illicit Drugs on Parkinson’s Disease’, *Life (Basel, Switzerland)*, 10(6), pp. 1–35. Available at: https://doi.org/10.3390/LIFE10060086.

Ferreon, A.C.M. *et al.* (2009) ‘Interplay of alpha-synuclein binding and conformational switching probed by single-molecule fluorescence’, *Proceedings of the National Academy of Sciences of the United States of America*, 106(14), pp. 5645–5650. Available at: https://doi.org/10.1073/PNAS.0809232106.

Fontaine, S.N. *et al.* (2016) ‘DnaJ/Hsc70 chaperone complexes control the extracellular release of neurodegenerative-associated proteins’, *The EMBO Journal*,

35(14), pp. 1537–1549. Available at: https://doi.org/10.15252/embj.201593489.

Fortin, D.L. *et al.* (2004) ‘Lipid rafts mediate the synaptic localization of alpha-synuclein’, *The Journal of neuroscience : the official journal of the Society for Neuroscience*, 24(30), pp. 6715–6723. Available at: https://doi.org/10.1523/JNEUROSCI.1594-04.2004.

Francelle, L., Outeiro, T.F. and Rappold, G.A. (2020) ‘Inhibition of HDAC6 activity protects dopaminergic neurons from alpha-synuclein toxicity’, *Scientific Reports 2020 10:1*, 10(1), pp. 1–14. Available at: https://doi.org/10.1038/s41598-020-62678-5.

Freeman, D. *et al.* (2013) ‘Alpha-Synuclein Induces Lysosomal Rupture and Cathepsin Dependent Reactive Oxygen Species Following Endocytosis’, *PLOS ONE*, 8(4), p. e62143. Available at: https://doi.org/10.1371/JOURNAL.PONE.0062143.

Friedman, L.G. *et al.* (2012) ‘Disrupted autophagy leads to dopaminergic axon and dendrite degeneration and promotes presynaptic accumulation of α-synuclein and LRRK2 in the brain’, *The Journal of neuroscience : the official journal of the Society for Neuroscience*, 32(22), pp. 7585–7593. Available at: https://doi.org/10.1523/JNEUROSCI.5809-11.2012.

Fuji, R.N. *et al.* (2015) ‘Effect of selective LRRK2 kinase inhibition on nonhuman primate lung’, *Science translational medicine*, 7(273), p. 273ra15. Available at: https://doi.org/10.1126/SCITRANSLMED.AAA3634.

Fujiwara, H. *et al.* (2002a) ‘alpha-Synuclein is phosphorylated in synucleinopathy lesions’, *Nature cell biology*, 4(2), pp. 160–164. Available at: https://doi.org/10.1038/NCB748.

Fujiwara, H. *et al.* (2002b) ‘α-Synuclein is phosphorylated in synucleinopathy lesions’, *Nature Cell Biology 2002 4:2*, 4(2), pp. 160–164. Available at: https://doi.org/10.1038/ncb748.

Fukuzono, T. *et al.* (2016) ‘Chaperone complex BAG2-HSC70 regulates localization of Caenorhabditis elegans leucine-rich repeat kinase LRK-1 to the Golgi’, *Genes to*

cells : devoted to molecular & cellular mechanisms, 21(4), pp. 311–324. Available at: https://doi.org/10.1111/GTC.12338.

Funayama, M. *et al.* (2002) 'A new locus for Parkinson's disease (PARK8) maps to chromosome 12p11.2-q13.1', *Annals of neurology*, 51(3), pp. 296–301. Available at: https://doi.org/10.1002/ANA.10113.

Funayama, M. *et al.* (2005) 'An LRRK2 mutation as a cause for the parkinsonism in the original PARK8 family', *Annals of neurology*, 57(6), pp. 918–921. Available at: https://doi.org/10.1002/ANA.20484.

Fusco, G. *et al.* (2017) 'Structural basis of membrane disruption and cellular toxicity by a-synuclein oligomers', *Science*, 358(6369), pp. 1440–1443. Available at: https://doi.org/10.1126/SCIENCE.AAN6160/SUPPL_FILE/AAN6160_FUSCO_SM.PDF.

Fussi, N. *et al.* (2018) 'Exosomal secretion of α-synuclein as protective mechanism after upstream blockage of macroautophagy', *Cell Death & Disease 2018 9:7*, 9(7), pp. 1–14. Available at: https://doi.org/10.1038/s41419-018-0816-2.

Gaig, C. *et al.* (2009) 'G2019S LRRK2 mutation causing Parkinson's disease without Lewy bodies', *BMJ Case Reports* [Preprint]. Available at: https://doi.org/10.1136/bcr.08.2008.0632.

Gaiter, D. *et al.* (2006) 'LRRK2 expression linked to dopamine-innervated areas', *Annals of neurology*, 59(4), pp. 714–719. Available at: https://doi.org/10.1002/ANA.20808.

Galvagnion, C. *et al.* (2016) 'Chemical properties of lipids strongly affect the kinetics of the membrane-induced aggregation of α-synuclein', *Proceedings of the National Academy of Sciences of the United States of America*, 113(26), pp. 7065–7070. Available at: https://doi.org/10.1073/PNAS.1601899113/SUPPL_FILE/PNAS.1601899113.SAPP.PDF.

Gamborg, M. *et al.* (2022) 'Parkinson's disease and intensive exercise therapy - An updated systematic review and meta-analysis', *Acta neurologica Scandinavica*,

145(5), pp. 504–528. Available at: https://doi.org/10.1111/ANE.13579.

Gamerdinger, M. *et al.* (2011) ‘BAG3 mediates chaperone-based aggresome-targeting and selective autophagy of misfolded proteins’, *EMBO reports*, 12(2), pp. 149–156. Available at: https://doi.org/10.1038/EMBOR.2010.203.

Gan-Or, Z. *et al.* (2008) ‘Genotype-phenotype correlations between GBA mutations and Parkinson disease risk and onset’, *Neurology*, 70(24), pp. 2277–2283. Available at: https://doi.org/10.1212/01.WNL.0000304039.11891.29.

Gan, H. *et al.* (2021) ‘The pivotal role of the NLRC4 inflammasome in neuroinflammation after intracerebral hemorrhage in rats’, *Experimental & molecular medicine*, 53(11), pp. 1807–1818. Available at: https://doi.org/10.1038/S12276-021-00702-Y.

Gandhi, P.N. *et al.* (2008) ‘The Roc domain of leucine-rich repeat kinase 2 is sufficient for interaction with microtubules’, *Journal of neuroscience research*, 86(8), pp. 1711–1720. Available at: https://doi.org/10.1002/JNR.21622.

García-Mata, R. *et al.* (1999) ‘Characterization and dynamics of aggresome formation by a cytosolic GFP- chimera’, *Journal of Cell Biology*, 146(6), pp. 1239–1254. Available at: https://doi.org/10.1083/jcb.146.6.1239.

Garcia-Reitböck, P. *et al.* (2010) ‘SNARE protein redistribution and synaptic failure in a transgenic mouse model of Parkinson’s disease’, *Brain*, 133(7), p. 2032. Available at: https://doi.org/10.1093/BRAIN/AWQ132.

Ge, P., Dawson, V.L. and Dawson, T.M. (2020) ‘PINK1 and Parkin mitochondrial quality control: a source of regional vulnerability in Parkinson’s disease’, *Molecular neurodegeneration*, 15(1). Available at: https://doi.org/10.1186/S13024-020-00367-7.

Geeraert, C. *et al.* (2010) ‘Starvation-induced hyperacetylation of tubulin is required for the stimulation of autophagy by nutrient deprivation’, *The Journal of biological chemistry*, 285(31), pp. 24184–24194. Available at: https://doi.org/10.1074/JBC.M109.091553.

Gegg, M.E., Menozzi, E. and Schapira, A.H.V. (2022) ‘Glucocerebrosidase-

associated Parkinson disease: Pathogenic mechanisms and potential drug treatments', *Neurobiology of Disease*, 166, p. 105663. Available at: https://doi.org/10.1016/J.NBD.2022.105663.

Gerfen, C.R. (2022) 'Segregation of D1 and D2 dopamine receptors in the striatal direct and indirect pathways: An historical perspective', *Frontiers in Synaptic Neuroscience*, 14. Available at: https://doi.org/10.3389/FNSYN.2022.1002960.

Ghanem, S.S. *et al.* (2022) 'α-Synuclein phosphorylation at serine 129 occurs after initial protein deposition and inhibits seeded fibril formation and toxicity', *Proceedings of the National Academy of Sciences of the United States of America*, 119(15). Available at: https://doi.org/10.1073/PNAS.2109617119.

Ghosh, D. *et al.* (2013) 'The parkinson's disease-associated H50Q mutation accelerates α-synuclein aggregation in vitro', *Biochemistry*, 52(40), pp. 6925–6927. Available at: https://doi.org/10.1021/BI400999D/SUPPL_FILE/BI400999D_SI_001.PDF.

Giasson, B.I. *et al.* (2001) 'A hydrophobic stretch of 12 amino acid residues in the middle of alpha-synuclein is essential for filament assembly', *The Journal of biological chemistry*, 276(4), pp. 2380–2386. Available at: https://doi.org/10.1074/JBC.M008919200.

Giesert, F. *et al.* (2013) 'Expression analysis of Lrrk1, Lrrk2 and Lrrk2 splice variants in mice', *PloS one*, 8(5). Available at: https://doi.org/10.1371/JOURNAL.PONE.0063778.

Gilsbach, B.K. *et al.* (2015) 'Structural Characterization of LRRK2 Inhibitors', *Journal of medicinal chemistry*, 58(9), pp. 3751–3756. Available at: https://doi.org/10.1021/JM5018779.

Giusto, E. *et al.* (2021) 'Pathways to Parkinson's disease: a spotlight on 14-3-3 proteins', *NPJ Parkinson's disease*, 7(1). Available at: https://doi.org/10.1038/S41531-021-00230-6.

Godena, V.K. *et al.* (2014) 'Increasing microtubule acetylation rescues axonal transport and locomotor deficits caused by LRRK2 Roc-COR domain mutations',

Nature Communications, 5. Available at: https://doi.org/10.1038/ncomms6245.

Goers, J. *et al.* (2003) 'Nuclear localization of α-synuclein and its interaction with histones', *Biochemistry*, 42(28), pp. 8465–8471. Available at: https://doi.org/10.1021/BI0341152/ASSET/IMAGES/LARGE/BI0341152F00008.JPEG.

Gold, W.A. *et al.* (2015) 'MeCP2 deficiency is associated with reduced levels of tubulin acetylation and can be restored using HDAC6 inhibitors', *Journal of molecular medicine (Berlin, Germany)*, 93(1), pp. 63–72. Available at: https://doi.org/10.1007/S00109-014-1202-X.

Goldman, S.M. *et al.* (2012) 'Solvent exposures and Parkinson disease risk in twins', *Annals of neurology*, 71(6), pp. 776–784. Available at: https://doi.org/10.1002/ANA.22629.

Gómez-Benito, M. *et al.* (2020) 'Modeling Parkinson’s Disease With the Alpha-Synuclein Protein', *Article*, 11, p. 1. Available at: https://doi.org/10.3389/fphar.2020.00356.

Gómez-Suaga, P. *et al.* (2012) 'Leucine-rich repeat kinase 2 regulates autophagy through a calcium-dependent pathway involving NAADP', *Human Molecular Genetics*, 21(3), pp. 511–525. Available at: https://doi.org/10.1093/hmg/ddr481.

Gomez, R.C. *et al.* (2019) 'Membrane association but not identity is required for LRRK2 activation and phosphorylation of Rab GTPases', *The Journal of cell biology*, 218(12), pp. 4157–4170. Available at: https://doi.org/10.1083/JCB.201902184.

Gopalai, A.A. *et al.* (2014) 'LRRK2 G2385R and R1628P mutations are associated with an increased risk of Parkinson's disease in the Malaysian population', *BioMed research international*, 2014. Available at: https://doi.org/10.1155/2014/867321.

Gorbatyuk, O.S. *et al.* (2008) 'The phosphorylation state of Ser-129 in human alpha-synuclein determines neurodegeneration in a rat model of Parkinson disease', *Proceedings of the National Academy of Sciences of the United States of America*, 105(2), pp. 763–768. Available at: https://doi.org/10.1073/PNAS.0711053105.

Gordon, R. *et al.* (2018) ‘Inflammasome inhibition prevents α-synuclein pathology and dopaminergic neurodegeneration in mice’, *Science translational medicine*, 10(465). Available at: https://doi.org/10.1126/SCITRANSLMED.AAH4066.

Gotthardt, K. *et al.* (2008) ‘Structure of the Roc-COR domain tandem of C. tepidum, a prokaryotic homologue of the human LRRK2 Parkinson kinase’, *The EMBO journal*, 27(16), pp. 2239–2249. Available at: https://doi.org/10.1038/EMBOJ.2008.150.

Grace, A.A. and Bunney, B.S. (1983) ‘Intracellular and extracellular electrophysiology of nigral dopaminergic neurons--1. Identification and characterization’, *Neuroscience*, 10(2). Available at: https://doi.org/10.1016/0306-4522(83)90135-5.

Grace, A.A. and Onn, S.P. (1989) ‘Morphology and electrophysiological properties of immunocytochemically identified rat dopamine neurons recorded in vitro’, *The Journal of neuroscience : the official journal of the Society for Neuroscience*, 9(10), pp. 3463–3481. Available at: https://doi.org/10.1523/JNEUROSCI.09-10-03463.1989.

Grassi, D. *et al.* (2018) ‘Identification of a highly neurotoxic α-synuclein species inducing mitochondrial damage and mitophagy in Parkinson’s disease’, *Proceedings of the National Academy of Sciences of the United States of America*, 115(11), pp. E2634–E2643. Available at: https://doi.org/10.1073/PNAS.1713849115/-/DCSUPPLEMENTAL.

Graves, N.J., Gambin, Y. and Sierecki, E. (2023) ‘α-Synuclein Strains and Their Relevance to Parkinson’s Disease, Multiple System Atrophy, and Dementia with Lewy Bodies’, *International Journal of Molecular Sciences*, 24(15), p. 12134. Available at: https://doi.org/10.3390/IJMS241512134.

Greggio, E. *et al.* (2008) ‘The Parkinson disease-associated leucine-rich repeat kinase 2 (LRRK2) is a dimer that undergoes intramolecular autophosphorylation’, *The Journal of biological chemistry*, 283(24), pp. 16906–16914. Available at: https://doi.org/10.1074/JBC.M708718200.

Grova, N. *et al.* (2019) ‘Epigenetic and neurological impairments associated with early life exposure to persistent organic pollutants’, *International Journal of Genomics*, 2019. Available at: https://doi.org/10.1155/2019/2085496.

Grozinger, C.M., Hassig, C.A. and Schreiber, S.L. (1999) ‘Three proteins define a class of human histone deacetylases related to yeast Hda1p’, *Proceedings of the National Academy of Sciences of the United States of America*, 96(9), pp. 4868–4873.

Gu, C., Fan, X. and Yu, W. (2023) ‘Functional Diversity of Mammalian Small Heat Shock Proteins: A Review’, *Cells*, 12(15). Available at: https://doi.org/10.3390/CELLS12151947.

Guaitoli, G. *et al.* (2016) ‘Structural model of the dimeric Parkinson’s protein LRRK2 reveals a compact architecture involving distant interdomain contacts’, *Proceedings of the National Academy of Sciences of the United States of America*, 113(30).

Guedes-Dias, P. *et al.* (2015) ‘HDAC6 inhibition induces mitochondrial fusion, autophagic flux and reduces diffuse mutant huntingtin in striatal neurons’, *Biochimica et biophysica acta*, 1852(11), pp. 2484–2493. Available at: https://doi.org/10.1016/J.BBADIS.2015.08.012.

Guerra De Souza, A.C., Prediger, R.D. and Cimarosti, H. (2016) ‘SUMO-regulated mitochondrial function in Parkinson’s disease’, *Journal of neurochemistry*, 137(5), pp. 673–686. Available at: https://doi.org/10.1111/JNC.13599.

Guerreiro, P.S. *et al.* (2013) ‘LRRK2 interactions with α-synuclein in Parkinson’s disease brains and in cell models’, *Journal of molecular medicine (Berlin, Germany)*, 91(4), pp. 513–522. Available at: https://doi.org/10.1007/S00109-012-0984-Y.

Guerrero-Ferreira, R. *et al.* (2018) ‘Cryo-EM structure of alpha-synuclein fibrils’, *eLife*, 7. Available at: https://doi.org/10.7554/eLife.36402.

Guo, H. *et al.* (2023) ‘Potential application of heat shock proteins as therapeutic targets in Parkinson’s disease’, *Neurochemistry International*, 162, p. 105453. Available at: https://doi.org/10.1016/J.NEUINT.2022.105453.

Guo, W. *et al.* (2017) ‘HDAC6 inhibition reverses axonal transport defects in motor neurons derived from FUS-ALS patients’, *Nature communications*, 8(1). Available at: https://doi.org/10.1038/S41467-017-00911-Y.

Haebig, K. *et al.* (2010) ‘ARHGEF7 (Beta-PIX) acts as guanine nucleotide exchange factor for leucine-rich repeat kinase 2’, *PloS one*, 5(10). Available at: https://doi.org/10.1371/JOURNAL.PONE.0013762.

Han, Y. *et al.* (2009) ‘Acetylation of histone deacetylase 6 by p300 attenuates its deacetylase activity’, *Biochemical and Biophysical Research Communications*, 383(1), pp. 88–92. Available at: https://doi.org/10.1016/j.bbrc.2009.03.147.

Hanss, Z. *et al.* (2021) ‘Mitochondrial and Clearance Impairment in p.D620N VPS35 Patient-Derived Neurons’, *Movement Disorders*, 36(3), pp. 704–715. Available at: https://doi.org/10.1002/MDS.28365.

Hao, R. *et al.* (2013) ‘Proteasomes activate aggresome disassembly and clearance by producing unanchored ubiquitin chains’, *Molecular cell*, 51(6), p. 819. Available at: https://doi.org/10.1016/J.MOLCEL.2013.08.016.

Haque, M.E. *et al.* (2020) ‘Targeting the microglial NLRP3 inflammasome and its role in Parkinson’s disease’, *Movement disorders : official journal of the Movement Disorder Society*, 35(1), pp. 20–33. Available at: https://doi.org/10.1002/MDS.27874.

Harder, Z., Zunino, R. and McBride, H. (2004) ‘Sumo1 conjugates mitochondrial substrates and participates in mitochondrial fission’, *Current biology : CB*, 14(4), pp. 340–345. Available at: https://doi.org/10.1016/J.CUB.2004.02.004.

Härtlova, A. *et al.* (2018) ‘LRRK2 is a negative regulator of Mycobacterium tuberculosis phagosome maturation in macrophages’, *The EMBO journal*, 37(12). Available at: https://doi.org/10.15252/EMBJ.201798694.

Hawk, B.J.D., Khounlo, R. and Shin, Y.K. (2019) ‘Alpha-Synuclein Continues to Enhance SNARE-Dependent Vesicle Docking at Exorbitant Concentrations’, *Frontiers in neuroscience*, 13. Available at: https://doi.org/10.3389/FNINS.2019.00216.

He, S. *et al.* (2020) ‘Alpha-Synuclein: The Interplay of Pathology, Neuroinflammation, and Environmental Factors in Parkinson’s Disease’, *Neuro-degenerative diseases*, 20(2–3), pp. 55–64. Available at: https://doi.org/10.1159/000511083.

He, W.T. *et al.* (2015) ‘Gasdermin D is an executor of pyroptosis and required for interleukin-1β secretion’, *Cell research*, 25(12), pp. 1285–1298. Available at: https://doi.org/10.1038/CR.2015.139.

Healy, D.G. *et al.* (2008) ‘Phenotype, genotype, and worldwide genetic penetrance of LRRK2-associated Parkinson’s disease: a case-control study’, *The Lancet Neurology*, 7(7), pp. 583–590. Available at: https://doi.org/10.1016/S1474-4422(08)70117-0.

Heikkila, R.E. *et al.* (1985) ‘Dopaminergic toxicity of rotenone and the 1-methyl-4-phenylpyridinium ion after their stereotaxic administration to rats: implication for the mechanism of 1-methyl-4-phenyl-1,2,3,6-tetrahydropyridine toxicity’, *Neuroscience letters*, 62(3), pp. 389–394. Available at: https://doi.org/10.1016/0304-3940(85)90580-4.

Helwig, M. *et al.* (2016) ‘Brain propagation of transduced α-synuclein involves non-fibrillar protein species and is enhanced in α-synuclein null mice’, *Brain : a journal of neurology*, 139(Pt 3), pp. 856–870. Available at: https://doi.org/10.1093/BRAIN/AWV376.

Henderson, M.X. *et al.* (2018) ‘LRRK2 activity does not dramatically alter α-synuclein pathology in primary neurons’, *Acta neuropathologica communications*, 6(1), p. 45. Available at: https://doi.org/10.1186/S40478-018-0550-0.

Henderson, M.X. *et al.* (2019) ‘LRRK2 inhibition does not impart protection from α-synuclein pathology and neuron death in non-transgenic mice’, *Acta neuropathologica communications*, 7(1), p. 28. Available at: https://doi.org/10.1186/S40478-019-0679-5/FIGURES/6.

Henderson, M.X., Trojanowski, J.Q. and Lee, V.M.Y. (2019) ‘α-Synuclein pathology in Parkinson’s disease and related α-synucleinopathies’, *Neuroscience letters*, 709. Available at: https://doi.org/10.1016/J.NEULET.2019.134316.

Henry, J. *et al.* (2010) ‘Parkinsonism and neurological manifestations of influenza throughout the 20th and 21st centuries’, *Parkinsonism & related disorders*, 16(9), pp. 566–571. Available at: https://doi.org/10.1016/J.PARKRELDIS.2010.06.012.

Herbst, S. *et al.* (2020) ‘LRRK2 activation controls the repair of damaged endomembranes in macrophages’, *The EMBO journal*, 39(18). Available at: https://doi.org/10.15252/EMBJ.2020104494.

Herzig, M.C. *et al.* (2011) ‘LRRK2 protein levels are determined by kinase function and are crucial for kidney and lung homeostasis in mice’, *Human molecular genetics*, 20(21), pp. 4209–4223. Available at: https://doi.org/10.1093/HMG/DDR348.

Hetz, C., Zhang, K. and Kaufman, R.J. (2020) ‘Mechanisms, regulation and functions of the unfolded protein response’, *Nature reviews. Molecular cell biology*, 21(8), pp. 421–438. Available at: https://doi.org/10.1038/S41580-020-0250-Z.

Hijaz, B.A. and Volpicelli-Daley, L.A. (2020) ‘Initiation and propagation of α-synuclein aggregation in the nervous system’, *Molecular Neurodegeneration*. BioMed Central Ltd. Available at: https://doi.org/10.1186/s13024-020-00368-6.

Ho, D.H. *et al.* (2018) ‘LRRK2 impairs autophagy by mediating phosphorylation of leucyl-tRNA synthetase’, *Cell Biochemistry and Function*, 36(8), pp. 431–442. Available at: https://doi.org/10.1002/cbf.3364.

Ho, D.H. *et al.* (2022) ‘LRRK2 Inhibition Mitigates the Neuroinflammation Caused by TLR2-Specific α-Synuclein and Alleviates Neuroinflammation-Derived Dopaminergic Neuronal Loss’, *Cells*, 11(5). Available at: https://doi.org/10.3390/CELLS11050861.

Ho, P.W.L. *et al.* (2020) ‘Age-dependent accumulation of oligomeric SNCA/α-synuclein from impaired degradation in mutant LRRK2 knockin mouse model of Parkinson disease: role for therapeutic activation of chaperone-mediated autophagy (CMA)’, *Autophagy*, 16(2), pp. 347–370. Available at: https://doi.org/10.1080/15548627.2019.1603545.

Ho, P.W.L. *et al.* (2022) ‘Long-term inhibition of mutant LRRK2 hyper-kinase activity reduced mouse brain α-synuclein oligomers without adverse effects’, *npj Parkinson’s Disease 2022 8:1*, 8(1), pp. 1–22. Available at: https://doi.org/10.1038/s41531-022-

00386-9.

Hockey, L.N. *et al.* (2015) ‘Dysregulation of lysosomal morphology by pathogenic LRRK2 is corrected by TPC2 inhibition’, *Journal of Cell Science*, 128(2), pp. 232–238. Available at: https://doi.org/10.1242/jcs.164152.

Hodara, R. *et al.* (2004) ‘Functional consequences of alpha-synuclein tyrosine nitration: diminished binding to lipid vesicles and increased fibril formation’, *The Journal of biological chemistry*, 279(46), pp. 47746–47753. Available at: https://doi.org/10.1074/JBC.M408906200.

Holmes, B.B. *et al.* (2013) ‘Heparan sulfate proteoglycans mediate internalization and propagation of specific proteopathic seeds’, *Proceedings of the National Academy of Sciences of the United States of America*, 110(33), pp. E3138–E3147. Available at: https://doi.org/10.1073/PNAS.1301440110/SUPPL_FILE/SM01.MOV.

Homma, Y., Hiragi, S. and Fukuda, M. (2021) ‘Rab family of small GTPases: an updated view on their regulation and functions’, *The FEBS journal*, 288(1), pp. 36–55. Available at: https://doi.org/10.1111/FEBS.15453.

Hook, S.S. *et al.* (2002) ‘Histone deacetylase 6 binds polyubiquitin through its zinc finger (PAZ domain) and copurifies with deubiquitinating enzymes’, *Proceedings of the National Academy of Sciences of the United States of America*, 99(21), pp. 13425–13430. Available at: https://doi.org/10.1073/PNAS.172511699.

Hsieh, C.H. *et al.* (2016) ‘Functional Impairment in Miro Degradation and Mitophagy Is a Shared Feature in Familial and Sporadic Parkinson’s Disease’, *Cell stem cell*, 19(6), pp. 709–724. Available at: https://doi.org/10.1016/J.STEM.2016.08.002.

Hsu, L.J. *et al.* (2000) ‘α-synuclein promotes mitochondrial deficit and oxidative stress’, *American Journal of Pathology*, 157(2), pp. 401–410. Available at: https://doi.org/10.1016/S0002-9440(10)64553-1.

Hu, J. *et al.* (2023) ‘Small-molecule LRRK2 inhibitors for PD therapy: Current achievements and future perspectives’, *European journal of medicinal chemistry*, 256. Available at: https://doi.org/10.1016/J.EJMECH.2023.115475.

Huang, C.C. *et al.* (2018) ‘Soluble α-synuclein facilitates priming and fusion by releasing Ca2+ from the thapsigargin-sensitive Ca2+ pool in PC12 cells’, *Journal of Cell Science*, 131(23). Available at: https://doi.org/10.1242/jcs.213017.

Huang, X. *et al.* (2019) ‘The Parkinson’s disease-associated mutation N1437H impairs conformational dynamics in the G domain of LRRK2’, *FASEB journal : official publication of the Federation of American Societies for Experimental Biology*, 33(4), pp. 4814–4823. Available at: https://doi.org/10.1096/FJ.201802031R.

Hubbert, C. *et al.* (2002) ‘HDAC6 is a microtubule-associated deacetylase’, *Nature*, 417(6887), pp. 455–458. Available at: https://doi.org/10.1038/417455A.

Hughes, A.J. *et al.* (1992) ‘Accuracy of clinical diagnosis of idiopathic Parkinson’s disease: A clinico-pathological study of 100 cases’, *Journal of Neurology Neurosurgery and Psychiatry*, 55(3), pp. 181–184. Available at: https://doi.org/10.1136/jnnp.55.3.181.

Hui, K.Y. *et al.* (2018) ‘Functional variants in the LRRK2 gene confer shared effects on risk for Crohn’s disease and Parkinson’s disease’, *Science translational medicine*, 10(423). Available at: https://doi.org/10.1126/SCITRANSLMED.AAI7795.

Ingelsson, M. (2016) ‘Alpha-synuclein oligomers-neurotoxic molecules in Parkinson’s disease and other lewy body disorders’, *Frontiers in Neuroscience*, 10(SEP), p. 216192. Available at: https://doi.org/10.3389/FNINS.2016.00408/BIBTEX.

Inglis, K.J. *et al.* (2009) ‘Polo-like kinase 2 (PLK2) phosphorylates alpha-synuclein at serine 129 in central nervous system’, *The Journal of biological chemistry*, 284(5), pp. 2598–2602. Available at: https://doi.org/10.1074/JBC.C800206200.

Inoshita, T. *et al.* (2022) ‘Parkinson disease-associated Leucine-rich repeat kinase regulates UNC-104-dependent axonal transport of Arl8-positive vesicles in Drosophila’, *iScience*, 25(12). Available at: https://doi.org/10.1016/J.ISCI.2022.105476.

Ioghen, O.C., Ceafalan, L.C. and Popescu, B.O. (2023) ‘SH-SY5Y Cell Line In Vitro Models for Parkinson Disease Research-Old Practice for New Trends’, *Journal of integrative neuroscience*, 22(1), p. 20. Available at:

https://doi.org/10.31083/J.JIN2201020.

Iqbal, A. *et al.* (2020) ‘Alpha-synuclein aggresomes inhibit ciliogenesis and multiple functions of the centrosome’, *Biology open*, 9(10). Available at: https://doi.org/10.1242/BIO.054338.

Ito, G. *et al.* (2007) ‘GTP binding is essential to the protein kinase activity of LRRK2, a causative gene product for familial Parkinson’s disease’, *Biochemistry*, 46(5), pp. 1380–1388. Available at: https://doi.org/10.1021/BI061960M.

Ito, G. and Utsunomiya-Tate, N. (2023) ‘Overview of the Impact of Pathogenic LRRK2 Mutations in Parkinson’s Disease’, *Biomolecules*, 13(5). Available at: https://doi.org/10.3390/BIOM13050845.

Iwai, A. *et al.* (1995) ‘The Precursor Protein of Non-Ap Component of Alzheimer’s Disease Amyloid Is a Presynaptic Protein of the Central Nervous System’, *Neuron*, 14, pp. 467–475.

Iwata, A., Riley, B.E., *et al.* (2005) ‘HDAC6 and microtubules are required for autophagic degradation of aggregated huntingtin’, *The Journal of biological chemistry*, 280(48), pp. 40282–40292. Available at: https://doi.org/10.1074/JBC.M508786200.

Iwata, A., Christianson, J.C., *et al.* (2005) ‘Increased susceptibility of cytoplasmic over nuclear polyglutamine aggregates to autophagic degradation’, *Proceedings of the National Academy of Sciences of the United States of America*, 102(37), pp. 13135–13140. Available at: https://doi.org/10.1073/pnas.0505801102.

Iwatsubo, T. (2003) ‘Aggregation of α-synuclein in the pathogenesis of Parkinson’s disease’, *Journal of Neurology, Supplement*, 250(3), pp. 11–14. Available at: https://doi.org/10.1007/s00415-003-1303-x.

Iyer, A., Sidhu, A. and Subramaniam, V. (2022) ‘How important is the N-terminal acetylation of alpha-synuclein for its function and aggregation into amyloids?’, *Frontiers in neuroscience*, 16. Available at: https://doi.org/10.3389/FNINS.2022.1003997.

Jacobson, S. *et al.* (2019) ‘Parkinson’s Disease and the Environment’, *Frontiers in Neurology* | *www.frontiersin.org*, 1, p. 218. Available at: https://doi.org/10.3389/fneur.2019.00218.

Jakes, R., Spillantini, M.G. and Goedert, M. (1994) ‘Identification of two distinct synucleins from human brain’, *FEBS Letters*, 345(1), pp. 27–32. Available at: https://doi.org/10.1016/0014-5793(94)00395-5.

Jang, H. *et al.* (2009) ‘Highly pathogenic H5N1 influenza virus can enter the central nervous system and induce neuroinflammation and neurodegeneration’, *Proceedings of the National Academy of Sciences of the United States of America*, 106(33), pp. 14063–14068. Available at: https://doi.org/10.1073/PNAS.0900096106.

Jayaraj, G.G., Hipp, M.S. and Ulrich Hartl, F. (2020) ‘Functional Modules of the Proteostasis Network’, *Cold Spring Harbor perspectives in biology*, 12(1). Available at: https://doi.org/10.1101/CSHPERSPECT.A033951.

Jellinger, K.A. (2009) ‘A critical evaluation of current staging of alpha-synuclein pathology in Lewy body disorders’, *Biochimica et biophysica acta*, 1792(7), pp. 730–740. Available at: https://doi.org/10.1016/J.BBADIS.2008.07.006.

Jensen, T.J. *et al.* (1995) ‘Multiple proteolytic systems, including the proteasome, contribute to CFTR processing’, *Cell*, 83(1), pp. 129–135. Available at: https://doi.org/10.1016/0092-8674(95)90241-4.

Jeong, G.R. *et al.* (2018) ‘Dysregulated phosphorylation of Rab GTPases by LRRK2 induces neurodegeneration’, *Molecular neurodegeneration*, 13(1). Available at: https://doi.org/10.1186/S13024-018-0240-1.

Jeong, G.R. and Lee, B.D. (2020a) *Pathological Functions of LRRK2 in Parkinson’s Disease*, *Cells*.

Jeong, G.R. and Lee, B.D. (2020b) ‘Pathological Functions of LRRK2 in Parkinson’s Disease’, *Cells*, 9(12). Available at: https://doi.org/10.3390/CELLS9122565.

Jian, W. *et al.* (2017) ‘Inhibition of HDAC6 increases acetylation of peroxiredoxin1/2 and ameliorates 6-OHDA induced dopaminergic injury’, *Neuroscience letters*, 658,

pp. 114–120. Available at: https://doi.org/10.1016/J.NEULET.2017.08.029.

Jo, H., Shim, K. and Jeoung, D. (2022) ‘Targeting HDAC6 to Overcome Autophagy-Promoted Anti-Cancer Drug Resistance’, *International Journal of Molecular Sciences*, 23(17). Available at: https://doi.org/10.3390/IJMS23179592.

Johansen, K.K. *et al.* (2018) ‘A Case of Parkinson’s Disease with No Lewy Body Pathology due to a Homozygous Exon Deletion in Parkin’, *Case reports in neurological medicine*, 2018, pp. 1–4. Available at: https://doi.org/10.1155/2018/6838965.

Johansen, T. and Lamark, T. (2020) ‘Selective Autophagy: ATG8 Family Proteins, LIR Motifs and Cargo Receptors’, *Journal of molecular biology*, 432(1), pp. 80–103. Available at: https://doi.org/10.1016/J.JMB.2019.07.016.

Johnston, J.A., Ward, C.L. and Kopito, R.R. (1998) ‘Aggresomes: A cellular response to misfolded proteins’, *Journal of Cell Biology*, 143(7), pp. 1883–1898. Available at: https://doi.org/10.1083/jcb.143.7.1883.

Jónsson, S.A., Mohanty, S. and Irbäck, A. (2012) ‘Distinct phases of free α-synuclein-A Monte Carlo study’, *Proteins: Structure, Function and Bioinformatics*, 80(9), pp. 2169–2177. Available at: https://doi.org/10.1002/prot.24107.

Jowaed, A. *et al.* (2010) ‘Methylation regulates alpha-synuclein expression and is decreased in Parkinson’s disease patients’ brains’, *The Journal of neuroscience : the official journal of the Society for Neuroscience*, 30(18), pp. 6355–6359. Available at: https://doi.org/10.1523/JNEUROSCI.6119-09.2010.

Junn, E. and Mouradian, M.M. (2002) ‘Human α-Synuclein over-expression increases intracellular reactive oxygen species levels and susceptibility to dopamine’, *Neuroscience Letters*, 320(3), pp. 146–150. Available at: https://doi.org/10.1016/S0304-3940(02)00016-2.

Kaksonen, M. and Roux, A. (2018) ‘Mechanisms of clathrin-mediated endocytosis’, *Nature reviews. Molecular cell biology*, 19(5), pp. 313–326. Available at: https://doi.org/10.1038/NRM.2017.132.

Kalebic, N. *et al.* (2013) ‘αTAT1 is the major α-tubulin acetyltransferase in mice’, *Nature communications*, 4. Available at: https://doi.org/10.1038/NCOMMS2962.

Kalia, L. V. *et al.* (2015) ‘Clinical Correlations With Lewy Body Pathology in LRRK2-Related Parkinson Disease’, *JAMA neurology*, 72(1), p. 100. Available at: https://doi.org/10.1001/JAMANEUROL.2014.2704.

Kalluri, R. and LeBleu, V.S. (2020) ‘The biology , function , and biomedical applications of exosomes’, *Science (New York, N.Y.)*, 367(6478). Available at: https://doi.org/10.1126/SCIENCE.AAU6977.

Kalogeropulou, A.F. *et al.* (2020) ‘Endogenous Rab29 does not impact basal or stimulated LRRK2 pathway activity’, *The Biochemical journal*, 477(22), pp. 4397–4423. Available at: https://doi.org/10.1042/BCJ20200458.

Kamp, F. *et al.* (2010) ‘Inhibition of mitochondrial fusion by α-synuclein is rescued by PINK1, Parkin and DJ-1’, *The EMBO Journal*, 29(20), p. 3571. Available at: https://doi.org/10.1038/EMBOJ.2010.223.

Kapitein, L.C. and Hoogenraad, C.C. (2015) ‘Building the Neuronal Microtubule Cytoskeleton’, *Neuron*. Cell Press, pp. 492–506. Available at: https://doi.org/10.1016/j.neuron.2015.05.046.

Karampetsou, M. *et al.* (2017) ‘Phosphorylated exogenous alpha-synuclein fibrils exacerbate pathology and induce neuronal dysfunction in mice’, *Scientific reports*, 7(1). Available at: https://doi.org/10.1038/S41598-017-15813-8.

Kawagoe, S., Ishimori, K. and Saio, T. (2022) ‘Structural and Kinetic Views of Molecular Chaperones in Multidomain Protein Folding’, *International journal of molecular sciences*, 23(5). Available at: https://doi.org/10.3390/IJMS23052485.

Kawaguchi, Y. *et al.* (2003) ‘The deacetylase HDAC6 regulates aggresome formation and cell viability in response to misfolded protein stress’, *Cell*, 115(6), pp. 727–738. Available at: https://doi.org/10.1016/S0092-8674(03)00939-5.

Kawahata, I., Yagishita, S., Hasegawa, K., Nagatsu, I., Nagatsu, T. and Ichinose, H. (2009) ‘Immunohistochemical analyses of the postmortem human brains from

patients with Parkinson's disease with anti-tyrosine hydroxylase antibodies', *Biog. Amines*, (23), pp. 1–7.

Kawahata, I., Finkelstein, D.I. and Fukunaga, K. (2022) 'Pathogenic Impact of α-Synuclein Phosphorylation and Its Kinases in α-Synucleinopathies'. Available at: https://doi.org/10.3390/ijms23116216.

Kett, L.R. *et al.* (2012) 'LRRK2 Parkinson disease mutations enhance its microtubule association', *Human molecular genetics*, 21(4), pp. 890–899. Available at: https://doi.org/10.1093/HMG/DDR526.

Khalid, M., Petroianu, G. and Adem, A. (2022) 'Advanced Glycation End Products and Diabetes Mellitus: Mechanisms and Perspectives', *Biomolecules*, 12(4). Available at: https://doi.org/10.3390/BIOM12040542.

Kiely, A.P. *et al.* (2013) 'α-Synucleinopathy associated with G51D SNCA mutation: a link between Parkinson's disease and multiple system atrophy?', *Acta neuropathologica*, 125(5), pp. 753–769. Available at: https://doi.org/10.1007/S00401-013-1096-7.

Kim, B., Suh, Y.H. and Joe, E. (2022) 'LRRK2 decreases microglial actin dynamics by filamentous actin depolymerization and Rac1 inhibition', *Animal cells and systems*, 26(6), pp. 380–387. Available at: https://doi.org/10.1080/19768354.2022.2158219.

Kim, C. *et al.* (2012) 'HDAC6 inhibitor blocks amyloid beta-induced impairment of mitochondrial transport in hippocampal neurons', *PloS one*, 7(8). Available at: https://doi.org/10.1371/JOURNAL.PONE.0042983.

Kim, C. *et al.* (2013) 'Neuron-released oligomeric α-synuclein is an endogenous agonist of TLR2 for paracrine activation of microglia', *Nature Communications 2013 4:1*, 4(1), pp. 1–12. Available at: https://doi.org/10.1038/ncomms2534.

Kim, C. *et al.* (2021) 'Effects of innate immune receptor stimulation on extracellular α-synuclein uptake and degradation by brain resident cells', *Experimental & Molecular Medicine 2021 53:2*, 53(2), pp. 281–290. Available at: https://doi.org/10.1038/s12276-021-00562-6.

Kim, G.W. *et al.* (2013) ‘Mice lacking α-tubulin acetyltransferase 1 are viable but display α-tubulin acetylation deficiency and dentate gyrus distortion’, *The Journal of biological chemistry*, 288(28), pp. 20334–20350. Available at: https://doi.org/10.1074/JBC.M113.464792.

Kim, Y.M. *et al.* (2011) ‘Proteasome inhibition induces α-synuclein SUMOylation and aggregate formation’, *Journal of the neurological sciences*, 307(1–2), pp. 157–161. Available at: https://doi.org/10.1016/J.JNS.2011.04.015.

Kirkin, V. (2020) ‘History of the Selective Autophagy Research: How Did It Begin and Where Does It Stand Today?’, *Journal of molecular biology*, 432(1), pp. 3–27. Available at: https://doi.org/10.1016/J.JMB.2019.05.010.

Kitada, T. *et al.* (1998) ‘Mutations in the parkin gene cause autosomal recessive juvenile parkinsonism’, *Nature*, 392(6676), pp. 605–608. Available at: https://doi.org/10.1038/33416.

Klucken, J. *et al.* (2004) ‘Hsp70 Reduces alpha-Synuclein Aggregation and Toxicity’, *The Journal of biological chemistry*, 279(24), pp. 25497–25502. Available at: https://doi.org/10.1074/JBC.M400255200.

Kolicheski, A. *et al.* (2022) ‘Early-Onset Parkinson’s Disease: Creating the Right Environment for a Genetic Disorder’, *Journal of Parkinson’s disease*, 12(8), pp. 2353–2367. Available at: https://doi.org/10.3233/JPD-223380.

Kondo, K., Obitsu, S. and Teshima, R. (2011) ‘α-Synuclein Aggregation and Transmission Are Enhanced by Leucine-Rich Repeat Kinase 2 in Human Neuroblastoma SH-SY5Y Cells’, *Biological and Pharmaceutical Bulletin*, 34(7), pp. 1078–1083. Available at: https://doi.org/10.1248/BPB.34.1078.

Konig, A., Miranda, H.V. and Outeiro, T.F. (2018) ‘Alpha-Synuclein Glycation and the Action of Anti-Diabetic Agents in Parkinson’s Disease’, *Journal of Parkinson’s disease*, 8(1), pp. 33–43. Available at: https://doi.org/10.3233/JPD-171285.

Kopito, R.R. (2000) ‘Aggresomes, inclusion bodies and protein aggregation’, *Trends in Cell Biology*, pp. 524–530. Available at: https://doi.org/10.1016/S0962-8924(00)01852-3.

Kordower, J.H. *et al.* (2008) ‘Lewy body-like pathology in long-term embryonic nigral transplants in Parkinson’s disease’, *Nature Medicine*, 14(5), pp. 504–506. Available at: https://doi.org/10.1038/nm1747.

Kosten, J. *et al.* (2014) ‘Efficient modification of alpha-synuclein serine 129 by protein kinase CK1 requires phosphorylation of tyrosine 125 as a priming event’, *ACS chemical neuroscience*, 5(12), pp. 1203–1208. Available at: https://doi.org/10.1021/CN5002254.

Kovacs, J.J. *et al.* (2005) ‘HDAC6 regulates Hsp90 acetylation and chaperone-dependent activation of glucocorticoid receptor’, *Molecular Cell*, 18(5), pp. 601–607. Available at: https://doi.org/10.1016/j.molcel.2005.04.021.

Kozikowski, A.P. *et al.* (2019) ‘Brain Penetrable Histone Deacetylase 6 Inhibitor SW-100 Ameliorates Memory and Learning Impairments in a Mouse Model of Fragile X Syndrome’, *ACS chemical neuroscience*, 10(3), pp. 1679–1695. Available at: https://doi.org/10.1021/ACSCHEMNEURO.8B00600.

Krüger, R. *et al.* (1998) ‘Ala30Pro mutation in the gene encoding α-synuclein in Parkinson’s disease’, *Nature Genetics*, 18(2), pp. 106–108. Available at: https://doi.org/10.1038/ng0298-106.

Krumova, P. *et al.* (2011) ‘Sumoylation inhibits alpha-synuclein aggregation and toxicity’, *The Journal of cell biology*, 194(1), pp. 49–60. Available at: https://doi.org/10.1083/JCB.201010117.

Kruppa, A.J. and Buss, F. (2021) ‘Motor proteins at the mitochondria-cytoskeleton interface’, *Journal of cell science*, 134(7). Available at: https://doi.org/10.1242/JCS.226084.

Kumar, A. V., Mills, J. and Lapierre, L.R. (2022) ‘Selective Autophagy Receptor p62/SQSTM1, a Pivotal Player in Stress and Aging’, *Frontiers in cell and developmental biology*, 10. Available at: https://doi.org/10.3389/FCELL.2022.793328.

Kunadt, M. *et al.* (2015) ‘Extracellular vesicle sorting of α-Synuclein is regulated by sumoylation’, *Acta neuropathologica*, 129(5), pp. 695–713. Available at:

https://doi.org/10.1007/S00401-015-1408-1.

Kuwahara, T. *et al.* (2012) ‘Phosphorylation of α-synuclein protein at Ser-129 reduces neuronal dysfunction by lowering its membrane binding property in Caenorhabditis elegans’, *The Journal of biological chemistry*, 287(10), pp. 7098–7109. Available at: https://doi.org/10.1074/JBC.M111.237131.

Kuwahara, T. *et al.* (2020) ‘Roles of lysosomotropic agents on LRRK2 activation and Rab10 phosphorylation’, *Neurobiology of disease*, 145. Available at: https://doi.org/10.1016/J.NBD.2020.105081.

Kwon, Y. *et al.* (2020) ‘Amitriptyline interferes with autophagy-mediated clearance of protein aggregates via inhibiting autophagosome maturation in neuronal cells’, *Cell Death & Disease 2020 11:10*, 11(10), pp. 1–17. Available at: https://doi.org/10.1038/s41419-020-03085-6.

L’Hernaul, S.W. and Rosenbaum, J.L. (1985) ‘Chlamydomonas alpha-tubulin is posttranslationally modified by acetylation on the epsilon-amino group of a lysine’, *Biochemistry*, 24(2), pp. 473–478. Available at: https://doi.org/10.1021/BI00323A034.

Lafarga, V. *et al.* (2012) ‘A novel GRK2/HDAC6 interaction modulates cell spreading and motility’, *The EMBO Journal*, 31(4), p. 856. Available at: https://doi.org/10.1038/EMBOJ.2011.466.

Lashuel, H.A. *et al.* (2002) ‘α-Synuclein, Especially the Parkinson’s Disease-associated Mutants, Forms Pore-like Annular and Tubular Protofibrils’, *Journal of Molecular Biology*, 322(5), pp. 1089–1102. Available at: https://doi.org/10.1016/S0022-2836(02)00735-0.

Lashuel, H.A. (2020) ‘Do Lewy bodies contain alpha-synuclein fibrils? and Does it matter? A brief history and critical analysis of recent reports’, *Neurobiology of disease*, 141. Available at: https://doi.org/10.1016/J.NBD.2020.104876.

Latif, S. *et al.* (2021) ‘Dopamine in Parkinson’s disease’, *Clinica chimica acta; international journal of clinical chemistry*, 522, pp. 114–126. Available at: https://doi.org/10.1016/J.CCA.2021.08.009.

Lavedan, C., Dehejia, A., *et al.* (1998) ‘Contig map of the Parkinson’s disease region on 4q21-q23’, *DNA research : an international journal for rapid publication of reports on genes and genomes*, 5(1), pp. 19–23. Available at: https://doi.org/10.1093/DNARES/5.1.19.

Lavedan, C., Leroy, E., *et al.* (1998) ‘Identification, localization and characterization of the human gamma-synuclein gene’, *Human genetics*, 103(1), pp. 106–112. Available at: https://doi.org/10.1007/S004390050792.

Law, B.M.H. *et al.* (2014) ‘A direct interaction between leucine-rich repeat kinase 2 and specific β-tubulin isoforms regulates tubulin acetylation’, *The Journal of biological chemistry*, 289(2), pp. 895–908. Available at: https://doi.org/10.1074/JBC.M113.507913.

LeDizet, M. and Piperno, G. (1987) ‘Identification of an acetylation site of Chlamydomonas alpha-tubulin’, *Proceedings of the National Academy of Sciences of the United States of America*, 84(16), pp. 5720–5724. Available at: https://doi.org/10.1073/PNAS.84.16.5720.

Lee, B.E., Suh, P.G. and Kim, J.I. (2021) ‘O-GlcNAcylation in health and neurodegenerative diseases’, *Experimental & molecular medicine*, 53(11), pp. 1674–1682. Available at: https://doi.org/10.1038/S12276-021-00709-5.

Lee, H.J. *et al.* (2004) ‘Clearance of alpha-synuclein oligomeric intermediates via the lysosomal degradation pathway’, *The Journal of neuroscience : the official journal of the Society for Neuroscience*, 24(8), pp. 1888–1896. Available at: https://doi.org/10.1523/JNEUROSCI.3809-03.2004.

Lee, H.J. *et al.* (2008) ‘Assembly-dependent endocytosis and clearance of extracellular α-synuclein’, *International Journal of Biochemistry and Cell Biology*, 40(9), pp. 1835–1849. Available at: https://doi.org/10.1016/j.biocel.2008.01.017.

Lee, H.J., Choi, C. and Lee, S.J. (2002) ‘Membrane-bound α-Synuclein Has a High Aggregation Propensity and the Ability to Seed the Aggregation of the Cytosolic Form’, *Journal of Biological Chemistry*, 277(1), pp. 671–678. Available at: https://doi.org/10.1074/JBC.M107045200.

Lee, H.J. and Lee, S.J. (2002) ‘Characterization of cytoplasmic alpha-synuclein aggregates. Fibril formation is tightly linked to the inclusion-forming process in cells’, *The Journal of biological chemistry*, 277(50), pp. 48976–48983. Available at: https://doi.org/10.1074/JBC.M208192200.

Lee, H.J., Patel, S. and Lee, S.J. (2005a) ‘Intravesicular localization and exocytosis of alpha-synuclein and its aggregates’, *The Journal of neuroscience : the official journal of the Society for Neuroscience*, 25(25), pp. 6016–6024. Available at: https://doi.org/10.1523/JNEUROSCI.0692-05.2005.

Lee, H.J., Patel, S. and Lee, S.J. (2005b) ‘Intravesicular localization and exocytosis of α-synuclein and its aggregates’, *Journal of Neuroscience*, 25(25), pp. 6016–6024. Available at: https://doi.org/10.1523/JNEUROSCI.0692-05.2005.

Lee, J.G. *et al.* (2016) ‘Unconventional secretion of misfolded proteins promotes adaptation to proteasome dysfunction in mammalian cells’, *Nature Cell Biology 2016 18:7*, 18(7), pp. 765–776. Available at: https://doi.org/10.1038/ncb3372.

Lee, J.T. *et al.* (2008) ‘Ubiquitination of alpha-synuclein by Siah-1 promotes alpha-synuclein aggregation and apoptotic cell death’, *Human molecular genetics*, 17(6), pp. 906–917. Available at: https://doi.org/10.1093/HMG/DDM363.

Lee, J.Y. *et al.* (2010) ‘HDAC6 controls autophagosome maturation essential for ubiquitin-selective quality-control autophagy’, *The EMBO journal*, 29(5), pp. 969–980. Available at: https://doi.org/10.1038/EMBOJ.2009.405.

Lee, J.Y. and Yao, T.P. (2010) ‘Quality control autophagy: A joint effort of ubiquitin, protein deacetylase and actin cytoskeleton’, *Autophagy*, 6(4), pp. 555–557. Available at: https://doi.org/10.4161/auto.6.4.11812.

Lehotzky, A. *et al.* (2004) ‘Dynamic targeting of microtubules by TPPP/p25 affects cell survival’, *Journal of cell science*, 117(Pt 25), pp. 6249–6259. Available at: https://doi.org/10.1242/JCS.01550.

Lehtonen, Š. *et al.* (2019) ‘Dysfunction of cellular proteostasis in Parkinson’s disease’, *Frontiers in Neuroscience*. Frontiers Media S.A. Available at: https://doi.org/10.3389/fnins.2019.00457.

Lei, Q., Yi, T. and Chen, C. (2018) 'NF-κB-Gasdermin D (GSDMD) Axis Couples Oxidative Stress and NACHT, LRR and PYD Domains-Containing Protein 3 (NLRP3) Inflammasome-Mediated Cardiomyocyte Pyroptosis Following Myocardial Infarction', *Medical science monitor : international medical journal of experimental and clinical research*, 24, pp. 6044–6052. Available at: https://doi.org/10.12659/MSM.908529.

Lesage, S. *et al.* (2011) 'Mutations in the glucocerebrosidase gene confer a risk for Parkinson disease in North Africa', *Neurology*, 76(3), pp. 301–303. Available at: https://doi.org/10.1212/WNL.0B013E318207B01E.

Lesage, S. *et al.* (2020) 'Genetic and Phenotypic Basis of Autosomal Dominant Parkinson's Disease in a Large Multi-Center Cohort', *Frontiers in Neurology*, 11, p. 682. Available at: https://doi.org/10.3389/FNEUR.2020.00682/BIBTEX.

Levine, B. and Klionsky, D.J. (2004) 'Development by self-digestion: Molecular mechanisms and biological functions of autophagy', *Developmental Cell*, pp. 463–477. Available at: https://doi.org/10.1016/S1534-5807(04)00099-1.

Levine, P.M. *et al.* (2017) 'O-GlcNAc modification inhibits the calpain-mediated cleavage of α-synuclein', *Bioorganic & medicinal chemistry*, 25(18), pp. 4977–4982. Available at: https://doi.org/10.1016/J.BMC.2017.04.038.

Levine, P.M. *et al.* (2019) 'α-Synuclein O-GlcNAcylation alters aggregation and toxicity, revealing certain residues as potential inhibitors of Parkinson's disease', *Proceedings of the National Academy of Sciences of the United States of America*, 116(5), pp. 1511–1519. Available at: https://doi.org/10.1073/PNAS.1808845116.

Lewis, Y.E. *et al.* (2017) 'O-GlcNAcylation of α-Synuclein at Serine 87 Reduces Aggregation without Affecting Membrane Binding', *ACS chemical biology*, 12(4), pp. 1020–1027. Available at: https://doi.org/10.1021/ACSCHEMBIO.7B00113.

Li, B. *et al.* (2018) 'Cryo-EM of full-length α-synuclein reveals fibril polymorphs with a common structural kernel', *Nature Communications 2018 9:1*, 9(1), pp. 1–10. Available at: https://doi.org/10.1038/s41467-018-05971-2.

Li, J., Uversky, V.N. and Fink, A.L. (2001) 'Effect of familial Parkinson's disease point mutations A30P and A53T on the structural properties, aggregation, and fibrillation of

human α-synuclein', *Biochemistry*, 40(38), pp. 11604–11613. Available at: https://doi.org/10.1021/BI010616G/ASSET/IMAGES/LARGE/BI010616GF00010.JPEG.

Li, J.Y. *et al.* (2008) 'Lewy bodies in grafted neurons in subjects with Parkinson's disease suggest host-to-graft disease propagation', *Nature Medicine*, 14(5), pp. 501–503. Available at: https://doi.org/10.1038/nm1746.

Li, K. *et al.* (2015) 'LRRK2 A419V variant is a risk factor for Parkinson's disease in Asian population', *Neurobiology of aging*, 36(10), pp. 2908.e11-2908.e15. Available at: https://doi.org/10.1016/J.NEUROBIOLAGING.2015.07.012.

Li, W.W. *et al.* (2007) 'Localization of alpha-synuclein to mitochondria within midbrain of mice', *Neuroreport*, 18(15), pp. 1543–1546. Available at: https://doi.org/10.1097/WNR.0B013E3282F03DB4.

Li, Y. *et al.* (2008) 'HDAC6 is required for epidermal growth factor-induced beta-catenin nuclear localization', *The Journal of biological chemistry*, 283(19), pp. 12686–12690. Available at: https://doi.org/10.1074/JBC.C700185200.

Li, Y. *et al.* (2018) 'Amyloid fibril structure of α-synuclein determined by cryo-electron microscopy', *Cell Research 2018 28:9*, 28(9), pp. 897–903. Available at: https://doi.org/10.1038/s41422-018-0075-x.

Li, Y., Shin, D. and Kwon, S.H. (no date) *Histone deacetylase 6 plays a role as a distinct regulator of diverse cellular processes*. John Wiley & Sons, Ltd (10.1111).

Li, Z. yang *et al.* (2017) 'A novel HDAC6 inhibitor Tubastatin A: Controls HDAC6-p97/VCP-mediated ubiquitination-autophagy turnover and reverses Temozolomide-induced ER stress-tolerance in GBM cells', *Cancer Letters*, 391, pp. 89–99. Available at: https://doi.org/10.1016/J.CANLET.2017.01.025.

Liao, J. *et al.* (2014) 'Parkinson disease-associated mutation R1441H in LRRK2 prolongs the "active state" of its GTPase domain', *Proceedings of the National Academy of Sciences of the United States of America*, 111(11), pp. 4055–4060. Available at: https://doi.org/10.1073/PNAS.1323285111.

Lichtenberg, M. *et al.* (2011) ‘The Parkinson’s disease protein LRRK2 impairs proteasome substrate clearance without affecting proteasome catalytic activity’, *Cell Death & Disease 2011 2:8*, 2(8), pp. e196–e196. Available at: https://doi.org/10.1038/cddis.2011.81.

Lin, C.H. *et al.* (2010) ‘LRRK2 G2019S Mutation Induces Dendrite Degeneration through Mislocalization and Phosphorylation of Tau by Recruiting Autoactivated GSK3β’, *The Journal of Neuroscience*, 30(39), p. 13138. Available at: https://doi.org/10.1523/JNEUROSCI.1737-10.2010.

Lin, C.H. *et al.* (2020) ‘A dual inhibitor targeting HMG-CoA reductase and histone deacetylase mitigates neurite degeneration in LRRK2-G2019S parkinsonism’, *Aging (Albany NY)*, 12(24), p. 25581. Available at: https://doi.org/10.18632/AGING.104165.

Lin, X. *et al.* (2009) ‘Leucine-Rich Repeat Kinase 2 Regulates the Progression of Neuropathology Induced by Parkinson’s Disease-related Mutant α-synuclein’, *Neuron*, 64(6), p. 807. Available at: https://doi.org/10.1016/J.NEURON.2009.11.006.

Lindersson, E. *et al.* (2004) ‘Proteasomal inhibition by alpha-synuclein filaments and oligomers’, *The Journal of biological chemistry*, 279(13), pp. 12924–12934. Available at: https://doi.org/10.1074/JBC.M306390200.

Lindström, V. *et al.* (2017) ‘Extensive uptake of α-synuclein oligomers in astrocytes results in sustained intracellular deposits and mitochondrial damage’, *Molecular and Cellular Neuroscience*, 82, pp. 143–156. Available at: https://doi.org/10.1016/j.mcn.2017.04.009.

Liu, G. *et al.* (2009) ‘alpha-Synuclein is differentially expressed in mitochondria from different rat brain regions and dose-dependently down-regulates complex I activity’, *Neuroscience letters*, 454(3), pp. 187–192. Available at: https://doi.org/10.1016/J.NEULET.2009.02.056.

Liu, M. *et al.* (2018) ‘Trichloroethylene and Parkinson’s Disease: Risk Assessment’, *Molecular neurobiology*, 55(7), pp. 6201–6214. Available at: https://doi.org/10.1007/S12035-017-0830-X.

Liu, W. *et al.* (2017) ‘LRRK2 promotes the activation of NLRC4 inflammasome during

Salmonella Typhimurium infection', *The Journal of experimental medicine*, 214(10), pp. 3051–3066. Available at: https://doi.org/10.1084/JEM.20170014.

Liu, Y. *et al.* (2012) 'Modulation of histone deacetylase 6 (HDAC6) nuclear import and tubulin deacetylase activity through acetylation', *Journal of Biological Chemistry*, 287(34), pp. 29168–29174. Available at: https://doi.org/10.1074/jbc.M112.371120.

Loeb, V. *et al.* (2010) 'The transgenic overexpression of alpha-synuclein and not its related pathology associates with complex I inhibition', *The Journal of biological chemistry*, 285(10), pp. 7334–7343. Available at: https://doi.org/10.1074/JBC.M109.061051.

Logan, T. *et al.* (2017) 'α-Synuclein promotes dilation of the exocytotic fusion pore', *Nature Neuroscience*, 20(5), pp. 681–689. Available at: https://doi.org/10.1038/nn.4529.

Long, J. *et al.* (2008) 'Ubiquitin recognition by the ubiquitin-associated domain of p62 involves a novel conformational switch', *The Journal of biological chemistry*, 283(9), pp. 5427–5440. Available at: https://doi.org/10.1074/JBC.M704973200.

Longo, F. *et al.* (2017) 'Age-dependent dopamine transporter dysfunction and Serine129 phospho-α-synuclein overload in G2019S LRRK2 mice', *Acta Neuropathologica Communications*, 5, p. 22. Available at: https://doi.org/10.1186/s40478-017-0426-8.

Lopresti, P. (2020) 'HDAC6 in Diseases of Cognition and of Neurons', *Cells*, 10(1), pp. 1–15. Available at: https://doi.org/10.3390/CELLS10010012.

Loria, F. *et al.* (2017) 'α-Synuclein transfer between neurons and astrocytes indicates that astrocytes play a role in degradation rather than in spreading', *Acta Neuropathologica*, 134(5), pp. 789–808. Available at: https://doi.org/10.1007/s00401-017-1746-2.

Losson, H. *et al.* (2020) 'HDAC6—An Emerging Target Against Chronic Myeloid Leukemia?', *Cancers*, 12(2). Available at: https://doi.org/10.3390/CANCERS12020318.

Lu, L. *et al.* (2013) ‘Voltage-dependent anion channel involved in the α-synuclein-induced dopaminergic neuron toxicity in rats’, *Acta biochimica et biophysica Sinica*, 45(3), pp. 170–178. Available at: https://doi.org/10.1093/ABBS/GMS114.

Lucas, R.M. *et al.* (2019) ‘LRRK2-mediated phosphorylation of HDAC6 regulates HDAC6-cytoplasmic dynein interaction and aggresome formation.’, *bioRxiv*, (April), p. 554881. Available at: https://doi.org/10.1101/554881.

Luk, K.C. *et al.* (2009) ‘Exogenous alpha-synuclein fibrils seed the formation of Lewy body-like intracellular inclusions in cultured cells’, *Proceedings of the National Academy of Sciences of the United States of America*, 106(47), pp. 20051–20056. Available at: https://doi.org/10.1073/PNAS.0908005106.

Luk, K.C. *et al.* (2012) ‘Pathological α-Synuclein Transmission Initiates Parkinson-like Neurodegeneration in Non-transgenic Mice’, *Science (New York, N.Y.)*, 338(6109), p. 949. Available at: https://doi.org/10.1126/SCIENCE.1227157.

Lundblad, M. *et al.* (2012) ‘Impaired neurotransmission caused by overexpression of α-synuclein in nigral dopamine neurons’, *Proceedings of the National Academy of Sciences of the United States of America*, 109(9), p. 3213. Available at: https://doi.org/10.1073/PNAS.1200575109.

Luth, E.S. *et al.* (2014) ‘Soluble, Prefibrillar α-Synuclein Oligomers Promote Complex I-dependent, Ca2+-induced Mitochondrial Dysfunction’, *The Journal of Biological Chemistry*, 289(31), p. 21490. Available at: https://doi.org/10.1074/JBC.M113.545749.

Ma, K.L., Song, L.K., Yuan, Y.H., Zhang, Y., Han, N., *et al.* (2014) ‘The nuclear accumulation of alpha-synuclein is mediated by importin alpha and promotes neurotoxicity by accelerating the cell cycle’, *Neuropharmacology*, 82, pp. 132–142. Available at: https://doi.org/10.1016/J.NEUROPHARM.2013.07.035.

Ma, K.L., Song, L.K., Yuan, Y.H., Zhang, Y., Yang, J.L., *et al.* (2014) ‘α-synuclein is prone to interaction with the GC-box-like sequence in vitro’, *Cellular and Molecular Neurobiology*, 34(4), pp. 603–609. Available at: https://doi.org/10.1007/S10571-014-0046-9/FIGURES/3.

Machiya, Y. *et al.* (2010) ‘Phosphorylated alpha-synuclein at Ser-129 is targeted to the proteasome pathway in a ubiquitin-independent manner’, *The Journal of biological chemistry*, 285(52), pp. 40732–40744. Available at: https://doi.org/10.1074/JBC.M110.141952.

Macisaac, S. *et al.* (2020) ‘Neuron-autonomous susceptibility to induced synuclein aggregation is exacerbated by endogenous Lrrk2 mutations and ameliorated by Lrrk2 genetic knock-out’, *Brain communications*, 2(1). Available at: https://doi.org/10.1093/BRAINCOMMS/FCZ052.

MacLeod, D.A. *et al.* (2013) ‘RAB7L1 interacts with LRRK2 to modify intraneuronal protein sorting and Parkinson’s disease risk’, *Neuron*, 77(3), pp. 425–439. Available at: https://doi.org/10.1016/J.NEURON.2012.11.033.

Madureira, M., Connor-Robson, N. and Wade-Martins, R. (2020) ‘“LRRK2: Autophagy and Lysosomal Activity”’, *Frontiers in Neuroscience*, 14. Available at: https://doi.org/10.3389/FNINS.2020.00498.

Magupalli, V.G. *et al.* (2020) ‘HDAC6 mediates an aggresome-like mechanism for NLRP3 and pyrin inflammasome activation’, *Science (New York, N.Y.)*, 369(6510). Available at: https://doi.org/10.1126/SCIENCE.AAS8995.

Mahul-Mellier, A.L. *et al.* (2014) ‘c-Abl phosphorylates α-synuclein and regulates its degradation: implication for α-synuclein clearance and contribution to the pathogenesis of Parkinson’s disease’, *Human molecular genetics*, 23(11), pp. 2858–2879. Available at: https://doi.org/10.1093/HMG/DDT674.

Mahul-Mellier, A.L. *et al.* (2020) ‘The process of Lewy body formation, rather than simply α-synuclein fibrillization, is one of the major drivers of neurodegeneration’, *Proceedings of the National Academy of Sciences of the United States of America*, 117(9), pp. 4971–4982. Available at: https://doi.org/10.1073/PNAS.1913904117/SUPPL_FILE/PNAS.1913904117.SD04.XLSX.

Di Maio, R. *et al.* (2016) ‘α-Synuclein binds TOM20 and inhibits mitochondrial protein import in Parkinson’s disease’, *Science translational medicine*, 8(342), p. 342ra78.

Available at: https://doi.org/10.1126/SCITRANSLMED.AAF3634.

Di Maio, R. *et al.* (2018) 'LRRK2 activation in idiopathic Parkinson's disease', *Science translational medicine*, 10(451). Available at: https://doi.org/10.1126/SCITRANSLMED.AAR5429.

Manca, S. *et al.* (2019) 'The Role of Alcohol-induced Golgi Fragmentation for Androgen Receptor Signaling in Prostate Cancer', *Molecular cancer research : MCR*, 17(1), p. 225. Available at: https://doi.org/10.1158/1541-7786.MCR-18-0577.

Mandel, N. and Agarwal, N. (2022) 'Role of SUMOylation in Neurodegenerative Diseases', *Cells*, 11(21). Available at: https://doi.org/10.3390/CELLS11213395.

Manning-Bog, A.B. *et al.* (2002) 'The Herbicide Paraquat Causes Up-regulation and Aggregation of α-Synuclein in Mice: PARAQUAT AND α-SYNUCLEIN', *Journal of Biological Chemistry*, 277(3), pp. 1641–1644. Available at: https://doi.org/10.1074/JBC.C100560200.

Manzoni, C. *et al.* (2016) 'MTOR independent regulation of macroautophagy by Leucine Rich Repeat Kinase 2 via Beclin-1', *Scientific Reports*, 6. Available at: https://doi.org/10.1038/srep35106.

Maraganore, D.M. *et al.* (2006) 'Collaborative Analysis of α-Synuclein Gene Promoter Variability and Parkinson Disease', *JAMA*, 296(6), pp. 661–670. Available at: https://doi.org/10.1001/JAMA.296.6.661.

Marchand, A. *et al.* (2020) 'LRRK2 Phosphorylation, More Than an Epiphenomenon', *Frontiers in Neuroscience*, 14, p. 527. Available at: https://doi.org/10.3389/FNINS.2020.00527/BIBTEX.

Marder, K. *et al.* (2015) 'Age-specific penetrance of LRRK2 G2019S in the Michael J. Fox Ashkenazi Jewish LRRK2 Consortium', *Neurology*, 85(1), pp. 89–95. Available at: https://doi.org/10.1212/WNL.0000000000001708.

Marín, I. (2008) 'Ancient origin of the parkinson disease gene LRRK2', *Journal of Molecular Evolution*, 67(1), pp. 41–50. Available at: https://doi.org/10.1007/s00239-008-9122-4.

Marotta, N.P. *et al.* (2015) ‘O-GlcNAc modification blocks the aggregation and toxicity of the protein α-synuclein associated with Parkinson’s disease’, *Nature chemistry*, 7(11), pp. 913–920. Available at: https://doi.org/10.1038/NCHEM.2361.

Martinez-Fonts, K. *et al.* (2020) ‘The proteasome 19S cap and its ubiquitin receptors provide a versatile recognition platform for substrates’, *Nature Communications 2020 11:1*, 11(1), pp. 1–16. Available at: https://doi.org/10.1038/s41467-019-13906-8.

Martinez-Vicente, M. *et al.* (2008a) ‘Dopamine-modified alpha-synuclein blocks chaperone-mediated autophagy’, *The Journal of clinical investigation*, 118(2), pp. 777–778. Available at: https://doi.org/10.1172/JCI32806.

Martinez-Vicente, M. *et al.* (2008b) ‘Dopamine-modified α-synuclein blocks chaperone-mediated autophagy’, *The Journal of Clinical Investigation*, 118(2), p. 777. Available at: https://doi.org/10.1172/JCI32806.

Martinon, F., Burns, K. and Tschopp, J. (2002) ‘The Inflammasome: A Molecular Platform Triggering Activation of Inflammatory Caspases and Processing of proIL-β’, *Molecular Cell*, 10(2), pp. 417–426. Available at: https://doi.org/10.1016/S1097-2765(02)00599-3.

Mata, I.F. *et al.* (2016) ‘The discovery of LRRK2 p.R1441S, a novel mutation for Parkinson’s disease, adds to the complexity of a mutational hotspot’, *American journal of medical genetics. Part B, Neuropsychiatric genetics : the official publication of the International Society of Psychiatric Genetics*, 171(7), pp. 925–930. Available at: https://doi.org/10.1002/AJMG.B.32452.

Matsuda, W. *et al.* (2009) ‘Single nigrostriatal dopaminergic neurons form widely spread and highly dense axonal arborizations in the neostriatum’, *The Journal of neuroscience : the official journal of the Society for Neuroscience*, 29(2), pp. 444–453. Available at: https://doi.org/10.1523/JNEUROSCI.4029-08.2009.

Matsumoto, G. *et al.* (2018) ‘N-Acyldopamine induces aggresome formation without proteasome inhibition and enhances protein aggregation via p62/SQSTM1 expression’, *Scientific reports*, 8(1). Available at: https://doi.org/10.1038/S41598-018-27872-6.

Matta, S. *et al.* (2012) ‘LRRK2 controls an EndoA phosphorylation cycle in synaptic endocytosis’, *Neuron*, 75(6), pp. 1008–1021. Available at: https://doi.org/10.1016/J.NEURON.2012.08.022.

Mayer, R.J. *et al.* (1989) ‘Intermediate filament-ubiquitin diseases: Implications for cell sanitization’, *Biochemical Society Symposia*, 55, pp. 193–201.

Mazzetti, S. *et al.* (2020) ‘Phospho-HDAC6 Gathers Into Protein Aggregates in Parkinson’s Disease and Atypical Parkinsonisms’, *Frontiers in Neuroscience*, 14, p. 624. Available at: https://doi.org/10.3389/fnins.2020.00624.

Mazzocchi, M. *et al.* (2020) ‘The class II histone deacetylases as therapeutic targets for Parkinson’s disease’, *Neuronal signaling*, 4(2), pp. 1–9. Available at: https://doi.org/10.1042/NS20200001.

McFarland, N.R. *et al.* (2014) ‘Chronic treatment with novel small molecule Hsp90 inhibitors rescues striatal dopamine levels but not α-synuclein-induced neuronal cell loss’, *PloS one*, 9(1). Available at: https://doi.org/10.1371/JOURNAL.PONE.0086048.

McFarthing, K. *et al.* (2022) ‘Parkinson’s Disease Drug Therapies in the Clinical Trial Pipeline: 2022 Update’, *Journal of Parkinson’s disease*, 12(4), pp. 1073–1082. Available at: https://doi.org/10.3233/JPD-229002.

McGregor, M.M. and Nelson, A.B. (2019) ‘Circuit Mechanisms of Parkinson’s Disease’, *Neuron*, 101(6), pp. 1042–1056. Available at: https://doi.org/10.1016/J.NEURON.2019.03.004.

McNaught, K.S.P. *et al.* (2002) ‘Aggresome-related biogenesis of Lewy bodies’, *The European journal of neuroscience*, 16(11), pp. 2136–2148. Available at: https://doi.org/10.1046/J.1460-9568.2002.02301.X.

Mehra, S., Sahay, S. and Maji, S.K. (2019) ‘α-Synuclein misfolding and aggregation: Implications in Parkinson’s disease pathogenesis’, *Biochimica et biophysica acta. Proteins and proteomics*, 1867(10), pp. 890–908. Available at: https://doi.org/10.1016/J.BBAPAP.2019.03.001.

Miki, Y. *et al.* (2011) ‘Accumulation of histone deacetylase 6, an aggresome-related protein, is specific to Lewy bodies and glial cytoplasmic inclusions’, *Neuropathology*, 31(6), pp. 561–568. Available at: https://doi.org/10.1111/j.1440-1789.2011.01200.x.

Milber, J.M. *et al.* (2012) ‘Lewy pathology is not the first sign of degeneration in vulnerable neurons in Parkinson disease’, *Neurology*, 79(24), pp. 2307–2314. Available at: https://doi.org/10.1212/WNL.0B013E318278FE32.

Miller, G.K. *et al.* (2023) ‘Effects of LRRK2 Inhibitors in Nonhuman Primates’, *Toxicologic pathology*, 51(5). Available at: https://doi.org/10.1177/01926233231205895.

Mir, R. *et al.* (2018) ‘The Parkinson’s disease VPS35[D620N] mutation enhances LRRK2-mediated Rab protein phosphorylation in mouse and human’, *The Biochemical journal*, 475(11), pp. 1861–1883. Available at: https://doi.org/10.1042/BCJ20180248.

Mirecka, Ewa A *et al.* (2014) ‘Sequestration of a β-Hairpin for Control of α-Synuclein Aggregation’, *Angewandte Chemie International Edition*, 53(16), pp. 4227–4230. Available at: https://doi.org/10.1002/ANIE.201309001.

Mitchell, E. *et al.* (2022) ‘Alcohol and Parkinson’s Disease: A Systematic Review and Meta-Analysis’, *Journal of Parkinson’s disease*, 12(8), pp. 2369–2381. Available at: https://doi.org/10.3233/JPD-223522.

Mo, Z. *et al.* (2018) ‘Aberrant GlyRS-HDAC6 interaction linked to axonal transport deficits in Charcot-Marie-Tooth neuropathy’, *Nature communications*, 9(1). Available at: https://doi.org/10.1038/S41467-018-03461-Z.

Moors, T.E. *et al.* (2021) ‘The subcellular arrangement of alpha-synuclein proteoforms in the Parkinson’s disease brain as revealed by multicolor STED microscopy’, 142, pp. 423–448. Available at: https://doi.org/10.1007/s00401-021-02329-9.

Morrow, C.S. *et al.* (2020) ‘Vimentin Coordinates Protein Turnover at the Aggresome during Neural Stem Cell Quiescence Exit’, *Cell stem cell*, 26(4), pp. 558-568.e9. Available at: https://doi.org/10.1016/J.STEM.2020.01.018.

Muda, K. *et al.* (2014) ‘Parkinson-related LRRK2 mutation R1441C/G/H impairs PKA phosphorylation of LRRK2 and disrupts its interaction with 14-3-3’, *Proceedings of the National Academy of Sciences of the United States of America*, 111(1). Available at: https://doi.org/10.1073/PNAS.1312701111.

Muqit, M.M.K. *et al.* (2004) ‘Parkin is recruited into aggresomes in a stress-specific manner: over-expression of parkin reduces aggresome formation but can be dissociated from parkin’s effect on neuronal survival’. Available at: https://doi.org/10.1093/hmg/ddh012.

Murphy, D.D. *et al.* (2000) ‘Synucleins are developmentally expressed, and alpha-synuclein regulates the size of the presynaptic vesicular pool in primary hippocampal neurons’, *The Journal of neuroscience : the official journal of the Society for Neuroscience*, 20(9), pp. 3214–3220. Available at: https://doi.org/10.1523/JNEUROSCI.20-09-03214.2000.

Murphy, K.E. *et al.* (2014) ‘Reduced glucocerebrosidase is associated with increased α-synuclein in sporadic Parkinson’s disease’, *Brain : a journal of neurology*, 137(Pt 3), pp. 834–848. Available at: https://doi.org/10.1093/BRAIN/AWT367.

Na, C.H. *et al.* (2012) ‘Synaptic protein ubiquitination in rat brain revealed by antibody-based ubiquitome analysis’, *Journal of proteome research*, 11(9), pp. 4722–4732. Available at: https://doi.org/10.1021/PR300536K.

Nagai-Ito, Y. *et al.* (2022) ‘The atypical Rab GTPase associated with Parkinson’s disease, Rab29, is localized to membranes’, *Journal of Biological Chemistry*, 0(0), p. 102499. Available at: https://doi.org/10.1016/J.JBC.2022.102499.

Nakamura, K. *et al.* (2008) ‘Optical reporters for the conformation of alpha-synuclein reveal a specific interaction with mitochondria’, *The Journal of neuroscience : the official journal of the Society for Neuroscience*, 28(47), pp. 12305–12317. Available at: https://doi.org/10.1523/JNEUROSCI.3088-08.2008.

Nakamura, K. *et al.* (2011) ‘Direct Membrane Association Drives Mitochondrial Fission by the Parkinson Disease-associated Protein α-Synuclein’, *Journal of Biological Chemistry*, 286(23), pp. 20710–20726. Available at:

https://doi.org/10.1074/JBC.M110.213538.

Nalls, M.A. *et al.* (2019) ‘Identification of novel risk loci, causal insights, and heritable risk for Parkinson’s disease: a meta-analysis of genome-wide association studies’, *The Lancet Neurology*, 18(12), pp. 1091–1102. Available at: https://doi.org/10.1016/S1474-4422(19)30320-5.

Narayanan, A. *et al.* (2019) ‘A first order phase transition mechanism underlies protein aggregation in mammalian cells’, *eLife*, 8. Available at: https://doi.org/10.7554/eLife.39695.

Naren, P. *et al.* (2023) ‘Microtubule acetylation dyshomeostasis in Parkinson’s disease’, *Translational Neurodegeneration*, 12(1). Available at: https://doi.org/10.1186/S40035-023-00354-0.

Negro, A. *et al.* (2002) ‘Multiple phosphorylation of alpha-synuclein by protein tyrosine kinase Syk prevents eosin-induced aggregation’, *FASEB journal : official publication of the Federation of American Societies for Experimental Biology*, 16(2), pp. 210–212. Available at: https://doi.org/10.1096/FJ.01-0517FJE.

Neves, M. *et al.* (2022) ‘Modulation of signaling pathways by DJ-1: An updated overview’, *Redox biology*, 51. Available at: https://doi.org/10.1016/J.REDOX.2022.102283.

Nguyen, M. and Krainc, D. (2018) ‘LRRK2 phosphorylation of auxilin mediates synaptic defects in dopaminergic neurons from patients with Parkinson’s disease’, *Proceedings of the National Academy of Sciences of the United States of America*, 115(21), pp. 5576–5581. Available at: https://doi.org/10.1073/PNAS.1717590115/-/DCSUPPLEMENTAL.

Nuber, S. *et al.* (2018) ‘Abrogating Native α-Synuclein Tetramers in Mice Causes a L-DOPA-Responsive Motor Syndrome Closely Resembling Parkinson’s Disease’, *Neuron*, 100(1), pp. 75-90.e5. Available at: https://doi.org/10.1016/J.NEURON.2018.09.014.

O’Hara, D.M. *et al.* (2020) ‘LRRK2 and α-Synuclein: Distinct or Synergistic Players in Parkinson’s Disease?’, *Frontiers in Neuroscience*, 14, p. 577. Available at:

https://doi.org/10.3389/FNINS.2020.00577/BIBTEX.

Obergasteiger, J. *et al.* (2020) ‘Kinase inhibition of G2019S-LRRK2 enhances autolysosome formation and function to reduce endogenous alpha-synuclein intracellular inclusions’, *Cell death discovery*, 6(1). Available at: https://doi.org/10.1038/S41420-020-0279-Y.

Oh, Y. *et al.* (2011) ‘Human Polycomb protein 2 promotes α-synuclein aggregate formation through covalent SUMOylation’, *Brain research*, 1381, pp. 78–89. Available at: https://doi.org/10.1016/J.BRAINRES.2011.01.039.

Öhrfelt, A. *et al.* (2011) ‘Identification of novel α-synuclein isoforms in human brain tissue by using an online nanoLC-ESI-FTICR-MS method’, *Neurochemical research*, 36(11), pp. 2029–2042. Available at: https://doi.org/10.1007/S11064-011-0527-X.

Okochi, M. *et al.* (2000) ‘Constitutive phosphorylation of the Parkinson’s disease associated alpha-synuclein’, *The Journal of biological chemistry*, 275(1), pp. 390–397. Available at: https://doi.org/10.1074/JBC.275.1.390.

Olanow, C.W. *et al.* (2004) ‘Lewy-body formation is an aggresome-related process: A hypothesis’, *Lancet Neurology*, 3(8), pp. 496–503. Available at: https://doi.org/10.1016/S1474-4422(04)00827-0.

Olzmann, J.A. *et al.* (2007) ‘Parkin-mediated K63-linked polyubiquitination targets misfolded DJ-1 to aggresomes via binding to HDAC6’, *The Journal of cell biology*, 178(6), pp. 1025–1038. Available at: https://doi.org/10.1083/JCB.200611128.

Onishi, M. *et al.* (2021) ‘Molecular mechanisms and physiological functions of mitophagy’, *The EMBO journal*, 40(3). Available at: https://doi.org/10.15252/EMBJ.2020104705.

Opazo, F. *et al.* (2008) ‘Accumulation and clearance of alpha-synuclein aggregates demonstrated by time-lapse imaging’, *Journal of neurochemistry*, 106(2), pp. 529–540. Available at: https://doi.org/10.1111/J.1471-4159.2008.05407.X.

Ordonez, D.G., Lee, M.K. and Feany, M.B. (2018) ‘α-synuclein Induces Mitochondrial Dysfunction through Spectrin and the Actin Cytoskeleton’, *Neuron*,

97(1), pp. 108-124.e6. Available at: https://doi.org/10.1016/J.NEURON.2017.11.036.

Orenstein, S.J. *et al.* (2013) 'Interplay of LRRK2 with chaperone-mediated autophagy', *Nature Neuroscience*, 16(4), pp. 394–406. Available at: https://doi.org/10.1038/nn.3350.

Osterberg, V.R. *et al.* (2015) 'Progressive aggregation of alpha-synuclein and selective degeneration of Lewy inclusion-bearing neurons in a mouse model of parkinsonism', *Cell reports*, 10(8), p. 1252. Available at: https://doi.org/10.1016/J.CELREP.2015.01.060.

Oueslati, A. *et al.* (2012) 'Mimicking phosphorylation at serine 87 inhibits the aggregation of human α-synuclein and protects against its toxicity in a rat model of Parkinson's disease', *The Journal of neuroscience : the official journal of the Society for Neuroscience*, 32(5), pp. 1536–1544. Available at: https://doi.org/10.1523/JNEUROSCI.3784-11.2012.

Oueslati, A. *et al.* (2013) 'Polo-like kinase 2 regulates selective autophagic α-synuclein clearance and suppresses its toxicity in vivo', *Proceedings of the National Academy of Sciences of the United States of America*, 110(41). Available at: https://doi.org/10.1073/PNAS.1309991110.

Oun, A. *et al.* (2023) 'Characterization of Lipopolysaccharide Effects on LRRK2 Signaling in RAW Macrophages', *International journal of molecular sciences*, 24(2). Available at: https://doi.org/10.3390/IJMS24021644.

Ouyang, H. *et al.* (2012) 'Protein aggregates are recruited to aggresome by histone deacetylase 6 via unanchored ubiquitin C termini', *The Journal of biological chemistry*, 287(4), pp. 2317–2327. Available at: https://doi.org/10.1074/JBC.M111.273730.

Øverbye, A., Fengsrud, M. and Seglen, P.O. (2007) 'Proteomic analysis of membrane-associated proteins from rat liver autophagosomes', *Autophagy*, 3(4), pp. 300–322. Available at: https://doi.org/10.4161/auto.3910.

Paciotti, S. *et al.* (2018) 'Are We Ready for Detecting α-Synuclein Prone to Aggregation in Patients? The Case of "Protein-Misfolding Cyclic Amplification" and

"Real-Time Quaking-Induced Conversion" as Diagnostic Tools', *Frontiers in neurology*, 9(JUN). Available at: https://doi.org/10.3389/FNEUR.2018.00415.

Paisán-Ruíz, C. *et al.* (2004) 'Cloning of the gene containing mutations that cause PARK8-linked Parkinson's disease', *Neuron*, 44(4), pp. 595–600. Available at: https://doi.org/10.1016/j.neuron.2004.10.023.

Pajarillo, E. *et al.* (2023) 'The role of microglial LRRK2 kinase in manganese-induced inflammatory neurotoxicity via NLRP3 inflammasome and RAB10-mediated autophagy dysfunction', *The Journal of Biological Chemistry*, 299(7). Available at: https://doi.org/10.1016/J.JBC.2023.104879.

Paleologou, K.E. *et al.* (2008) 'Phosphorylation at Ser-129 but not the phosphomimics S129E/D inhibits the fibrillation of alpha-synuclein', *The Journal of biological chemistry*, 283(24), pp. 16895–16905. Available at: https://doi.org/10.1074/JBC.M800747200.

Paleologou, K.E. *et al.* (2010) 'Phosphorylation at S87 is enhanced in synucleinopathies, inhibits alpha-synuclein oligomerization, and influences synuclein-membrane interactions', *The Journal of neuroscience : the official journal of the Society for Neuroscience*, 30(9), pp. 3184–3198. Available at: https://doi.org/10.1523/JNEUROSCI.5922-09.2010.

Pan, P.Y. *et al.* (2017) 'Parkinson's Disease-Associated LRRK2 Hyperactive Kinase Mutant Disrupts Synaptic Vesicle Trafficking in Ventral Midbrain Neurons', *The Journal of neuroscience : the official journal of the Society for Neuroscience*, 37(47), pp. 11366–11376. Available at: https://doi.org/10.1523/JNEUROSCI.0964-17.2017.

Pang, S.Y.Y. *et al.* (2022) 'LRRK2, GBA and their interaction in the regulation of autophagy: implications on therapeutics in Parkinson's disease', *Translational neurodegeneration*, 11(1). Available at: https://doi.org/10.1186/S40035-022-00281-6.

Parkkinen, L., Hartikainen, P. and Alafuzoff, I. (2007) 'Abundant glial alpha-synuclein pathology in a case without overt clinical symptoms', *Clinical neuropathology*, 26(6), pp. 276–283. Available at: https://doi.org/10.5414/NPP26276.

Parmigiani, R.B. *et al.* (2008) 'HDAC6 is a specific deacetylase of peroxiredoxins

and is involved in redox regulation', *Proceedings of the National Academy of Sciences of the United States of America*, 105(28), p. 9633. Available at: https://doi.org/10.1073/PNAS.0803749105.

Pasanen, P. *et al.* (2014) 'Novel α-synuclein mutation A53E associated with atypical multiple system atrophy and Parkinson's disease-type pathology', *Neurobiology of aging*, 35(9), pp. 2180.e1-2180.e5. Available at: https://doi.org/10.1016/J.NEUROBIOLAGING.2014.03.024.

Patrick, K.L. *et al.* (2019) 'Exploring the "Multiple-Hit Hypothesis" of Neurodegenerative Disease: Bacterial Infection Comes Up to Bat', *Frontiers in cellular and infection microbiology*, 9(MAY). Available at: https://doi.org/10.3389/FCIMB.2019.00138.

Paxinou, E. *et al.* (2001) 'Induction of alpha-synuclein aggregation by intracellular nitrative insult', *The Journal of neuroscience : the official journal of the Society for Neuroscience*, 21(20), pp. 8053–8061. Available at: https://doi.org/10.1523/JNEUROSCI.21-20-08053.2001.

Peng, B. *et al.* (2020) 'Role of Alcohol Drinking in Alzheimer's Disease, Parkinson's Disease, and Amyotrophic Lateral Sclerosis', *International journal of molecular sciences*, 21(7). Available at: https://doi.org/10.3390/IJMS21072316.

Peng, C. *et al.* (2018) 'Cellular milieu imparts distinct pathological α-synuclein strains in α-synucleinopathies', *Nature*, 557(7706), pp. 558–563. Available at: https://doi.org/10.1038/S41586-018-0104-4.

Pérez-Carrión, M.D. *et al.* (2022) 'LRRK2 and Proteostasis in Parkinson's Disease', *International journal of molecular sciences*, 23(12). Available at: https://doi.org/10.3390/IJMS23126808.

Perez Carrion, M. *et al.* (2018) 'The LRRK2 Variant E193K Prevents Mitochondrial Fission Upon MPP+ Treatment by Altering LRRK2 Binding to DRP1', *Frontiers in molecular neuroscience*, 11. Available at: https://doi.org/10.3389/FNMOL.2018.00064.

Pernet, L. *et al.* (2014) 'HDAC6–ubiquitin interaction controls the duration of HSF1

activation after heat shock', *Molecular Biology of the Cell*, 25(25), p. 4187. Available at: https://doi.org/10.1091/MBC.E14-06-1032.

Perry, G. *et al.* (2008) 'Leucine-rich repeat kinase 2 colocalizes with alpha-synuclein in Parkinson's disease, but not tau-containing deposits in tauopathies', *Neuro-degenerative diseases*, 5(3–4), pp. 222–224. Available at: https://doi.org/10.1159/000113708.

Petroi, D. *et al.* (2012) 'Aggregate clearance of α-synuclein in Saccharomyces cerevisiae depends more on autophagosome and vacuole function than on the proteasome', *Journal of Biological Chemistry*, 287(33), pp. 27567–27579. Available at: https://doi.org/10.1074/jbc.M112.361865.

Piccoli, G. *et al.* (2011) 'LRRK2 controls synaptic vesicle storage and mobilization within the recycling pool', *The Journal of neuroscience : the official journal of the Society for Neuroscience*, 31(6), pp. 2225–2237. Available at: https://doi.org/10.1523/JNEUROSCI.3730-10.2011.

Pinho, B.R. *et al.* (2016) 'Pharmacological modulation of HDAC1 and HDAC6 in vivo in a zebrafish model: Therapeutic implications for Parkinson's disease', *Pharmacological research*, 103, pp. 328–339. Available at: https://doi.org/10.1016/J.PHRS.2015.11.024.

Pinho, R. *et al.* (2019) 'Nuclear localization and phosphorylation modulate pathological effects of alpha-synuclein', *Human Molecular Genetics*, 28(1), pp. 31–50. Available at: https://doi.org/10.1093/HMG/DDY326.

Pissadaki, E.K. and Bolam, J.P. (2013) 'The energy cost of action potential propagation in dopamine neurons: clues to susceptibility in Parkinson's disease', *Frontiers in computational neuroscience*, 7(FEB). Available at: https://doi.org/10.3389/FNCOM.2013.00013.

Plotegher, N., Gratton, E. and Bubacco, L. (2014) 'Number and Brightness analysis of alpha-synuclein oligomerization and the associated mitochondrial morphology alterations in live cells', *Biochimica et biophysica acta*, 1840(6), pp. 2014–2024. Available at: https://doi.org/10.1016/J.BBAGEN.2014.02.013.

Polymeropoulos, M.H. *et al.* (1997) ‘Mutation in the α-synuclein gene identified in families with Parkinson’s disease’, *Science*, 276(5321), pp. 2045–2047. Available at: https://doi.org/10.1126/science.276.5321.2045.

Portran, D. *et al.* (2017) ‘Tubulin acetylation protects long-lived microtubules against mechanical ageing’, *Nature cell biology*, 19(4), pp. 391–398. Available at: https://doi.org/10.1038/NCB3481.

Pronin, A.N. *et al.* (2000) ‘Synucleins are a novel class of substrates for G protein-coupled receptor kinases’, *The Journal of biological chemistry*, 275(34), pp. 26515–26522. Available at: https://doi.org/10.1074/JBC.M003542200.

Prudencio, M. *et al.* (2021) ‘Serum neurofilament light protein correlates with unfavorable clinical outcomes in hospitalized patients with COVID-19’, *Science translational medicine*, 13(602). Available at: https://doi.org/10.1126/SCITRANSLMED.ABI7643.

Prusiner, S.B. (2001) ‘Shattuck lecture--neurodegenerative diseases and prions’, *The New England journal of medicine*, 344(20), pp. 1516–1526. Available at: https://doi.org/10.1056/NEJM200105173442006.

Puccini, J.M. *et al.* (2015) ‘Leucine-rich repeat kinase 2 modulates neuroinflammation and neurotoxicity in models of human immunodeficiency virus 1-associated neurocognitive disorders’, *The Journal of neuroscience : the official journal of the Society for Neuroscience*, 35(13), pp. 5271–5283. Available at: https://doi.org/10.1523/JNEUROSCI.0650-14.2015.

Pugacheva, E.N. *et al.* (2007) ‘HEF1-dependent Aurora A activation induces disassembly of the primary cilium’, *Cell*, 129(7), p. 1351. Available at: https://doi.org/10.1016/J.CELL.2007.04.035.

Purlyte, E. *et al.* (2018) ‘Rab29 activation of the Parkinson’s disease-associated LRRK2 kinase’, *The EMBO journal*, 37(1), pp. 1–18. Available at: https://doi.org/10.15252/EMBJ.201798099.

Putcha, P. *et al.* (2010) ‘Brain-permeable small-molecule inhibitors of Hsp90 prevent alpha-synuclein oligomer formation and rescue alpha-synuclein-induced toxicity’,

The Journal of pharmacology and experimental therapeutics, 332(3), pp. 849–857. Available at: https://doi.org/10.1124/JPET.109.158436.

Qing, H., Zhang, Y., *et al.* (2009a) 'Lrrk2 interaction with alpha-synuclein in diffuse Lewy body disease', *Biochemical and biophysical research communications*, 390(4), pp. 1229–1234. Available at: https://doi.org/10.1016/J.BBRC.2009.10.126.

Qing, H., Zhang, Y., *et al.* (2009b) 'Lrrk2 interaction with α-synuclein in diffuse Lewy body disease', *Biochemical and Biophysical Research Communications*, 390(4), pp. 1229–1234. Available at: https://doi.org/10.1016/J.BBRC.2009.10.126.

Qing, H., Wong, W., *et al.* (2009) 'Lrrk2 phosphorylates alpha synuclein at serine 129: Parkinson disease implications', *Biochemical and biophysical research communications*, 387(1), pp. 149–152. Available at: https://doi.org/10.1016/J.BBRC.2009.06.142.

Ramírez, M.B. *et al.* (2017) 'GTP binding regulates cellular localization of Parkinson's disease-associated LRRK2', *Human molecular genetics*, 26(14), pp. 2747–2767. Available at: https://doi.org/10.1093/HMG/DDX161.

Ravikumar, B., Duden, R. and Rubinsztein, D.C. (2002) 'Aggregate-prone proteins with polyglutamine and polyalanine expansions are degraded by autophagy', *Human Molecular Genetics*, 11(9), pp. 1107–1117. Available at: https://doi.org/10.1093/HMG/11.9.1107.

Reed, N.A. *et al.* (2006) 'Microtubule acetylation promotes kinesin-1 binding and transport', *Current biology : CB*, 16(21), pp. 2166–2172. Available at: https://doi.org/10.1016/J.CUB.2006.09.014.

Reimer, L. *et al.* (2018) 'Inflammation kinase PKR phosphorylates α-synuclein and causes α-synuclein-dependent cell death', *Neurobiology of disease*, 115, pp. 17–28. Available at: https://doi.org/10.1016/J.NBD.2018.03.001.

Reith, A.D. *et al.* (2012) 'GSK2578215A; A potent and highly selective 2-arylmethyloxy-5-substitutent-N-arylbenzamide LRRK2 kinase inhibitor', *Bioorganic & medicinal chemistry letters*, 22(17), p. 5625. Available at: https://doi.org/10.1016/J.BMCL.2012.06.104.

Ren, X. and Chen, J.F. (2020) ‘Caffeine and Parkinson’s Disease: Multiple Benefits and Emerging Mechanisms’, *Frontiers in neuroscience*, 14. Available at: https://doi.org/10.3389/FNINS.2020.602697.

Rey, N.L. *et al.* (2016) ‘Widespread transneuronal propagation of α-synucleinopathy triggered in olfactory bulb mimics prodromal Parkinson’s disease’, *The Journal of Experimental Medicine*, 213(9), p. 1759. Available at: https://doi.org/10.1084/JEM.20160368.

Reyes, J.F. *et al.* (2014) ‘Alpha-synuclein transfers from neurons to oligodendrocytes’, *Glia*, 62(3), pp. 387–398. Available at: https://doi.org/10.1002/GLIA.22611.

Reyes, J.F. *et al.* (2019) ‘Binding of α-synuclein oligomers to Cx32 facilitates protein uptake and transfer in neurons and oligodendrocytes’, *Acta Neuropathologica*, 138(1), pp. 23–47. Available at: https://doi.org/10.1007/S00401-019-02007-X/FIGURES/7.

Reynolds, N.P. *et al.* (2011) ‘Mechanism of membrane interaction and disruption by α-synuclein’, *Journal of the American Chemical Society*, 133(48), pp. 19366–19375. Available at: https://doi.org/10.1021/JA2029848/SUPPL_FILE/JA2029848_SI_001.PDF.

Rideout, H.J. *et al.* (2001) ‘Proteasomal inhibition leads to formation of ubiquitin/alpha-synuclein-immunoreactive inclusions in PC12 cells’, *Journal of neurochemistry*, 78(4), pp. 899–908. Available at: https://doi.org/10.1046/J.1471-4159.2001.00474.X.

Rideout, H.J. and Stefanis, L. (2002) ‘Proteasomal inhibition-induced inclusion formation and death in cortical neurons require transcription and ubiquitination’, *Molecular and Cellular Neuroscience*, 21(2), pp. 223–238. Available at: https://doi.org/10.1006/mcne.2002.1173.

de Rijk, M.C. *et al.* (1997) ‘A population perspective on diagnostic criteria for Parkinson’s disease.’, *Neurology*, 48(5), pp. 1277–1281. Available at: https://doi.org/10.1212/wnl.48.5.1277.

Riolo, M.T. *et al.* (2012) ‘Histone deacetylase 6 (HDAC6) deacetylates survivin for its nuclear export in breast cancer’, *The Journal of biological chemistry*, 287(14), pp. 10885–10893. Available at: https://doi.org/10.1074/JBC.M111.308791.

Ritz, B. *et al.* (2015) ‘Traffic-Related Air Pollution and Parkinson’s Disease in Denmark: A Case–Control Study’, *Environmental Health Perspectives*, 124(3), pp. 351–356. Available at: https://doi.org/10.1289/EHP.1409313.

Rocha, E.M. *et al.* (2020) ‘LRRK2 inhibition prevents endolysosomal deficits seen in human Parkinson’s disease’, *Neurobiology of disease*, 134. Available at: https://doi.org/10.1016/J.NBD.2019.104626.

Rolls, M.M., Thyagarajan, P. and Feng, C. (2021) ‘Microtubule dynamics in healthy and injured neurons’, *Developmental neurobiology*, 81(3), pp. 321–332. Available at: https://doi.org/10.1002/DNEU.22746.

Ross, O.A. *et al.* (2011) ‘Association of LRRK2 exonic variants with susceptibility to Parkinson’s disease: a case-control study’, *The Lancet. Neurology*, 10(10), pp. 898–908. Available at: https://doi.org/10.1016/S1474-4422(11)70175-2.

Rossaert, E. *et al.* (2019) ‘Restoration of histone acetylation ameliorates disease and metabolic abnormalities in a FUS mouse model’, *Acta neuropathologica communications*, 7(1), p. 107. Available at: https://doi.org/10.1186/S40478-019-0750-2.

Rostami, J. *et al.* (2017) ‘Human Astrocytes Transfer Aggregated Alpha-Synuclein via Tunneling Nanotubes’, *Journal of Neuroscience*, 37(49), pp. 11835–11853. Available at: https://doi.org/10.1523/JNEUROSCI.0983-17.2017.

Rostami, J. *et al.* (2020) ‘Astrocytes have the capacity to act as antigen-presenting cells in the Parkinson’s disease brain’, *Journal of Neuroinflammation*, 17(1), pp. 1–18. Available at: https://doi.org/10.1186/S12974-020-01776-7/FIGURES/8.

Rostovtseva, T.K. *et al.* (2015) ‘α-Synuclein Shows High Affinity Interaction with Voltage-dependent Anion Channel, Suggesting Mechanisms of Mitochondrial Regulation and Toxicity in Parkinson Disease’, *The Journal of biological chemistry*, 290(30), pp. 18467–18477. Available at: https://doi.org/10.1074/JBC.M115.641746.

Rothaug, M. *et al.* (2015) ‘LAMP-2 deficiency leads to hippocampal dysfunction but normal clearance of neuronal substrates of chaperone-mediated autophagy in a mouse model for Danon disease’, *Acta neuropathologica communications*, 3, p. 6. Available at: https://doi.org/10.1186/S40478-014-0182-Y.

Rott, R. *et al.* (2008) ‘Monoubiquitylation of alpha-synuclein by seven in absentia homolog (SIAH) promotes its aggregation in dopaminergic cells’, *The Journal of biological chemistry*, 283(6), pp. 3316–3328. Available at: https://doi.org/10.1074/JBC.M704809200.

Rott, R. *et al.* (2017) ‘SUMOylation and ubiquitination reciprocally regulate α-synuclein degradation and pathological aggregation’, *Proceedings of the National Academy of Sciences of the United States of America*, 114(50), pp. 13176–13181.

Rousseaux, M.W.C. *et al.* (2018) ‘Depleting Trim28 in adult mice is well tolerated and reduces levels of’, *eLife*, 7, pp. 1–16. Available at: https://doi.org/10.7554/eLife.36768.

Ryan, B.J. *et al.* (2015) ‘Mitochondrial dysfunction and mitophagy in Parkinson’s: From familial to sporadic disease’, *Trends in Biochemical Sciences*. Elsevier Ltd, pp. 200–210. Available at: https://doi.org/10.1016/j.tibs.2015.02.003.

S, M. *et al.* (2020) ‘Neuron-autonomous Susceptibility to Induced Synuclein Aggregation Is Exacerbated by Endogenous Lrrk2 Mutations and Ameliorated by Lrrk2 Genetic Knock-Out’, *Brain communications*, 2(1). Available at: https://doi.org/10.1093/BRAINCOMMS/FCZ052.

Sahoo, S. *et al.* (2022) ‘Role of Ubiquitin-Proteasome and Autophagy-Lysosome Pathways in α-Synuclein Aggregate Clearance’, *Molecular neurobiology*, 59(9), pp. 5379–5407. Available at: https://doi.org/10.1007/S12035-022-02897-1.

Sahu, I. and Glickman, M.H. (2021) ‘Structural Insights into Substrate Recognition and Processing by the 20S Proteasome’, *Biomolecules*, 11(2), pp. 1–15. Available at: https://doi.org/10.3390/BIOM11020148.

Saliba, R.S. *et al.* (2002) ‘The cellular fate of mutant rhodopsin: quality control, degradation and aggresome formation’, *Journal of cell science*, 115(Pt 14), pp.

2907–2918. Available at: https://doi.org/10.1242/JCS.115.14.2907.

Sano, K. *et al.* (2021) ‘Tyrosine 136 phosphorylation of α-synuclein aggregates in the Lewy body dementia brain: involvement of serine 129 phosphorylation by casein kinase 2’, *Acta neuropathologica communications*, 9(1). Available at: https://doi.org/10.1186/S40478-021-01281-9.

dos Santos, I.B. *et al.* (2018) ‘Lysosomal Cathepsin Release Is Required for NLRP3-Inflammasome Activation by Mycobacterium tuberculosis in Infected Macrophages’, *Frontiers in immunology*, 9(JUL). Available at: https://doi.org/10.3389/FIMMU.2018.01427.

Sanyal, A. *et al.* (2020) ‘Lysosome and Inflammatory Defects in GBA1-Mutant Astrocytes Are Normalized by LRRK2 Inhibition’, *Movement Disorders*, 35(5), pp. 760–773. Available at: https://doi.org/10.1002/MDS.27994.

Saunders-Pullman, R., Raymond, D. and Elango, S. (2019) *LRRK2 Parkinson Disease*.

Savyon, M. and Engelender, S. (2020) ‘SUMOylation in α-Synuclein Homeostasis and Pathology’, *Frontiers in aging neuroscience*, 12. Available at: https://doi.org/10.3389/FNAGI.2020.00167.

Schapansky, J. *et al.* (2014) ‘Membrane recruitment of endogenous LRRK2 precedes its potent regulation of autophagy’, *Human molecular genetics*, 23(16), pp. 4201–4214. Available at: https://doi.org/10.1093/HMG/DDU138.

Schindelin, J. *et al.* (2012) ‘Fiji: an open-source platform for biological-image analysis’, *Nature methods*, 9(7), pp. 676–682. Available at: https://doi.org/10.1038/NMETH.2019.

Schmidt, S., Vogt Weisenhorn, D.M. and Wurst, W. (2022) ‘Chapter 5 – “Parkinson’s disease – A role of non-enzymatic posttranslational modifications in disease onset and progression?”’, *Molecular Aspects of Medicine*, 86, p. 101096. Available at: https://doi.org/10.1016/J.MAM.2022.101096.

Schmidt, S.H. *et al.* (2019) ‘The dynamic switch mechanism that leads to activation

of LRRK2 is embedded in the DFGψ motif in the kinase domain', *Proceedings of the National Academy of Sciences of the United States of America*, 116(30), pp. 14979–14988. Available at: https://doi.org/10.1073/PNAS.1900289116/-/DCSUPPLEMENTAL.

Schmidt, S.H. *et al.* (2021) 'Conformation and dynamics of the kinase domain drive subcellular location and activation of LRRK2', *Proceedings of the National Academy of Sciences of the United States of America*, 118(23). Available at: https://doi.org/10.1073/PNAS.2100844118/-/DCSUPPLEMENTAL.

Schofield, A. V. *et al.* (2013) 'Tubulin polymerization promoting protein 1 (Tppp1) phosphorylation by Rho-associated coiled-coil kinase (rock) and cyclin-dependent kinase 1 (Cdk1) inhibits microtubule dynamics to increase cell proliferation', *The Journal of biological chemistry*, 288(11), pp. 7907–7917. Available at: https://doi.org/10.1074/JBC.M112.441048.

Scott, D.A. *et al.* (2010) 'A pathologic cascade leading to synaptic dysfunction in α-synuclein-induced neurodegeneration', *Journal of Neuroscience*, 30(24), pp. 8083–8095. Available at: https://doi.org/10.1523/JNEUROSCI.1091-10.2010.

Scott, J.D. *et al.* (2017) 'Discovery of a 3-(4-Pyrimidinyl) Indazole (MLi-2), an Orally Available and Selective Leucine-Rich Repeat Kinase 2 (LRRK2) Inhibitor that Reduces Brain Kinase Activity', *Journal of Medicinal Chemistry*, 60(7), pp. 2983–2992. Available at: https://doi.org/10.1021/ACS.JMEDCHEM.7B00045/SUPPL_FILE/JM7B00045_SI_003.PDF.

Scroggins, B.T. *et al.* (2007) 'An acetylation site in the middle domain of Hsp90 regulates chaperone function', *Molecular cell*, 25(1), pp. 151–159. Available at: https://doi.org/10.1016/J.MOLCEL.2006.12.008.

Seegobin, S.P. *et al.* (2020) 'Progress in LRRK2-Associated Parkinson's Disease Animal Models', *Frontiers in neuroscience*, 14. Available at: https://doi.org/10.3389/FNINS.2020.00674.

Seibenhener, M.L. and Wooten, M.W. (2012) 'Isolation and culture of hippocampal

neurons from prenatal mice', *Journal of visualized experiments : JoVE* [Preprint], (65). Available at: https://doi.org/10.3791/3634.

Seidel, K. *et al.* (2015) 'The brainstem pathologies of Parkinson's disease and dementia with Lewy bodies', *Brain pathology (Zurich, Switzerland)*, 25(2), pp. 121–135. Available at: https://doi.org/10.1111/BPA.12168.

Seigneurin-Berny, D. *et al.* (2001) 'Identification of Components of the Murine Histone Deacetylase 6 Complex: Link between Acetylation and Ubiquitination Signaling Pathways', *Molecular and Cellular Biology*, 21(23), p. 8035. Available at: https://doi.org/10.1128/MCB.21.23.8035-8044.2001.

Sekiya, H. *et al.* (2022) 'Discrepancy between distribution of alpha-synuclein oligomers and Lewy-related pathology in Parkinson's disease', *Acta Neuropathologica Communications*, 10(1), pp. 1–13. Available at: https://doi.org/10.1186/S40478-022-01440-6/FIGURES/7.

Selenica, M.L. *et al.* (2014) 'Histone deacetylase 6 inhibition improves memory and reduces total tau levels in a mouse model of tau deposition', *Alzheimer's research & therapy*, 6(1). Available at: https://doi.org/10.1186/ALZRT241.

Senior, S.L. *et al.* (2008) 'Increased striatal dopamine release and hyperdopaminergic-like behaviour in mice lacking both alpha-synuclein and gamma-synuclein', *The European journal of neuroscience*, 27(4), pp. 947–957. Available at: https://doi.org/10.1111/J.1460-9568.2008.06055.X.

Serio, T.R. *et al.* (2000) 'Nucleated conformational conversion and the replication of conformational information by a prion determinant', *Science*, 289(5483), pp. 1317–1321. Available at: https://doi.org/10.1126/science.289.5483.1317.

Shabek, N. *et al.* (2012) 'The size of the proteasomal substrate determines whether its degradation will be mediated by mono- or polyubiquitylation', *Molecular cell*, 48(1), pp. 87–97. Available at: https://doi.org/10.1016/J.MOLCEL.2012.07.011.

Shahmoradian, S.H. *et al.* (2019) 'Lewy pathology in Parkinson's disease consists of crowded organelles and lipid membranes', *Nature Neuroscience 2019 22:7*, 22(7), pp. 1099–1109. Available at: https://doi.org/10.1038/s41593-019-0423-2.

Shakya, S. and Westlake, C.J. (2021) 'Recent advances in understanding assembly of the primary cilium membrane', *Faculty reviews*, 10. Available at: https://doi.org/10.12703/R/10-16.

Shanley, M.R. *et al.* (2015) 'LRRK2 Facilitates tau Phosphorylation through Strong Interaction with tau and cdk5', *Biochemistry*, 54(33), pp. 5198–5208. Available at: https://doi.org/10.1021/ACS.BIOCHEM.5B00326.

Sharon, R. *et al.* (2003) 'The formation of highly soluble oligomers of α-synuclein is regulated by fatty acids and enhanced in Parkinson's disease', *Neuron*, 37(4), pp. 583–595. Available at: https://doi.org/10.1016/S0896-6273(03)00024-2.

Shen, C. *et al.* (2018) 'Dynactin is involved in Lewy body pathology', *Neuropathology*, 38(6), pp. 583–590. Available at: https://doi.org/10.1111/neup.12512.

Sheng, Z. *et al.* (2012) 'Ser1292 autophosphorylation is an indicator of LRRK2 kinase activity and contributes to the cellular effects of PD mutations.', *Science translational medicine*, 4(164).

Sherer, T.B. *et al.* (2003) 'Subcutaneous Rotenone Exposure Causes Highly Selective Dopaminergic Degeneration and α-Synuclein Aggregation', *Experimental Neurology*, 179(1), pp. 9–16. Available at: https://doi.org/10.1006/EXNR.2002.8072.

Shida, T. *et al.* (2010) 'The major α-tubulin K40 acetyltransferase αTAT1 promotes rapid ciliogenesis and efficient mechanosensation', *Proceedings of the National Academy of Sciences of the United States of America*, 107(50), pp. 21517–21522. Available at: https://doi.org/10.1073/PNAS.1013728107/-/DCSUPPLEMENTAL/SD01.XLS.

Shin, N. *et al.* (2008) 'LRRK2 regulates synaptic vesicle endocytosis', *Experimental cell research*, 314(10), pp. 2055–2065. Available at: https://doi.org/10.1016/J.YEXCR.2008.02.015.

Shu, L. *et al.* (2019) 'A Comprehensive Analysis of Population Differences in LRRK2 Variant Distribution in Parkinson's Disease', *Frontiers in aging neuroscience*, 11(JAN). Available at: https://doi.org/10.3389/FNAGI.2019.00013.

Siddiqui, A. *et al.* (2012) ‘Selective binding of nuclear alpha-synuclein to the PGC1alpha promoter under conditions of oxidative stress may contribute to losses in mitochondrial function: Implications for Parkinson’s disease’, *Free Radical Biology and Medicine*, 53(4), pp. 993–1003. Available at: https://doi.org/10.1016/J.FREERADBIOMED.2012.05.024.

Siegel, D. *et al.* (2021) ‘A redox-mediated conformational change in NQO1 controls binding to microtubules and α-tubulin acetylation’, *Redox biology*, 39. Available at: https://doi.org/10.1016/J.REDOX.2020.101840.

Singh, F. *et al.* (2021) ‘Pharmacological rescue of impaired mitophagy in Parkinson’s disease-related LRRK2 G2019S knock-in mice’, *eLife*, 10. Available at: https://doi.org/10.7554/ELIFE.67604.

Singh, R. *et al.* (2019) ‘DYRK1B regulates Hedgehog-induced microtubule acetylation’, *Cellular and molecular life sciences : CMLS*, 76(1), pp. 193–207. Available at: https://doi.org/10.1007/S00018-018-2942-5.

Singleton, A.B. *et al.* (2003) ‘α-Synuclein Locus Triplication Causes Parkinson’s Disease’, *Science*, 302(5646), p. 841. Available at: https://doi.org/10.1126/science.1090278.

Sitzia, G., Skiteva, O. and Chergui, K. (2022) ‘Neuronal Firing and Glutamatergic Synapses in the Substantia Nigra Pars Reticulata of LRRK2-G2019S Mice’. Available at: https://doi.org/10.3390/biom12111635.

Smeyne, R.J. *et al.* (2021) ‘Infection and Risk of Parkinson’s Disease’, *Journal of Parkinson’s disease*, 11(1), pp. 31–43. Available at: https://doi.org/10.3233/JPD-202279.

Smith, W.W. *et al.* (2005) ‘Alpha-synuclein phosphorylation enhances eosinophilic cytoplasmic inclusion formation in SH-SY5Y cells’, *The Journal of neuroscience : the official journal of the Society for Neuroscience*, 25(23), pp. 5544–5552. Available at: https://doi.org/10.1523/JNEUROSCI.0482-05.2005.

Smith, W.W. *et al.* (2006) ‘Kinase activity of mutant LRRK2 mediates neuronal toxicity’, *Nature neuroscience*, 9(10), pp. 1231–1233. Available at:

https://doi.org/10.1038/NN1776.

Snead, D.M. *et al.* (2022) ‘Structural basis for Parkinson’s disease-linked LRRK2’s binding to microtubules’, *Nature structural & molecular biology*, 29(12), pp. 1196–1207. Available at: https://doi.org/10.1038/S41594-022-00863-Y.

Snyder, H. *et al.* (2003) ‘Aggregated and monomeric α-synuclein bind to the S6′ proteasomal protein and inhibit proteasomal function’, *Journal of Biological Chemistry*, 278(14), pp. 11753–11759. Available at: https://doi.org/10.1074/jbc.M208641200.

Soldner, F. *et al.* (2016) ‘Parkinson-associated risk variant in enhancer element produces subtle effect on target gene expression’, *Nature*, 533(7601), p. 95. Available at: https://doi.org/10.1038/NATURE17939.

Sonustun, B. *et al.* (2022) ‘Pathological Relevance of Post-Translationally Modified Alpha-Synuclein (pSer87, pSer129, nTyr39) in Idiopathic Parkinson’s Disease and Multiple System Atrophy’, *Cells*, 11(5). Available at: https://doi.org/10.3390/CELLS11050906.

Sosero, Y.L. and Gan-Or, Z. (2023) ‘LRRK2 and Parkinson’s disease: from genetics to targeted therapy’, *Annals of Clinical and Translational Neurology* [Preprint]. Available at: https://doi.org/10.1002/ACN3.51776.

Souza, J.M. *et al.* (2000) ‘Dityrosine cross-linking promotes formation of stable alpha -synuclein polymers. Implication of nitrative and oxidative stress in the pathogenesis of neurodegenerative synucleinopathies’, *The Journal of biological chemistry*, 275(24), pp. 18344–18349. Available at: https://doi.org/10.1074/JBC.M000206200.

Spillantini, M.G. *et al.* (1997) ‘α-Synuclein in Lewy bodies’, *Nature*, 388(6645), pp. 839–840. Available at: https://doi.org/10.1038/42166.

Spillantini, M.G. *et al.* (1998) ‘alpha-Synuclein in filamentous inclusions of Lewy bodies from Parkinson’s disease and dementia with lewy bodies’, *Proceedings of the National Academy of Sciences of the United States of America*, 95(11), pp. 6469–6473. Available at: https://doi.org/10.1073/PNAS.95.11.6469.

Spillantini, M.G., Divane, A. and Goedert, M. (1995) ‘Assignment of human alpha-synuclein (SNCA) and beta-synuclein (SNCB) genes to chromosomes 4q21 and 5q35’, *Genomics*, 27(2), pp. 379–381. Available at: https://doi.org/10.1006/GENO.1995.1063.

Sreenivasmurthy, S.G. *et al.* (2022) ‘Bromo-protopine, a novel protopine derivative, alleviates tau pathology by activating chaperone-mediated autophagy for Alzheimer’s disease therapy’, *Frontiers in molecular biosciences*, 9. Available at: https://doi.org/10.3389/FMOLB.2022.1030534.

Stafa, K. *et al.* (2014) ‘Functional interaction of Parkinson’s disease-associated LRRK2 with members of the dynamin GTPase superfamily’, *Human molecular genetics*, 23(8), pp. 2055–2077. Available at: https://doi.org/10.1093/HMG/DDT600.

Stefanis, L. *et al.* (2019) ‘How is alpha-synuclein cleared from the cell?’, *Journal of Neurochemistry*. Blackwell Publishing Ltd, pp. 577–590. Available at: https://doi.org/10.1111/jnc.14704.

Steger, M. *et al.* (2016) ‘Phosphoproteomics reveals that Parkinson’s disease kinase LRRK2 regulates a subset of Rab GTPases’, *eLife*, 5. Available at: https://doi.org/10.7554/ELIFE.12813.

Steger, M. *et al.* (2017) ‘Systematic proteomic analysis of LRRK2-mediated Rab GTPase phosphorylation establishes a connection to ciliogenesis’, *eLife*, 6. Available at: https://doi.org/10.7554/ELIFE.31012.

Stephens, A.D. *et al.* (2020) ‘Extent of N-terminus exposure of monomeric alpha-synuclein determines its aggregation propensity’, *Nature Communications*, 11(1). Available at: https://doi.org/10.1038/S41467-020-16564-3.

Stuendl, A. *et al.* (2016) ‘Induction of α-synuclein aggregate formation by CSF exosomes from patients with Parkinson’s disease and dementia with Lewy bodies’, *Brain*, 139(2), pp. 481–494. Available at: https://doi.org/10.1093/BRAIN/AWV346.

Su, M. *et al.* (2011) ‘HDAC6 regulates aggresome-autophagy degradation pathway of α-synuclein in response to MPP+-induced stress’, *Journal of Neurochemistry*, 117(1), pp. 112–120. Available at: https://doi.org/10.1111/j.1471-4159.2011.07180.x.

Su, R. and Zhou, T. (2021) ‘Alpha-Synuclein Induced Immune Cells Activation and Associated Therapy in Parkinson’s Disease’, *Frontiers in Aging Neuroscience*, 13, p. 710. Available at: https://doi.org/10.3389/FNAGI.2021.769506/BIBTEX.

Sugeno, N. *et al.* (2008) ‘Serine 129 phosphorylation of alpha-synuclein induces unfolded protein response-mediated cell death’, *The Journal of biological chemistry*, 283(34), pp. 23179–23188. Available at: https://doi.org/10.1074/JBC.M802223200.

Sun, J. *et al.* (2019) ‘Functional cooperation of α-synuclein and VAMP2 in synaptic vesicle recycling’, *Proceedings of the National Academy of Sciences of the United States of America*, 116(23), pp. 11113–11115. Available at: https://doi.org/10.1073/PNAS.1903049116.

Taes, I. *et al.* (2013) ‘Hdac6 deletion delays disease progression in the SOD1G93A mouse model of ALS’, *Human molecular genetics*, 22(9), pp. 1783–1790. Available at: https://doi.org/10.1093/HMG/DDT028.

Tahavvori, A. *et al.* (2023) ‘Involvement of antioxidant enzymes in Parkinson’s disease’, *Pathology, research and practice*, 249. Available at: https://doi.org/10.1016/J.PRP.2023.154757.

Takahashi, T. *et al.* (2002) ‘Tyrosine 125 of α-synuclein plays a critical role for dimerization following nitrative stress’, *Brain Research*, 938(1–2), pp. 73–80. Available at: https://doi.org/10.1016/S0006-8993(02)02498-8.

Takanashi, M. *et al.* (2018) ‘Isolated nigral degeneration without pathological protein aggregation in autopsied brains with LRRK2 p.R1441H homozygous and heterozygous mutations’, *Acta neuropathologica communications*, 6(1), p. 105. Available at: https://doi.org/10.1186/S40478-018-0617-Y.

Tan, E.K. *et al.* (2005) ‘The G2019S LRRK2 mutation is uncommon in an Asian cohort of Parkinson’s disease patients’, *Neuroscience letters*, 384(3), pp. 327–329. Available at: https://doi.org/10.1016/J.NEULET.2005.04.103.

Tan, J.M.M. *et al.* (2008) ‘Lysine 63-linked ubiquitination promotes the formation and autophagic clearance of protein inclusions associated with neurodegenerative diseases’, *Human molecular genetics*, 17(3), pp. 431–439. Available at:

https://doi.org/10.1093/HMG/DDM320.

Tanaka, M. *et al.* (2004) ‘Aggresomes formed by alpha-synuclein and synphilin-1 are cytoprotective’, *The Journal of biological chemistry*, 279(6), pp. 4625–4631. Available at: https://doi.org/10.1074/JBC.M310994200.

Tanik, S.A. *et al.* (2013) ‘Lewy Body-like α-Synuclein Aggregates Resist Degradation and Impair Macroautophagy’, *The Journal of Biological Chemistry*, 288(21), p. 15194. Available at: https://doi.org/10.1074/JBC.M113.457408.

Tanner, C.M. *et al.* (2011) ‘Rotenone, paraquat, and Parkinson’s disease’, *Environmental health perspectives*, 119(6), pp. 866–872. Available at: https://doi.org/10.1289/EHP.1002839.

Taylor, M. and Alessi, D.R. (2020) ‘Advances in elucidating the function of leucine-rich repeat protein kinase-2 in normal cells and Parkinson’s disease’, *Current opinion in cell biology*, 63, pp. 102–113. Available at: https://doi.org/10.1016/J.CEB.2020.01.001.

Taymans, J.-M. *et al.* (2023) ‘Perspective on the current state of the LRRK2 field’, *NPJ Parkinson’s Disease*, 9(1). Available at: https://doi.org/10.1038/S41531-023-00544-7.

Tenreiro, S. *et al.* (2014) ‘Phosphorylation modulates clearance of alpha-synuclein inclusions in a yeast model of Parkinson’s disease’, *PLoS genetics*, 10(5). Available at: https://doi.org/10.1371/JOURNAL.PGEN.1004302.

Themistokleous, C. *et al.* (2023) ‘Role of Autophagy Pathway in Parkinson’s Disease and Related Genetic Neurological Disorders’, *Journal of molecular biology*, 435(12), p. 168144. Available at: https://doi.org/10.1016/J.JMB.2023.168144.

Tofaris, G.K. *et al.* (2003) ‘Ubiquitination of alpha-synuclein in Lewy bodies is a pathological event not associated with impairment of proteasome function’, *The Journal of biological chemistry*, 278(45), pp. 44405–44411. Available at: https://doi.org/10.1074/JBC.M308041200.

Tofaris, G.K. *et al.* (2006) ‘Pathological Changes in Dopaminergic Nerve Cells of the

Substantia Nigra and Olfactory Bulb in Mice Transgenic for Truncated Human α-Synuclein(1–120): Implications for Lewy Body Disorders', *The Journal of Neuroscience*, 26(15), p. 3942. Available at: https://doi.org/10.1523/JNEUROSCI.4965-05.2006.

Tofaris, G.K. *et al.* (2011) 'Ubiquitin ligase Nedd4 promotes α-synuclein degradation by the endosomal-lysosomal pathway', *Proceedings of the National Academy of Sciences of the United States of America*, 108(41), pp. 17004–17009. Available at: https://doi.org/10.1073/PNAS.1109356108/-/DCSUPPLEMENTAL/SAPP.PDF.

Tofaris, G.K. (2022) 'Initiation and progression of α-synuclein pathology in Parkinson's disease', *Cellular and molecular life sciences : CMLS*, 79(4). Available at: https://doi.org/10.1007/S00018-022-04240-2.

Tofaris, G.K., Layfield, R. and Spillantini, M.G. (2001) 'alpha-synuclein metabolism and aggregation is linked to ubiquitin-independent degradation by the proteasome', *FEBS letters*, 509(1), pp. 22–26. Available at: https://doi.org/10.1016/S0014-5793(01)03115-5.

Tolosa, E. *et al.* (2021) 'Challenges in the diagnosis of Parkinson's disease', *The Lancet Neurology*, 20(5), pp. 385–397. Available at: https://doi.org/10.1016/S1474-4422(21)00030-2.

Tomiyama, H. *et al.* (2006) 'Clinicogenetic study of mutations in LRRK2 exon 41 in Parkinson's disease patients from 18 countries', *Movement Disorders*, 21(8), pp. 1102–1108. Available at: https://doi.org/10.1002/MDS.20886.

Tong, Y. *et al.* (2010) 'Loss of leucine-rich repeat kinase 2 causes impairment of protein degradation pathways, accumulation of alpha-synuclein, and apoptotic cell death in aged mice', *Proceedings of the National Academy of Sciences of the United States of America*, 107(21), pp. 9879–9884. Available at: https://doi.org/10.1073/PNAS.1004676107.

Tracz, M. and Bialek, W. (2021) 'Beyond K48 and K63: non-canonical protein ubiquitination', *Cellular & molecular biology letters*, 26(1). Available at: https://doi.org/10.1186/S11658-020-00245-6.

Trinh, J. *et al.* (2023) ‘LRRK2 Parkinson Disease’, *GeneReviews*® [Preprint].

Trist, B.G., Hare, D.J. and Double, K.L. (2019) ‘Oxidative stress in the aging substantia nigra and the etiology of Parkinson’s disease’, *Aging cell*, 18(6). Available at: https://doi.org/10.1111/ACEL.13031.

Tysnes, O.-B. and Storstein, A. (2017) ‘Epidemiology of Parkinson’s disease’, *Journal of Neural Transmission*, 124(8), pp. 901–905. Available at: https://doi.org/10.1007/s00702-017-1686-y.

Usmani, A., Shavarebi, F. and Hiniker, A. (2021) ‘The Cell Biology of LRRK2 in Parkinson’s Disease’, *Molecular and cellular biology*, 41(5). Available at: https://doi.org/10.1128/MCB.00660-20.

Uversky, V.N., Li, J. and Fink, A.L. (2001) ‘Evidence for a Partially Folded Intermediate in α-Synuclein Fibril Formation’, *Journal of Biological Chemistry*, 276(14), pp. 10737–10744. Available at: https://doi.org/10.1074/JBC.M010907200.

Valente, E.M. *et al.* (2004) ‘Hereditary early-onset Parkinson’s disease caused by mutations in PINK1’, *Science (New York, N.Y.)*, 304(5674), pp. 1158–1160. Available at: https://doi.org/10.1126/SCIENCE.1096284.

Varkey, J. *et al.* (2010) ‘Membrane curvature induction and tubulation are common features of synucleins and apolipoproteins’, *The Journal of biological chemistry*, 285(42), pp. 32486–32493. Available at: https://doi.org/10.1074/JBC.M110.139576.

Vicente Miranda, H. *et al.* (2017) ‘Glycation potentiates α-synuclein-associated neurodegeneration in synucleinopathies’, *Brain : a journal of neurology*, 140(5), pp. 1399–1419. Available at: https://doi.org/10.1093/BRAIN/AWX056.

Vides, E.G. *et al.* (2022) ‘A feed-forward pathway drives LRRK2 kinase membrane recruitment and activation’, *eLife*, 11. Available at: https://doi.org/10.7554/ELIFE.79771.

Vidović, M. and Rikalovic, M.G. (2022) ‘Alpha-Synuclein Aggregation Pathway in Parkinson’s Disease: Current Status and Novel Therapeutic Approaches’, *Cells*, 11(11). Available at: https://doi.org/10.3390/CELLS11111732.

Vilariño-Güell, C. *et al.* (2011) 'VPS35 Mutations in Parkinson Disease', *The American Journal of Human Genetics*, 89(1), pp. 162–167. Available at: https://doi.org/10.1016/J.AJHG.2011.06.001.

Vogiatzi, T. *et al.* (2008) 'Wild type alpha-synuclein is degraded by chaperone-mediated autophagy and macroautophagy in neuronal cells', *The Journal of biological chemistry*, 283(35), pp. 23542–23556. Available at: https://doi.org/10.1074/JBC.M801992200.

Vollstedt, E.J. *et al.* (2023) 'Embracing Monogenic Parkinson's Disease: The MJFF Global Genetic PD Cohort', *Movement disorders : official journal of the Movement Disorder Society*, 38(2), pp. 286–303. Available at: https://doi.org/10.1002/MDS.29288.

Volpicelli-Daley, L.A. *et al.* (2011) 'Exogenous α-Synuclein Fibrils Induce Lewy Body Pathology Leading to Synaptic Dysfunction and Neuron Death', *Neuron*, 72(1), p. 57. Available at: https://doi.org/10.1016/J.NEURON.2011.08.033.

Volpicelli-Daley, L.A. *et al.* (2016) 'G2019s-LRRK2 expression augments α-synuclein sequestration into inclusions in neurons', *Journal of Neuroscience*, 36(28), pp. 7415–7427. Available at: https://doi.org/10.1523/JNEUROSCI.3642-15.2016.

Volpicelli-Daley, L.A., Luk, K.C. and Lee, V.M.Y. (2014) 'Addition of exogenous α-synuclein preformed fibrils to primary neuronal cultures to seed recruitment of endogenous α-synuclein to Lewy body and Lewy neurite-like aggregates', *Nature protocols*, 9(9), pp. 2135–2146. Available at: https://doi.org/10.1038/NPROT.2014.143.

Wang, B. *et al.* (2018) '14-3-3 Proteins Reduce Cell-to-Cell Transfer and Propagation of Pathogenic α-Synuclein', *Journal of Neuroscience*, 38(38), pp. 8211–8232. Available at: https://doi.org/10.1523/JNEUROSCI.1134-18.2018.

Wang, L. *et al.* (2008) 'The chaperone activity of heat shock protein 90 is critical for maintaining the stability of leucine-rich repeat kinase 2', *The Journal of neuroscience : the official journal of the Society for Neuroscience*, 28(13), pp. 3384–3391. Available at: https://doi.org/10.1523/JNEUROSCI.0185-08.2008.

Wang, L., Klionsky, D.J. and Shen, H.M. (2022) ‘The emerging mechanisms and functions of microautophagy’, *Nature Reviews Molecular Cell Biology 2022 24:3*, 24(3), pp. 186–203. Available at: https://doi.org/10.1038/s41580-022-00529-z.

Wang, R. *et al.* (2019) ‘ATP13A2 facilitates HDAC6 recruitment to lysosome to promote autophagosome-lysosome fusion’, *The Journal of cell biology*, 218(1), pp. 267–284. Available at: https://doi.org/10.1083/JCB.201804165.

Wang, W. *et al.* (2011) ‘A soluble α-synuclein construct forms a dynamic tetramer’, *Proceedings of the National Academy of Sciences of the United States of America*, 108(43), pp. 17797–17802.

Wang, X. *et al.* (2012) ‘LRRK2 regulates mitochondrial dynamics and function through direct interaction with DLP1’, *Human molecular genetics*, 21(9), pp. 1931–1944. Available at: https://doi.org/10.1093/HMG/DDS003.

Ward, C.L. and Kopito$, R.R. (1994) ‘THE JOURNAL OF BIOLOGICAL CHEMISTRY Intracellular Turnover of Cystic Fibrosis Transmembrane C.onductance Regulator INEFFICIENT PROCESSING AND RAPID DEGRADATION O F WILD-TYPE AND MUTANT PROTEINS*’, 269(41), pp. 2571–25718. Available at: https://doi.org/10.1016/S0021-9258(18)47306-1.

Watabe, M. and Nakaki, T. (2011) ‘Protein kinase CK2 regulates the formation and clearance of aggresomes in response to stress’, *Journal of Cell Science*, 124(9), pp. 1519–1532. Available at: https://doi.org/10.1242/jcs.081778.

Watanabe, R. *et al.* (2020) ‘The In Situ Structure of Parkinson’s Disease-Linked LRRK2’, *Cell*, 182(6), pp. 1508-1518.e16. Available at: https://doi.org/10.1016/J.CELL.2020.08.004.

Watanabe, Y. *et al.* (2012) ‘p62/SQSTM1-dependent autophagy of Lewy body-like α-synuclein inclusions’, *PloS one*, 7(12). Available at: https://doi.org/10.1371/JOURNAL.PONE.0052868.

Wauters, F. *et al.* (2020) ‘LRRK2 mutations impair depolarization-induced mitophagy through inhibition of mitochondrial accumulation of RAB10’, *Autophagy*, 16(2), pp. 203–222. Available at: https://doi.org/10.1080/15548627.2019.1603548.

Waxman, E.A. and Giasson, B.I. (2008) ‘Specificity and regulation of casein kinase-mediated phosphorylation of alpha-synuclein’, *Journal of neuropathology and experimental neurology*, 67(5). Available at: https://doi.org/10.1097/NEN.0B013E31816FC995.

Webb, J.L. *et al.* (2003) ‘Alpha-Synuclein is degraded by both autophagy and the proteasome’, *The Journal of biological chemistry*, 278(27), pp. 25009–25013. Available at: https://doi.org/10.1074/JBC.M300227200.

Weetman, J. *et al.* (2013) ‘Increased SUMO-1 expression in the unilateral rotenone-lesioned mouse model of Parkinson’s disease’, *Neuroscience letters*, 544, pp. 119–124. Available at: https://doi.org/10.1016/J.NEULET.2013.03.057.

Wei, D. *et al.* (2018) ‘α-Tubulin Acetylation Restricts Axon Overbranching by Dampening Microtubule Plus-End Dynamics in Neurons’, *Cerebral cortex (New York, N.Y. : 1991)*, 28(9), pp. 3332–3346. Available at: https://doi.org/10.1093/CERCOR/BHX225.

Weng, J.-H. *et al.* (2023) ‘Capturing Differences in the Regulation of LRRK2 Dynamics and Conformational States by Small Molecule Kinase Inhibitors’, *ACS chemical biology*, 18(4), pp. 810–821. Available at: https://doi.org/10.1021/ACSCHEMBIO.2C00868.

Wentink, A.S. *et al.* (2020) ‘Molecular dissection of amyloid disaggregation by human HSP70’, *Nature 2020 587:7834*, 587(7834), pp. 483–488. Available at: https://doi.org/10.1038/s41586-020-2904-6.

West, A.B. *et al.* (2005) ‘Parkinson’s disease-associated mutations in leucine-rich repeat kinase 2 augment kinase activity’, *Proceedings of the National Academy of Sciences of the United States of America*, 102(46), pp. 16842–16847. Available at: https://doi.org/10.1073/PNAS.0507360102.

West, A.B. *et al.* (2007) ‘Parkinson’s disease-associated mutations in LRRK2 link enhanced GTP-binding and kinase activities to neuronal toxicity’, *Human molecular genetics*, 16(2), pp. 223–232. Available at: https://doi.org/10.1093/HMG/DDL471.

Weston, L.J. *et al.* (2021) ‘In vivo aggregation of presynaptic alpha-synuclein is not

influenced by its phosphorylation at serine-129', *Neurobiology of disease*, 152. Available at: https://doi.org/10.1016/J.NBD.2021.105291.

Westphal, C.H. and Chandra, S.S. (2013) 'Monomeric synucleins generate membrane curvature', *The Journal of biological chemistry*, 288(3), pp. 1829–1840. Available at: https://doi.org/10.1074/JBC.M112.418871.

Wigley, C.W. *et al.* (1999) 'Dynamic association of proteasomal machinery with the centrosome', *The Journal of cell biology*, 145(3), pp. 481–490. Available at: https://doi.org/10.1083/JCB.145.3.481.

Williams, K.A. *et al.* (2013) 'Extracellular signal-regulated kinase (ERK) phosphorylates histone deacetylase 6 (HDAC6) at serine 1035 to stimulate cell migration', *The Journal of biological chemistry*, 288(46), pp. 33156–33170. Available at: https://doi.org/10.1074/JBC.M113.472506.

Winner, B. *et al.* (2011) 'In vivo demonstration that α-synuclein oligomers are toxic', *Proceedings of the National Academy of Sciences of the United States of America*, 108(10), pp. 4194–4199. Available at: https://doi.org/10.1073/PNAS.1100976108/SUPPL_FILE/PNAS.201100976SI.PDF.

Wong, E.S.P. *et al.* (2008) 'Autophagy-mediated clearance of aggresomes is not a universal phenomenon', *Human molecular genetics*, 17(16), pp. 2570–2582. Available at: https://doi.org/10.1093/HMG/DDN157.

Wooten, M.W. *et al.* (2008) 'Essential Role of Sequestosome 1/p62 in Regulating Accumulation of Lys63-ubiquitinated Proteins', *Journal of Biological Chemistry*, 283(11), pp. 6783–6789. Available at: https://doi.org/10.1074/JBC.M709496200.

Wu, C.X. *et al.* (2019) 'Parkinson's disease-associated mutations in the GTPase domain of LRRK2 impair its nucleotide-dependent conformational dynamics', *The Journal of biological chemistry*, 294(15), pp. 5907–5913. Available at: https://doi.org/10.1074/JBC.RA119.007631.

Xia, Q. *et al.* (2015) 'Loss of TDP-43 Inhibits Amyotrophic Lateral Sclerosis-Linked Mutant SOD1 Aggresome Formation in an HDAC6-Dependent Manner', *Journal of Alzheimer's disease : JAD*, 45(2), pp. 373–386. Available at:

https://doi.org/10.3233/JAD-142244.

Xie, Z. *et al.* (2017) ‘Molecular Mechanisms for the Coupling of Endocytosis to Exocytosis in Neurons’. Available at: https://doi.org/10.3389/fnmol.2017.00047.

Xilouri, M. *et al.* (2016) ‘Impairment of chaperone-mediated autophagy induces dopaminergic neurodegeneration in rats’, *Autophagy*, 12(11), pp. 2230–2247. Available at: https://doi.org/10.1080/15548627.2016.1214777.

Xiong, R. *et al.* (2015) ‘A Novel Hsp90 Inhibitor Activates Compensatory Heat Shock Protein Responses and Autophagy and Alleviates Mutant A53T α-Synuclein Toxicity’, *Molecular pharmacology*, 88(6), pp. 1045–1054. Available at: https://doi.org/10.1124/MOL.115.101451.

Xu, X., Kozikowski, A.P. and Pozzo-Miller, L. (2014) ‘A selective histone deacetylase-6 inhibitor improves BDNF trafficking in hippocampal neurons from Mecp2 knockout mice: implications for Rett syndrome’, *Frontiers in cellular neuroscience*, 8(MAR). Available at: https://doi.org/10.3389/FNCEL.2014.00068.

Xu, Y. *et al.* (2018) ‘DNAJC5 facilitates USP19-dependent unconventional secretion of misfolded cytosolic proteins’, *Cell Discovery 2018 4:1*, 4(1), pp. 1–18. Available at: https://doi.org/10.1038/s41421-018-0012-7.

Xu, Z. *et al.* (2017) ‘Microtubules acquire resistance from mechanical breakage through intralumenal acetylation’, *Science (New York, N.Y.)*, 356(6335), pp. 328–332. Available at: https://doi.org/10.1126/SCIENCE.AAI8764.

Yamada, K. and Iwatsubo, T. (2018) ‘Extracellular α-synuclein levels are regulated by neuronal activity’, *Molecular neurodegeneration*, 13(1). Available at: https://doi.org/10.1186/S13024-018-0241-0.

Yan, J. *et al.* (2013) ‘SQSTM1/p62 interacts with HDAC6 and regulates deacetylase activity’, *PloS one*, 8(9). Available at: https://doi.org/10.1371/JOURNAL.PONE.0076016.

Yan, J. *et al.* (2022) ‘LRRK2 deficiency mitigates colitis progression by favoring resolution of inflammation and restoring homeostasis of gut microbiota’, *Genomics*,

114(6). Available at: https://doi.org/10.1016/J.YGENO.2022.110527.

Yan, S. *et al.* (2020) 'Pharmacological Inhibition of HDAC6 Attenuates NLRP3 Inflammatory Response and Protects Dopaminergic Neurons in Experimental Models of Parkinson's Disease', *Frontiers in aging neuroscience*, 12. Available at: https://doi.org/10.3389/FNAGI.2020.00078.

Yang, Y.W. *et al.* (2017) 'Increased risk of Parkinson disease with diabetes mellitus in a population-based study', *Medicine*, 96(3). Available at: https://doi.org/10.1097/MD.0000000000005921.

Yankova, G., Bogomyakova, O. and Tulupov, A. (2021) 'The glymphatic system and meningeal lymphatics of the brain: New understanding of brain clearance', *Reviews in the Neurosciences*, 32(7), pp. 693–705. Available at: https://doi.org/10.1515/REVNEURO-2020-0106/ASSET/GRAPHIC/J_REVNEURO-2020-0106_FIG_001.JPG.

Yao, C. *et al.* (2013) 'Kinase inhibitors arrest neurodegeneration in cell and C. elegans models of LRRK2 toxicity', *Human molecular genetics*, 22(2), pp. 328–344. Available at: https://doi.org/10.1093/HMG/DDS431.

Ye, H. *et al.* (2020) 'Retromer subunit, VPS29, regulates synaptic transmission and is required for endolysosomal function in the aging brain', *eLife*, 9. Available at: https://doi.org/10.7554/ELIFE.51977.

Ye, H. *et al.* (2022) 'Genetics and Pathogenesis of Parkinson's Syndrome'. Available at: https://doi.org/10.1146/annurev-pathmechdis.

Yi, S. *et al.* (2022) 'Pathogenesis of α-Synuclein in Parkinson's Disease: From a Neuron-Glia Crosstalk Perspective', *International journal of molecular sciences*, 23(23). Available at: https://doi.org/10.3390/IJMS232314753.

Yoo, H. *et al.* (2022) 'Role of post-translational modifications on the alpha-synuclein aggregation-related pathogenesis of Parkinson's disease', *BMB reports*, 55(7), pp. 323–335. Available at: https://doi.org/10.5483/BMBREP.2022.55.7.073.

Yoon, J.H. *et al.* (2017) 'LRRK2 functions as a scaffolding kinase of ASK1-mediated

neuronal cell death', *Biochimica et biophysica acta. Molecular cell research*, 1864(12), pp. 2356–2368. Available at: https://doi.org/10.1016/J.BBAMCR.2017.09.001.

Yoshino, H. *et al.* (2017) 'Homozygous alpha-synuclein p.A53V in familial Parkinson's disease', *Neurobiology of aging*, 57, pp. 248.e7-248.e12. Available at: https://doi.org/10.1016/J.NEUROBIOLAGING.2017.05.022.

Ysselstein, D. *et al.* (2019) 'LRRK2 kinase activity regulates lysosomal glucocerebrosidase in neurons derived from Parkinson's disease patients', *Nature communications*, 10(1). Available at: https://doi.org/10.1038/S41467-019-13413-W.

Yu, L., Chen, Y. and Tooze, S.A. (2018) 'Autophagy pathway: Cellular and molecular mechanisms', *Autophagy*, 14(2), pp. 207–215. Available at: https://doi.org/10.1080/15548627.2017.1378838.

Zaarur, N. *et al.* (2008) 'Triggering Aggresome Formation: DISSECTING AGGRESOME-TARGETING AND AGGREGATION SIGNALS IN SYNPHILIN 1', *Journal of Biological Chemistry*, 283(41), pp. 27575–27584. Available at: https://doi.org/10.1074/JBC.M802216200.

Zaffagnini, G. *et al.* (2018) 'p62 filaments capture and present ubiquitinated cargos for autophagy', *The EMBO journal*, 37(5). Available at: https://doi.org/10.15252/EMBJ.201798308.

Zajicek, A. and Yao, W.D. (2021) 'Remodeling without destruction: non-proteolytic ubiquitin chains in neural function and brain disorders', *Molecular psychiatry*, 26(1), pp. 247–264. Available at: https://doi.org/10.1038/S41380-020-0849-7.

Zampese, E. and Surmeier, D.J. (2020) 'Calcium, Bioenergetics, and Parkinson's Disease', *Cells*, 9(9). Available at: https://doi.org/10.3390/CELLS9092045.

Zarranz, J.J. *et al.* (2004) 'The New Mutation, E46K, of α-Synuclein Causes Parkinson and Lewy Body Dementia', *Annals of Neurology*, 55(2), pp. 164–173. Available at: https://doi.org/10.1002/ana.10795.

Zenko, D. *et al.* (2023) 'Monitoring α-synuclein ubiquitination dynamics reveals key

endosomal effectors mediating its trafficking and degradation', *Science advances*, 9(24), p. eadd8910. Available at: https://doi.org/10.1126/SCIADV.ADD8910/SUPPL_FILE/SCIADV.ADD8910_MOVIES_S1_TO_S11.ZIP.

Zhang, B. *et al.* (2019) 'Stereotaxic Targeting of Alpha-Synuclein Pathology in Mouse Brain Using Preformed Fibrils', *Methods in molecular biology (Clifton, N.J.)*, 1948, p. 45. Available at: https://doi.org/10.1007/978-1-4939-9124-2_5.

Zhang, L. *et al.* (2014) 'Tubastatin A/ACY-1215 improves cognition in Alzheimer's disease transgenic mice', *Journal of Alzheimer's disease : JAD*, 41(4), pp. 1193–1205. Available at: https://doi.org/10.3233/JAD-140066.

Zhang, S. *et al.* (2015) 'LK6/Mnk2a is a new kinase of alpha synuclein phosphorylation mediating neurodegeneration', *Scientific reports*, 5. Available at: https://doi.org/10.1038/SREP12564.

Zhang, S. *et al.* (2018) 'Intercellular transfer of pathogenic α-synuclein by extracellular vesicles is induced by the lipid peroxidation product 4-hydroxynonenal', *Neurobiology of Aging*, 61, pp. 52–65. Available at: https://doi.org/10.1016/J.NEUROBIOLAGING.2017.09.016.

Zhang, S. *et al.* (2021) 'Mechanistic basis for receptor-mediated pathological α-synuclein fibril cell-to-cell transmission in Parkinson's disease', *Proceedings of the National Academy of Sciences of the United States of America*, 118(26). Available at: https://doi.org/10.1073/PNAS.2011196118.

Zhang, X.-H. *et al.* (2021) 'A Review of Progress in Histone Deacetylase 6 Inhibitors Research: Structural Specificity and Functional Diversity'. Available at: https://doi.org/10.1021/acs.jmedchem.0c01782.

Zhang, X. *et al.* (2007) 'HDAC6 Modulates Cell Motility by Altering the Acetylation Level of Cortactin', *Molecular Cell*, 27(2), pp. 197–213. Available at: https://doi.org/10.1016/j.molcel.2007.05.033.

Zhang, X. and Qian, S.B. (2011) 'Chaperone-mediated hierarchical control in targeting misfolded proteins to aggresomes', *Molecular biology of the cell*, 22(18),

pp. 3277–3288. Available at: https://doi.org/10.1091/MBC.E11-05-0388.

Zhang, Y. *et al.* (2003) ‘HDAC-6 interacts with and deacetylates tubulin and microtubules in vivo’, *The EMBO journal*, 22(5), pp. 1168–1179. Available at: https://doi.org/10.1093/EMBOJ/CDG115.

Zhang, Y. *et al.* (2006) ‘Two catalytic domains are required for protein deacetylation’, *The Journal of biological chemistry*, 281(5), pp. 2401–2404. Available at: https://doi.org/10.1074/JBC.C500241200.

Zhang, Y., Kwon, SoHee, *et al.* (2008) ‘Mice lacking histone deacetylase 6 have hyperacetylated tubulin but are viable and develop normally’, *Molecular and cellular biology*, 28(5), pp. 1688–1701. Available at: https://doi.org/10.1128/MCB.01154-06.

Zhang, Y., Kwon, Sohee, *et al.* (2008) ‘Mice Lacking Histone Deacetylase 6 Have Hyperacetylated Tubulin but Are Viable and Develop Normally †’, *MOLECULAR AND CELLULAR BIOLOGY*, 28(5), pp. 1688–1701. Available at: https://doi.org/10.1128/MCB.01154-06.

Zhao, H.T. *et al.* (2017) ‘LRRK2 Antisense Oligonucleotides Ameliorate α-Synuclein Inclusion Formation in a Parkinson’s Disease Mouse Model’, *Molecular Therapy. Nucleic Acids*, 8, p. 508. Available at: https://doi.org/10.1016/J.OMTN.2017.08.002.

Zhao, J. *et al.* (2015) ‘LRRK2 dephosphorylation increases its ubiquitination’, *The Biochemical journal*, 469(1), pp. 107–120. Available at: https://doi.org/10.1042/BJ20141305.

Zhao, J. *et al.* (2023) ‘HDAC6 Deficiency Has Moderate Effects on Behaviors and Parkinson’s Disease Pathology in Mice’, *International journal of molecular sciences*, 24(12), p. 9975. Available at: https://doi.org/10.3390/IJMS24129975.

Zhao, Y. *et al.* (2020) ‘LRRK2 kinase inhibitors reduce alpha-synuclein in human neuronal cell lines with the G2019S mutation’, *Neurobiology of Disease*, 144, p. 105049. Available at: https://doi.org/10.1016/j.nbd.2020.105049.

Zhou, H. *et al.* (2019) ‘Tetramethylpyrazine Analogue T-006 Promotes the Clearance of Alpha-synuclein by Enhancing Proteasome Activity in Parkinson’s Disease

Models', *Neurotherapeutics : the journal of the American Society for Experimental NeuroTherapeutics*, 16(4), pp. 1225–1236. Available at: https://doi.org/10.1007/S13311-019-00759-8.

Zhou, W. and Freed, C.R. (2004) 'Tyrosine-to-Cysteine Modification of Human α-Synuclein Enhances Protein Aggregation and Cellular Toxicity', *Journal of Biological Chemistry*, 279(11), pp. 10128–10135. Available at: https://doi.org/10.1074/JBC.M307563200.

Zhou, W., Ryan, J.J. and Zhou, H. (2004) 'Global analyses of sumoylated proteins in Saccharomyces cerevisiae. Induction of protein sumoylation by cellular stresses', *The Journal of biological chemistry*, 279(31), pp. 32262–32268. Available at: https://doi.org/10.1074/JBC.M404173200.

Zhu, J., Coyne, C.B. and Sarkar, S.N. (2011) 'PKC alpha regulates Sendai virus-mediated interferon induction through HDAC6 and β-catenin', *The EMBO journal*, 30(23), pp. 4838–4849. Available at: https://doi.org/10.1038/EMBOJ.2011.351.

Zhu, M. and Fink, A.L. (2003) 'Lipid Binding Inhibits α-Synuclein Fibril Formation', *Journal of Biological Chemistry*, 278(19), pp. 16873–16877. Available at: https://doi.org/10.1074/JBC.M210136200.

Zhu, M., Li, J. and Fink, A.L. (2003) 'The Association of α-Synuclein with Membranes Affects Bilayer Structure, Stability, and Fibril Formation', *Journal of Biological Chemistry*, 278(41), pp. 40186–40197. Available at: https://doi.org/10.1074/JBC.M305326200.

Zimprich, A. *et al.* (2004) 'Mutations in LRRK2 cause autosomal-dominant parkinsonism with pleomorphic pathology', *Neuron*, 44(4), pp. 601–607. Available at: https://doi.org/10.1016/j.neuron.2004.11.005.

Zimprich, A. *et al.* (2011) 'A Mutation in VPS35, Encoding a Subunit of the Retromer Complex, Causes Late-Onset Parkinson Disease', *The American Journal of Human Genetics*, 89(1), pp. 168–175. Available at: https://doi.org/10.1016/J.AJHG.2011.06.008.

Zunke, F. *et al.* (2018) 'Reversible Conformational Conversion of α-Synuclein into

Toxic Assemblies by Glucosylceramide', *Neuron*, 97(1), pp. 92-107.e10. Available at: https://doi.org/10.1016/J.NEURON.2017.12.012.